Investigations of a Direct Injection Diesel Engine Run on Non Petroleum Fuel Blends

Abhishek Sharma

Department of Mechanical Engineering
National Institute of Technology Rourkela

Investigations of a Direct Injection Diesel Engine Run on Non Petroleum Fuel Blends

Dissertation submitted in partial fulfillment
of the requirements of the degree of

Doctor of Philosophy
in
Mechanical Engineering
by

Abhishek Sharma

(Roll Number: 511ME132)

based on research carried out
under the supervision of

Prof. S. Murugan

April, 2017

Department of Mechanical Engineering
National Institute of Technology Rourkela

Department of Mechanical Engineering
National Institute of Technology Rourkela

April 22, 2017

Certificate of Examination

Roll Number: 511ME132

Name: *Abhishek Sharma*

Title of Dissertation: Investigations of a Direct Injection Diesel Engine Run on Non Petroleum Fuel Blends

We the below signed, after checking the dissertation mentioned above and the official record book (s) of the student, hereby state our approval of the dissertation submitted in partial fulfillment of the requirement of the degree of Doctor of Philosophy in Mechanical Engineering at National Institute of Technology, Rourkela. We are satisfied with the volume, quality, correctness, and originality of the work.

S. Murugan
Supervisor

Ashok Kumar Satapathy
Member (DSC)

Santanu Paria
Member (DSC)

S. Jayanthu
Member (DSC)

Ujjwal K. Saha
External Examiner

`

R. K. Sahoo
Chairman (DSC)

S. S. Mahapatra
Head of the Department

Department of Mechanical Engineering
National Institute of Technology Rourkela

April 22, 2017

Prof. S. Murugan
Associate Professor
Department of Mechanical Engineering

Supervisor's Certificate

This is to certify that the work presented in this dissertation entitled *"Investigations of a Direct Injection Diesel Engine Run on Non Petroleum Fuel Blends"* by *"Abhishek Sharma"*, Roll Number: 511ME132, is a record of original research carried out by him under my supervision and guidance in partial fulfillment of the requirements of the degree of *Doctor of philosophy* in *Mechanical Engineering*. Neither this dissertation nor any part of it has been submitted for any degree or diploma to any institute or university in India or abroad.

\- - - - - - - - - - - - - - - -
S. Murugan
Supervisor

I dedicate this thesis to my parents, ***Shri Om Prakash Diwan*** and ***Smt. Kavita Diwan***, whose unconditional love, care and support laid the foundations for the discipline necessary to complete this work.

Also, I would like to dedicate my thesis to my beloved ***grandparents and my daughter Dhani***.

Declaration of Originality

I, Abhishek Sharma, Roll Number: 511ME132, hereby declare that this dissertation entitled *"Investigations of a Direct Injection Diesel Engine Run on Non Petroleum Fuel Blends"* represents my original work carried out as a doctoral student of NIT Rourkela and, to the best of my knowledge, it contains no material previously published or written by another person, nor any material presented for the award of any degree or diploma of NIT Rourkela or any other institution. Any contribution made to this research by others, with whom I have worked at NIT Rourkela or elsewhere, is explicitly acknowledged in the dissertation. Works of other authors cited in this dissertation have been duly acknowledged under the section "References". I have also submitted my original research records to the scrutiny committee for evaluation of my dissertation.

I am fully aware that in case of my non-compliance detected in the future, the Senate of NIT Rourkela may withdraw the degree awarded to me on the basis of the present dissertation.

April 22, 2017

NIT Rourkela

Abhishek Sharma

Acknowledgement

I am extremely fortunate to be involved in a challenging research work of this kind. It has enriched my life, giving me an opportunity to work in a new area of alternative fuel for diesel engine. This work enhanced my thinking abilities and understanding capability and after the completion of my work, I experienced a feeling of self-gratification.

I would like to express my deep sense of gratitude to my guide Prof. S Murugan, Associate Professor, Department of Mechanical Engineering who is an embodiment of knowledge, perseverance and tolerance for his excellent guidance, suggestions, extraordinary effort and support during my research work. Without his continual guidance this thesis would not have been materialized.

I am ever grateful to Prof. Animesh Biswas, Director who motivated me to do research work and given me a constant support all time during this study. I also sincerely thank Prof. Sunil Kumar Sarangi, for his support in submitting the thesis. I would also like to express my sincere gratitude to Prof. S.S. Mahapatra, Professor & Head of the Department of Mechanical Engineering for his encouragement and illuminating feedbacks during my research work.

I take this opportunity to express my deep sense of gratitude to the members of my Doctoral Scrutiny Committee members, Prof. R.K. Sahoo (Chairman), and Prof. Ashok Kumar Satapathy, Department of Mechanical Engineering, and Prof. Santanu Paria, Chemical Engineering Department, and Prof. S. Jayanthu, Mining Engineering Department, for their valuable suggestion while carrying out this research work.

I would like to acknowledge the assistance of my fellow research scholars for helping me in every way they could and for making the past couple of years more delightful. I also express my special thanks to all our research scholars for their support during my experimentation and documentation. I am indebted to other supporting staff for their constant help throughout the work.

I am extremely thankful to my friends Abhishek Kumar Jain, Abhimanyu Bassi, Akhtar Khan, Anuja Bharat, Amit Pandey, Akshay Prabhash Sharma, Anshuman Mitra, Abhishek Patwardhan, Amit Gupta, Alok Agrawal, Brahma Prakash Arya, Brijesh Pratap Singh, Jhamendra Sahu, Gaurav Gupta, Gurmukh Dhullion, Himandri Majumder, Hari Sankar Bendu, Kunal Shukla, Monika Verma, Mayank Choubey, M. Naresh, Naveen Pandey, Nishant Tiwari, Naseem Khayum, Nimesh Pandey, Pawan Kumar, Rohit Dhyani, Raghuwar Singh Rathore, Rajat Rusia, R. Prakash, Sumeet Verma, Sharad Agrawal, Saurabh Chandrakar, Saurabh Bhaghmar, Shrikant Zade, Surabhi Diwan, Saumya Diwan, Sandesh Chawla, Toshan Chandrakar, Tekendra Bhatt, Vivek Mishra, Vikash Upadhyay, Vaneshwar Sahu for helping me in every way they could and for making the past few years more delightful.

Most importantly, my heartfelt gratitude is for my parents Shri Om Prakash Diwan and Smt. Kavita Diwan, who have always supported me in my academic pursuits and encouraged me to do my best. I wish to give my profound love and care to my beloved daughter Ms. Avaya Sharma for her indirect involvement in completion of my work. I also express thanks and gratitude to my teachers, friends and all other family members who have been a constant source of inspiration and support for me through one way or the other from the very childhood and who stood by me whatsoever, at all phases of my life. At last, I thank the Almighty for giving me an opportunity to work in such an environment with such good and knowledgeable people around.

(Abhishek Sharma)

Abstract

The accumulation of waste automobile tyres causes a severe environmental problem, and also contaminates the soil and reduces the fertility. The anthropogenic gases raise from the disposal area is one of the reasons for the increase in greenhouse gases (GHGs). The burning of automobile tyres is toxic and harmful to the human being. Therefore, it is very much essential to dispose the waste tyres in an efficient way.

Pyrolysis process is one of the methods to recycle the waste automobile tyres in to useful energy. In the pyrolysis process, long chain polymers are thermally broken down into smaller hydrocarbon in the oxygen free environment. The process yields three principal products, viz., tyre pyrolysis oil (TPO), pyro gas and carbon black. The TPO consists of C, H, O, N and S containing organic compounds and water. The organic compounds range from C5 to C20. The TPO contains fractions of volatility consistent with gasoline, kerosene and diesel. As a result, the TPO was examined as an alternative fuel in both spark ignition (SI) engines and compression ignition (CI) engines. The solid carbon black can be used in industrial application such as re-treading, coating of insulation and industrial filters.

The main drawback of TPO is its lower cetane number due to which it can not be used as sole fuel in diesel engine. The cetane number of TPO is in the range of 25-30. This issue can be resolved by blending TPO with a fuel of higher cetane number. In this regard, the TPO was blended with Jatropha methyl ester (JME), whose cetane number is higher than that of diesel, and used as an alternative fuel in a single cylinder, four stroke, air cooled, direct injection (DI) diesel engine developing 4.4 kW. In this research study, seven modules of work were carriedout that include six experimental and one optimization. Experiments have been conducted by using five different blends where TPO was blended, from 10 to 50% at steps of 10% on a volume basis with JME. The blends were denoted as JMETPO10, JMETPO20, JMETPO30, JMETPO40 and JMETPO50, where the numeric value represents the percentage value of the TPO in the Jatropha methyl ester tyre pyrolysis oil (JMETPO) blend. The combustion, performance and emission behaviour of the engine fueled with the JMETPO blends, were compared with those of diesel and JME operations. The test results indicated that, the JMETPO20 blend exhibited reasonably better performance and lower emissions than

those by other JMETPO blends. The brake thermal efficiency for the JMETPO20 blend was close to that of diesel at full load. Further, the brake specific carbon monoxide (BSCO), brake specifc hydrocarbon (BSHC) emission and smoke opacity also reduced by 9.1%, 8.6% and 26% respectively, compared to those in case of diesel at full load. Interestingly, the combustion, performance and emission behaviour of the engine deviated after 20% TPO in the blend.

In the second module of the research work, a new approach was employed to develop hybrid multi criteria decision making techniques namely VlseKriterijumska Optimizacija I Kompromisno Resenje (in Serbian) (VIKOR) for ranking the blend alternatives. The proposed model, principal component analysis was integrated with a technique VIKOR to determine an optimum JMETPO blend. The experimental results of the combustion, performance and emission parameters of the test engine operated with different JMETPO blends at different load conditions were used for optimization. It was noticed that experimental trial number 32 had the smallest VIKOR index (Qi) value for JMETPO20 blend compared to other JMETPO blends. Thus, it was concluded that, the minimum VIKOR index can be obtained when engine was operated with the JMETPO20 blend at full load. Thus, the final ranking for the JMETPO blends based on VIKOR analysis was JMETPO20> JMETPO10> JMETPO30> JMETPO40> JMETPO50.

In the third module, the effect of varying the injection timing on the combustion, performance and emission characteristics of the test engine was experimentally investigated, when the engine was run with the JMETPO20 blend. The original injection timing was altered by adjusting the number of shims fitted under the plunger in the pump, by addition or removal of shims. In addition to the original injection timing of 23 ˚CA bTDC, other injection timings at which the study was carriedout were 20, 21.5, 24.5 and 26 ˚CA bTDC. The results indicated that, the blend gave a better performance and lower emissions when operated with an advanced injection timing of 24.5 ˚CA bTDC as compared to other injection timings.

In the fourth module, the tests were conducted at the optimum injection timing to study the effect of the nozzle opening pressure on the combustion, performance and emission characteristics of the test engine fueled with JMETPO20 blend. In order to find an optimum

nozzle opening pressure for the blend, tests were conducted at an optimized injection timing with five nozzle opening pressure s viz. 210, 220, 230, 240 and 250 bar in addition to the original nozzle opening pressure of 200 bar, and the findings were compared with those of diesel operation. Based on the combustion, performance and emission of the engine, the nozzle opening pressure of 220 bar gave a better performance results and lower smoke, and BSHC and BSCO emissions compared to other nozzle opening pressure investigated.

Further, study was carriedout at investigating the effect of varying the compression ratio at optimized injection timing and nozzle opening pressure on the behaviour of the test engine, using optimum blend, i.e. JMETPO20. The engine was subjected to one lower (16.5) and one higher (18.5) compression ratio in addition to the standard compression ratio of 17.5. At the higher compression ratio of 18.5 and full load, shorter ignition delay, maximum cylinder pressure and higher heat release rate were found for the blend, compared to those in case of the original compression ratio. The increase in the compression ratio from 17.5 to 18.5 for the blend improved the brake thermal efficiency by about 8% compared to that of the original compression ratio at full load. The BSCO, BSHC emissions and smoke opacity were reduced by about 10.5%, 32%, and 17.4% respectively, with respect to those of the original compression ratio at full load.

The oxidation stability of biodiesel plays an important role for its long term storage. Although it is possible to obtain the required oxidation stability of any biodiesel by using synthetic antioxidants, at the same time, it will increase the cost of the resultant fuel as antioxidants are expensive. The phenolic compounds present in the pyrolysis oil may act as natural antioxidants to biodiesel. TPO derived from waste automobile tyres through pyrolysis contains few phenolic compounds. Therefore, in the sixth module of this research work, an attempt was made to analyse the influence of blending different amounts of TPO with JME on the oxidation stability of the blend. For this purpose, 20%, 40% and 60% (on volume basis) of TPO were blended with the JME. This work reveals that, blending TPO with JME, there was a significant improvement in the oxidation stability of JMETPO blends. In addition to this, an experimental investigation was also carriedout by using the JMETPO20 blend, to evaluate the behaviour of the diesel engine run on the biodiesel blend, with and without synthetic

antioxidants. Based on the experimental findings, this study suggests that blending 20% TPO with 80% JME can reduce dosage of antioxidant by about 50%.

Finally a comparative study was conducted in this module to examine the durability issues of a direct injection diesel engine run on the JMETPO20 blend and diesel. For this purpose, the engine operated with the JMETPO20 blend and diesel was run for 100 h, which consist of 14 test cycles of 7 h each as per the IS 10000 standards. Visual examination of the vital parts of the engine components such as cylinder head, piston crown, and nozzle injector tip etc. was also carried out to find the carbon deposit after the durability test. After the durability test, several tribological characteristics of the used lubricating oil were evaluated after every 25 h of engine operation in order to analyze the consequence of fuel chemistry on the life of the lubricating oil. Measurement of different metal debris concentrations present in the lubricating oil samples drawn from the JMETPO20 blend and diesel operated engine was carriedout by the atomic absorption spectroscopy. On the whole, it is concluded that, the JMETPO20 blend can be used as an alternative fuel for CI engine with few minor modifications in the engine geometry.

Keywords**: **Diesel engine; biodiesel; pyrolysis oil; performance; combustion; emission; durability;

Contents

List of Figures

List of Tables

Nomenclatures

AAS	Atomic absorption spectroscopy
ADC	Analog to digital converter
ASTM	American society for testing and materials
BDC	Bottom dead centre
BHA	Butylated hydroxyanisole
BHT	Butylated hydroxytoluene
BP	Brake power
BSEC	Brake specific energy consumption
BSFC	Brake specific fuel consumption
BSHC	Brake specific hydrocarbon
BSCO	Brake specific carbon monoxide
BSNO	Brake specific nitric oxide
BTE	Brake thermal efficiency
bTDC	Before top dead center
CA	Crank angle
CI	Compression ignition
CO	Carbon monoxide
CO2	Carbon dioxide
CR	Compression ratio
DAS	Data acquisition system
DA	Digital to analog
DEE	Diethyl ether
DI	Direct injection
DTPO	Distilled tire pyrolysis oil
EGR	Exhaust gas recirculation
EGT	Exhaust gas temperature
EPA	Environmental protection agency
FT-IR	Fourier transform infrared
FTIR	Fourier transform infrared spectroscopy
FAME	Fatty acid methyl ester
FID	Flame ionisation detector
GC-MS	Gas chromatography mass spectrometry
GHG	Greenhouse gas
HC	Hydrocarbon
HHV	Higher heating value
HRR	Heat release rate
IC	Internal combustion
ID	Ignition delay
IP	Induction period
IT	Injection timing
JME	Jatropha methyl ester
kWh	kilowatt hour
kW	kilowatts

LHV	Lower heating value
MBEBP	4-methyl-6-tert-butyphenol
MCDM	Multi-criteria decision making
NDIR	Non dispersive infrared
NO	Nitric oxide
NO_2	Nitrogen dioxide
NO_x	Oxides of nitrogen
NOP	Nozzle opening pressure
O_2	Oxygen
P_{max}	Maximum cylinder pressure
PG	Propyl gallate
ppm	Parts per million
PM	Particulate matter
PY	Pyrogallol
RT	Retention time
ROPR	Rate of pressure rise
SFC	Specific fuel consumption
SI	Spark ignition
SMD	Sauter mean diameter
SOME	Soybean oil methyl ester
TBHQ	Tert-butyl hydroquinone
TDC	Top dead centre
TPO	Tire pyrolysis oil
UTO	Used transformer oil
WLO	Waste lubricating oil
WPO	Waste plastic oil

Chapter 1

Introduction

1.1 General

Energy has always been the primary element that humanity has depended for survival. Energy consumption in the world is increasing faster than the supply. It is estimated that the existing fossil fuel reserves will be sufficient for only a few decades. The heat engines based transportation and decentralized power generation mainly depend upon fossil fuels. On the other hand, the environmental quality has been continuously degrading from last two centuries due to increase in fossil fuel consumption. In order to overcome these two issues, there have been many attempts made by the world in the last four decades to substitute the fossil fuels, particularly petroleum fuels by various alternative energy sources that include renewable and non-conventional energy sources. This chapter discusses about energy sustainability, heat engines and their applications, requirement of alternative fuel for diesel engines and some potential alternative fuels. This chapter also provides the information on the potential utilization and their environmental impacts of liquid fuels for diesel engines obtained by converting waste products.

1.2 Energy sustainability

Global energy demand is increasing dramatically due to increasing industrialization, overwhelming rise in number of automotive vehicles and growing population. Table 1.1 gives the world energy consumption and percentage of energy share of different energy sources [1]. It is apparent from the table that, in the year 2014 fuel consumption was almost doubled compared to that in the year 1980. According to the reports of the International Energy Agency (IEA) estimation, global energy demand is expected to increase by about 53% by 2030. Currently, approximately 86.3% of world energy demand is fulfilled by fossil fuels, in which crude oil supports by about 32.6%, whereas coal and natural gas by about 30% and 23.7% respectively [2]. Conversely, nuclear energy and hydroelectric energy contribute only small proportions by about 4.4% and 6.8%, respectively. Over the past 25 years, total energy supply has increased steadily. However, with the current consumption rates, the reserves of

crude oil and natural gas will diminish after approximately 41.8 and 60.3 years, respectively. The total primary fuel consumption by world has reached by about 12928.3 million tonnes of oil equivalent (Mtoe) in 2014 which is 95% higher than that in 1980, as given in Table 1.1.

Table 1.1 World primary energy consumption and percentage of share

Source	1980		2012		2015	
	Mtoe	**Share (%)**	**Mtoe**	**Share (%)**	**Mtoe**	**Share (%)**
Petroleum	2979.8	44.9	4130.5	33.11	4331.3	32.94
Coal	1807.9	27.3	3730.1	29.90	3839.9	29.22
Natural gas	1296.8	19.6	2987.1	23.94	3135.2	23.84
Nuclear	161	2.4	560.4	4.49	583.1	4.43
Hydropower	384.3	5.8	831.1	6.66	892.9	6.8
Renewables	-	-	237.4	1.90	364.9	2.77
Total	6629.8	100	12476.6	100	13147.3	100

Table 1.2 provides energy consumption of some of the developed countries and percentage of energy share in the year 2014 [1]. Globally, the equivalent of by about more than 11 billion tons of oil in fossil fuel is consumed every year. Crude oil reserves are vanishing at a rate of 4 billion tons a year. If this rate continues, oil deposits will be finished by 2052 [3].

Table 1.2 Some of the developed countries energy consumption and percentage of share in the year 2015

Source	US		UK		Canada		Sweden		Japan	
	Mtoe	**Share (%)**	**Mtoe**	**Share (%)**	**Mtoe**	**Share (%)**	**Mtoe**	**Share (%)**	**Mtoe**	**Share (%)**
Petroleum	851.6	37.34	71.6	37.45	100.3	30.40	14.1	26.60	189.6	42.27
Coal	396.3	17.38	23.4	12.24	19.8	6.00	2.1	3.96	119.4	26.62
Natural gas	713.6	31.29	61.4	32.12	92.2	27.95	0.8	1.51	102.1	22.76
Nuclear	189.9	8.33	15.9	8.34	23.6	7.15	12.9	24.34	1	0.22
Hydropower	57.4	2.52	1.4	0.75	86.7	26.28	16.9	31.89	21.9	4.89
Renewables	71.7	3.14	17.4	9.10	7.3	2.22	6.2	11.70	14.5	3.24
Total	2280.5	100	191.1	100	329.9	100	53	100	448.5	100

Moreover, the rate of energy consumption in the world is not steady, as it increases dramatically with the increase in global population and living standards. The energy consumption and percentage of energy share of some of the developing countries in the year 2015 are given in Table 1.3 [1]. India is one of the fastest developing countries in the world with a stable economic growth, which multiplies the demand for petroleum fuels manifold. It was reported that in the year 2011, India was the fourth largest energy consumer in the world after the United States, China, and Russia. India depends mainly on the imported crude oil due to lack of fossil fuel reserves, and this has a great impact on the economy. Therefore, India has to consistently look for an alternative to meet the future energy demand.

Table 1.3 Some of the developing countries energy consumption and percentage of share in the year 2015

Source	**India**		**China**		**South Africa**		**Pakistan**		**Philippines**	
	Mtoe	**Share (%)**	**Mtoe**	**Share (%)**	**Mtoe**	**Share (%)**	**Mtoe**	**Share (%)**	**Mtoe**	**Share (%)**
Petroleum	195.5	27.91	559.7	18.57	31.1	25.04	25.2	32.2	18.4	48.81
Coal	407.2	58.13	1920.4	63.72	85	68.44	4.7	6.0	11.4	30.24
Natural gas	45.5	6.50	177.6	5.89	4.5	3.62	39.0	49.9	3.0	7.96
Nuclear	8.6	1.23	38.6	1.28	2.4	1.93	1.1	1.4	0.0	0.00
Hydropower	28.1	4.02	254.9	8.46	0.2	0.16	7.8	10.0	2.2	5.84
Renewables	15.5	2.21	62.7	2.08	1	0.81	0.4	0.5	2.7	7.16
Total	700.5	100	3014.0	100	124.2	100	78.2	100	37.7	100

1.3 Heat engines

Heat engine is a device which transforms the chemical energy of a fuel into thermal energy and utilizes this energy to produce mechanical work. Heat engine can be broadly classified into two types i.e. internal combustion (IC) engines and external combustion (EC) engines. One of the outstanding applications of IC engines is in the field of transportation on land, sea and air. The other applications of IC engines include industry applications and prime movers for electrical power generations. The advantages of IC engines over EC engines are greater

mechanical simplicity, lower ratio of weight, higher overall efficiency and lesser requirement of water for dissipation of energy through cooling system.

Several research works have been carriedout in small-scale power generation, despite the propagation of large-scale centralized power generation. Decentralized power generation with renewable energy technologies has the potential to solve these issues particularly in remote areas. Renewable and non-conventional energy sources are perfectly suited for decentralized power generation and they have a substantial potential to provide reliable and secure energy supply as decentralized power generation. Some of the renewable energy technologies that are used in villages and rural areas as are small biogas plants, solar street lighting systems; solar water heating systems, biomass based power generators etc. can play a vital role in decentralized power generation for irrigation and electrification [4].

1.4 Requirement of alternative fuel for diesel engines

Some of the important requirements of alternative fuels for diesel engines are given below;

(i) A good CI engine fuel should be enough volatile in the operating rage of temperature to produce good air-fuel mixing.

(ii) A good CI engine fuel should have a shorter ignition delay to avoid knocking. The ignition delay also affects the starting, warm up, and leads to the production of smoke opacity in CI engines.

(iii) The fuel should mix with air faster and better.

(iv) Fuel must be able to flow freely at all expected ambient temperatures.

(v) The fuel should not cause corrosion and wear of the vital engine parts during operation. These requirements are directly related to the presence of sulphur, ash and residue in the fuel.

(vi) The fuel should have a high flash point and a high fire point.

(vii) Cloud point is another concern with diesel fuel at lower temperatures.

1.5 Potential liquid alternative fuel for CI engines

1.5.1 Vegetable oils

Vegetable oils are derived from plants that are composed of triglycerides. Vegetable oils can be classified broadly in two category i.e. edible oils and non edibles oils. The examples of the

edible oil seed crops are Palm oil, Soybean oil, Sun flower oil, Canola oil, Rice bran etc. and non-edible oil seed crops are Jatropha, Mahua, Karanja, Neem, Rubber seed etc. In the last three decades, vegetable oils have become more attractive candidate for the replacement of petroleum based fuels, because they are renewable in nature and made from renewable resources and environmentally friendly as well [5]. Different methods to use a vegetable oil as a substitute fuel in diesel engines are described below.

1.5.1.1 Direct use of vegetable oils

When Rudolf Diesel demonstrated his patented diesel engine in a France conference, he used peanut oil as a fuel for running the diesel engine. Since then, it has been a proven source as an alternative source of energy for diesel engine. After significant research works carriedout, it was concluded that the direct use of neat vegetable oils is not suitable for diesel engines; because of their higher viscosities than that of diesel. Hence, their structures have to be modified to bring their properties closer to those of diesel. There have been many problems associated with using vegetable oils directly in diesel engines which are as follows;

(i) The presence of chemically bound oxygen in vegetable oil lowers their heating values.

(ii) The high viscosity and high flash point of vegetable oils attributes to lower volatility characteristics.

(iii) Cold weather starting problem due to significantly higher cloud and pour points than that of diesel.

(iv) Plugging and gumming of filters, lines and injectors

(v) Coking of injectors and high carbon deposits on piston, piston rings, valves, engine head and injector tips are the major problems associated with direct use of straight vegetable oils.

(vi) Engine knocking

(vii) Excessive engine wear

(viii) Thickening and gelling of the lubricating oil as a result of contamination by the vegetable oils.

1.5.1.2 Blending

Fuel modification is mainly aimed at reducing the viscosity to avoid flow and combustion-related problems. Blending of a vegetable oil with diesel or other fuel is one of the techniques

to bring the viscosity close to a specification range. The blending of different vegetable oil with mineral diesel were experimented and documented by various researchers**.** Some examples of them include Sunflower oil [6], Soybean oil [7], Palm oil [8], Canola oil [9] in edible oil category and Jatropha [10], Karanja oil [11], Mahua oil [12], Neem oil [13], Cotton seed oil [14], in non-edible oil category. In 1980, Caterpillar (Brazil) company used pre-combustion chamber engines with a mixture of 10% vegetable oil to maintain total power without any engine modification. It was reported that replacement of 100% diesel fuel by vegetable oil was not practical, but a 20% blend of vegetable oil with diesel works satisfactorily in the existing diesel engine and parameters at which engines are operating [15]. The blending of vegetable oils reduces the viscosity, but its molecular structure remains unchanged; hence polyunsaturated character and low volatility problems remains exist. It is reported by many researchers that brake specific fuel consumption (BSFC) and exhaust gas temperature for blends of vegetable oil with diesel were found to be higher compared to diesel [16]. It was also noticed that, BSFC increased as the proportion of vegetable oil in the blend increased. In most of the cases, it was concluded that the performance and emission characteristics of the diesel engine were found to be very close to base diesel for lower blend concentrations only [17]. The extra consumption of vegetable oil, a drop in engine power and thermal efficiency is due to the consequences of the low net calorific value, high density and high viscosity of vegetable oils compared to that of diesel [18]. The high viscosity of vegetable oils affects the injection process and leads to poor fuel atomization which leads to incomplete combustion of fuel resulting to heavy smoke opacity and carbon deposit on the injector and valve seat. These problems can be resolved, if the vegetable oils are chemically reformed to biodiesel, which is similar in properties to diesel [19].

1.5.1.3 Preheating

Preheating is one of the most effective methods to reduce the viscosity of vegetable oils. Vegetable oils need to be heated to a temperature such that, it is high enough to give a low viscosity similar to diesel, but not so high as to damage the injection system. However, the fuel injection system is made up of parts that are very close fitting and high fuel intake temperature may have adverse effects on these parts. Data indicate that temperature varies between 25-100 ˚C for preheating of vegetable oils to lower its viscosity to that of diesel and generally above 70 ˚C, vegetable oils have a viscosity approaching that of mineral diesel [20-

21]. A number of researchers have investigated the performance and emission characteristics of a diesel engines that were run on preheated vegetable oils; such as Palm oil [22], Rapseed oil [23], Jatropha oil [24] etc. They reported that, use of preheated vegetable oils in diesel engines resulted in improved brake thermal efficiency (BTE) [25]. In most cases nitric oxide (NO) and hydrocarbon (HC) emissions of the diesel engine fueled with preheated vegetable oils is higher in comparison with diesel [26-27].

1.5.1.4 Microemulsion of vegetable oils

Micro-emulsions with solvents such as methanol, ethanol and isobutanol have been tried to reduce the viscosity of vegetable oil. A micro-emulsion is defined as a colloidal equilibrium dispersion of optically isotropic fluid microstructures with dimensions generally in the 1-150 nm range formed spontaneously from two normally immiscible liquids. They can improve the spray characteristics by explosive vaporisation of the low boiling constituents [28]. There have been several research works reported in the scientific literature regarding the formulation and characterization of the microemulsions of vegetable oils such as Cotton oil [29], Rapseed oil [30], Palm oil [31] etc. and animal fats, as well as their potential to substitute diesel fuel by a certain amount [32-33]. It was reported that the emulsion of vegetable oils is suitable as a diesel engine fuel due to the improvements of the atomization process. However, increases of the BSFC, ignition delay, HC and carbon monoxide (CO) emissions were also reported. On the other hand, in some experimental conditions, decrease in HC and/or CO emissions for vegetable oil emulsion compared with diesel and/or neat vegetable oils also were reported [34].

1.5.1.5 Pyrolysis

Pyrolysis is the process of breaking down complex structure of hydrocarbons into simpler by the application of heat in the absence of air. Vegetable oils and animal fats can be pyrolyzed. The pyrolysis of vegetable oils such as Soybean oil [35], Palm oil [36], and Canola oil [37] etc. have been investigated and further utilized in diesel engines. The pyrolysis of fats has been investigated for more than 100 years, especially in those areas of the world that lack deposits of petroleum [38]. This process is carriedout at higher temperatures of about 250-500 ˚C and at higher heating rates. The bio-oil produced by pyrolysis of vegetable oils has been considered as fuels used in combustors, engines or gas turbines, and also has the potential to

supply a number of valuable chemicals [39]. The bio-oils are complex and chemically unstable mixtures, and this depends upon feedstocks, products uses, suitable reactors and processes for the product applications. Also more work is needed on the stabilization and upgrading of bio-oils with some modifications to equipment configuration before using them for heat or power generation [40]. These are the some issues which is blocking its industrialization processes and easy use.

1.5.1.6 Transesterification

The esters of vegetable oils are produced by transesterification process. The triglycerides of vegetable oils are converted into simple mono esters by this process. In transesterification process triglyceride is reacted with alcohol in the presence of a catalyst, to produce glycerol and fatty acid esters. A catalyst is usually used to enhance the reaction rate and yield. This process reduces its viscosity and unsaturation. The most important variables that influence the transesterification reaction are oil temperature, ratio of alcohol to oil, type and concentration of catalyst, stirring rate, intensity of mixing and purity of reactants [41].

The transesterification process, also called alcoholysis is an equilibrium reaction, during which the vegetable oil reacts with alcohol (e.g. methanol, ethanol, propanol or butanol) to make fatty acid methyl esters (FAME), fatty acid ethyl esters (FAEE), fatty acid butyl esters (FABE), and glycerol in the presence of a catalyst (NaOH or KOH). The process reduces the viscosity of the end product. The schematic representation of tranesterification process for the production of biodiesel is given in Figure 1.1.

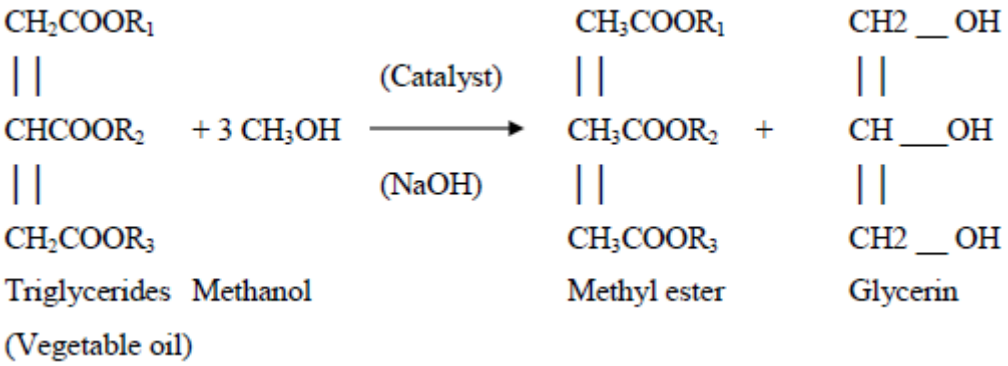

Fig. 1.1 Schematic diagram of the transesterification process

Both methanol and ethanol are used in this process, but methanol is often preferred because of its availability, lower cost and high reactivity. However, ethanol has advantages such as it derivable from agricultural products, renewable and environmental friendly [42].

1.5.2. Biodiesel

The fatty methyl or ethyl or butyl ester derived from vegetable oils, animal fat or algae is commonly referred as biodiesel. It is a fuel composed of mono-alkaline esters of long chain fatty acids which is produced from vegetable oils (edible and non-edible), animal fats and algae by the tranesterification process. Vegetable oils are often seen as a more suitable source for biodiesel production compared to animal fats and algae. Biodiesel is a non-toxic, renewable, biodegradable and environment friendly with the potential to mitigate engine exhaust emissions [43].

1.5.2.1 Sources of biodiesel production

In the last few decades, the biodiesel production has been receiving an intensive attention, because it is considered as a possible substitute or extender of conventional diesel. Many countries have started using biodiesel derived from edible or non-edible oil seeds for heat and power applications, particularly for transportation applications. Figure 1.2 represents the world's biggest biodiesel producers in 2015, by country (in billion liters) in the world [44]. The feedstock used for biodiesel production varies from country to country. In India, the use of edible oils like Soybean oil, Sunflower oil, Coconut oil, Palm oil to produce biodiesel is not practical as these oils are being consumed as food and there is an enormous gap in their demand and supply in the country. Thus, for Indian conditions, solely non-edible oil seed plants can be considered for the biodiesel production. Table 1.4 provides the details of different types of non-edible seed considered for biodiesel production, and the total planted area in various states of India [45]. Several researchers in India have tried different non-edible feed stocks such as Jatropha curcas, Pongamia pinnata, Linseed, Madhuca indica, Rapseed, Cotton seed and Rubber seed etc. for the production of biodiesel [46-49]. Among the non edible seeds produced in India, Jatropha curcas is the most preferred only because of its high oil content and biodiesel yield.

The "National policy on Biofuels" programme by the Ministry of New and Renewable Energy (MNRE) has already launched in the year 2009, to increase biodiesel production and to be used as replacement of diesel particularly in the transportation [50]. The Government of India has identified waste land where non-edible oil seed plant can be cultivated, to meet the goal of replacement of 20% of India's diesel consumption by 2017. Already many state governments have taken initiation for plantations of Jatropha for biodiesel production [51].

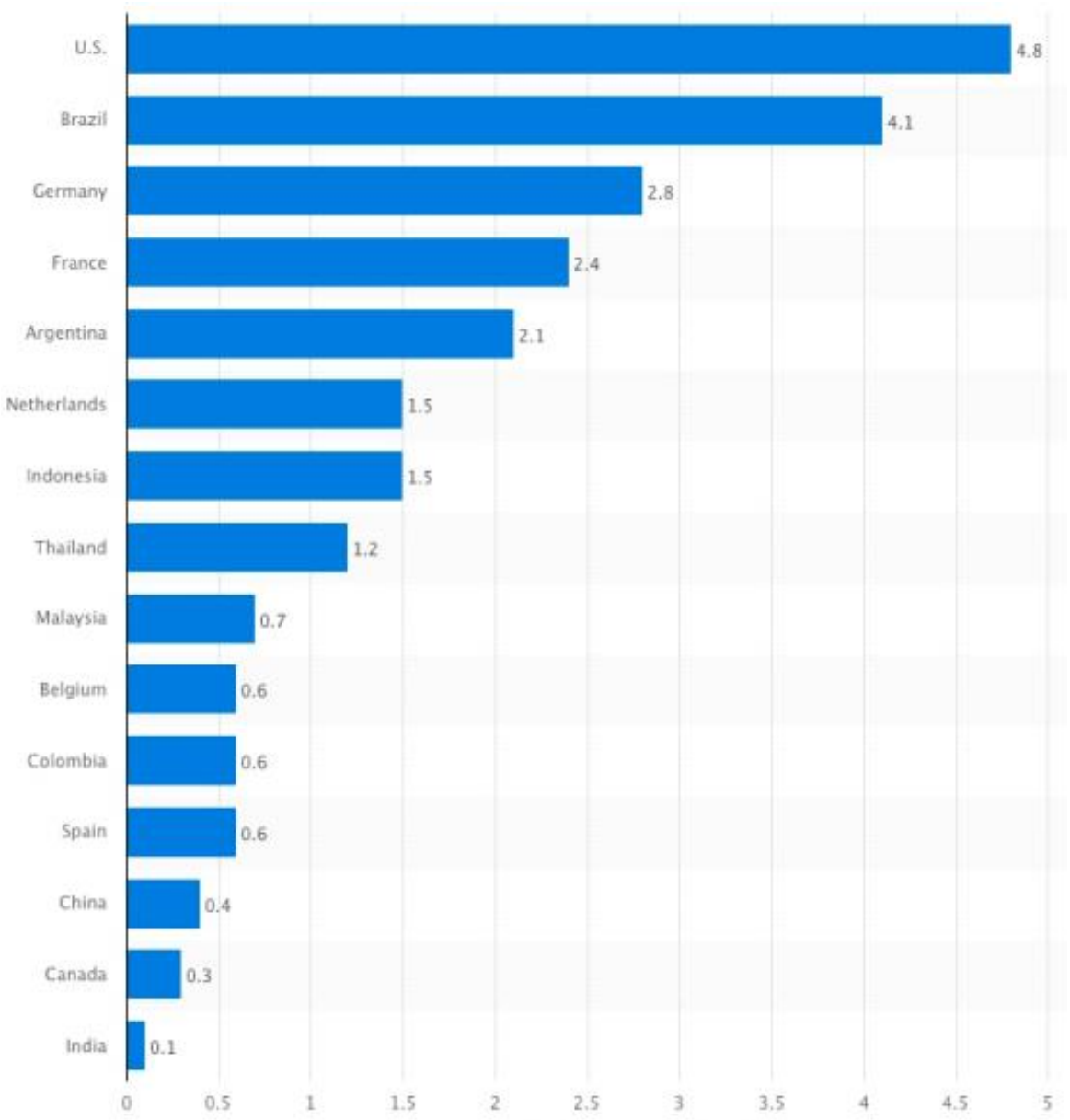

Fig. 1.2 World's biggest biodiesel producers in 2015, by country (in billion liters)

It is estimated that the existing potential of tree-borne oil seeds in the country is 3-3.5 million tons but only 0.5-0.69 million tons are being collected [52]. Some of the biodiesel feedstocks with their oil content are shown in Table 1.5.

Table 1.4 Land area (ha) under cultivation of different tree bearing non-edible seeds for production of biodiesel in India

S. No.	Name of State	Jatropha	Karanja	Neem	Mahua
1.	Andhra Pradesh	1500	7,009	59,856	5620
2.	Assam	100	712	3,101	3
3.	Arunachal Pradesh	235	28	12	34
4.	Bihar	200	180	7,979	1301
5.	Chhattisgarh	3,04,152	1,895	14,657	7793
6.	Dadra Nagar Haveli	45	53	232	245
7.	Gujarat	1,300	718	42,794	1554
8.	Delhi	-	168	3,333	-
9.	Haryana	1,405	553	12,534	55
10.	Himachal Pradesh	489	843	845	10
11.	Jammu & Kashmir	9	5	212	-
12.	Jharkhand	800	1,416	9,940	2,570
13.	Karnataka	670	3,580	41,666	3,037
14.	Kerala	50	685	16,457	1,047
15.	Madhya Pradesh	3,74,648	4,235	50,066	15,884
16.	Maharashtra	2360	2,201	59,903	5,341
17.	Manipur	450	19	668	-
18.	Meghalaya	446	347	216	3
19.	Mizoram	380	-	-	-
20.	Nagaland	490	-	-	-
21.	Orissa	-	1,506	13,324	5,367
22.	Puduchery	-	1,830	17,207	37
23.	Punjab	300	319	12,836	37
24.	Rajasthan	10,554	595	60,768	3,257
25.	Sikkim	150		51	3
26.	Tamilnadu	900	4,176	96,413	1,324
27.	Tripura	150	393	44,021	
28.	Uttar Pradesh	12,000	1,929	70,193	6,482
29.	Uttarakhand	13,500	513	2,527	838
30.	West Bengal	21,500	481	19,125	658
31.	Total	74,8782	36,000	61,7359	62,500

Table 1.5 Oil content and the biodiesel yield of different oil sources

Nature	Oil Source	Oil content (%)	Biodiesel yield (%)
Edible	Soybean	15-20	>95
	Sunflower	25-35	97.1
	Palm	30-60	89.2
	Peanut	45-55	89
	Corn	48	85-96
	Camelina	29.9-38.3	97.9
	Canola	43	80-95
	Pumpkin	50	97.5
	Rice bran	15-23	< 96
	Coconut	63-65	98
	Olive	45-70	92
Non-Edible	Jatropha (Jatropha curcas)	20–60	98
	Karanja/ Honge (Pongamia pinnata)	25–50	97-98
	Mahua (Madhuca indica)	35–50	98
	Cottonseed	17–25	96.9
	Rapeseed	38-46	95-96
	Neem (Azadirachta indica)	20–30	88-94
	Putranjiva (Putranjiva roxburghii)	42	91
	Tobacco (Nicotiana tabacum)	36-41	88
	Polanga (Calophyllum inophyllum)	65	85
	Cardoon (Cynaracardunculus)	25-26	92
	Castor (Ricinus communis)	45-50	90
	Jojoba (Simmondsia chinensis)	45-55	93
	Moringa (Moringa oleifera)	45–50	82
	Poon (Sterculia foetida)	50–55	88
	Sea mango (Cerbera odollam)	54	83.8
Animal Fat	Tallow	41	98.28
	Poultry	-	99.7
Others	Used cooking oil	-	94.6
	Micro algae	20-50	60

1.5.2.2 Biodiesel in CI engines

Research works on utilization of biodiesel obtained from variety of feedstocks in diesel engines have been extensively carriedout in the last few decades in the world. In India, several research works have been documented in the past on the utilization of biodiesel in diesel engines, both stationary and mobile applications. It is reported that the biodiesel fueled engine offers almost equal thermal efficiency close to diesel fueled engines. Utilization of methyl esters of edible oils such as Sunflower, Soybean, Palm, Rapeseed etc. in diesel engines have been investigated by many researchers [53]. However, the use of edible oils for

biodiesel production is not encouraged, because it otherwise affects the food supply chain [54]. Research works have also been documented on the combustion, performance and emission characteristics of a diesel engine, run on blends of methyl/ethyl/butyl esters of Jatropha, Karanja, and Mahua, Cotton seed oil, Rubber seed oil and Linseed oil with diesel [55-57]. Some of them have also investigated the utilization of these esters in diesel engines with engine modification, while others have studied their effects on varied engine components. A complete review of research works related to the utilization of Jatropha biodiesel are given in Chapter 2.

It is reported that 20% biodiesel blended with 80% diesel fuel (B20) gives comparable performance and emission with that of diesel, when it is used in a conventional diesel engine. Nowadays, engines are manufactured for a configuration so that 100% biodiesel (B100) can be used with little or no modification. Biodiesel fueled engine results in considerable decrease of HC, CO and particulate matter (PM) emissions. It is has almost no sulphur, no aromatics and its higher cetane number enhances the combustion quality of fuel [58]. Also, it is reported that for every 10% increase of biodiesel content in the diesel-biodiesel blend, the engine will produce 1% more NO emission [59]. This is the major issue related to most biodiesels from the emission point of view.

1.5.2.3 Biodiesel merits

The following are the advantages of using biodiesel as a substitute of diesel fuel.

(i) It can be directly used as a fuel in diesel engines without any major engine modification, and it gives almost equal fuel efficiency and results in significant reduction of HC, CO, smoke and particulate matter emission compared to conventional diesel.

(ii) Biodiesel is cheaper than diesel and can be a ‘‘on farm fuel’’ where the farmer can grow the seed oil crops, produced biodiesel and can use in the field itself.

(iii) It contains about 10% oxygen in the molecules, which improves the ignition quality resulting in an enhanced combustion of the fuel inside the cylinder. Biodiesel has a higher cetane number which makes the vehicle performance better as higher cetane number improves the quality of the fuel’s ignition.

(iv) Its use can extend the life of diesel engine, because it has better lubricating properties than diesel.

(v) It can also be made by using waste cooking oils and animal fats. Therefore, rather than disposing substances away, the flexibility to convert them into biodiesel becomes more attractive. In this manner biodiesel reduces the environmental effect of a waste product.

(vi) Biodiesel is energy efficient. If the production of biodiesel is compared with the production of the regular type, producing the latter consumes more energy. Biodiesel does not need to be drilled, transported, or refined like petroleum diesel. Producing biodiesel is easier and is less time consuming.

(vii) It can be made from domestic resources such as Soybeans, Jatropha, Cotton seed, Rubber seed, and Mustard seed oil etc. This would help to reduce a country's dependency on imported petroleum fuels.

(viii) Biodiesel is safe to handle and transport because it has a flash point about 110 ˚C compared to diesel whose flash point is 45-55 ˚C.

1.5.2.4 Limitations of biodiesel

The following are the limitations of biodiesel when it is used as a substitute to diesel fuel for compression ignition (CI) engine.

(i) The major drawbacks of biodiesel are its higher viscosity, lower energy content, higher cloud and pour point than diesel.

(ii) Biodiesel fueled engine produces higher emission of nitrogen oxides compared to a diesel fueled engine.

(iv)The oxidation stability of biodiesel is very poor which discourages its long term use. The other important issue with biodiesel is fuel ageing commences rapidly, which causes deposit formation; and can cause corrosion in vehicle material.

(v) Low volatility compared to diesel.

1.5.2.5 Stability problem associated with biodiesel

Although biodiesel can be a prominent substitute for diesel fuel in many aspects, it has some drawbacks which include cold start problem, higher density and viscosity, injector coking, produces higher emission of nitrogen oxides compared to a diesel fueled engine, high cost of the feedstock due to its limited availability and its inferior stability during a long term storage etc. [60].

Biodiesel is more susceptible to degradation compared to mineral diesel due to the presence of significant amount of unsaturated fatty acids with double bonds in it which also affect its properties when it is stored for long term [61-62]. The biodiesel composition varies based on the feedstock utilized for production. As the portion of unsaturated fatty acid ester increases in biodiesel, it becomes more unstable. Examples of saturated fatty acids are butyric acid, myristic acid, palmitic acid and stearic acid whereas unsaturated fatty acids are oleic acid, linolenic acid and linoleic acids. The trend of increasing stability for both acids and esters was found as linolenic < linoleic <oleic [63]. Most of the plant derived vegetable oils contain poly-unsaturated fatty acids in the form of methylene interrupted configuration that has more than one cis double bonds separated by a single methylene (-CH2 -) unit. The molecular structure of the common fatty acid ester biodiesel molecules is given below in Figure 1.3.

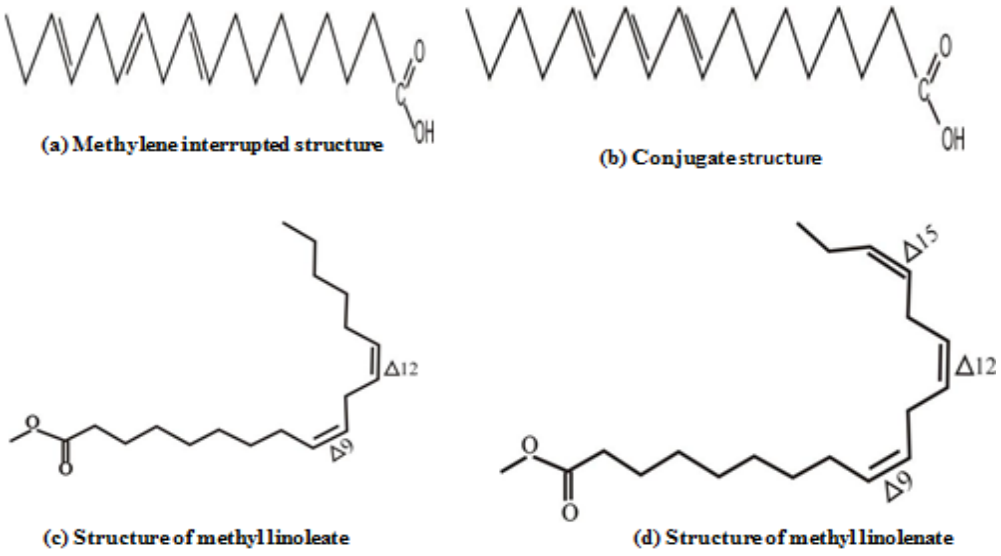

Fig. 1.3 Molecular structure of the common fatty acid ester biodiesel molecules

Stability is one of the vital desirable properties of any fuel. The stability of biodiesel is lower than mineral diesel. Numerous processes, including oxidation in aerobic conditions, hydrolysis in the presence of moisture, thermal decomposition by additional heat, contamination of impurities, etc., cause for the instability of biodiesel that may change the fuel properties significantly [64]. Among these processes, oxidation is one of the important stability problems identified with biodiesel, because it has a lower resistance to oxidation and might simply be affected by air oxidation when it is kept for a long-term [65]. The term oxidation stability is a general term, that differs from 'storage stability' and 'thermal

stability', as the oxidative degradation may occur during long term storage, transportation and end use [66].

The various mechanisms due to which oxidation occurs are (i) autoxidation in presence of atmospheric oxygen, (ii) thermal degradation from excess heat, (iii) hydrolysis in presence of moisture or water during storage and in fuel lines, (iv) microbial contamination from contact with dust particles or water droplets containing fungi or bacteria into the fuel etc. As the portion of unsaturated fatty acid ester increases in biodiesel, it becomes more unstable. The susceptibility to oxidation of a biodiesel increases with the number of double bonds, their relative location, and degree of conjugation of double bonds present. Therefore, as the portion of unsaturated fatty acid esters in biodiesel increases it is more prone to oxidation [67].

The chemistry of oxidation process can be described by set of reactions such as initiation, propagation and termination resulting in aldehydes, alcohols and carbonic acids. This can be formulated as:

Initiation

$$RH \longrightarrow R^{\cdot}$$

Propagation

$$R^{\cdot} + O \longrightarrow ROO^{\cdot}$$
$$ROO^{\cdot} + RH \longrightarrow R{-}OOH + R^{\cdot}$$

Termination

$$R^{\cdot} + R^{\cdot} \longrightarrow R{-}R$$
$$ROO^{\cdot} + R^{\cdot} \longrightarrow R{-}OO{-}R$$

When an oxidation process occurs, the fatty acid methyl ester generally forms a radical next to the double bond. This radical quickly binds with the oxygen molecule in the air, which is a biradical. This creates peroxide radical. The fast radical destruction cycle starts after that. This peroxide radical promptly forms another radical from the unsaturated fatty methyl ester, which in turn binds with oxygen in the air. At this point of time, the destructive radical auto-oxidation cycle begins. During this process, up to 100 new radicals are made rapidly from one single radical, meaning that decomposition occurs at an exponentially fast rate and results in

formation of a series of by-products. These species shaped during the oxidation process cause the fuel to eventually deteriorate. At last the oil spoils and became rancid very quickly [68]. When oxidation occurs to biodiesel many changes in its properties happens. Properties like density, acid value and peroxide value increase, whereas the iodine value and methyl esters content decrease [69]. Accelerated oxidation of biodiesel additionally brings about an increase in a polymer content that starts the gum and sediment formation. It impacts the corrosion of engine components, through which the fuel comes in contact up to combustion chamber like fuel injector, piston ring, piston liner, etc. Other physico-chemical properties that are sensitive to biodiesel oxidation include cetane number, flash point, refractive index and di-electric constant [70]. The formation of deposits and gum and the darkening of fuels generally happen when biodiesel is kept for long term [71]. Addition of a synthetic antioxidant in biodiesel has a positive role for improving the oxidation stability, but at the same time it increases the cost of fuel. However, in order to reduce the cost, some other fuel which may act as a natural antioxidant can be used.

1.5.3 Ethanol

Ethanol is an oxygenated fuel, produced from fermentation of biological renewable sources such as molasses, sugar cane, or starch. Because of the reduced environmental pollution with ethanol, it is considered as one of the possible fuels for diesel replacement in CI engines. Ethanol was first suggested as an automotive fuel in USA in the 1930s, but was widely used only after 1970. With the rapid expanding production of ethanol and its lower cost relative to fossil fuel in countries such as Brazil, interest in using ethanol as a blending candidate with diesel has naturally occurred.

In India, ethanol is produced from sugarcane molasses for blending with gasoline. In the beginning January 2003, Government of India mandated the use of 5% ethanol blend in gasoline through its ambitious Ethanol Blending Program (EBP) in a number of states. With continuation of this, the Government of India approved the National Policy on Biofuels on December 24, 2009 to promote and encourage the energy generation by using renewable energy resources as alternate fuel to supplement transport petroleum fuels and had proposed an indicative target to replace 20% of petroleum fuel consumption with biofuels [72].

Ethanol can be used with diesel in different techniques. The most used methods are blending [73] and fumigation [74]. In blending method, ethanol is mixed with diesel before injecting inside the cylinder. To stabilize the miscibility of blending ethanol with diesel extra additives are required. Hence there is a limitation on amount of ethanol which can be used for blending operation. Ethanol fumigation has been defined simply as the introduction of ethanol into the intake air up stream of the manifold either by spraying, carbureting or injecting. This method of introduction has the advantage of providing a portion of the total fuel supply premixed with the intake air thus improving air utilization.

The advantages of using ethanol as automotive fuels are that they are renewable and oxygenated, containing by about 35% oxygen. They reduce vehicular emission of HC and CO and eliminate emission of lead, benzene, butadiene etc. [75]. While the calorific value of ethanol is lower than that of gasoline by about 40% it makes up a part by increased efficiency. Blends below 10% of ethanol do not present problems. However, blends above 20% present certain difficulties such as (i) higher aldehyde emissions, (ii) corrosiveness, affecting metallic parts (iii) higher latent heat of vaporization causing starting problem, (iv) higher evaporation losses due to higher vapour pressure and (v) require large fuel tank due to lower calorific value [76]. Ethanol is corrosive in nature, absorbs moisture readily and can affect metallic parts (ferrous/non-ferrous). However with the 10% ethanol blend no compatibility problems have been found.

1.5.4 Diethyl ether

Diethyl ether (DEE) can be produced from renewable feedstock and waste. It is a colorless liquid with high volatility and flammability. DEE is considered to be a low-emission, high quality diesel engine fuel. Its advantages are very high cetane number, reasonable energy density and low auto ignition temperature, with high oxygen content [77]. It has high miscibility with both diesel and biodiesel. When used as a diesel engine fuel, DEE offers significantly reduced CO, HC, NO and PM emissions. But, the limitations of DEE are its high oxygen content, low auto ignition temperature, broad flammability limits, its propensity for peroxidation in storage and its anesthetic effects on human health that raise some concerns. Research also indicates that blending of DEE with diesel also lowers emission and improves

the performance of the engine. It is reported that a 5% blend of DEE with diesel was optimum [78].

1.6 Liquid fuels derived from other organic substances

1.6.1 Tyre pyrolysis oil

The number of waste automobile tyres in the world increases every year, due to the increase in the vehicle population. It is estimated that about 2-3 billion ton waste automobile tyres are disposed annually in the world [79]. The waste automobile tyres are majorly disposed from the USA, Europium countries, Australia, Japan, China and India. The waste tyre is composed of rubber, chemicals, steel wire, fabrics and cotton. The accumulation of the waste automobile tyres causes a severe environmental problem and also contaminates the soil and reducing its fertility. The burning of automobile tyres is toxic and harmful to the human being, and therefore it is banned in most of the countries in the world. The anthropogenic gases rising from the disposal area is one of the reasons for the greenhouse gas (GHG) [80]. Therefore, it is very much essential to dispose the waste tyres in an efficient way with safety. The possible solution is pyrolysis and gasification.

Pyrolysis process is one of the thermochemical methods to convert the waste automobile tyres into useful energy. Several researchers have demonstrated the pyrolysis process for converting carbonaceous such as automobile tyres, rubber, agro waste, plastic etc. It is a simple technique to convert scrap tyres in to value added products. In the pyrolysis process, long chain polymers are thermally broken down at high temperatures (300-900 ˚C) into smaller hydrocarbon in the oxygen free environment. There have been several fundamental documented studies on the pyrolysis of waste automobile tyres. The research includes methods of pyrolysis (i.e. vacuum pyrolysis, flash pyrolysis, fluidized bed). Different operating parameters such as the heating rate, reactor temperature and reactor design have been examined [81]. Different types of tyres have also been investigated in the recent past for a better yield of value added products. Some of the researchers have investigated the type of reactors such as fixed-bed (batch), screw kiln, rotary kiln, rotating cone, vortex centrifuge, vacuum and fluidised-bed etc. A few catalysts (CaO, $Ca(OH)_2$) were also tried, for higher production of liquid pyrolysis oil [82].

The products from pyrolysis of waste automobile tyres yields three value added products; tyre pyrolysis oil (TPO), pyrogas and carbon black. The TPO a dark-brown liquid can be a potential alternative fuel for CI engines, but the main drawback is its lower cetane number, which is in the range of 25-30. The production of pyrolysis oil from waste automobile tyres has gained momentum in the last few years across the world. In recent years, a significant number of pilot plants have been installed with the production capacity in the range of 5-20 tons in the countries, such as China, India, Canada, France, Italy and Spain.

1.6.2 Waste plastic oil

Plastics are produced from petroleum derivatives and are composed primarily of hydrocarbons, but also contain additives such as antioxidants, colorants, and other stabilizers. Plastics are classified in to two types; (i) Thermoplastics and (ii) Thermosetting. After use, the plastics are decomposed in large quantity. Recycling of some of the selected plastics is possible which can yield energy, fuel and chemical. Different type of plastic that can be converted into energy, fuel and chemicals are polyethylene terephthalate (PET), polyethylene (PE), polypropylene (PP), polystyrene (PS), high density polyethylene (HDPE), low density polyethylene (LDPE), polyvinyl chloride (PVC) etc. Thermochemical methods such as pyrolysis and gasification are used to convert waste plastic into energy, fuels and value added chemicals. Research investigations have been conducted on the use of plastic oil in diesel engines [83].

Although numerous research works have been done in the advancements of plastic conversion into useful products, some of the issues need to solve. One potential problem identified in pyrolysis of waste plastic is the formation of chlorine compounds, especially hydrochloric acid during pyrolysis [84]. This causes corrosion to the pyrolysis equipment, as well as lowering the viability of the liquid product to be used as a fuel [85]. Some researchers have been able to remove chlorine to some extent by dechlorination methods. Many research works has been carriedout done by blending oil obtained by waste plastic with heavy oil for marine applications. The results showed that waste plastic oil when mixed with heavy oils reduces the viscosity significantly and improves the engine performance. However, very little work has been done to test their use in high-speed diesel engines [86].

1.6.3 Bio-oil

When a biomass material is subjected to pyrolysis, three principal products are obtained from the biomass i.e. bio-oil (liquid), pyro gas (gas), and char (solid). In pyrolysis process, the biomass-particularly solid or liquid is fed into a reactor which is indirectly heated up. During heating, the vapours evolved from the reactor are condensed in a condenser, preferably water cooled.

Bio-oil is a high density oxygenated liquid that can be used as a replacement for fossil fuels in some applications. But, the physical and chemical properties of bio-oils are very different to mineral diesel. The bio-oil has high oxygen content and moisture content, but poor volatility, high viscosity, corrosiveness and cold flow properties which limit its use as additives in transportation fuel, rather than being used as transportation fuel by itself [87]. It can be used in diesel engines, turbines or boilers. In the last decades, bio-oil derived from the fast pyrolysis of different biomass species has been proposed as an appealing alternative to the use of diesel fuel in automobiles. The investigations on the use of bio oil in diesel engines were carriedout by many researchers. Some of the common problems associated with the use of bio-oil in diesel engines are (i) difficulty in starting the engine, both injection duration and ignition delay parameters were higher, higher fuel consumption, CO and PM emission than diesel operation [88-89].

1.6.4 Waste lubricating oil

Waste lubricant oil is one of the most important sources which can be converted as a useful fuel for engine applications. It gradually loses its lubricant properties, and the oil absorbs many dust and metal particles from the engine block, due to the extreme conditions encountered. As there are inorganic matters such as lead, copper and halogens (C1, F, Br, and so on) in the structure of these oils, it cannot be used as an engine fuel without purification and being converted into the fuel to be used in order to minimize the harmful effects on living beings and environment. These effects can be eliminated when they are purified, and then converted into fuels. The waste lubricant oil is processed and refined by various steps to eliminate the impurities involve in the structure of these oils and used as an extenders of diesel fuel by many researchers [90-91].

1.6.5 Used transformer oil

A significant quantity of used transformer oil is disposed of annually in the world. The used transformer oil is considered as a poorly biodegradable. The problem associated with used transformer oil is that it affects soil and waterways. Government regulatory agents have already initiated to solve this, issue and are imposing penalties for spills. The effective utilization used transformer oil may reduce environmental problems rather disposing it in the open land. Recently the suitability of used transformer oil as an alternative fuel was examined [92]. In that research work, different blends of used transformer oil and diesel were used as alternative fuels in a single cylinder, four stroke, air cooled, direct injection diesel engine. The blend percentage was varied from 10-60% at a regular interval of 10% on volume basis. They reported the increase in BTE with reduction of smoke opacity for used transformer oil and its diesel blends compared to diesel. The NO emission was higher for used transformer oil and its diesel blends than that of diesel. Further, the authors conducted experiments with different injection timing, nozzle opening pressure, compression ratio and dual fuel mode for improving the performance of the engine fueled with used transformer oil and its diesel blends [93].

1.7 Present investigation

In this research study, possibility of replacing biodiesel by some other non-conventional fuel and solving some of the problems associated with biodiesel stability were explored. The complete review of literature and the objectives of the research work are given at the end of Chapter 2 Literature review.

1.8 Thesis outline

The remainder of this thesis is organized as follows:

Chapter 2

This chapter provides a detailed review of research works that were carriedout on utilization of Jatropha methyl ester in CI engines. The review particularly relates the assessment of combustion, performance and emission parameters of different CI engines that was run on JME with fuel and engine modification. The review also provides few literatures on oxidation stability of biodiesel. Further, this chapter also presents the application of tyre pyrolysis oil in CI engines.

Chapter 3

This chapter includes a description of the raw materials involved in the production of JME and tyre pyrolysis oil (TPO). It presents the details of characterization of the test fuels considered in this study.

Chapter 4

This chapter describes the experimental apparatus used in this research study. It also provides necessary information on different instruments used, their working principle, instrumental accuracy and procedure of the engine test experiments. In addition to this, this chapter also addresses about step by step procedure for VIKOR optimization technique to determine best blend.

Chapter 5

This chapter provides the results and discussion of the experimental results that were obtained for the combustion, performance and emission from running a single cylinder, four stroke, air cooled, DI diesel engine on diesel, JME and JMETPO blends with and without engine and fuel modification. This chapter also discusses about the selection of optimum blend based on VIKOR optimization technique.

Chapter 6

This chapter presents the conclusion and the possible extension of this work.

.

Chapter 2

Literature Review

2.1 General

As mentioned earlier in the Introduction chapter, Jatropha oil is considered as one of the potential feedstocks for the biodiesel production in India. Therefore, the researcher has developed interest to carryout this research work in the area of utilization of Jatropha methyl ester (JME) and reviewed various research articles in the area of biodiesel utilization in compression ignition (CI) engines. This chapter presents the review of research works related to the study of the of combustion, performance and emission parameters of the CI engines run on JME by adopting different fuel and engine modification techniques. Further, the chapter presents the critical review of the problems associated with biodiesel and the solutions arrived to overcome these problems. As the proposed research work is aimed to use a non-conventional fuel with biodiesel and to investigate on the stability issues of biodiesel, the possible methods to solve those problems are also reviewed and presented.

2.2 Jatropha methyl ester fueled diesel engine

Various alternative fuels for CI engines have been explored by many researchers over the past few decades. Among the various possibilities, biodiesel from vegetable oils, animal fats and algae was proposed as a potential liquid alternative fuel by several researchers around the world, because it is renewable, oxygenated biodegradable, non-toxic, and environment friendly. In India owing to food security use of vegetable oils for production of biodiesel has not been encouraged. Therefore, several researchers in India have tried different non-edible feedstocks such as Jatropha curcas, Pongamia pinnata, Madhuca indica and Linseed etc. for the production of biodiesel. Among these non-edible seeds produced in India, Jatropha is the most preferred because of its high oil content and biodiesel yield. The merit of JME depends on the feedstock quality, chemical composition of feedstock, method of tranesterification process, type of catalyst used, storage and handling process etc. The simplest method of using JME as an alternative fuel in a CI engine is blending with diesel or some other fuels. In recent years, investigations have been carried out worldwide by several researchers for evaluating

the engine combustion, performance and emission characteristics of diesel engine run on the JME and its blends. It was found that 20% JME blended with 80% diesel fuel (B20) exhibits acceptable performance and emission with that of diesel, when it is used in a conventional diesel engine. Table 2.1 presents the summary of the review on the combustion, performance, and emission parameters of diesel engines fueled with the JME and its blends with diesel in different test conditions reported by the researchers. It is understood from the Table 2.1 that the JME fueled engine gives high thermal efficiency with high fuel consumption as the JME percentage increases in the blend. However, in some cases it also exhibits low thermal efficiency than diesel. It has been reported that, the JME fueled engine reduces carbon monoxide (CO), hydrocarbon (HC) and particulate matter (PM) emissions; however nitric oxide (NO) emission is increased than the diesel fuel operation. Several techniques like retarded fuel injection timing, addition of antioxidant or blending of a fuel of more saturated fatty acid with JME are employed for reducing NO emission from CI engines.

The problems associated with biodiesel are its high viscosity and auto ignition temperature compared to that of diesel. To minimize these drawbacks as well as to increase the fuel bound oxygen (to enhance the combustion process) and to keep lubricity at reasonable levels, oxygenated additives such as n-butanol and diethyl ether (DEE) are generally added in a small quantity. The n-butanol and ethanol have emerged as a potential oxygenated additive to improve the fuel properties of both diesel and biodiesels. Table 2.2 presents the summary of the review on the combustion, performance and emission parameters of diesel engine fueled with the JME and its blends with alcohols/biodiesel (obtained from other feedstock) etc. documented by the researchers. It may be mentioned that, the standard design of a diesel engine is not suitable for a fuel of a different origin. For other fuels, certain operating parameters of the engine have to be optimized, in view of the combustion, performance and emission characteristics. It is important to note that, the engine behaviour is predominantly affected by the fuel-air mixture supplied to the diesel engine, fuel injection rate, injection timing (IT), nozzle opening pressure, nozzle geometry, compression ratio (CR) and design of combustion chamber etc. Numerous research works have been documented on the optimum design parameters such as for CI engines run on JME and its blends. The studies related to the effect of engine modifications on the combustion, performance and emission behaviour of a CI engine fueled with the JME and its blends in the recent past are summarized in Table 2.3.

Table 2.1 Review on the engine combustion, performance and emission results obtained from diesel engine fueled with JME and its blends with diesel

***** Where XXX indicates percentage of JME blended with diesel.

Code used: BP = Brake power; BTE = Brake thermal efficiency; BSFC= Brake specific fuel consumption; BSEC = Brake specific energy consumption; EGT = Exhaust gas temperature; P_{max} = Maximum cylinder pressure; ID = Ignition delay; CA = Crank angle; CD = Combustion duration; ROPR = Rate of pressure rise; HRR = Heat release rate; PM = Particulate matter

Table 2.2 Review on the engine combustion, performance and emission results obtained from diesel engine when JME is blended with alcohols/biodiesel obtained from other feedstock

Table 2.3 Summary on the effect of modification of various engine parameters on diesel engine behavior fueled with JME and its blends

***** Where XXX indicates percentage of JME blended with diesel.

Code used: IT= Injection timing; IP=Injection pressure; CR= Compression ratio BP = Brake power; BTE = Brake thermal efficiency; BSFC= Brake specific fuel consumption; BSEC = Brake specific energy consumption; EGT = Exhaust gas temperature; P_{max} = Maximum cylinder pressure; ID = Ignition delay; CA = Crank angle; CD = Combustion duration; ROPR = Rate of pressure rise; HRR = Heat release rate; PM = Particulate matter

2.3 Oxidation stability of Jatropha methyl ester

The problems associated with the storage and utilization of biodiesel has already been discussed in the Introduction section. The research works related to these problems are discussed below.

The most commonly used chain breaking antioxidants for improving oxidation stability are classified in phenolic and amine types. Many research articles have been published related to the long term storage of biodiesel and to improve its oxidation stability by adding these two types. The examples of such antioxidants used in those studies were butylated hydroxytoluene (BHT), 4-allyl-2,6-dimethoxyphenol, tert-butyl hydroquinone (TBHQ), butylated hydroxyanisole (BHA), 4-methyl-6-tert-butyphenol (MBEBP), propyl gallate (PG), and pyrogallol (PY) etc. [150-152].

Jain et al. [153] have investigated the effect of adding five antioxidants with the JME and its blend on the oxidation stability and PY was found to be the best antioxidant among the five. The concentration of antioxidants used were from 50 to 600 ppm and it was found in optimum case that the amount of PY antioxidant required for the JME was around 100 ppm, while it was around 50 ppm for the B30 blend to obtain the oxidation stability as per EN 14112 specification.

Sarin et al. [154] have examined four phenolic antioxidants (BHT, bis-2,6-ditertairybutyl phenol derivative, mixed butylated phenol and octylated butylated diphenyl amine) in their study to improve the oxidation stability of JME and BHT with a concentration of 200 ppm was found as the most effective antioxidant. Further, the authors blended palm oil biodiesel by 20% 40%, 50%, 60%, and 80% on a volume basis with the JME, and reported that 60% of palm biodiesel could be blended with the JME to obtain a better oxidation stability of it as per EN 14112. The authors have reported that, by blending palm biodiesel into JME, the oxidation stability of the blend enhanced. The reason was the presence of more saturated fatty acid esters in palm biodiesel. The effect of antioxidants on biodiesel varies from biodiesel to biodiesel, as different feedstock is used for biodiesel production, and also the presence of fatty acid ester composition varies for different biodiesels. The same authors [155] also studied the effect of metal contaminants on the oxidation stability of JME, and reported that induction

period reduced significantly even with the presence of small concentrations (ppm) of metal contaminants. The oxidation stability of metal contaminated JME was reported to increase with increase in amount of phenolic antioxidant 2,6-ditertiarybutyl hydroxytoluene. In order to meet the oxidation stability as per EN-14112 specification of iron and nickel contaminated JME, and manganese contaminated JME, the minimum amount of antioxidant was required by about 500 ppm and 700 ppm respectively. Also, for cobalt and copper contaminated JME, minimum concentration of 900 ppm and 1000 ppm respectively were required to meet as per EN-14112 specifications.

As a continuation of previous study, Sarin et al. [156] have studied the synergistic effect of both metal deactivators as well as synthetic antioxidants on metal contaminated JME sample. They found, when 5 ppm and 10 ppm of metal deactivator was blended with BHT to enhance the IP of JME to meet EN-14112 specification, there was reduction of usage of minimum of 200 ppm and 250 ppm of BHT for iron, nickel and manganese contaminated JME, and 300 ppm and 350 ppm of BHT for cobalt and copper contaminated JME respectively. Finally they concluded that, there could be an effective reduction of using antioxidants by doping small amount of the metal deactivators in the metal contaminated biodiesel.

Varatharajan et al. [157] have studied the effect of antioxidants on the NO emission of JME containing 0.025%-m of the additives p-phenylenediamine, ethylenediamine, L-ascorbic acid, a-tocopherol acetate, and BHT from a single-cylinder diesel engine at full load. The test results showed that p-phenylenediamine produced a mean reduction in NO of 43.55% compared to that of 100% biodiesel. However, the addition of antioxidants increased HC and CO emissions compared to that of 100% biodiesel at full load. The reason mentioned for this reduction was possibly due to the suppression of free radical formation by antioxidants.

Addition of a synthetic antioxidant in biodiesel has a positive role for improving the oxidation stability, but at the same time, it increases the cost of fuel. However, in order to reduce the cost, some other fuel which may act as natural antioxidants can be used. For this purpose, Sarin et al [158] have further more conducted a study on determining the effect of blending of some other biodiesel with the JME to improve the oxidation stability. They have found that the oxidation stability of JME, Pongamia and Palm oil methyl ester were 3.95 h, 2.54 h and

9.24 h respectively. They also reported that the minimum amount of 40% (by weight) palm oil methyl ester was required to be blended with neat JME to get the oxidation stability of as per EN-14112 specification.

In another study by Chen et al. [159], the JME was blended with palm oil methyl ester (PME) and soybean oil methyl ester (SME) in different proportions to improve the oxidation stability. They found that the oxidation stability of the JMEPME blend could be more than 6 h when the PME contained 60 wt.% or higher in the blend and it was due to the result of an increased saturated fatty acid methyl ester in the blend. There was no major improvement noticed in oxidation stability, while the SME was blended with the JME. Further the authors have added a few antioxidants such as α-T, BHA, BHT, DTBHQ (2,5-di-tert-butyl-hydroquinone), Ethanox 4760E, MBMTBP (2,20-methylene-bis-(4-methyl-6- tert-butylphenol)), PDA (N,N'-di-sec-butyl-p-phenylenediamine), PG, PY (pyrogallol), and TBHQ to improve the oxidation stability of JME. The authors have reported the effectiveness of the antioxidants at improving the oxidation stability of the JME was found to be in the order of PY >PG>Ethanox 4760E > PDA > MBMTBP > BHT > TBHQ>BHT > DTBHQ > a-tocopherol and the concentration of 100 to 250 ppm PY antioxidant to JME was suggested to meet the desired oxidation stability as per EN-14112 specification.

2.4 Tyre pyrolysis oil-A source of natural antioxidant

It is reported that phenols or phenolic compounds presents in any form may improve the oxidation stability of biodiesel. One example of such substance in which phenol or phenolic compound present is pyrolysis oil derived from biomass, waste tyre or plastic.

The tyre pyrolysis oil (TPO) consists of C, H, O, N and S containing organic compounds and water. It is a mixture of organic compounds range from C_5 to C_{20} with different proportions of aliphatic and aromatic. It is important to note that the TPO also contains some phenolic compounds which would be favorable to improve the oxidation stability of biodiesel, and to reduce the oxides of nitrogen. The TPO contains fractions of volatility consistent with gasoline, kerosene and diesel. These fractions cannot be separated because of their proximate boiling points [160]. As a result, the TPO was tried as an alternative fuel in both spark ignition (SI) engines and compression ignition (CI) engines, with or without fuel modification

and only a few documents are available for reference. The solid carbon black can be used in industrial application such as re-treading, coating of insulation and industrial filters.

Only a limited number of studies have been previously performed to investigate the effects of the TPO-diesel blends on the engine performance and emissions as an alternative fuel for diesel engines. Preliminary research investigations by Murugan et al. [161] have studied the effects of lower and higher percentage of the TPO-diesel blends on the combustion, performance and emissions characteristics of a single cylinder, four stroke, water cooled, DI diesel engine, running at 1500 rpm. They have reported that the BTE of the engine was only marginally influenced by the use of the TPO-diesel blends compared to using diesel alone at blends of 10% (TPO10), 30% (TPO30) and 50% (TPO50) of TPO with diesel. They have also reported that, there was no seizing of the engine or injector nozzle blocking with the use of these blends. The HC emissions were significantly increased by 15% and 21% when TPO30 and TPO50 blends respectively were used under full load conditions compared to that of diesel. This was attributed to the higher concentration of PAH in TPO compared to that of diesel. In addition, NO emissions were found to be 4.5% and 10% higher for the TPO30 and TPO50 blends respectively compared to that of diesel under full load conditions. The smoke emission was increased by 7% compared to diesel when the TPO50 blend was used at full load. In addition of this, they reported that the maximum cylinder pressure (P_{max}), ignition delay (ID), heat release rate (HRR) and rate of pressure rise (ROPR) of the engine fueled with these blends increased with an increase in TPO concentration in the blend. The reason for this was mention the higher viscosity and poor volatility of the TPO-diesel blends. In their further investigation it was found that the maximum volume of the TPO which could be blended with diesel was found to be 70% and beyond this engine was not able to run [162].

Murugan et al. [163] have also studied the influence of the distillation process on raw TPO properties and the engine combustion, performance and emission behaviour were performed in a DI diesel engine by using TPO30 blend and 30% distilled TPO blended with 70% diesel (DTPO30). The distillation process improved the fuel properties of crude TPO, and the engine test results showed that, the engine performance and emissions improved considerably. The test results indicated that NO was reduced by about 8% compared to TPO30 and by about 10% compared to diesel. The HC emission was reduced by about 2% compared to TPO30.

The CO and smoke emissions were found to be increased for DTPO30 compared to those of TPO30 and diesel. In their further extensive investigation [163-165] by using distilled TPO-diesel blends they found that the engine could not operate satisfactorily on 100% distilled TPO, but could at a blend of 90% distilled TPO and 10% diesel. A small (2%) reduction in BTE and an 11% increase in HC emission were observed, but an 18% decrease in NO was reported at peak load using a blend of 90% distilled TPO compared to that of diesel operation. However, there was a marked increase in the smoke emission compared to that of diesel.

In another work [166] by the same authors, the experimental investigation was carried out on a single cylinder, four stroke, direct injection diesel engine, with a dual fuel mode to study the effect of an ignition improver. Stable engine operation was observed when ignition improver was used. Di ethyl ether (DEE) was used as an ignition improver, which was admitted at three different flow rates (65, 130 and 170 g/h). The peak pressure for TPO–DEE with 130 g/h flow rate was higher by about 3 bar whereas ID was longer by about 2.8 ˚CA than diesel at full load. In addition of this the BTE was decreased by 2.5% than diesel while the HC, CO and smoke emissions were increased by about 2%, 4.5% and 38% respectively.

Dogan et al. [167] have investigated the effect of different TPO-diesel blends on performance and emission characteristics of a DI diesel engine at full load and different engine speeds (1400, 2000, 2600 and 3200 rpm). The authors have reported that blending of refined and desulfurized TPO with diesel does not have a substantial influence on the engine output torque, the engine power, BSEC and BTE with respect to those of the diesel fuel. The author also concluded that smoke opacity, CO and HC emissions decreased, while NO emission increased as TPO content increased in the blend, but the results were very sensitive to the operating modes tested. Finally author made conclusion of their study that, the TPO-diesel blends can be used in diesel engines without significant loss in engine performance up to 70% TPO blended with diesel while improving some engine emissions, especially for smoke opacity, CO and HC emissions.

Frigo et al. [168] have carriedout a preliminary engine investigation on a single-cylinder diesel engine run on two TPO-diesel (TPO blended by 20% and 40% with diesel) blend at different loads (50%, 75% and 100%) and engine speeds (2000, 2500 and 3000 rpm). They

observed, at 3000 rpm a reduction on both HC and NO emissions, whereas CO emissions increased as TPO increased in the blend. The results mentioned that, engine ran satisfactorily without occurring any mechanical problem during experiment and no significant carbon deposit was found on the combustion chamber and on the piston in the final engine examination.

Martinez et al. [169] have investigated the performance and emissions of a 4-cylinder, four stroke, turbocharged, intercooled, 2.0 L Nissan diesel automotive engine with common-rail injection system by using TPO5 (5% TPO blended with diesel) blend. The blend did not show any significant changes on the combustion parameters; just marginally longer combustion duration with the TPO blend was observed. Both the BSFC and BTE seemed to be deteriorated at low engine load, while at higher engine load the values of these parameters were almost equal to diesel. The HC emission for the blend was higher at low engine load, but similar to that of diesel when the engine load increased. In addition, TPO5 led to higher smoke opacity respect to those found for diesel in all operating modes. The authors suggested that, the liquid fuel converted from pyrolysis of waste tyres could be used in automotive engines, and also this helps for converting waste into useful product.

2.5 Knowledge Gap and Motivation for the Present Investigation

The literature survey presented above reveals following knowledge gap in earlier investigations that help to set the objectives of this research work:

- Reports are available in the literature on the studies of combustion, performance and emission characteristics of diesel engine fueled with TPO-diesel blend; but there exists hardly any report on utilization of TPO blended with other than diesel.
- The main drawback of TPO is its lower cetane number, which is in the range of 25-30. TPO can not be used as a sole fuel in diesel engine. This problem can be solved by blending TPO with fuels of high cetane number.
- A lot of research works have been carried out in the past using JME and its blends with diesel. But no attempt has so far been reported on the utilization of blends of Jatropha methyl ester- tyre pyrolysis oil in diesel engines.
- Evaluation of suitable blend is based on the exploratory analysis of the performance, emission and combustion parameters of the single cylinder, constant speed direct

injection (DI) diesel engine at different load conditions. Besides, there are only a few reports available on implementation of a hybrid multi-criteria decision modelling approach for the prediction of optimum blend.

- The oxidation stability of JME is lower than mineral diesel. Addition of a synthetic antioxidant in biodiesel has a positive role for improving the oxidation stability, but at the same time it increases the cost of fuel. However, in order to reduce the cost, some other fuel which may act as natural antioxidants can be used. The TPO derived from the pyrolysis of waste automobile tyres contains a few phenolic compounds in it which may act like antioxidants.

2.6 Objectives of the present research

The main objective of the present investigation is to replace diesel fuel completely by a non-petroleum fuel. For this purpose, one renewable fuel and one non- conventional fuel were used for this investigation. The renewable fuel is JME which is derived from Jatropha oil and the non-conventional fuel is TPO.

The specific objectives of the present investigation are as follows:

(i) To evaluate the behaviour in terms of the combustion, performance and emission characteristics of a single cylinder, DI diesel engine, run on a non-petroleum fuel; i.e. JMETPO blends and comparisons of those results with diesel and JME operation.

(ii) To find the optimum JMETPO blend by using a hybrid multi-criteria decision modelling approach; VlseKriterijumska Optimizacija I Kompromisno Resenje (in Serbian) (VIKOR) analysis with experimentally measured combustion, performance and emission parameters.

(iii) To study the effect of injection timing on the combustion, performance and emission parameters of engine fueled with optimum blend and find the optimum injection timing.

(iv) To study the effect of nozzle opening pressure on the combustion, performance and emission parameters of engine fueled with optimum blend and find the optimum nozzle opening pressure.

(v) To study the effect of compression ratio on the combustion, performance and emission parameters of engine fueled with optimum blend and find the compression ratio.

(vi) To study the effect of blending TPO with JME on oxidation stability and also evaluate the behaviour of the diesel engine run on the optimum blend, with and without synthetic antioxidants.

(vii) Durability analysis of single cylinder DI diesel engine operating with the JMETPO20 blend.

Chapter 3

Production and Characterization of Fuels

3.1 General

This chapter provides a description of Jatropha oil as a feedstock for biodiesel production, transesterification process, and then parameters affecting the transesterification process. Further, the information about the waste tyre as a potential feedstock for pyrolysis process, details about pyrolysis process, and characterization of tyre pyrolysis oil (TPO) are described in this chapter. Furthermore, the characterization of the test fuels using advanced instruments such as FTIR, GC-MS is presented. In addition to these, the chapter also presents the physico-chemical properties of the test fuels used in this study.

3.2 Jatropha methyl ester production

For the present investigation, Jatropha oil was selected as a raw material for the production of Jatropha methyl ester (JME). The photograph of Jatropha oil is shown in Figure 3.1.

Fig. 3.1 Photograph of Jatropha oil

The fatty acid compounds present in Jatropha oil are given in Table 3.1. Transesterification is the method of biodiesel production from vegetable oils and fats. Transesterification is a well-defined chemical process where mono-alkyl esters are produced by the reaction of triglyceride

with an alcohol [170]. The glycerol is a common by-product that is formed during the transesterification process. These mono-alkyl esters are normally referred to as biodiesel.

Table 3.1 Fatty acid composition of Jatropha oil

Fatty acid	Structure	Formula	Composition (% wt)
Palmitic	16:0	$C_{16}H_{32}O_2$	14.1–15.3
Stearic	18:0	$C_{18}H_{36}O_2$	3.7–9.8
Oleic	18:1	$C_{18}H_{34}O_2$	34.3–45.8
Linoleic	18:2	$C_{18}H_{32}O_2$	29–44.2

The tranesterification process for the production of JME is given in Figure 3.2. The optimal inputs for the transesterification of Jatropha oil are identified to be 40% methanol and 1.0% NaOH. The maximum ester yield is achieved after 90 min reaction time at 60^{o}C. The photograph of the JME is shown in Figure 3.3.

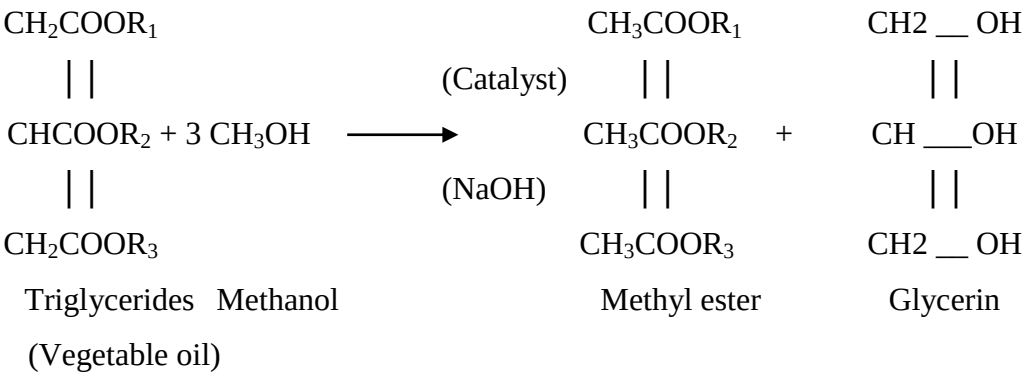

Fig. 3.2 Schematic diagram of the transesterification process

After the process of transesterification, biodiesel offers properties closer to mineral diesel. The most important advantage, the kinematic viscosity is reduced to almost the same level as diesel. The cetane number and the calorific value are also improved.

Fig. 3.3 Photograph of Jatropha methyl ester

Countries like Germany, Italy, France, USA, etc., have developed their own biodiesel standards. However, for India IS: 15607 are followed as a standard for the biodiesel production. All above stated standards are reported in Table 3.2, which shows the limiting values of some of the properties of JME in ASTM and IS: 15607 standard [171]. The limiting value of carbon residue is almost same for the entire above standards. Among the general parameters for biodiesel, the viscosity is one of the important parameters which affect the spray formation when biodiesel is injected in a diesel engine. The viscosity of fatty acid methyl ester can reach very high levels, and hence it is important to control it within the acceptable levels to avoid negative impacts on a fuel injector system performance. Therefore, the viscosity specifications proposed are nearly same as that of the diesel fuel.

Table 3.2 Physico-chemical properties of biodiesel as per ASTM and IS standard

Property (units)	ASTM D- 6751 test methods	ASTM D-6751 limits	IS -15607 test methods	IS- 15607 limits
Kinematic viscosity at 40 ˚C (cSt)	D -445	1.9-6	IS 1448 P:25	2.5-6
Calorific value (MJ/kg)	D -4809	-		
Flash point (˚C)	D -93	Min. 130	IS 1448 P:21	Min 120
Fire point (˚C)	D -93			
Cetane number	D- 613	Min. 47	IS 1448 P:9	Min. 51
Sulfur (% mass)	D-5453	Max 0.05	D-5453	Max 0.05
Neutralization value (mgKOH/g)	D- 664	Max 0.80	IS 1448 P:1	Max 0.5
Free glycerin (% mass)	D -6584	Max 0.02	D -6584	Max 0.02
Total glycerin (% mass)	D -6584	Max 0.24	D -6584	Max 0.24
Oxidation stability of biodiesel at 110 ˚C (h)	EN 14112	3	EN 14112	Min. 6

3.3 Production of tyre pyrolysis oil

In this investigation, tyre pyrolysis oil (TPO) was obtained from a pilot pyrolysis plant situated at Rourkela, India. The detailed production process of TPO and its characterization are described below.

3.3.1 Pyrolysis process

Pyrolysis is a thermochemical decomposition of organic material by heating them in the absence of oxygen; the process is carriedout at near atmospheric pressure and in the temperature range between 300 and 600 °C [172]. In the pyrolysis process, long chain polymers are thermally broken down into smaller hydrocarbon in the oxygen free environment. Pyrolysis, the thermal fragmentation of waste tyres in the absence of air, produces three principal yields i.e. the tyre pyrolysis oil (TPO), carbon black (solid residue) and the remaining fraction as non-condensable gases mainly CO, CO_2, H_2, and CH_4 etc. in varying proportions [173]. The oil may be used directly as a fuel, added to petroleum refinery stocks, upgraded using catalysts to a premium grade fuel or used as a chemical feedstock. The gases from pyrolysis of waste tyres are typically composed of C_1-C_4 hydrocarbons and hydrogen with a high calorific value, of sufficient energy content to act as fuel to provide the heat for the pyrolysis process. The solid char consists of the carbon black filler and also char produced during the pyrolysis of the rubber. It may be used as a solid fuel, as carbon black or upgraded to produce an activated carbon.

A different variety of reactors, such as fixed-bed (batch), screw kiln, rotating cone, vacuum, spouted and fluidized bed have been used for pyrolysis of waste tyres [174]. The fixed bed, batch reactors have been widely used to investigate pyrolysis of waste tyres. The reactor is typically heated externally by an electric furnace, and nitrogen or another inert gas is used as a carrier gas. All these reactors/configurations have advantages and disadvantages in terms of technical, economical and ecological parameters and are used for different energy applications such as distributed heat or electricity generation and for the production of liquid fuels and char.

There are many classifications of types of pyrolysis depending on the operating conditions, such as the heating rate, the volatiles residence time and the temperature, but mainly there are two pyrolysis techniques i.e. slow and fast (also called as flash, and carriedout at higher heating rates and shorter vapour residence times than the fast pyrolysis) [175]. This technique is characterized by slow heating rates, relatively long residence times of solid and vapour, and usually a lower reaction temperature than fast pyrolysis. On the other hand, fast pyrolysis is characterized by high heating rates and short residence times. Fast pyrolysis generally

requires the feedstock to be supplied as fine particles; and the reactor design must facilitate rapid removal of the hot vapours from the presence of the hot solids. Pyrolysis process can be also classified on the basis of the environment used such as oxidative pyrolysis, hydro-pyrolysis, steam-pyrolysis, catalytic-pyrolysis and vacuum pyrolysis, and also depending on the heater system as the microwave or plasma pyrolysis [176].

In the present study the TPO was collected from a tyre pyrolysis plant of capacity five ton per batch. The feedstock used in the plant was waste automobile tyres. The composition of the waste automobile tyres used as a feedstock in the plant is given in Table 3.3.

Table 3.3 Composition of waste automobile tyres

Compound	(wt.%)
Natural Rubber	28
Synthetic Rubber	16
carbon Black	29.5
Metal	14.5
Other Additives	12

The proximate analysis of any fuel gives its amount of moisture, volatile matter, fixed carbon and ash. The proximate and elemental analysis of the waste automobile tyres used in the plant is shown in Table 3.4. Figure 3.4 shows the photographic views of raw material for pyrolysis, pyrolysis reactor and the products obtained from the pyrolysis process.

Table 3.4 Proximate and elemental analysis of the waste truck tyre

Proximate analysis (wt %)	**Ultimate analysis (wt %)**
Volatile matter: 66.64	Carbon: 83.87
Fixed carbon: 27.96	Hydrogen: 7.09
Moisture content: 0.62	Oxygen: 2.17
Ash content: 4.78	Nitrogen : 0.24
	Sulphur: 1.23
	Moisture: 0.62
	Ash: 4.78
Total: 100	100

The reactor used in the pyrolysis unit was of a horizontal and rotating type. The temperature rise of the reactor was maintained between 30-40˚C/h. The highest temperature of pyrolysis was 550˚C at which maximum yield of oil was obtained. The automobile tyre was cut into a number of pieces and the bead, steel wires and fabrics were removed. The thick rubber at the

periphery of the tyre was alone made into small chips. The tyre chips were washed, dried and fed into the pyrolysis reactor unit.

Fig. 3.4 Photographs of the tyre pyrolysis plant and its end products

The pyrolysis reactor used was a fully insulated chamber. Inert environment was created in the pyrolysis reactor by supplying nitrogen from a cylinder, and then externally heated by means of a heater. A temperature controller was used to control the temperature of the reactor. The products of pyrolysis in the form of vapour were sent to a water cooled condenser, and the condensed liquid was collected as pyrolytic oil. The oil was drained through the outlet of the oil collection tank. The non-condensable gases were collected in a gas bag, weighed, and then released to atmosphere. The TPO collected was crude in nature. Approximate yields from the process were 50 wt% TPO, 40 wt% gases and 10 wt% char. The electricity charges incurred in Indian currency for the production of 50000 litres of TPO per month is approximately Rs.8000.

3.3.2 Characterization of tyre pyrolysis oil

The recovered TPO is a dark-brown/black coloured liquid which resemble petroleum fractions. The TPO was characterized by Fourier transform infrared (FTIR) spectroscopy, gas chromatography with flame ionization detection (GC-FID) and gas chromatography-mass spectrometry (GC-MS). The elemental compositions, H/C atomic ratios and gross calorific values (GCV) of the TPO are presented in this section.

3.3.3 Identification of group compounds by FTIR

The Fourier Transform Infrared (FTIR) spectroscopy is a very useful technique for identifying functional groups and types of bonds in a molecule [177]. This technique allows not only a qualitative analysis but also a semi-quantitative analysis based on area of the absorption bands appearing at specific wavenumbers in the spectra. Nevertheless, it allows functional group analysis and characterizing covalent bonding formation to reveal the chemical properties of the liquids. Figure 3.5 shows the working principle of a FTIR spectrometer and the description is given below.

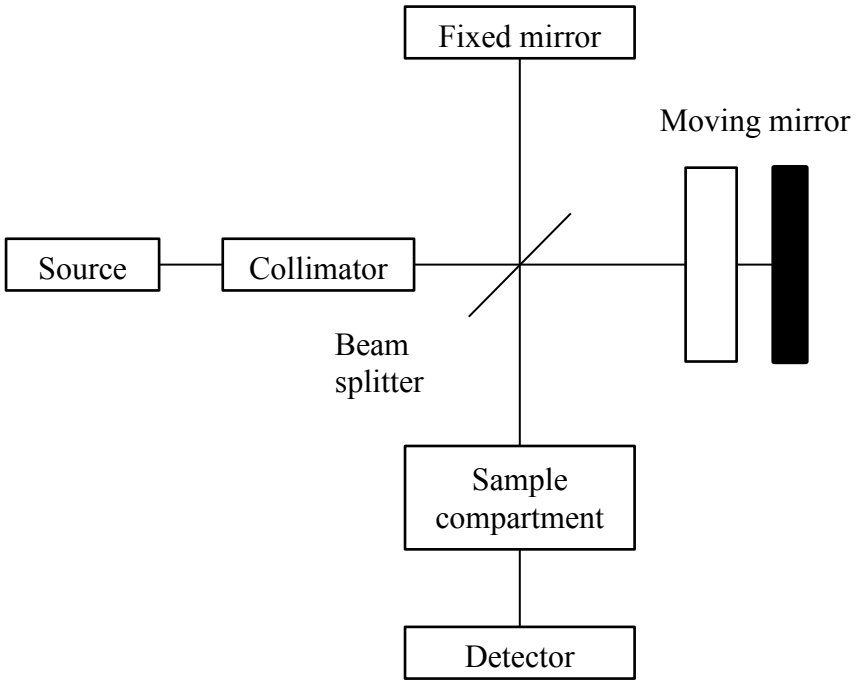

Fig. 3.5 Block diagram of working principle of an FTIR spectrometer

A common FTIR spectrometer consists of a source, interferometer, sample compartment, detector, amplifier, A/D convertor, and a computer. The source generates radiation, which passes the sample through the interferometer and reaches the detector. Then the signal is amplified and converted to a digital signal by the amplifier and analog-to-digital converter, respectively.

The FTIR analysis for TPO and diesel was performed using Perkin Elmer RX1 which is available in the department of chemical engineering, NIT Rourkela. The photograph of the FTIR instrument used in this study is shown in Figure 3.6.

Fig. 3.6 Photograph of Perkin Elmer RX 1

The FTIR test was carried out with a Perkin Elmer RX1 instrument which has a scan range of 450-4000 cm^{-1} with a resolution of 8 cm^{-1}. According to the FTIR spectra, the TPO contains a variety of aromatic compounds with aliphatic chains, aliphatic compounds, and oxygenated functional groups, such as phenolic, hydroxyl or carbonyl groups. The data shows therefore that the present liquids contain mainly aliphatic and aromatic compounds. The FTIR spectrums of conventional diesel and TPO were recorded after scanning on FTIR is shown in Figures 3.7 and 3.8 respectively. Also the family, bond types for the diesel fuel and TPO are given in Table 3.5 and 3.6 respectively.

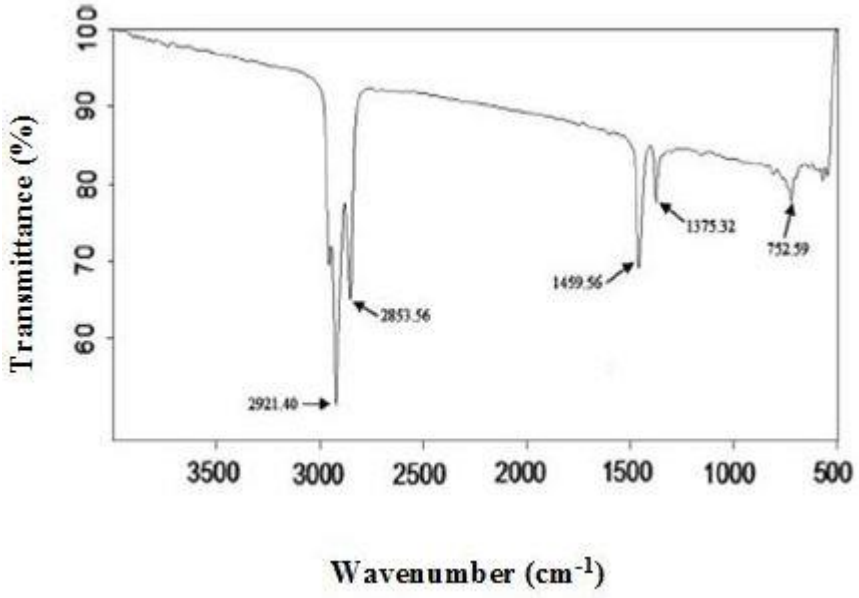

Fig. 3.7 FTIR of diesel

Table 3.5 FT-IR functional groups and indicated compounds present in tyre pyrolysis oil

Bond	Wave number(cm^{-1})	Wave length(μm)
C-H Stretch	3401.88	2.7 – 3.3
C≡C, C≡N Stretch	2122.08	4.2-4.8
C=C, Stretch	1644.12	5.9-6.3
O-H, Bending	1369.25	6.9-8.3
C-O,C-N Stretch	1230.16	7.7-11.1
Phosphate	1089.86	9.0-10.0
C-H	720.06	11.1-16.7

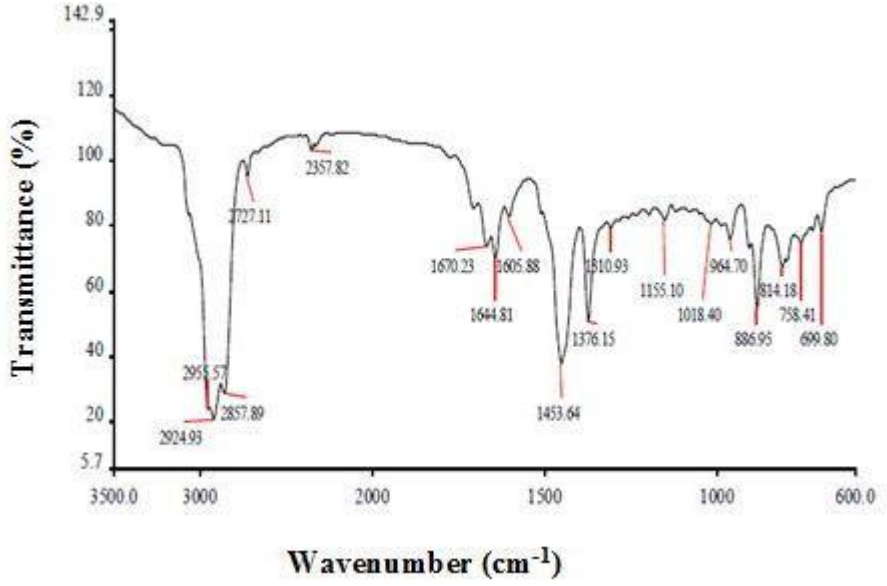

Fig. 3.8 FTIR of tyre pyrolysis oil

Table 3.6 FT-IR functional groups and indicated compounds present in diesel

Bond	Wave number(cm^{-1})	Wave length(μm)
C-H,Stretch	2921.33	3.0-3.7
C-H, Stretch	2812.72	3.0-3.7
C=C, C=N, Stretch	1605.47	5.9-6.3
O-H, Bending	1461.19	6.9-8.3
Nitrate	1376.55	7.2-7.4
C- Cl	722.05	13-14
C-Br	468.67	15-20

In case of diesel, the strong absorbance frequencies 2921.40 and 2853.56 cm^{-1} represent C–H stretching. The absorbance peaks 1459.56 cm^{-1} represented the C–H bending which indicates the presence of alkanes. From the FTIR graph it is seen that major transmittance spectrums peaks for both of the fuels are alkanes. Based on the above figure, it is clear that both of the oil is saturated hydrocarbon. The presence of hydrocarbon groups C–H indicates that the TPO has a potential to be used as fuel in diesel engine. Similar kind of FTIR results for waste tyre derived oil has been reported by many researchers [177-178].

3.3.4 GC-MS analysis of tyre pyrolysis oil

A gas chromatography-Mass spectrometry (GC-MS) analysis was carriedout for determining the composition of the TPO. The objective of GC-MS was to get an idea of the nature and type of compounds of TPO, in order to establish the possible ways of reusing or treating of them [9]. The Perkin Elmer GC-MS (model clarus 500) was used for analyzing the composition of TPO. The photograph of the instrument used in this study, which is available in the department of chemical engineering NIT Rourkela, is shown in Figure 3.9.

Fig. 3.9 Perkin Elmer GC-MS instrument

Also the working principle of GC-MS is shown in Figure 3.10 and it is described below. A capillary column coated with a 0.25 µm film of DB-5 with a length of 30 m and diameter 0.25 mm was used. The GC was equipped with a split injector at 200 ˚C with a split ratio of 1:10. The helium gas of 99.995% purity was used as the carrier gas at a flow rate of 1.51 ml/min. The oven's initial temperature was set at 70 ˚C for 2 min and then increased to 300 ˚C at a rate of 10 ˚C /min and maintained for 7 min. All the compounds were identified by means of the software developed by the National Institute of Standards (NIST-USA) library. The mass spectrometer was operated at an interface temperature of 240 ˚C, with an ion source temperature of 200 ˚C in the range of 40-1000 m/z.

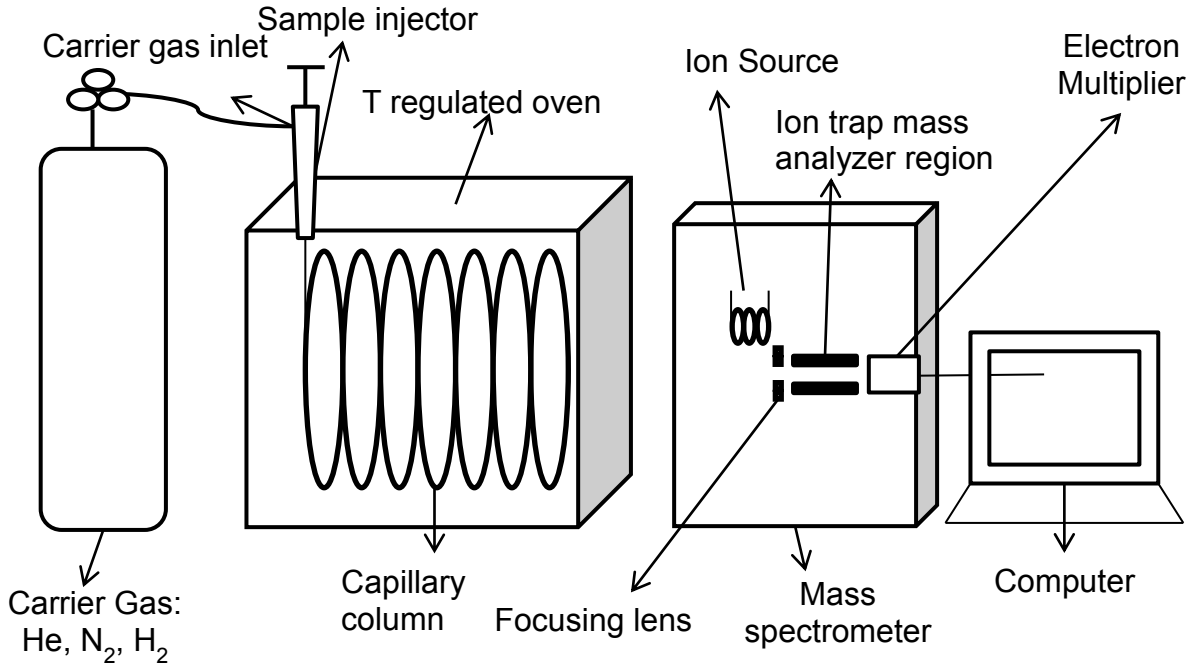

Fig. 3.10 Working principle of GC-MS analyzer

The chemical compounds were detected form chromatogram based on trace mass (% area) and retention time (t). Table 3.7 lists some of the compounds identified in diesel. The TPO is a chemically very complex containing more than 300 different compounds. The TPO has been fractionated into broad chemical class fractions and found to be composed of aliphatic, aromatic, heteroatom and polar fractions. The chemical composition of TPO from GC-MS is given Figure 3.11 and the compounds present are listed in Table 3.8.

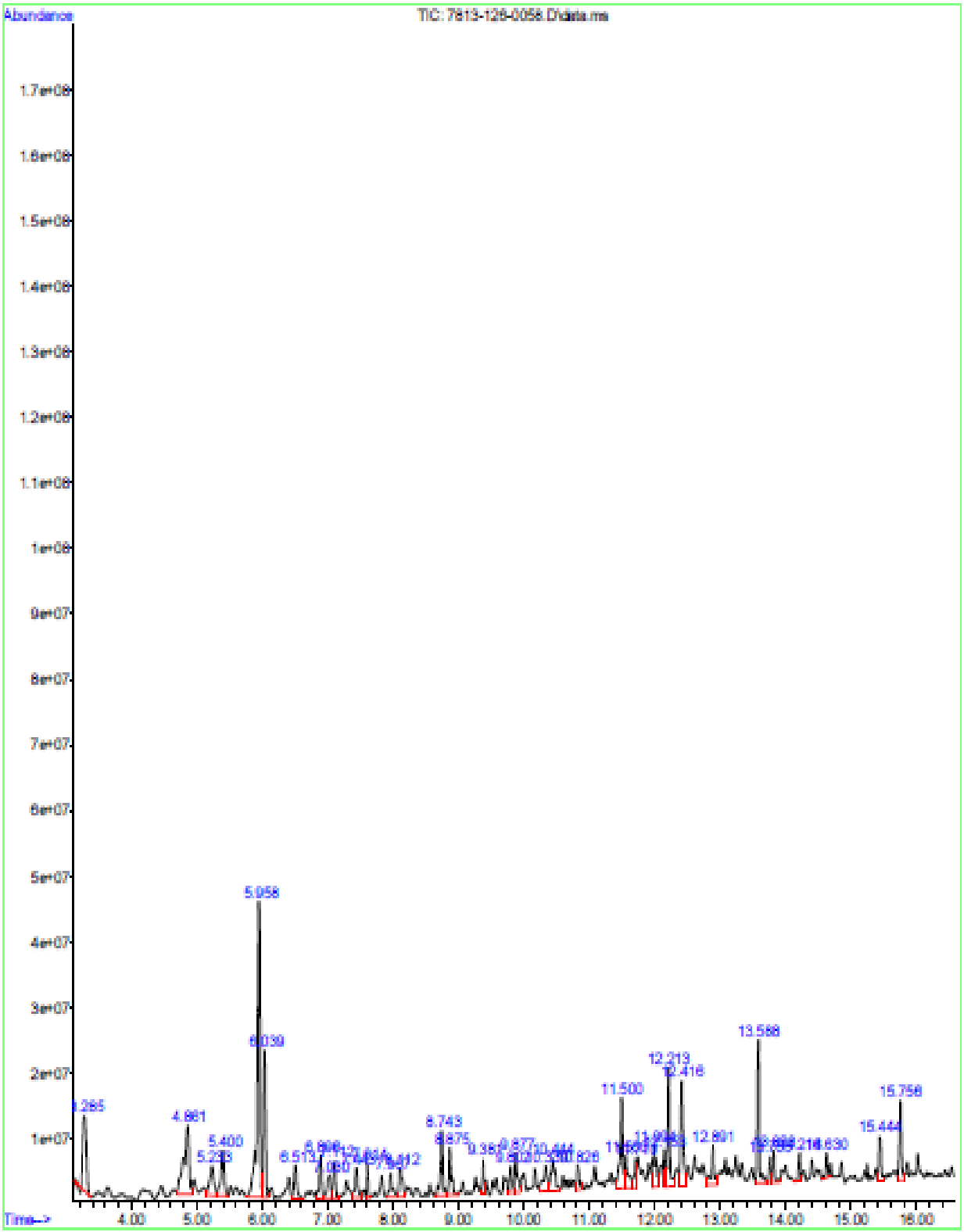

Fig. 3.11 GC-MS result of the tyre pyrolysis oil

Table 3.7 Chemical composition of diesel from GC-MS analysis

S No.	Time (min)	% Area	Compound name
1	3.065	0.98	1-Ethyl-2-methylcyclohexane
2	3.240	0.57	(2E)-2-Tridecen-1-ol
3	3.304	0.63	3-Methylnonane
4	3.359	1.06	Propylcyclohexane
5	3.682	0.75	2,2,3,3-Tetramethylpentane
6	3.737	0.84	2-Methylnonane
7	3.782	1.04	m-Ethylmethylbenzene
8	3.831	0.95	5-Ethyl-2-methylheptane
9	3.903	0.48	1,2,3-Trimethylbenzene
10	4.094	0.74	1-Methyl-2-Pentylcyclohexane
11	4.274	3.51	Decane
12	4.588	0.45	4-Methyldecane
13	4.839	0.59	Decane, 2-cyclohexyl-
14	5.080	0.44	1,3-Diethylbenzene
15	5.126	0.81	Malonic acid, 4-methylpent-2-yl tetradecyl ester
16	5.233	0.53	Benzenepropanal
17	5.250	0.75	2-Methyldecane
18	5.351	0.95	3-Methyldecane
19	5.822	2.14	n-Undecane
20	5.979	0.42	Benzene, (1-Ethyloctadecyl)-
21	6.054	0.55	1-Chlorooctadecane
22	6.167	0.80	Cyclohexanone, 5-Methyl-2-(1-Methylethylidene)-, (R)-
23	6.222	0.63	1,2,3,4-Tetramethylbenzene
24	6.425	0.68	Cyclohexane, 1,1'-(1,2-Ethanediyl)BIS
25	6.549	0.45	1-Methyl-2-Isopropenylbenzene
26	6.715	0.98	1,7,7-Trimethyl-2-Vinylbicyclo[2.2.1]Hept-2-ene
27	6.799	0.98	1-Iodo-2-Methylundecane
28	6.894	0.81	3-Methylundecane
29	7.199	0.44	1-(Cyclohexylmethyl)-2-methylcyclohexane
30	7.250	0.46	1,7,7-Trimethyl-2-vinylbicyclo[2.2.1]hept-2-ene
31	7.356	2.71	Dodecane
32	7.525	0.84	2,6-Dimethylundecane
33	7.741	0.66	1-Octadecanesulphonyl chloride
34	8.004	0.56	Octane, 2-cyclohexyl-
35	8.197	0.70	4-Methyldodecane
36	8.279	0.85	2-Methyldodecane
37	8.380	1.36	6-Ethylundecane
38	8.467	0.53	1,2,3,4-Tetrahydro-5-Methylnaphthalene
39	8.814	4.07	n-Tridecane
40	8.942	0.75	3,4-Difluorobenzoic acid, pentadecyl ester
41	9.023	0.50	n-Dodecane
42	9.171	0.50	Phosphorous acid, tris(decyl) ester

43	9.236	0.51	1,2,3,4-Tetrahydro-2,6-dimethylnaphthalene
44	9.477	0.81	2-Butyl-1-Octanol
45	9.525	0.49	2,4-Dimethyldodecane
46	9.677	0.70	2-Methyltridecane
47	9.766	0.84	2-Bromo dodecane
48	9.826	0.83	2,6,10-Trimethyldodecane
49	10.189	4.45	n-Tetradecane
50	10.787	0.77	7-Methylpentadecane
51	10.940	1.64	n-Hexadecane
52	10.994	0.74	2-Methyltetradecane
53	11.083	0.62	3-Methyltetradecane
54	11.480	4.87	Pentadecane
55	11.961	0.44	3-(2-Methyl-propenyl)-1H-indene
56	12.025	0.49	Furazan-3-carboxamide, 4-amino-N-(2- tetrahydrofurfuryl)-
57	12.039	0.50	6-Amino-1-methyl-2,4-dioxo-1,2,3,4-tetrahydro-5 pyrimidinyl(methyl)formamide
58	12.080	0.51	Tetradecane
59	12.154	0.84	4-Methylpentadecane

Table 3.8 Chemical composition of tyre pyrolysis oil from GC-MS analysis

S No.	**Time (min)**	**% Area**	**Compound name**
1	5.976	0.80	2-Methyl-1,3-butadiene
2	6.235	2.62	2-Hydroxy-2-pentanone
3	18.686	1.43	2-Methyl-5,3-cyclohexanone
4	7.425	1.42	2-Hydroxyl-Pntanol
5	17.87	4.718	1-Methyl-naphthalene
6	25.15	0.504	2-Methoxy-4-(1-propenyl)-phenol
7	8.657	3.85	2-Methyl-butanal
8	16.373	2.69	1-2-Butyl -Pentanol
9	14.984	0.65	Pyridine-3,4-dimethyl
10	12.557	1.58	1-Hydroxoy-3-ethylbenzene
11	30.15	1.156	9H-Fluorene
12	37.92	0.714	Phenanthrene
13	17.899	2.59	Phenol-3-3dimethylfuranone
14	9.134	2.11	3-Cyclopentanoic acid
15	15.67	5.20	Limonene
16	9.11	2.02	3-Methyl-phenol
17	9.796	3.23	Furan-methanol
18	7.24	2.908	1H-Indene
19	21.034	1.59	1,2,3,5-Tetramethylbenzene
20	10.426	2.38	3-Methyl-2,2-dimethyl-hexanediol
21	15.398	0.38	1-2-Furanyl-butanone
22	15.913	2.66	3-Methoxy-4-hydroxyphenylactic acid

23	11.752	1.98	2,3-Pentadiene
24	19.739	4.55	2- Benzoic acid
25	26.840	3.07	Hydroquinone
26	12.442	5.85	2,5- Hexanedione
27	12.97	4.575	Naphthalene
28	13.638	2.07	2-Cyclopenten-2-one
29	6.734	0.55	3-Methylcylohexene-1-acetone
30	12.914	2.11	5-Hydroxy-3-enoic acid
31	45.55	7.549	Hexadecanoic acid
32	23.574	2.05	3-Hydroxymethylfurfural
33	51.68	4.495	Octadecanoic acid
34	11.045	0.96	Pyridine 2-2dimethyl hydroxybenzene
35	17.423	4.45	2-Methyl-2-phenyl acetate
36	30.245	1.75	3-Furancarboxyfurfural
37	31.396	3.74	3-Methyl-2-cyclopenten-2-one
38	37.81	1.075	Tetradecanoic acid
39	21.945	2.11	3-Pentanoic acid

The main aromatic compounds found in the oil are benzene, toluene, xylenes (dimethylbenzenes), styrene, limonene and indene and their alkylated homologues. In addition, the TPO contain polycyclic aromatic hydrocarbons from 2-ring naphthalene to 5-ring benzopyrenes. The main aliphatic compounds are alkanes, with straight chain hydrocarbons from C_6-C_{37} and lower concentrations of alkenes. The content of aromatics and olefins in the liquid is rather high, which may limit its direct application as a fuel. The liquid fraction may be processed in a refinery by feeding the TPO to hydrocracking units for reducing aromatic and olefin content. The table indicates that TPO contains a few phenolic compounds which include Phenol-3-3dimethyl furanone, 3-Methyl-phenol, 2-Methoxy-4-(1-propenyl)-phenol and 1-Hydroxyl-2 methoxybenzene etc. in some proportions. Table 3.9 provides information about the phenolic compounds present in TPO with their specifications, which may act as antioxidants to biodiesel.

Table 3.9 Phenolic compound present in tyre pyrolysis oil

S.NO.	Compound Name	Specification
1	2- Benzoic acid	Molecular formula: $C_7H_6O_2$ CAS no.:65-85-0 Molecular weight:122.12
2	1-Hydroxoy-3-ethylbenzene	Molecular formula: $C_8H_{10}O$ CAS no.:620-17-7 Molecular weight:122.164
3	3-Methoxy-4-hydroxyphenylactic acid	Molecular formula: $C_9H_{10}O_4$ CAS no.:306-8-1 Molecular weight:182.18
4	Phenol-3-3dimethyl furanone	Molecular formula: $C_{12}H_{14}O_2$ CAS no.: 292148-43-7 Molecular weight:190.238
5	1-Hydroxyl-2methoxybenzene	Molecular formula: $C_7H_8O_2$ CAS no.:90-05-1 Molecular weight:124.14
6	3-Methyl-phenol	Molecular formula: C_7H_8O CAS no.: 108-39-4 Molecular weight:108.138
7	2-Methoxy-4-(1-propenyl)-phenol	Molecular formula: $C_{10}H_{612}O_2$ CAS no.:97-54-1 Molecular weight:164.201

3.3.5 Physicochemical properties of tyre pyrolysis oil

Table 3.11 represents the ultimate analysis which includes the quantitative determination of carbon, hydrogen, nitrogen, sulfur, and oxygen and other fuel properties of TPO and petroleum diesel for comparison. The physico-chemical properties of a liquid fuel define the characteristics of the fuel in terms of its potential performance in a combustion system, storage and transport issues, likely emissions, distillation range, etc.

The flash point of a liquid fuel represents the temperature that flammable gases are produced and will ignite and indicates the fire hazards associated with storage, transport and use of the any fuel. The flash point of the TPO is generally low when compared to petroleum refined

fuels due to its crude nature with a range of boiling point fractions, including volatile hydrocarbons. The carbon residue test is a measure of the tendency of the oil to form carbon under poor combustion conditions which may lead to carbon coking of diesel engine fuel injector nozzles or spray combustion burners. The TPO's carbon residues are quite high compared to diesel, suggesting that nozzle or spray burner blockage with extensive time of use may be an issue. The viscosity of a fuel influences the flow of the fuel through pipework, valves and pumps and also fuel atomization in engines and spray burners. The viscosity of the tyre oils was similar to that of petroleum diesel. The sulphur content of the TPO is 0.95 wt.%.

3.4 Preparation of Jatropha methyl ester-tyre pyrolysis oil blends

The present study is aimed to evaluate the effect of blending TPO with JME in five different percentages as fuels, on the combustion, performance and emission characteristics of a direct injection (DI) diesel engine. The blend was stirred well with the help of a mechanical agitator, to get a homogeneous stable mixture. Figure 3.12 shows the photographic view of the mechanical agitator used for stirring in this study.

Fig. 3.12 Photographic view of the mechanical agitator

All the JMETPO blends were kept under observation for 30 days, to ensure its stability. It was noticed that the TPO was not separated from the JME in the blend. The compositions of different blend used in this investigation and their notations are given in Table 3.10. The TPO at low percentages (10-50% at regular intervals of 10% on a volume basis), was blended with JME at 90 to 50% respectively, to get the fuel blends for the investigation. The blend was kept under observation for 30 days, to ensure its stability.

Table 3.10 Percentage of fuel available in different blends

Blends	JME	diesel	TPO
B80	80%	20%	
B60	60%	40%	
B40	40%	60%	
JMETPO10	90%		10%
JMETPO20	80%		20%
JMETPO30	70%		30%
JMETPO40	60%		40%
JMETPO50	50%		50%
JMETPO60	40%		60%

It was noticed that the TPO was not separated from the JME in the blend. The photographs of the JMETPO blends are shown in Figure 3.13.

Fig. 3.13 Photographs of the JMETPO blends

Table 3.11 Physico-chemical properties of diesel, JME, TPO and JMETPO blends

Properties	ASTM Test Method	JME	diesel	TPO	JMETPO10	JMETPO20	JMETPO30	JMETPO40	JMETPO50
Specific gravity	D 4052	0.881	0.830	0.913	0.884	0.887	0.891	0.894	0.898
Viscosity (cSt)	D 445	5.6	2.6	3.35	5.45	5.2	5	4.9	4.81
Calorific Value (MJ/kg)	D 4809	39.4	43.8	38.1	39.1	38.82	38.72	38.6	38.2
Flash point (˚C)	D 93	156	50	49	140	132	125	119	112
Fire point (˚C)	D 93	171	56	58	156	145	139	128	123
Cetane number	D 613	55	50	28	53	52	50	48	47
Carbon (%)	D 3178	77.1	86.2	86.92	78.1	79.26	80.12	82.1	83.5
Hydrogen (%)	D 3178	11.81	13.2	10.46	11.65	11.31	11.18	11.05	10.9
Nitrogen (%)	D 3179	0.119	Nil	0.65	0.178	0.23	0.27	0.3	0.32
Sulphur (%)	D 3177	0.001	0.3	0.95	0.08	0.18	0.3	0.39	0.45
Oxygen by difference (%)	E 385	10.97	Nil	1.02	10.1	9.02	8.9	8.78	8.7

3.5 Sauter mean diameter of test fuels

The physical properties of fuels like viscosity, density, bulk modulus and surface tension affect the droplet size that plays important role in spray formation. The Sauter mean diameter (SMD) is an average of the particle size of a liquid or fuel. The finer and more homogeneous the atomization, the more complete will be the physical preparation of the fuel, and more easily effective the combustion. Studies include the measurement of the droplet size using an age-old magnesium oxide (MgO) coating technique, and converting it into the more sophisticated Laser beam technique. Though the MgO technique is erroneous, it is simple and can be attempted in any laboratory environment compared to alternative methods that are more sophisticated and very costly. The Malvern particle analyzer is not available in the institute. Therefore, the authors attempted to collect the raw data using the MgO technique, and converted it into the more useful equivalent Malvern particle data.

The experimental set up employed to collect the spray is shown in Figure 3.14.

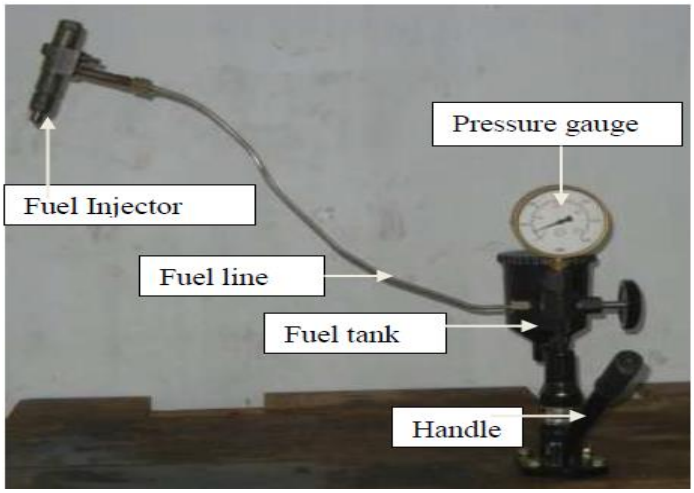

Fig. 3.14 Photographic view of the injector test bench

In this study, the MgO coated plates were introduced before the fuel spray. The distance between the MgO coated plate and the nozzle tip was 762 mm. The impressions of the droplet created on the coating of the plate were seen through a 10X microscope, choosing different regions on the plate. In order to minimize the error, two samples were selected from the spray collected on a glass plate, and were manually counted as given in Table 3.9. The numbers of droplets of different sizes were manually counted, viewing through the microscope and recorded. The injection pressure was fixed at 200 bar and the fuel samples of

JME and the JMETPO20 blend were tested and compared with the diesel sample. The crude data was converted into the more sophisticated measure used by the Laser Beam technique from Malvern particle analyzer data, using an empirical equation

Table 3.9 presents the sample study of the measurement of the droplet size of the diesel, JME and TPO, using the MgO technique at a room temperature of 27 ˚C. The SMD was determined using the following empirical equation:

$$(SMD)_{Mgo} = \frac{\frac{4\pi}{3}\left[N_1\left(\frac{D_1}{2}\right)^3 + N_1\left(\frac{D_2}{2}\right)^3 + N_1\left(\frac{D_3}{2}\right)^3 + \cdots\right]}{4\pi\left[N_1\left(\frac{D_1}{2}\right)^3 + N_1\left(\frac{D_1}{2}\right)^3 + N_1\left(\frac{D_1}{2}\right)^3 + \cdots\right]}$$

where, N1, N2, N3……are the numbers of droplets collected on the coated glass plate.
D1, D2, D3……...are the respective diameters of those droplets.

Figure 3.15 shows the droplet image of diesel, JME, and the JMETPO20 blend by using MgO coating technique, at an injection pressure of 200 bar and a room temperature of 27 ˚C through a single hole nozzle injector.

Table 3.13 shows the number of droplets at different ranges of diameter of diesel, JME, and the JMETPO20 blend. Droplets number were counted manually using NI vision software, it is clearly seen that, the maximum number of droplets fall within the range of less than 15 microns and minimum in 60-70 microns.

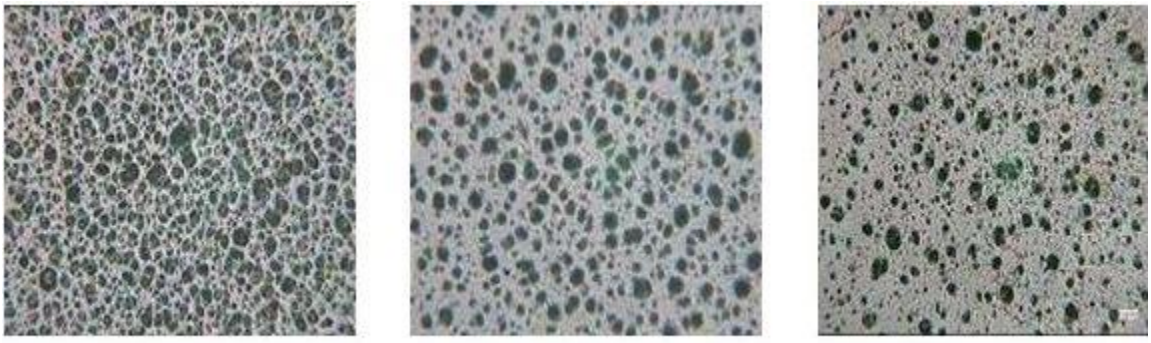

Fig. 3.15 Droplet images of diesel, JME and the JMETPO20 blend

Table 3.12 Droplet size of diesel, JME and the JMETPO20 blend

S. No.	Range of Droplet Diameter (Micron)	diesel (Average value of two samples)	JME (Average value of two samples)	JMETPO20 blend (Average value of two samples)
1	<15	1045	560	710
2	15-30	152	176	160
3	30-45	65	98	66
4	45-60	18	29	22
5	60-75	11	15	12

Chapter 4

Experimentation and Optimization

4.1 General

Awareness on the equipment or test rig to be used, different measuring instruments and techniques are essential before carrying out any particular research. This enables the researchers to identify and select appropriate devices, equipment and instruments for the research work. This chapter describes the experimental setup with necessary instruments which were used to evaluate the combustion, performance and emission characteristics of the diesel engine at different operating parameters. The information about the engine setup, instrumentation and methodology used in this study are also described in the following sections.

4.2 General description of the test engine

In the present investigation, experiments were carriedout on a single cylinder, four stroke, constant speed, air cooled, naturally aspirated, direct injection (DI) diesel engine, with a rated power of 4.4 kW at 1500 rpm. The technical specifications of the engine are given in Appendix 1. Figures 4.1 and 4.2 show the schematic layout of the experimental setup and photograph of the test engine respectively. The engine was coupled with an alternator which was connected to a load cell for loading purpose on the engine. The air consumption was measured using a sharp-edged orifice plate and U-tube manometer. A burette fitted with two optical sensors, one at a high level and, the other at a low level, was employed for measuring the quantity of fuel flow to the engine. The liquid flow through the high level optical sensor, gives a signal to the computer to start the time. Once the fuel reached the lower level optical sensor, the sensor would give a signal to the computer to stop the time and refill the burette. The time taken for the consumption of fuel of a fixed volume was recorded. The engine exhaust gas temperature was measured using a K type (Chromel-Aluminium) thermocouple connected to a digital indicator. The Kistler type piezoelectric pressure transducer was mounted on the cylinder head for the measurement of the cylinder pressure. A 11 bit 2050 step crank angle encoder is mounted on the camshaft to measure the engine crank angle. A

crank angle encoder with top dead center (TDC) marker was used to detect the engine crank angle.

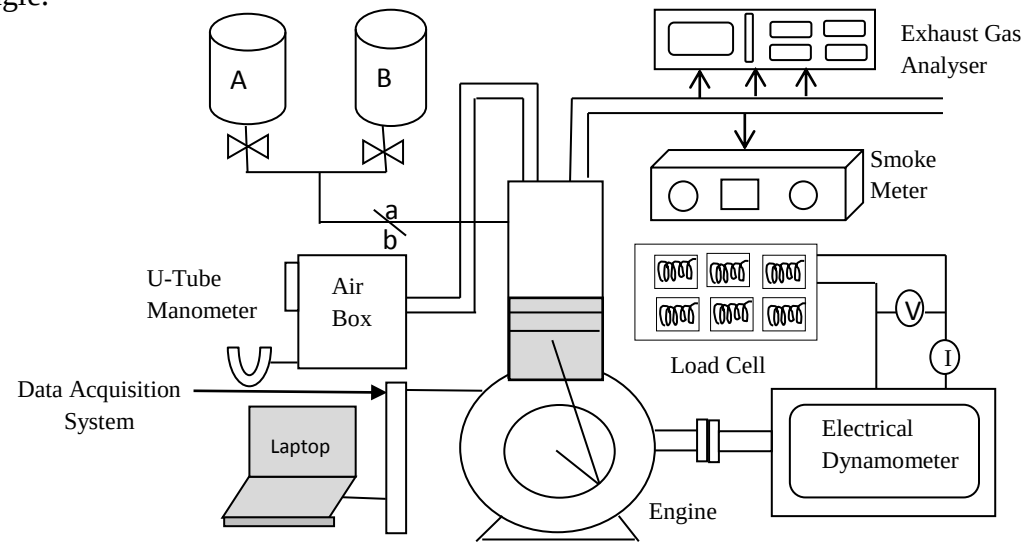

Fig. 4.1 Schematic layout of the experimental setup

The engine setup was attached with a control panel, which had the capability to communicate with the pressure sensor, and to convert the signal from the pressure sensor to the analogue voltage signal, which was ultimately fed to the data acquisition system (DAS). The exhaust gas compounds such as CO, CO_2, HC, NO, and O_2 were measured with the help of an AVL DiGas 444 exhaust gas analyser.

Fig. 4.2 Photographic view of the test engine

The smoke opacity of the exhaust gas was measured by an AVL 437 diesel smoke meter. The details of each and every component/instrument used in the research study are described in the following subsections. The time consumed for fuel flow, heating value and density of fuel were given as inputs to the data acquisition system. The data acquisition system (DAS) calculates the engine parameters such as brake thermal efficiency, fuel consumption and used as excel sheet provided in it.

4.3 Loading device

The engine was coupled with an alternator which is connected to a load cell for loading purpose on the engine. As the armature of the alternator is rotated by the engine, the field current/field strength will be induced, which tends to pull the field coils and the casing along with it. This rotation can be opposed in the same way as with the hydraulic dynamometer. This induced field strength is usually dissipated as heat through the banks of the electrical resistances. The load and speed can be increased or decreased on the alternator and thereby on the engine, by switching on or off the load resistances in the load cell bank, and by varying the field strength. An increase in power helps the engine to overcome the resistance from the alternator and maintain a set speed on the engine controller.

4.4 Fuel flow measurement

Fuel consumption was measured with the help of optical sensor and DAS. The fuel from the tank was connected to a solenoid valve; the outlet of the solenoid valve was connected to a glass burette and the same was connected to the engine through a manual ball valve. The photographic view of glass burette is shown in Figure 4.3. A burette fitted with two optical sensors, one at a high level and, the other at a low level, was employed for measuring the quantity of fuel flow to the engine. The liquid flow through the high level optical sensor, gave a signal to the computer to start the time. Once the fuel reached the lower level optical sensor, the sensor would give a signal to the computer, to stop the time and refill the burette. The time taken for the consumption of fuel of a fixed volume was recorded. Fuel consumption can also be measured manually with the help of a digital stopwatch and burette.

Fig. 4.3 Photographic view of glass burette

4.5 Air flow measurement

The air flow to the engine was routed through the cubical air tank. The air tank fulfills the purpose of regulating the flow of air to the tank. The inlet of the air tank was provided with an orifice, and a U-tube manometer connected with an orifice mounted on air box in the suction was used for measuring the intake air flow rate. One end of the manometer was left free to ambient and the other end was connected to the surge tank. It gave the reading of the difference in the water level in two columns, which was used to calculate the water head in terms of the pressure difference.

4.6 Temperature measurement

Temperature of the exhaust gas was measured with the help of K-type thermocouple fitted in exhaust pipe. Thermocouples work by having two different wires at the same temperature, and the two wires create a voltage at the joined end that could be related to temperature. The K-type thermocouples use nickel and chromium or aluminum for the wire set.

4.7 Cylinder pressure measurement

The cylinder pressure crank angle diagram is used to analyse the engine combustion behaviour, as the cylinder pressure has an effect on the performance parameters and emission levels of the engine. In this study, the in cylinder gas pressure was measured using a Kistler made quartz piezo-electric transducer (model 5395A) in conjunction with a Kistler charge amplifier mounted on the cylinder head of the test engine. A photographic view of the Kistler pressure transducer is shown in Figure 4.4.

Fig. 4.4 Photographic view of Kistler pressure transducer

The word "piezo electricity" means electricity resulting from pressure. It is derived from Greek. Piezo means to squeeze or press, which stands for amber, an ancient source of electric charge. Piezoelectricity is the direct result of the piezoelectric effect. The specifications of the pressure transducer are given in Appendix 2. The sensor was connected to the charge amplifier with a robust integrated high temperature Viton cable which converted the electric charge generated in a piezoelectric pressure sensor to voltages that can be input into conventional measurement and data recording equipment. The good linearity and repeatable measurements were recorded over a long period of time. The sealing took place at the shoulder of adapter that required a flat and smooth machined sealing area. The charge amplifier received a power supply between 7-32 VDC and had a range of 0-100 bar (40mV/ brand works with a time constant of 5 s). Figure 4.5 shows the photographic view of the pressure transducer mounted on the cylinder head.

Fig. 4.5 Photographic view of the pressure transducer mounted on the engine head

4.7.1 Pressure transducer calibration

Calibration is a process when the output signal of the sensor is compared to the value measured by an accurate device, and the relationship between the measured and the accurate value is determined. The calibration of the pressure transducer was done periodically to avoid measurement error. The Kistler piezo electric transducer of model 5395A was subjected to a dynamic calibration procedure using a standard dead weight tester. The dead weight tester generated the known pressure by hydraulically lifting precise weights with a piston with an accurately known cross-sectional area. The charge output signal of these transducers was used as the input to a charge amplifier via a high impedance cable. The charge amplifier converts the low level charge (which is of the order of several Pico-Coulombs) to a proportional voltage, which can be recorded with standard data acquisition equipment. In this procedure, a known pressure was applied to the transducer. Then, the output was grounded to zero volts, thereby eliminating signal decay. The pressure was then abruptly dropped to the atmospheric level, by rapidly releasing the hydraulic pressure holding up the weights and allowing them to fall. The resulting voltage change was recorded as a function of time, using a digital oscilloscope programmed to trigger on a voltage drop. The voltage change caused by the pressure change was determined using a peak-to-peak calculation feature on the scope. Dynamic pressures were taken at intervals of 200 psi from 200 to 1000 psi. Ten measurements were taken at each dynamic pressure. These were then averaged, and graphed against the corresponding voltage output. The linearity of the transducer was found to be better than 1%. The repeatability was observed to be about 2 to 3%.

4.8 Charge amplifier

The charge amplifier was used to convert the electrical charge output of the pressure transducer into proportional voltage. It consisted of an operational amplifier with a feedback through a variable capacitor, which was changed according to the range selected. This combination acted as an integrator for the current inputs from the transducer and the integral of the change variation appears as the output voltage. This voltage output was proportional to the total charge at any instant. In order to ensure the accuracy of the pressure measurement, the charge amplifier was allowed to warm up for four hours before the measurements were taken. The specifications of the charge amplifier are given in Appendix 3.

4.9 Analog to digital converter

An analog to digital converter (ADC) (12-bit) captures data about an actual system and stores that information in a format that can be easily retrieved for purposes of engineering or scientific review analysis. Another requirement of a DAS should be that, it captures information programmatically or automatically-in other words, without any hands-on human intervention or guidance. Using the DAS graphical analysis, evaluating the differential equation, computing the mathematical expression, display, control and recording were done for various engine operating parameters, like instantaneous pressure, crank angle, ignition delay, heat release rate, brake thermal efficiency, fuel consumption and exhaust gas temperature etc. A computer was used to process the data and store it during the investigation.

4.10 Measurement of crank angle

Crank angle encoder provides the basis for all crank-angle-related measurements of internal combustion engines. A 11 bit 2050 step crank angle encoder was fitted on the camshaft of the engine to measure the angular position of the crankshaft. A crank angle encoder with top dead center (TDC) marker was used to sense the position of TDC. The photographic view of the TDC marker is shown on Figure 4.6. It is a high precision optical pickup instrument with a pulse count of 360 ppr (pulse per revolution) used for torsional analysis for IC engines. The output from the crank angle encoder and pressure transducer was connected to a charge amplifier. From the charge amplifier, the output signal was transferred to a computer through an ADC. In this system, the analogue single was converted into digital impulses at fixed crank angles. The digital signal was then transmitted to the computer where it was stored. All the

data measured by sensors were processed, analysed and displayed with the help of a data acquisition system (DAS).

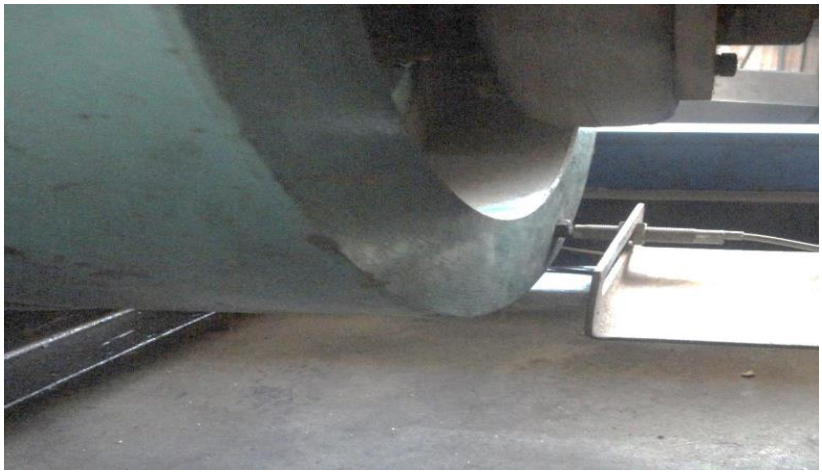

Fig. 4.6 Photographic view of top dead center marker

4.11 Combustion parameter calculation

4.11.1 Heat release rate

The heat release rate is an important parameter for the analysis of the combustion phenomenon in the engine cylinder, as the combustion duration and ignition delay can be easily estimated from the heat release rate-crank angle (CA) diagram. The heat release rate in this study was calculated, by using the cylinder pressure data. The heat release rate at each ˚CA was determined by the following formula, which is governed by the first law of thermodynamics.

The basic heat release rate analysis was established by Krieger and Borman [179]. The basic heat release method used in this study comprised three assumptions. The first is that the air-fuel mixture inside the cylinder behaves as an ideal gas. The second is that the charge in the cylinder is a uniform single zone of constant composition from the intake valve closing to the exhaust valve opening. The last one is that, the energy released due to fuel combustion can be considered as a heat addition to the cylinder. When the first law of thermodynamics was applied to this system,

$$\frac{dU}{dT} = \dot{Q} - \dot{W} \qquad (4.1)$$

$$mC_v \frac{dT}{dt} = \dot{Q} - P\frac{dv}{dt} \quad (4.2)$$

Where $\dot{Q}$ represents the sum of the heat transfer rate across the cylinder wall and the heat generation rate due to the combustion and is the rate of work done by the system boundary.

The ideal gas assumption, Eq. 4.3 can be applied at this point to above Eq. 4.2 and it becomes Eq. 4.4. After rearranging it, Eq. 4.5 is obtained and replacing the time term with crank angle, θ gives Eq. 4.6.

$$PV = mRT \quad (4.3)$$

$$\frac{dT}{dt} = \frac{1}{mR}\left(P\frac{dV}{dT} + V\frac{dP}{dt}\right) \quad (4.4)$$

$$\dot{Q} = \left(\frac{C_v}{R} + 1\right)P\frac{dV}{dT} + \frac{C_v}{R}V\frac{dP}{dt} \quad (4.5)$$

$$\frac{dQ}{d\theta} = P\frac{\gamma}{\gamma-1}\left(\frac{dV}{d\theta}\right) + \frac{1}{\gamma-1}V\frac{dP}{d\theta} \quad (4.6)$$

Where dQ/dθ is the heat release rate (kJ/deg), P is the in cylinder gas pressure (bar), V is in cylinder volume (m^3), and γ is the ratio of specific heats.

4.11.2 Ignition delay

Ignition delay is a period measured in terms of crank angle between the beginning of fuel injection and the beginning of combustion [180]. From the heat release rate curve, the start of combustion is determined as the point at which the heat release curve changes from a negative axis to a positive one.

4.11.3 Combustion duration

The combustion duration is described as the time duration required by the combustion process to reach 90% of its mass fractions burned [181].

4.11.4 Rate of pressure rise

The maximum rate of pressure rise $(dp/d\theta)_{max}$ in an engine combustion chamber has a substantial impact on the maximum cylinder pressure and smoothness of the engine operation [182]. The rate of pressure rise with respect to the crank angle is recorded from the following expression:

$$ROPR = dp/d\theta \quad (4.7)$$

In general, it is considered that combustion is normal when $(dp/d\theta)_{max}$ is lower than 3 bar/ ˚CA whereas the engine is considered to be knocking, if is greater than 7 to 8 bar/ ˚CA.

4.12 Performance parameter calculation

4.12.1 Brake thermal efficiency

The brake thermal efficiency (BTE) reflects quality of combustion and provides comparable of assessing how efficient the energy in the fuel was converted to mechanical power output [183]. The brake thermal efficiency is given by the ratio between the power output and the product of the fuel mass flow rate and lower heating value of the fuel.

BTE = (brake power x 3600 x 100)/ (volumetric fuel flow rate per hour x fuel density x calorific value of fuel)). (4.8)

4.12.2 Brake specific energy consumption

The formula used to calculate the brake specific fuel consumption (BSFC) is given below:

BSFC = (volumetric fuel flow rate per hour x fuel density/brake power) (4.9)

The brake specific fuel consumption is not a reliable factor when two fuels of different calorific values and densities are blended together. The brake specific energy consumption (BSEC) is described as the multiplication of the BSFC and lower calorific value of the fuel [184].

4.13 Exhaust emission measurement

4.13.1 CO, HC, CO_2 and NO emissions measurement

The engine exhaust emissions were measured with the help of an AVL DiGas 444 analyser. The working principle of the sensors for measuring the HC, CO, NO, CO_2 and O_2 are described in following sub sections. The CO and CO_2 in the exhaust of the engine are measured with the help of the gas analyser that works on the non-dispersive infrared (NDIR) principle [185]. Figure 4.7 gives the pictorial information of the gas analyser which uses the NDIR principle. The instrument has two remote sampling heads controlled by a main control unit, and is capable of sampling CO and CO_2 simultaneously in two locations. Each constituent gas in a sample will absorb some infra-red rays at a particular frequency. By shining an infra-red beam through a sample cell (containing CO or CO_2), and measuring the amount of infra-red absorbed by the sample at the necessary wavelength, the NDIR detector is able to measure the volumetric concentration of the CO or CO_2 in the sample.

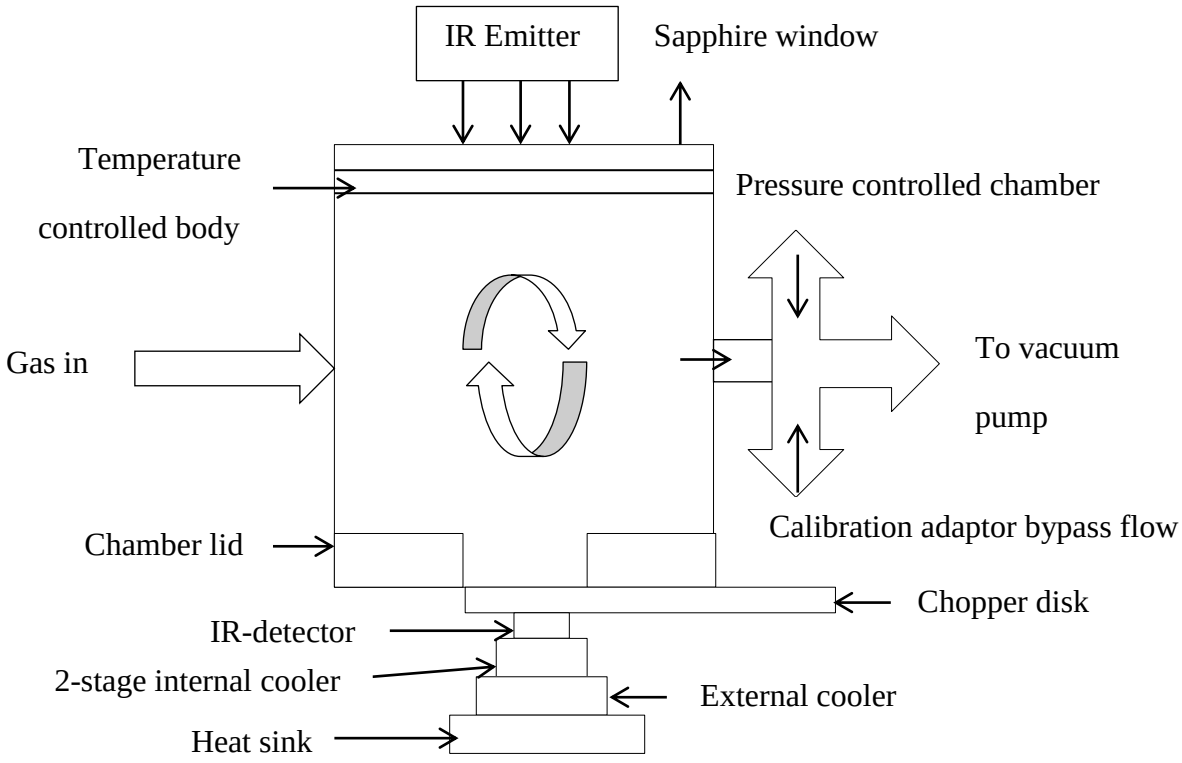

Fig. 4.7 NDIR principle for measuring the CO/CO_2 species in the exhaust

A chopper wheel mounted in front of the detector continually corrects the offset and gain of the analyser, and allows a single sampling head to measure the concentrations of two different gases. The flame ionisation detector (FID) is the industry standard method of measuring HC concentration [186]. Figure 4.8 illustrates the working principle of the FID technique that is used to measure the HC component in the engine exhaust. The sample gas is introduced into a hydrogen flame inside the FID. Any hydrocarbons in the sample will produce ions when they are burnt. The ions are detected using a metal collector which is biased with a high DC voltage. The current across this collector is thus proportional to the rate of ionization, which in turn, depends upon the concentration of HC in the sample gas.

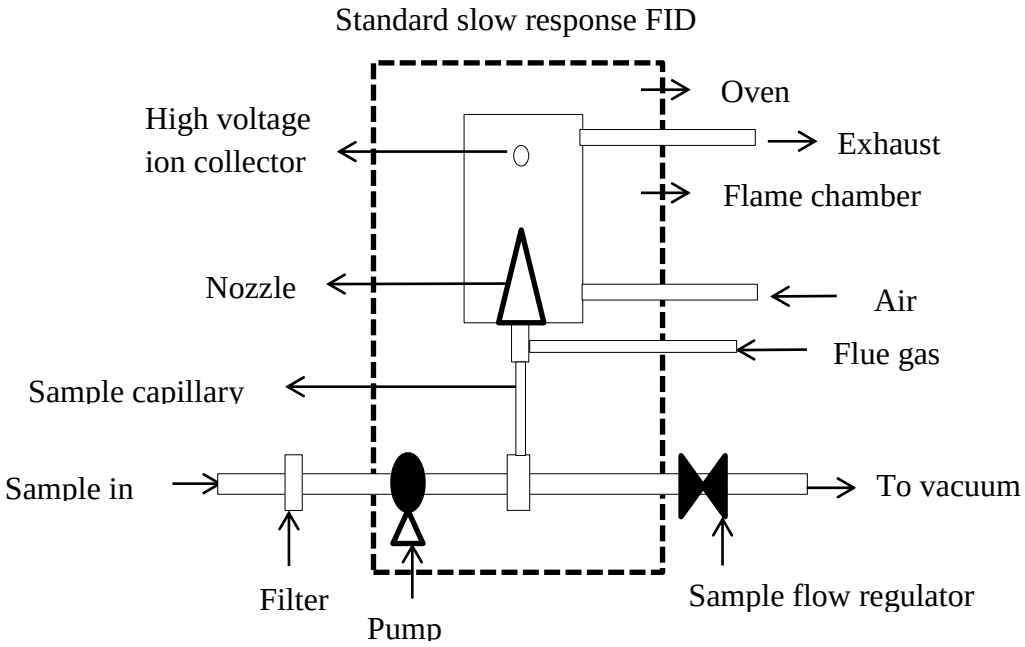

Fig. 4.8 FID principles for HC measurement

The ionization process is very rapid, and hence, the slow time response of the conventional FIDs is mainly due to sample handling. A typical slow analyser might have a response time of 1-2 seconds.

The electrochemical principle for the NO measurement is used to find out the controlled and uncontrolled emissions from the combustion sources, such as boilers, heaters, engines and turbines. Generally, it measures the emissions of NO, nitrogen dioxide (NO_2), and the sum of their concentrations (NO_x). The electrochemical principle is based upon the use of the

electrochemical sensors, in which the reacting gases are used to generate electrical signals proportional to the gas concentrations. It consists of the sensing electrode (or working electrode) and a counter electrode separated by a thin layer of electrolyte. The working principle is shown in Figure 4.9.

The exhaust gas first passes through a small capillary type opening, diffuses through a hydrophobic barrier, and then it reaches the electrode surface. These approaches can prevent the leaking of the electrolyte from the sensor.

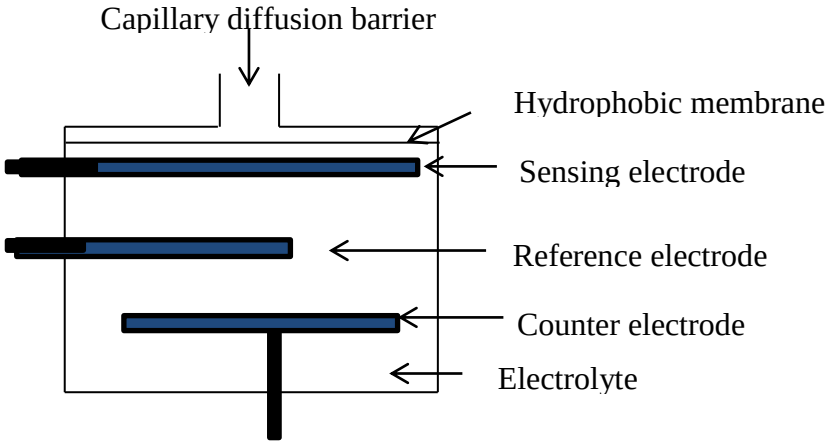

Fig. 4.9 Electrochemical principle for NO measurement

Then, the gas that diffuses through the barrier can react at the surface of the sensing electrode involving either an oxidation or reduction mechanism. According to the desired gas of interest, the reactions are catalyzed by the electrode materials. With a resistor connected across the electrodes, a current proportional to the gas concentration flows between the anode and the cathode. The current is measured to determine the gas concentration. Because the current is generated in the process, the electrochemical sensor is often described as an amperometric gas sensor or a micro fuel cell [187].

All the above mentioned principles are incorporated in a gas analyser provided by AVL Ltd. Therefore, the researcher used AVL Digas 444 analyser in this investigation. A photographic view of the AVL DiGas 444 analyser is shown in Figure 4.10. Specification of the gas analyzer is given in Appendix 4. The exhaust pipe of the engine with a length of by about one

foot was modified by using a T- joint with a ball valve for the emission measurements. While measuring the engine exhaust emission, the ball valve was opened for the insertion of the probe connected to the digital gas analyser. The probe is inserted into the engine's exhaust pipe by opening the ball valve. Before taking the emission test, a leak check was carriedout in the digital gas analyser. The leak check was conducted by closing the probe's nozzle manually. The purpose of the leak check is to discharge the residual gases through the gas analyser's exhaust tube.

Fig. 4.10 Photographic view of five gas analyzer

The recommended periodic calibration of the gas analyzer was carriedout, in order to ensure the accuracy of measurement. The gas analyzer's electronics, optics and its response to environmental factors were checked through calibration. The general calibration procedure involves the injection of calibration gases of known concentration, and validating the response. The compositions of CO, CO_2 and HC gases are; 3.5% volume of CO, 14% volume of CO_2, 2000 ppm volume of propane and the remainder nitrogen, whereas the calibration gas for the NO component is 2200 to 3000 ppm volume of the NO and the remainder N_2. The instrument outputs are then adjusted to the known inputs to correct the variations in the electronic response due to temperature effects, drift, or other interferences. Thus, the accuracy of the analyser is assured, and an accurate response to the sampled gas is achieved after calibration.

4.13.2 Smoke opacity measurement

The smoke opacity of the exhaust gas was measured by an AVL 437 diesel smoke meter. A photographic view of the diesel smoke meter is shown in Figure 4.11. The operating principle is based on the attenuation of a light beam caused by the exhaust gases in a measuring chamber of defined measuring length, and nonreflecting surface filled homogeneously with the exhaust gas. The loss of light intensity between the light source and a receiver is measured and reported in % opacity, the calculation being based on the Beer-Lambert law.

Fig. 4.11 Photographic view of the diesel smoke meter

The absorption coefficient "k" was also reported by the smoke meter, in accordance with the ECE-R24/ISO 3173. Condensation inside the instrument is avoided, as the measuring chamber is thermostatically heat controlled at 70 ± 5 ˚C. To ensure accuracy and repeatability observations were recorded, at each case of the engine operation, for a span of 120 s at intervals of 20 s, which was greater than the instrument measurement value resolution time of 10 s. The complete technical specification of the AVL 437C diesel smoke meter is given in Appendix 5.

Calibration of the smoke meter was done periodically. It was done by warming the heating elements up to 70 ˚C. The pre-heating was carried out to prevent the temperature falling below dew point, and thus, to avoid measurement error or condensation of smoke. Fresh air was allowed to enter the measurement chamber which was drawn through the fitter paper, underwent measurement and set the zero point for calibration. The halogen bulb current irradiated the column of the fresh air volume, and the signals from the detector were measured by the microprocessor and set as the reference value for 0% opacity. The linearity was checked by gently pushing the linearity check knob down, up to its dead position. The calibration plate was thus measured in front of the detector, and the measured opacity value

was indicated and printed on the protocol print out. The probe of the exhaust gas analyzer was inserted at the end of the exhaust pipe during the measurement of emissions. Once the engine reached stable operation, the probe was inserted into the exhaust pipe and the measurements were taken.

4.14 Instrument accuracy and uncertainty analysis

The details of the measuring range, accuracy and percentage uncertainties for the instruments used in the present investigation are Appendix A4. The overall uncertainty of the experiment was calculated by the addition of the uncertainties of the individual instruments, and is given below [188].

Total percentage of uncertainty of this experiment is

= Square root of { (uncertainty of total fuel consumption)^2 + (uncertainty of brake power)^2 + (uncertainty of specific fuel consumption)^2 + (uncertainty of brake thermal efficiency)^2 + (uncertainty of CO)^2 + (uncertainty of HC)^2 + (uncertainty of NO)^2 + (uncertainty of pressure transducer)^2 + (uncertainty of EGT)^2 + } (4.10)

$=\sqrt{\{(1.5)^2+(0.2)^2+(1)^2+(1)^2+(0.2)^2+(0.2)^2+(0.2)^2+(0.05)^2+(1.0)^2+(0.15)^2\}} = \pm 2.33$

Thus the total uncertainty for the whole experimentation was found to be ±2.33.

4.15 Calculations of brake specific exhaust emissions

Exhaust emissions are generally presented on a brake specific basis expect for the smoke opacity. In order to calculate the brake specific emissions from the measured exhaust gas concentration, usually based on volume percentage or parts per million, balanced chemical equations were used. The formulae used to convert the emissions from ppm and % vol into g/kWh are given below:

HC emissions in g/kWh

HC (g/kWh) = [{(mf+ma)/(29*1000)} * HC (in ppm)*13/BP] (4.11)

CO emissions in g/kWh

CO (g/kWh) = [{(mf+ma)/29)*10} * CO (in %vol)*28/BP] (4.12)

NO emissions in g/kWh

NO (g/kWh) = [{(mf+ma)/(29*1000)} * NO (in ppm)*32.4/BP] (4.13)

4.16 Experimental procedure

Before start of the engine experiments, the fuel tank, engine oil level, load cell, dynamometer, AVL DiGas444 exhaust gas analyser and AVL437 smoke meter were checked. The test engine was cranked and warmed up for an hour. Consecutively, the dynamometer, all analyzers and meters for measurements attached to the engine were switched on and the proper preparations and settings for measurements were made as recommended by the manufacturers of the instruments.

4.16.1 Engine experiment with diesel, JME and the JMETPO blends

Initially, the engine was started using diesel fuel and the experiments were conducted, under the original injection timing of 23 ˚CA bTDC, nozzle opening pressure of 200 bar and compression ratio of 17.5, as set by the engine manufacturer for obtaining the reference data. Further, the engine was run with the Jatropha methyl ester (JME) in the same operating conditions. The engine was run at no load, 25%, 50%, 75% and 100% loads for both the test fuels. In every test, all the combustion, performance and emission parameters were measured. Subsequently, tests were conducted with different blends of Jatropha methyl ester (JME) with tyre pyrolysis oil (TPO) to study the effects of blend on the combustion, performance and emission characteristics of the engine. The content of TPO in the blend was varied from 10% to 50% with a regular interval of 10% on a volume basis. The blends were denoted as JMETPO10, JMETPO20, JMETPO30, JMETPO40 and JMETPO50, where the numeric value represents the percentage value of the TPO in the Jatropha methyl ester tyre pyrolysis oil (JMETPO) blend. All the readings were taken only after the engine attained stable condition. At the end of the test for each JMETPO blend, the fuel was switched back to diesel and the engine was kept running atleast for 15 minutes before going for next JMETPO blend to flush the test fuel from the fuel line and the injection systems. Each test was conducted 3 times, ensuring the repeatability of the result. The values given in this study are the averages of these results. Each test was repeated three times and was averaged to ensure the reproducibility of data.

4.16.2 Best blend selection based on MCDM-VIKOR

The multi-criteria decision making (MCDM) based VIKOR method has been introduced by Opricovic in 1998 to optimize difficult problems that associated with several industries viz. manufacturing, automotive, chemical, aerospace etc. In recent days, the practical problems involve multiple input and output criteria which are of different units and opposite in nature (beneficial and non-beneficial). The VIKOR method targets on ranking and choosing an optimal alternate from a set of alternatives and provides compromise solution for a problem with conflicting criteria and thus reaching to a final solution. It is an effective tool for the selection of optimum fuel blend consists multiple responses.

The proposed method comprises of the following steps [189]

(1) The multiple outcomes obtained during the experimentation firstly converted in the form of a decision matrix. The decision matrix can be expressed as below (Eq^{n} 4.14).

$$A = \begin{bmatrix} a_{11} & a_{12} & . & a_{1j} & a_{1n} \\ a_{21} & a_{22} & . & a_{2j} & a_{2n} \\ . & . & . & . & . \\ a_{i1} & a_{i2} & . & a_{ij} & . \\ . & . & . & . & . \\ a_{m1} & a_{m2} & . & a_{mj} & a_{mn} \end{bmatrix} \qquad (4.14)$$

Here, the promising alternatives are shown in the row ($i = 1, 2, ..., m$) and the corresponding measured outcomes for each alternative are displayed in the column ($j = 1, 2, ……., n$).

(2) Normalize the decision matrix quantities between 0 and 1. The data normalization is carried out using the following equation (Eq^{n} 4.15).

$$a'_{ij} = \frac{a_{ij}}{\sqrt{\sum_{i=1}^{m} a_{ij}^2}} \qquad (4.15)$$

where, a'_{ij} exhibits the normalized value. The normalized decision matrix can be written as below (Eq^{n} 4.16).

$$A' = \begin{bmatrix} a'_{11} & a'_{12} & . & a'_{1j} & a'_{1n} \\ a'_{21} & a'_{22} & . & a'_{2j} & a'_{2n} \\ . & . & . & . & . \\ a'_{i1} & a'_{i2} & . & a'_{ij} & . \\ . & . & . & . & . \\ a'_{m1} & a'_{m2} & . & a'_{mj} & a'_{mn} \end{bmatrix} \qquad (4.16)$$

(3) Compute the beneficial (Ideal) and non-beneficial (Non-ideal) solutions. These values can be calculated using the equations specified below (Eq^n 4.17 and Eq^n 4.18).

$$A^+(beneficial) = \left\{ \left(\max a_{ij} \mid j \in J \right) or \left(\min a_{aj} \mid j \in J' \right) \mid i = 1, 2, ..., m \right\}$$

$$= \left(a_1^+, a_2^+, ..., a_j^+, ..., a_n^+ \right) \qquad (4.17)$$

$$A^-(non-beneficial) = \left\{ \left(\min a_{ij} \mid j \in J \right) or \left(\max a_{ij} \mid j \in J' \right) \mid i = 1, 2, ..., m \right\}$$

$$= \left(a_1^-, a_2^-, ..., a_j^-, ..., a_n^- \right) \qquad (4.18)$$

Where, $J = \left\{ j = 1, 2, ..., n \mid a_{ij} \right\}$ is used for higher-is-better type output characteristic and $J' = \left\{ j = 1, 2, ..., n \mid a_{ij} \right\}$ is used for lower-is-better type output response.

(4) Determine the utility measure and the regret measure by using the following equations (Eq^n 4.19 and Eq^n 4.20).

Utility measure $\left(U_i \right) = \sum_{j=1}^{n} w_j \frac{a_j^+ - a'_{ij}}{a_j^+ - a_j^-}$ (4.19)

Regret measure $\left(R_i \right) = \underset{i}{Max} \left[w_j \frac{a_j^+ - a'_{ij}}{a_j^+ - a_j^-} \right]$ (4.20)

where, U_i and R_i denote the utility measure and the regret measure respectively, and w_j denotes the weight assumed for *j*th attribute.

(5) At the end, compute the VIKOR index (Q_i) using the equation given below (Eq^n 4.21).

$$Q_i = \frac{v\left(U_i - U^+\right)}{U^- - U^+} + \frac{(1-v)\left(R_i - R^+\right)}{R^- - R^+} \qquad (4.21)$$

where, Q_i denotes the VIKOR index value $i = 1, 2, \ldots\ldots, m$; similarly, v represents the weight of the maximum group utility (generally taken as 0.5), and

$$U^+ = \underset{i}{Min} U_i \,;\; U^- = \underset{i}{Max}\, U_i \;;\; R^+ = \underset{i}{Min}\, R_i \,;\; R^- = \underset{i}{Max}\, R_i$$

(6) Rank the alternatives based on VIKOR index (Q_i). The alternative with the smallest Q_i value is considered as the best solution.

4.16.3 Variation of injection timing

Already, experiments were conducted using diesel, JME, and the JMETPO20 blend, with the original injection timing of 23 ˚CA bTDC (as set by the engine manufacturer) for obtaining the reference data. Generally, CI engines are designed to operate only with diesel. For other fuels, certain operating parameters of the engine have to be optimized, in view of the combustion, performance and emission characteristics [190]. It is important to note that the engine behaviour is predominantly affected by the fuel-air mixture supplied to the diesel engine. The fuel quantity is governed by the fuel injection rate, injection timing and nozzle geometry [191]. Besides, injection timing plays a vital role in the performance and emission characteristics of a diesel engine, as the pressure and temperature change significantly as the piston approaches the top dead centre (TDC). In this context, further, the experiments were conducted at different injection timings for the optimum blend i.e. JMETPO20. Before starting this study, the fuel pump was dismantled to change the injection timing. Figure 4.12 shows the photographic view of the fuel pump with shim. The original injection timing was altered by adjusting the number of shims fitted under the plunger in the pump, by addition or removal of shims. Figure 4.13 shows the photographic view of the shim. For changing the injection timing, the number of shims was varied. Every single shim of thickness 0.25 mm shifts the injection timing by about 1.5 ˚CA.

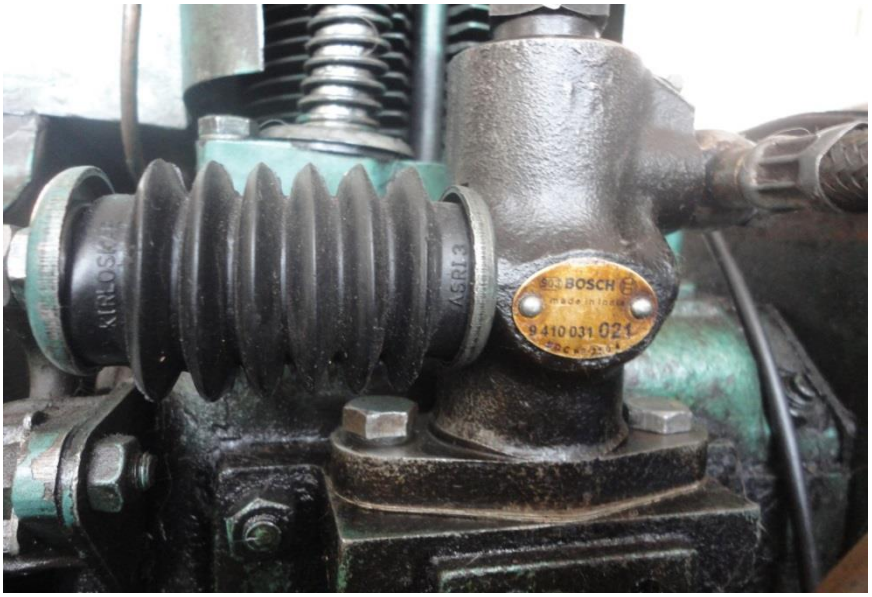

Fig. 4.12 Photographic view of the fuel pump with shim

The experiments were carriedout using the optimum JMETPO20 blend at five injection timings, of 26, 24.5, 23, 21.5 and 20 ˚CA bTDC. For the original injection timing of 23 ˚CA bTDC, three shims were used in the fuel pump. The study was carried out with 1.5 and 3 ˚CA advancement, and 1.5 and 3 ˚CA retarding injection timing for the JMETPO20 blend, and the results were compared with those of diesel, JME, and the JMETPO20 blend at the original injection timing.

Fig. 4.13 Photographic view of the shim

4.16.4 Variation on nozzle opening pressure

In the previous section, experiments were carriedout using the JMETPO20 blend on a CI engine at varied injection timings and it was found that an advanced injection timing of 24.5 ˚CA bTDC improved the overall performance of the engine compared to other the injection timings. Thus the injection timing of 24.5 ˚CA bTDC was set as optimum injection timing for the JMETPO20 blend based on the performance and emission parameters of the engine. One of the significant operating parameters which affect the engine behaviour is nozzle opening pressure, because it influences the atomization of fuel and mixture formation. Several researchers documented that operating the engine with higher nozzle opening pressure might give a better performance and lower emissions, if the fuel has a higher viscosity [192-194]. In this regard, further, the experiments were conducted with the optimum injection timing of 24.5 ˚CA bTDC, using the JMETPO20 blend at five nozzle opening pressures, of 210, 220, 230, 240, and 250 bar. The nozzle opening pressure was tested with the help of the nozzle pressure tester, as shown in Figure 4.14.

Fig. 14 Photographic view of the nozzle pressure tester assembly

Before starting the test for different nozzle opening pressures, the fuel injector was removed from the engine head, and the injector was dismantled. The adjustable screw located in the top of the injector was adjusted to get the required nozzle opening pressure. Then, the injector was inserted into the cylinder head and mounted. Figure 4.15 shows the dismantled view of the fuel injector. The experiments were conducted at that particular nozzle opening pressure.

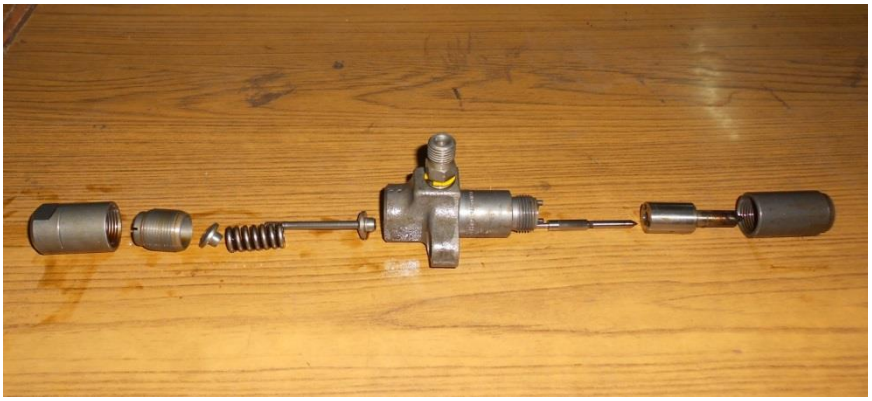

Fig. 4.15 Dismantled view of the fuel injector

4.16.5 Variation of compression ratio

In the previous module of research work, experiments were carriedout on a diesel engine using the JMETPO20 blend at optimum injection timing of 24.5 ˚CA bTDC and different nozzle opening pressures. It was noticed that, an advanced injection timing of 24.5 ˚CA bTDC and higher nozzle opening pressure of 220 bar improved the overall performance of the engine.

Several researchers have reported on the optimum design parameters for diesel engines when fueled with alternative fuels, because the conventional diesel engine is designed only for diesel fuel. Many researchers have reported results pertaining to the effects of varying injection timing, nozzle opening pressure and compression ratio on thermal efficiency, specific fuel consumption (SFC) and exhaust emissions of CI engines [195-198]. It is reported that the engine performance may be improved by many ways, such as increasing the compression ratio, and nozzle opening pressure and advancing the fuel injection timing. The use of a higher compression ratio usually enhances the fuel-air mixture density, due to the increase in the pressure and temperature of the compressed mixture in the combustion chamber, leading to a rise in peak cylinder pressure and the burning speed of the fuel-air mixture.

Therefore, an experimental investigation was carriedout to study the effects of operating the engine fueled with the JMETPO20 blend at different compression ratios, one higher (18.5) and one lower (16.5) in addition to the original compression ratio of 17.5 keeping the injection timing and nozzle opening pressure of the engine at optimum conditions.

In this module, the experiments were conducted with the advanced injection timing of 24.5 ˚CA and higher nozzle opening pressure of 220 bar, using the JMETPO20 blend for the compression ratios of 16.5, 17.5 and 18.5. The compression ratio of the engine was altered by changing the clearance volume, by the replacement of gaskets of different thickness in between the cylinder and the cylinder head. Figure 4.16 shows the photographic view of the gasket fitted with cylinder block.

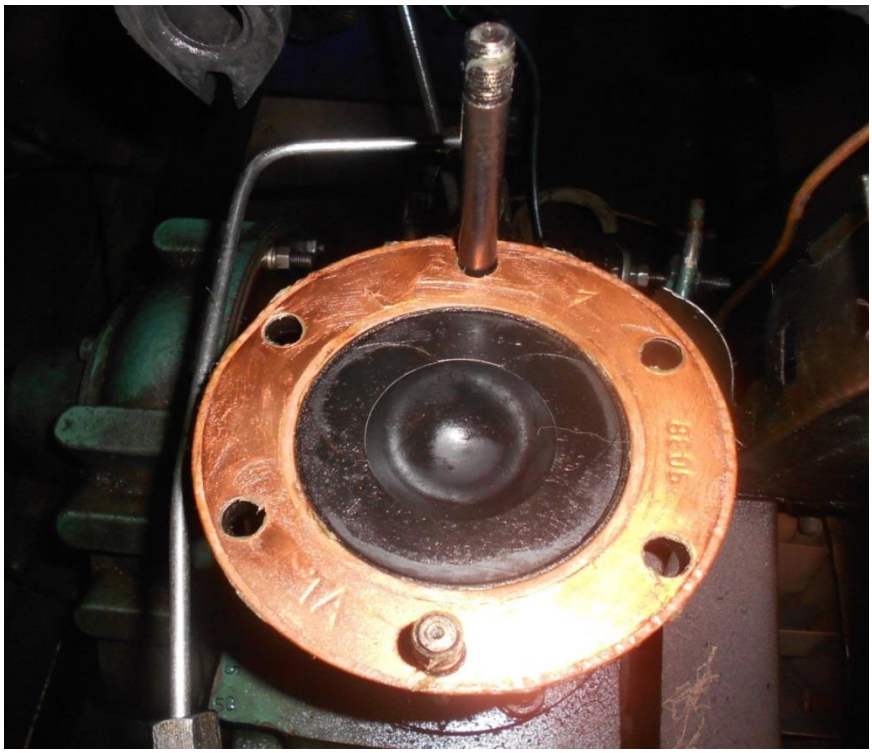

Fig. 4.16 Standard gasket fitted with cylinder block

The compression ratio below 16.5 resulted in a poor performance, and a compression ratio above 18.5 was not attainable, owing to the engine structural constraint.

The steps involved in the calculation of the compression ratio are as follows:

$$\text{Compression Ratio (CR)} = \frac{\text{Maximum cylinder volume (Vs+ Vc)}}{\text{Clearance volume (Vc)}}$$

Maximum cylinder volume = Swept volume (Vs) + Clearance volume (Vc)

$Vs = \frac{\pi\ \mathrm{d}^2}{4} \times L$ **(**Where, d = bore = 8.75 cm, L= Stroke = 11 cm)

$$CR = 17.5 = \frac{Vs + Vc}{Vc}$$

$$17.5 = \frac{Vs}{Vc} + 1$$

$$16.5 = \frac{Vs}{Vc}$$

$$V_c = \frac{V_s}{16.5} = \frac{661.45}{16.5} = 40.08\ cm^3$$

Gasket volume = 7.21 cm^3 (d= 8.75 cm, t= 0.12 cm)

For CR=18.5, Vc= $\frac{Vs}{17.5} = \frac{661.45}{17.5} = 37.79\ cm^3$

Clearance Volume excluding gasket volume+ Gasket volume = 37.79 cm^3

32.87 + Gasket volume = 37.79 cm^3

Gasket volume required for compression ratio of 18.5 = 4.92 cm^3

Gasket thickness required = 0.08 cm

In the same manner, the gasket volume and thickness required for CR=16.5 was calculated. The calculated gasket volume and thickness corresponding to the different compression ratios are given below in Table 4.1.

Table 4.1 Gasket volume and thickness required for different compression ratios

Compression ratio	**Gasket volume (cm^3)**	**Gasket thickness (cm)**
16.5	9.8	0.16
17.5	7.21	0.12
18.5	4.92	0.08

4.16.6 Oxidation stability of the JMETPO blends

Addition of a synthetic antioxidant to biodiesel has a positive role for improving the oxidation stability, but at the same time it increases the cost of fuel. However, in order to reduce the cost, some other fuel which may act as natural antioxidants can be used. The tyre pyrolysis oil (TPO) derived from the pyrolysis of waste automobile tyres contains a few phenolic compounds in it. These phenolic compounds may possibly act like antioxidants. Therefore, this investigation was aimed to investigate the effect of blending of TPO with JME on their oxidation stability and results were compared with those of the diesel-JME blends. Since the values of oxidation stability of the resultant blends did not reach the required values as per IS-15607 specification, three synthetic antioxidants i.e. TBHQ, PY and PG with a concentration of 200 ppm were mixed with the JMETPO20 (80%JME+20%TPO) blend.

The oxidation stability of biodiesel produced from different feedstocks and their blends with diesel was determined in terms of induction period (IP). The IP was calculated as per the Rancimat method EN 14112 for neat biodiesel and the modified Rancimat method EN 15751 for its diesel blends [199]. Figure 4.17 represents the schematic diagram of Rancimat apparatus. In the Rancimat apparatus, initially a stream of purified air is passed through the sample exposed to heat treatment at a specified temperature of 110 ˚C. Then the air is bubbled through the sample for the oxidation of the sample to occur. As a consequence of this process, some gases are released along with the air, which is then passed into a flask containing deionised water. The flask contains an electrode, which is linked to the apparatus for an estimation of the conductivity and its recording. The IP is measured in terms of time at which the conductivity initiates to rise very fast. The constant measurement of this conductivity provides an oxidation curve.

The point of inflection of this curve is known as the induction period. The volatile acidic gases are mainly formic acid, which also contained acetic acid and some other acids, are formed during the oxidation process and are absorbed in the water, which is the principal cause for the accelerated rise in the conductivity and the IP measurement.

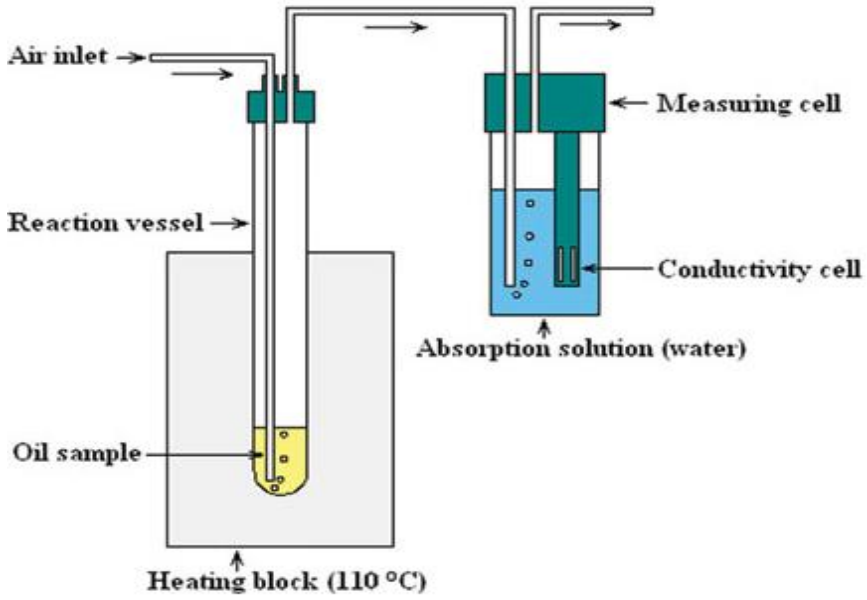

Fig. 4.17 Schematic diagram of Rancimat method

Two sets of readings one for JME-TPO and other for JME-diesel blends were recorded in this investigation. The compositions of different JME-TPO in comparison with the diesel-JME blends are given in Table 4.5. It can be noted from the table that, the JMETPO20, JMETPO40 and JMETPO60 blends have the same percentage of JME as in the B80, B60 and B40 blends respectively. At first, the oxidation stability of JME, JMETPO20, JMETPO40 and JMETPO60 blends were determined using the Rancimat apparatus and were compared with the oxidation stability of B80, B60 and B40 blends respectively. Further, three phenolic antioxidants with a dosage of 200 ppm were mixed with the JMETPO20 blend and the results of the oxidation stability were determined and compared with the B80 blend, when the same antioxidants were used with a concentration of 400 ppm.

In the next experiments, three phenolic synthetic antioxidants namely TBHQ, PY and PG were added in small quantity (200 ppm) to the JMETPO20 blend, and the resultant blends were tested as fuel in the test engine. The performance and exhaust emission results were recorded for the engine run on the JMETPO20 blend with the synthetic antioxidants and the results were compared with those of diesel, JME and JMETPO20 blend without doping of synthetic antioxidants.

4.16.7 Durability tests

Agarwal et al. [200-201] studied the wear pattern of in-cylinder engine components and lubricating oil tribology of a diesel engine fueled with B20 linseed oil methyl ester by conducting a 512 h endurance test. They reported that, wear debris were found to be lower by about 30% for the B20 fueled engine than that of diesel which was attributed to the inherent lubricating properties of the linseed oil methyl ester. For the B20 operated engine, the lubricating oil contamination was found to be low and lubricating oil life was reported longer compared to that of diesel operated engine. Another study was carriedout by Sinha et.al [202] to study the wear of in-cylinder parts and lubricating oil degradation, when 100 h endurance test was conducted in a transportation diesel engine with B20 rice bran oil methyl ester. It was reported that, for the B20 fueled engine, the wear magnitude of piston rings, bearings, cylinder liner, and cylinder head were lower than that of diesel. They also detected that, carbon deposits on the different vital parts of engine were lower for the blend in comparison with diesel attributing to the lower soot formation during combustion.

A study was done by Liaquat et al. [203] by conducting a 250 h durability test in a diesel engine operated with B20 Jatropha biodiesel and the outcomes were analyzed with respect to those of diesel. The authors analyzed the results obtained by scanning electron microscopy (SEM) and energy dispersive X-ray spectroscopy (EDX), and reported that carbon deposits on the nozzle injector tip was more for the B20 operated engine than that of diesel. They also observed the excessive wear metal concentrations and lowered value of lubricating oil viscosity for the B20 fueled engine. Wander et al. [204] have carriedout a durability test in a diesel engine operated with two types of biodiesel i.e. biodiesel produced by Soybean oil and Castor oil. From the lubricating oil analysis, they reported that there was no excessive amount of metals found for engine run on biodiesel compared to that of diesel operation, while higher carbon deposits were observed.

In the present investigation the JMETPO20 fueled engine, was run for 100 h with this optimum engine operating parameters to study short term durability issues. The visual inspection of the engine components, carbon deposits on the vital engine parts and wear assessment of lubricating oil samples drawn from the JMETPO20 blend and diesel fueled

engines were carriedout in order to compare the feasibility of the blend for long term application.

In the first phase, experiment was carriedout with 100 h of short term endurance test for diesel. The tests on the engine were carriedout as per the method recommended in IS10000, 1980 and the test cycle is given in Table 4.3**.**

Before the test, the engine was filled with new lubricating oil (SAE 20W 40) as recommended by the manufacturer and also the engine was dismantled and reassembled with a new fuel pump, fuel filter and fuel injector nozzle. Then the reassembled engine was run for 100 h with diesel as fuel. Further engine operating parameters such as injection timing, nozzle opening pressure and compression ratio were set at optimum for the JMETPO20 blend, as found earlier by the authors.

Then a similar short-term endurance test was repeated with the engine running with the JMETPO20 blend and the results of lubricating oil tribology were analyzed and compared with diesel operated engine. During short-term endurance test, the effect due to the use of the JMETPO20 blend on different vital parts of the engine was studied. The assessment of wear of several parts of the JMETPO20 blend and diesel fueled engines was carriedout after dismantling the various parts of the engine. For various tribological wear assessment analyses, the lubricating oil samples were drawn after a regular interval of 25 h of engine operation for both the test fuels. During each test cycle, the engine ran satisfactorily throughout the entire test and did not show any trouble, when run with the JMETPO20 blend. Figure 4.18 shows the photographic views of the dismantled engine before the start of endurance test.

Fig. 4.18 Photograph of the dismantled engine during durability test

The preliminary run for the engine fueled with the JMETPO20 blend was carriedout to make sure that, the engine run without any problem, by operating the engine for their running-in period. Initially constant speed engines were put to a preliminary run of 49 h under the operating temperature recommended by the engine manufacturer, in nonstop cycles of 7 h each, as per the engine loading cycle for the preliminary run shown in Table 4.2 [205]. In the preliminary run, concern was given to the engine vibration and its smoothness.

Table 4.2 Loading cycle pattern for preliminary runs of constant speed engine

Load applied (% of rated load)	Running time (h)
25	1.5
50	2
75	1.5
100	2

4.16.7.1 Atomic absorption spectroscopy

Atomic absorption spectroscopy (AAS) is a very common technique known to detect the wear metal debris concentration in the used engine lubricating oil. Its working principle is based on the absorption of light, where atoms in the vapor-state absorb radiation at a particular wavelength that is specifically defined and the amount of absorption indicates a specific atomic element. The hollow cathode lamp was used as a source of radiation where a beam of a particular wavelength projects (through a pure air-acetylene flame) on to a sensor and the quantity of radiation received at the photo sensor was noted. The fluid sample was introduced into the flame and vaporized. The quantity of radiation arriving at the photo sensor was

decreased in extent to the amount of the well-defined element present in the sample. The schematic layout of AAS is shown in Figure 4.19.

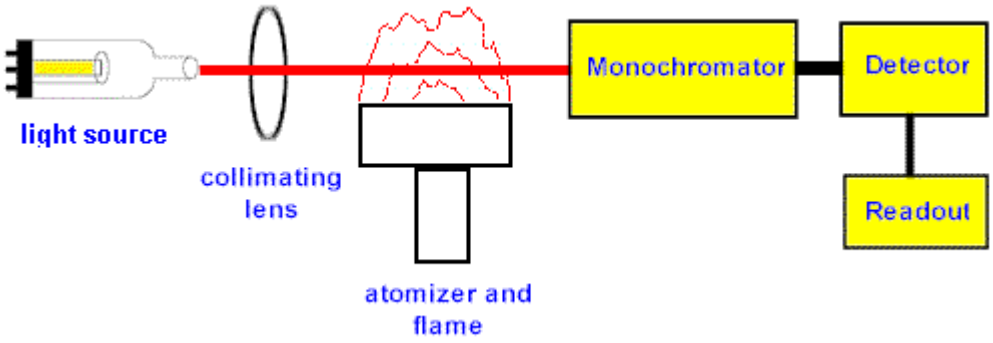

Fig. 4.19 Schematic diagram of atomic absorption spectroscopy

This spectrometric analysis can be used to get the information related to the amount of the particular element avaiable in the sample. This test of AAS was done to find the concentration of various metal elements such as Fe, Cr, Cu, Zn, Mg, Pb, and Co present in the lubricating oil samples after and before the endurance test when engine was run with the JMETPO20 blend and diesel.

Chapter 5

Results and Discussion

5.1. General

In this research study, attempts were made to explore the possibilities of running a diesel engine fully on a non-petroleum fuel blend. For this, experiments were carried out in a naturally aspirated, single cylinder, four stroke, air cooled, direct injection (DI) diesel engine with a rated power of 4.4 kW at a constant speed of 1500 rpm run on different Jatropha methyl ester (JME)-tyre pyrolysis oil (TPO) blends, and the results are compared with diesel and presented in the same order. The TPO at low percentages (10-50% at regular intervals of 10% on a volume basis), was blended with the JME at 90 to 50% respectively, to get the fuel blends for the investigation. Initially diesel, JME and the JMETPO blends were tested in an unmodified engine conditions i.e. injection timing of 23 ˚CA bTDC, nozzle opening pressure of 200 bar and compression ratio of 17.5:1. The results of the combustion, performance and emission characteristics of the engine run on JMETPO blends were analysed and compared with those of the diesel operation of the same engine. Further, principal component analysis (PCA) was integrated with a technique VlseKriterijumska Optimizacija I Kompromisno Resenje (in Serbian) (VIKOR) to determine an optimum blend. The experimental results of the combustion, performance and emission parameters of the diesel engine operated with different JMETPO blends at different load conditions were used for optimization. Furthermore, the experiments were carriedout with the optimum blend to find the optimum engine design parameters such as injection timing, nozzle opening pressure and compression ratio for it. The results obtained by blending TPO with the JME on their oxidation stability are also further discussed in the following sections. In addition to these, the performance and exhaust emission studies were carriedout in test engine run on the optimum blend with the synthetic antioxidants, and the results were compared with those of diesel, JME and JMETPO20 blend without doping of synthetic antioxidants. Finally, this chapter also presents the results that were obtained from the 100 h short term endurance test, conducted on the same engine with the optimum blend.

5.2 Combustion, performance and emission characteristics of the engine fueled with JME-TPO blends

This section discusses the results of the combustion, performance and emission parameters obtained from the test engine run on diesel, JME and different JMETPO blends. Some of the important results of this section have already been published in a reputed journal which is given in the list of paper published. The designations of the test fuels and their compositions used in this study are given below.

Fuel	JME (by volume)	TPO (by volume)	Diesel (by volume)
Diesel	-	-	100%
JME	100%	-	-
JMETPO10	90%	10%	-
JMETPO20	80%	20%	-
JMETPO30	70%	30%	-
JMETPO40	60%	40%	-
JMETPO50	50%	50%	-

5.2.1 Combustion Parameters

5.2.1.1 Cylinder pressure history

Figure 5.1 depicts the comparison of the cylinder pressure histories of the JME and JMETPO blends with diesel at full load condition. In a compression ignition (CI) engine, the peak cylinder pressure depends on the burned fuel fraction during the premixed burning phase, i.e., the initial stages of combustion. The cylinder pressure characterizes the ability of the fuel to mix well with air and burn [206].

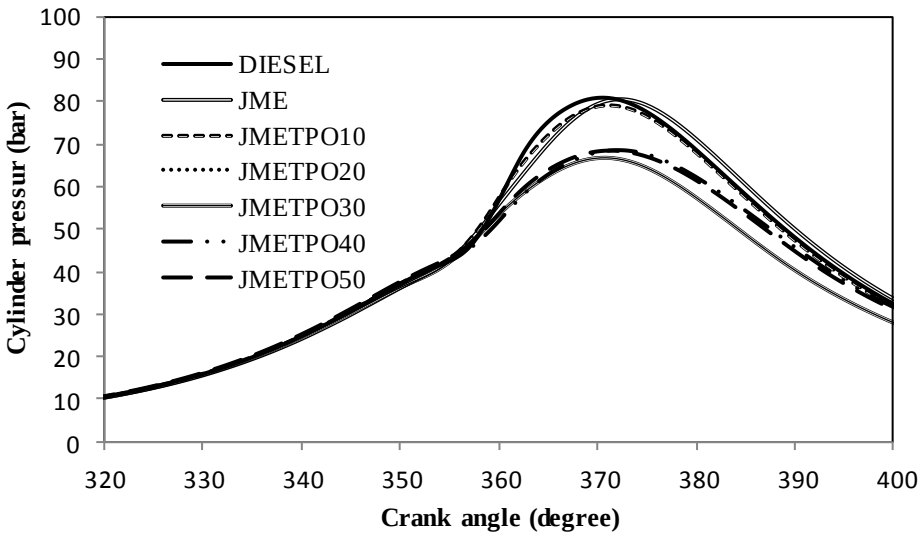

Fig. 5.1 Variation of cylinder pressure with crank angle at full load

The JMETPO blends follow a cylinder pressure pattern similar to that of diesel at full load condition. The commencement of ignition for JME is by about 2 ˚CA earlier than that of diesel at full load. In the case of the JMETPO10 and JMETPO20 blends, it is earlier by about 1 ˚CA than that of diesel. The oxygen content and higher cetane number of JME are the reasons for the earlier ignition of these blends and JME, than that of diesel at full load. When the TPO percentage is increased to 30, 40 and 50 in the JMETPO blend, the commencement of ignition is earlier by about 1 ˚CA than that of diesel at full load. The reduced oxygen content of JMETPO30, JMETPO40 and JMETPO50 may postpone the ignition to later than that of JME, JMETPO10 and JMETPO20 at full load.

5.2.1.2 Ignition delay

The ignition delay period in a CI engine is a very important parameter that influences subsequent combustion processes, engine performance, and exhaust emissions. The ignition delay is evaluated as the time difference measured in the crank angle between the start of injection and the start of ignition [207]. The variations of ignition delay with brake power for the fuels tested in this study are portrayed in Figure 5.2. It can be observed from the figure, that the ignition delay of diesel is longer in comparison with JME, JMETPO10, and JMETPO20 at full load. This may be due to the higher cetane number of JME, which gives better ignition quality. In addition to this, the presence of oxygen results in improved chemical reactions and more complete combustion.

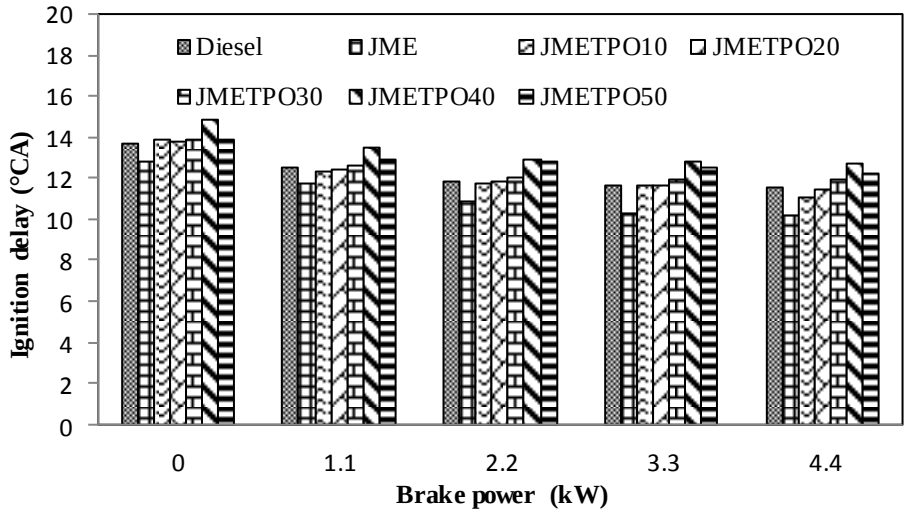

Fig. 5.2 Variation of ignition delay with brake power

It is to be noted that, further increasing the percentage of TPO in blend, the ignition delay becomes longer for the JMETPO30, JMETPO40, and JMETPO50 blends, due to the lower cetane number of the injected fuel. The values of ignition delay for diesel, JME,

JMETPO10, JMETPO20, JMETPO30, JMETPO40 and JMETPO50 are 11.5, 10.2, 11, 11.4, 11.9, 12.7 and 12.1 ˚CA respectively at full load. The JMETPO10 shows the shortest ignition delay at full load among all the blends tested in this study.

5.2.1.3 Heat release rate

The amount of heat release in the premixed combustion of a CI engine depends on the ignition delay, air fuel mixing rate and the heating value of the fuel [208]. Figure 5.3 illustrates the heat release rate pattern with respect to the crank angle at full load.

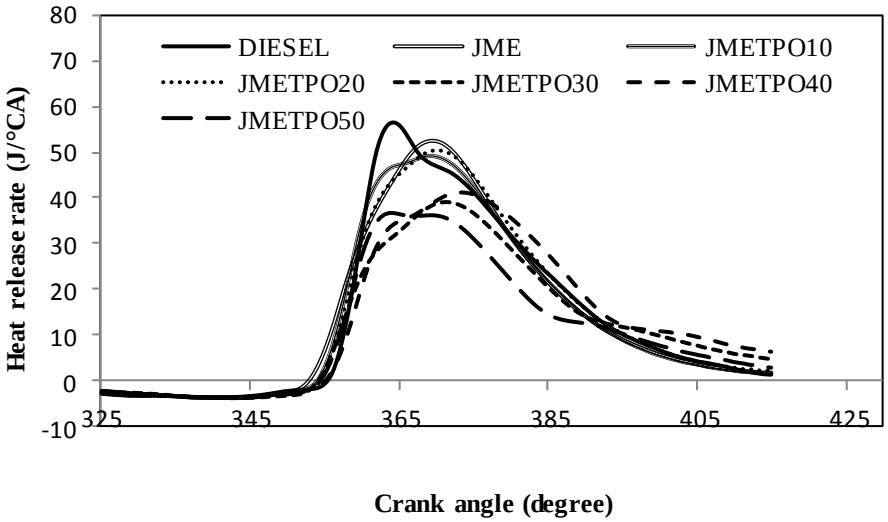

Fig. 5.3 Variation of heat release rate with crank angle at full load

It is apparent from the figure, that the maximum heat release rate is the highest for diesel and the lowest for JMETPO50 at full load. The diesel curve is followed by that of JME, JMETPO20, JMETPO10, JMETPO40, JMETPO50 and JMETPO30 at full load. The accumulation of diesel is more in the delay period, which releases the maximum heat, as it has a higher calorific value. The heat release rates for JME and its TPO blends are lower due to their shorter ignition delays and higher viscosities than that of diesel at full load. The JMETPO20 gives the maximum heat release rate compared to the other JMETPO blends at full load. The different boiling point compounds present in TPO may undergo chemical reactions with JME, and result in a higher heat release rate. The maximum heat release rates for diesel and JME are 56.4 and 52.4 J/˚CA respectively at full load. The maximum heat release rate for JMETPO20 is recorded as 50.4 J/˚CA at full load.

5.2.1.4 Combustion duration

The combustion duration is described as the time duration required by the combustion process to reach 90% of its mass fractions burned [209]. Figure 5.4 depicts the variation of the combustion duration for diesel, JME and JMETPO blends with brake power. It can be observed from the figure, that the combustion duration increases with increase in the brake power for all the tested fuels, which may be due to the increase in the quantity of fuel injected. It is also evident from the figure, that the combustion duration is shorter for JME, JMETPO10, and JMETPO20 compared to that of diesel operation at full load. This may be attributed to the oxygen content of JME which improves the oxidation and ensures the completion of initial stage of diffusion combustion in the fuel rich zones and results in higher in-cylinder temperatures.

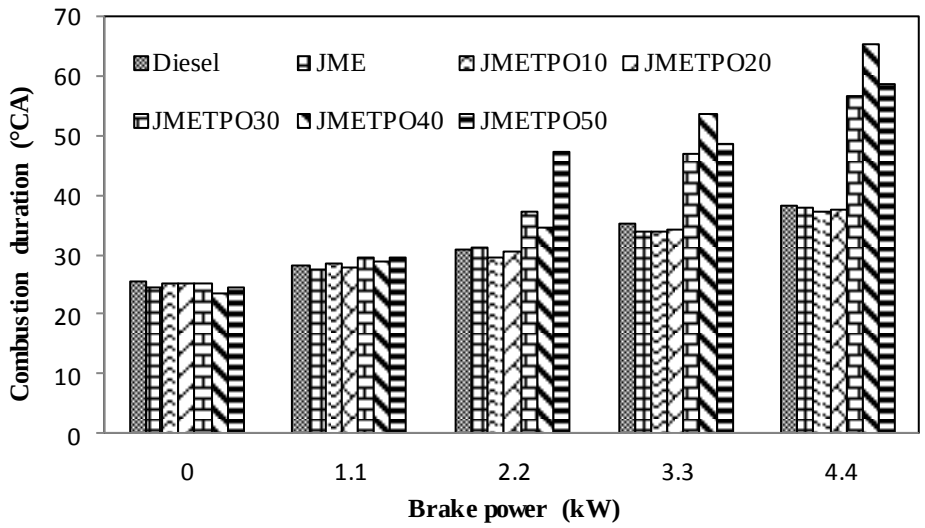

Fig. 5.4 Variation of combustion duration with brake power

Similar results are reported by Tse et al. [210] in his investigation of the combustion and particulate emissions analysis of a waste cooking oil methyl ester (WCOME)-diesel blend fueled DI diesel engine. Increasing the TPO percentage in the JMETPO blends, results in longer combustion duration. This may be due to the high boiling point compounds present in TPO, and its lower cetane number, which takes more time for the chemical reaction [211]. At full load, the values of the combustion duration for diesel are 38.3 ˚CA, while the values are 37.9, 37.3, 37.8, 56.9, 65.4, and 58.9 ˚CA for JME, JMETPO10, JMETPO20, JMETPO30, JMETPO40 and JMETPO50 respectively.

5.2.1.5 Maximum cylinder pressure

The variation of the maximum cylinder pressure at different values of brake power is shown in Figure 5.5. The maximum cylinder pressure is the highest for diesel, than that of JME and its TPO blends at full load. The reason is that more diesel fuel is accumulated in the delay period as a result of longer ignition delay.

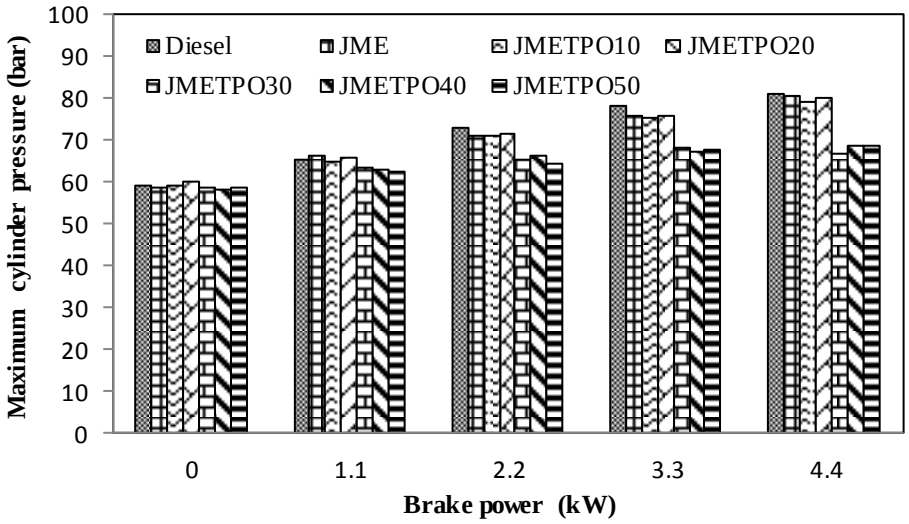

Fig. 5.5 Variation of maximum cylinder pressure with brake power

The maximum cylinder pressures for diesel, JME, JMETPO10 JMETPO20, JMETPO30, JMETPO40 and JMETPO50 at full load operation are approximately 81, 80.6, 79.2, 80, 66.8, 68.6 and 68.5 bar respectively. The maximum cylinder pressure decreases with the increase in the percentage of TPO in the blend after 20%. In the case of JMETPO30, JMETPO40 and JMETPO50 the maximum cylinder pressures are lower as a result of lower heat release rates. The JMETPO20 gives the highest maximum cylinder pressure of 80 bar in comparison with the other JMETPO blends at full load.

5.2.1.6 Maximum rate of pressure rise

Figure 5.6 depicts the variations in maximum rate of pressure rise with brake power for diesel, JME and JMETPO blends. The rate of pressure rise is the first derivative of cylinder pressure, that relates to the smoothness of the engine operation. The maximum rate of pressure rise increases initially with load, and then decreases due to the prominent influence of the premixed phase at lower loads, while the role of the diffusion phase of combustion remains significant at higher loads [212]. It is known that the premixed combustion rate depends upon the ignition delay period. The maximum rate of pressure rise is higher for diesel at full load. This is due to the fact that, ignition delay period of

diesel is longer than JME and the premixed heat release is higher for the diesel fuel operation. Similar reasons are mentioned by Rajendiran et al. [213], in their research work on the combustion analysis of a diesel engine fueled with different palm oil methyl ester (POME)-diesel blends.

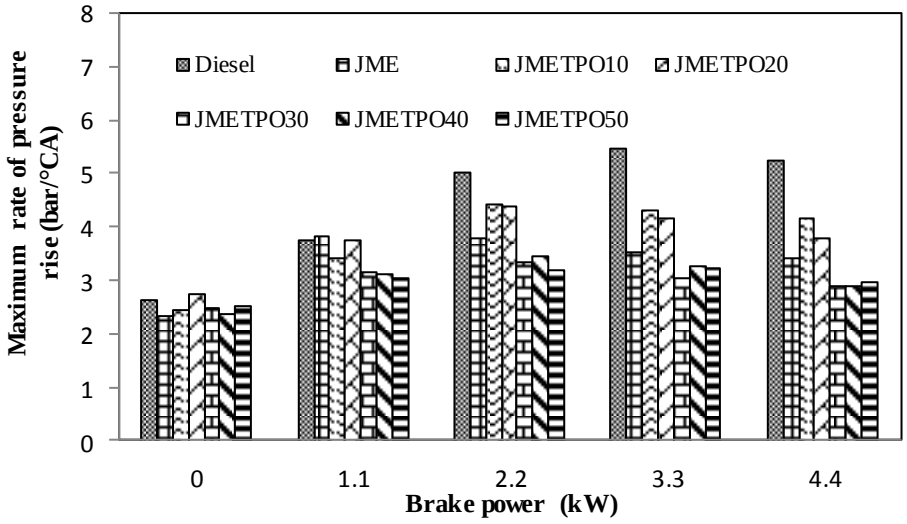

Fig. 5.6 Variation of maximum rate of pressure rise with brake power

The maximum rates of pressure rise are 5.3, 3.4, 4.2, 3.8, 2.9, 2.9, and 3 bar/˚CA for diesel, JME, JMETPO10, JMETPO20, JMETPO30, JMETPO40 and JMETPO50 at full load respectively. Interestingly, the rates of pressure rise for the JMETPO blends are much lower than that of diesel except JMETPO10 and JMETPO20 at full load. At low and part load operations, the rate of pressure rise is unpredictable, because of the aromatic nature of the TPO.

5.2.2 Performance parameters

5.2.2.1 Brake thermal efficiency

Figure 5.7 portrays the variations in the brake thermal efficiency with brake power for diesel, JME and the JMETPO blends. Brake thermal efficiency is the ratio between the power output and the energy introduced through fuel injection, the latter being the product of the injected fuel mass flow rate and the lower heating value of the fuel. The brake thermal efficiency for diesel is 29.89% at full load, which is the highest among all the fuels tested in this study. For JME, JMETPO10, JMETPO20, JMETPO30, JMETPO40 and JMETPO50, it is 28.61, 29.87, 29.88, 26.6, 26.9 and 27.86% respectively at full load. The brake thermal efficiency of diesel, JME and JMETPO blends increases with increase in brake power. As the brake power increases the heat generated in the cylinder increases, and hence, the thermal efficiency increases.

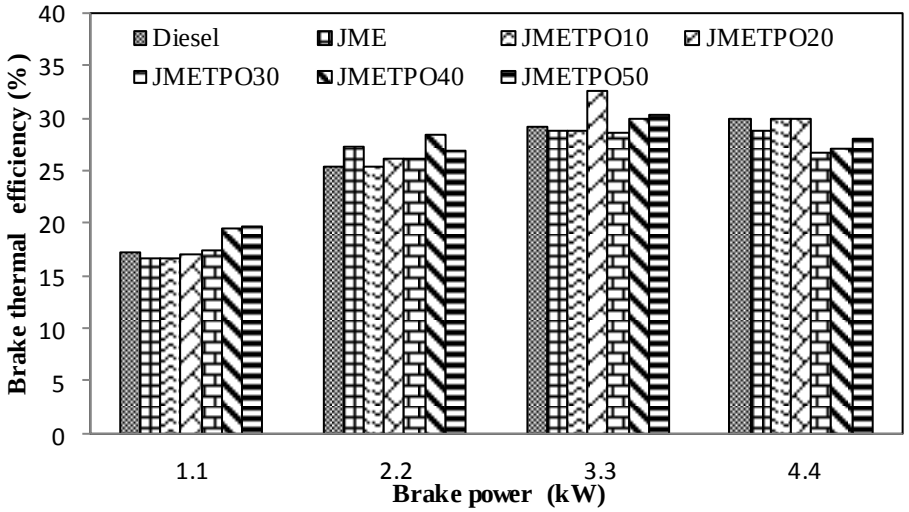

Fig. 5.7 Variation of brake thermal efficiency with brake power

The brake thermal efficiency of the JMETPO blends is lower than that of diesel and JME at full load, as a result of higher density, and poor volatility [214]. At low loads, the thermal efficiency is much lower for the JMETPO blends than that of diesel. At full load the brake thermal efficiency is higher for JMETPO20 compared to the other blends. Gopal et al. [215] reported similar reason for the results they obtained in a diesel engine run on palm oil biodiesel and its diesel blend.

5.2.2.2 Brake specific energy consumption

The brake specific fuel consumption (BSFC) is not a very reliable factor to compare the two fuels, as the calorific value and the density of the blends are marginally different [216]. The brake specific energy consumption (BSEC) is described as the multiplication of the BSFC and lower calorific value of the fuel. Figure 5.8 depicts the variation of BSEC for diesel, JME and the JMETPO blends, with respect to brake power. The BSEC for diesel is by about 11.86 MJ/kWh at full load. For the fuels JME, JMETPO10, JMETPO20, JMETPO30, JMETPO40 and JMETPO50, it is 12.55, 12.67, 12.79, 13.5, 13.69 and 13.92 MJ/kWh respectively. With the increase in brake power, the BSEC decreases for diesel, and JME as well as for all the JMETPO blends. The engine consumes more fuel with the JMETPO blends than with diesel, to develop the same power output, due to the lower calorific value of the JMETPO blends. This is because the energy content of both JME and TPO is lower compared to that of diesel, which leads to injection of higher quantities of the fuel for the same power output in comparison with diesel.

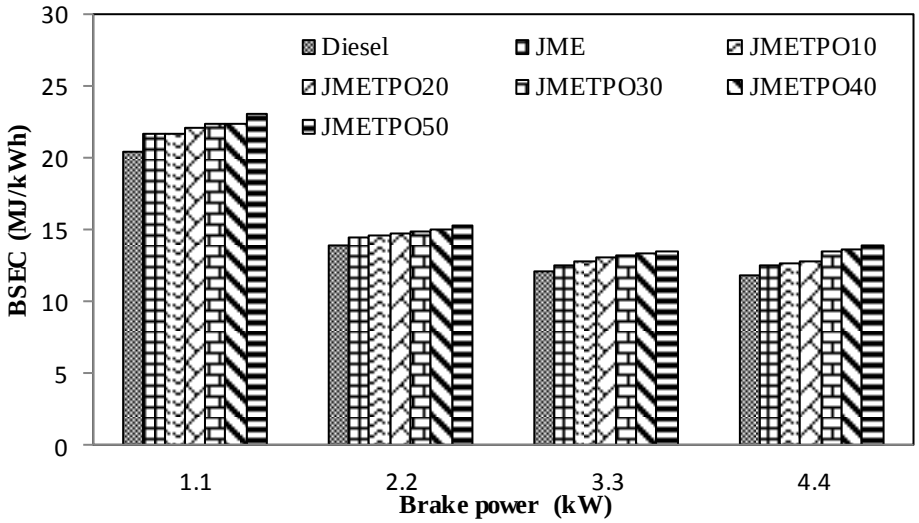

Fig. 5.8 Variation of BSEC with brake power

Similar result was reported by Labeckas and Slavinskas [217] that the BSEC increased with the increasing proportion of rapeseed oil methyl ester (ROME) in the blends. The BSEC is the lowest for JMETPO10; further increasing TPO percentage results higher BSEC due to its lower calorific value.

5.2.2.3 Exhaust gas temperature

Figure 5.9 illustrates the variations of the exhaust gas temperature with brake power for different fuels tested in this study. The exhaust gas temperature gives an indication about the amount of heat going waste with the exhaust gases.

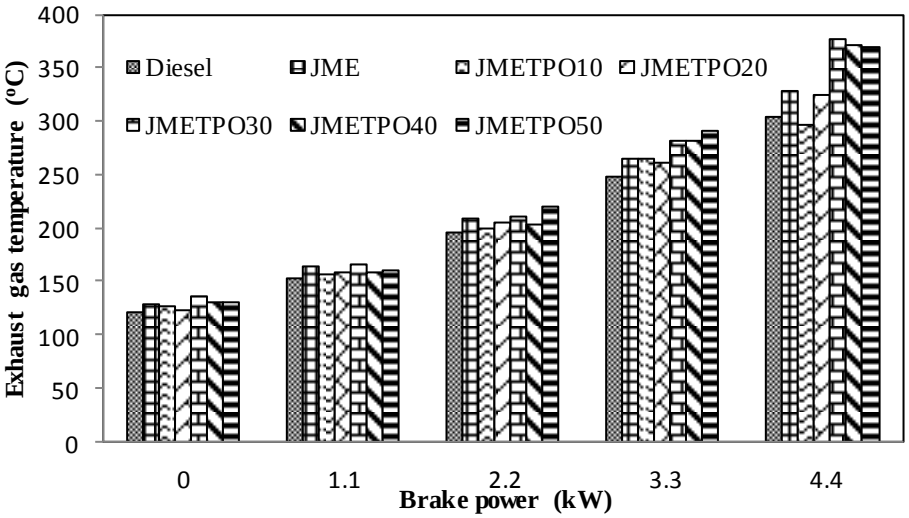

Fig. 5.9 Variation of exhaust gas temperature with brake power

It can be observed from the figure that, with the increase in brake power the exhaust gas temperature increases for all the tested fuels. This is due to the fact that the amount of fuel

injected into the combustion chamber of the diesel engine increased with the engine load to obtain the same engine torque [218]. The exhaust gas temperature value for diesel at full load was 303 ˚C. It can also be observed that the values of the exhaust gas temperature are found to be about 329, 297, 325, 376, 371 and 369 ˚C for JME, JMETPO10, JMETPO20, JMETPO30, JMETPO40 and JMETPO50 respectively at full load. As a result of increased combustion duration, a higher exhaust gas temperature is recorded for the JMETPO blends.

5.2.3 Emission parameters

5.2.3.1 Brake specific carbon monoxide emission

Figure 5.10 shows the trend of brake specific carbon monoxide (BSCO) emission for diesel, JME and the JMETPO blends, with respect to brake power. Carbon monoxide (CO) emission is an intermediate combustion product and is formed mainly due to incomplete combustion of fuel. If combustion is complete, then CO is oxidized to CO_2. If the combustion is incomplete due to shortage of air or due to low gas temperature, CO will be formed. Usually, the CO emission of diesel engines is low, because diesel combustion is occurred with lean mixture and has an abundant amount of air [219]. It can be observed from the figure that, the BSCO emission in g/kWh decreases with increase in brake power.

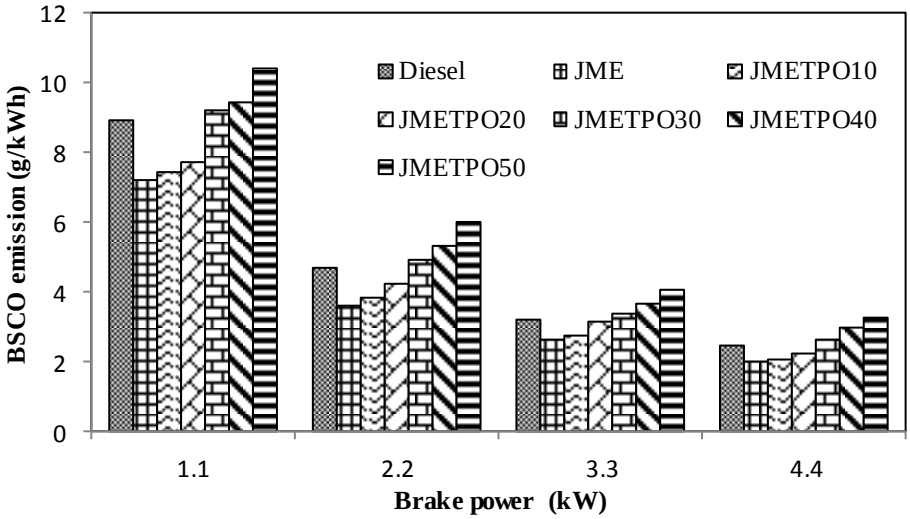

Fig. 5.10 Variation of BSCO emission with brake power

The BSCO emission is lower for JME, JMETPO10 and JMETPO20 compared to that of diesel at full load, because the excess oxygen present in the JME is helpful for better combustion. Nabi et al. [220] documented a similar reason for the results they obtained from a diesel engine run on cotton oil methyl ester (COME) and its diesel blends. The values of BSCO emission for diesel, JME, JMETPO10, JMETPO20, JMETPO30,

JMETPO40 and JMETPO50 are 2.45, 1.99, 2.07, 2.22, 2.6, 2.94 and 3.28 g/kWh respectively, at full load operation.

5.2.3.2 Brake specific hydrocarbon emission

The variation of brake specific hydrocarbon (BSHC) emission with respect to brake power for diesel, JME and the JMETPO blends is shown in Figure 5.11. Hydrocarbon (HC) emission is product of incomplete combustion. Thus at higher engine loads, the higher combustion temperature promotes more complete combustion and hence less HC emission [221]. The BSHC emission is lower at part load, but tends to increase at higher loads for all the fuels investigated in this study.

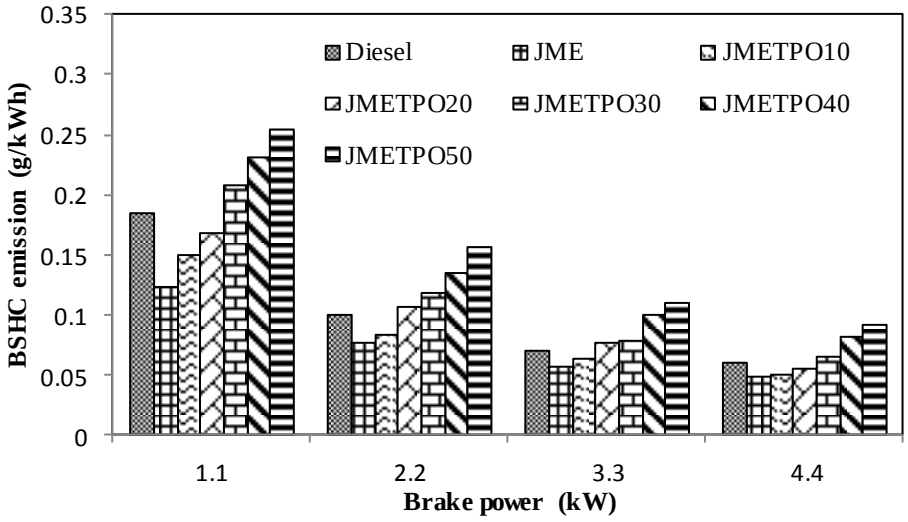

Fig. 5.11 Variation of BSHC emission with brake power

For JME, JMETPO10 and JMETPO20, the BSHC emission is found to be lesser compared to that of diesel. This could be due to the complete combustion of JME**.** Similar reason was reported by Canakci [222], when they conducted experiments in a diesel engine fueled with soybean oil methyl ester (SOME) and its diesel blends. But further addition of the TPO in the blend results in higher HC emission. This is because; the TPO has higher aromatic content, and hence may result in incomplete combustion and more BSHC emission for JMETPO30, JMETPO40 and JMETPO50 compared to the other fuels tested. The BSHC values for diesel, JME, JMETPO10, JMETPO20, JMETPO30, JMETPO40 and JMETPO50 are 0.059, 0.047, 0.049, 0.054, 0.065, 0.081, and 0.092 g/kWh at full load.

5.2.3.3 Brake specific nitric oxide emission

Two important factors affecting the formation of nitric oxide (NO) in a CI engine are the combustion temperature and the availability of oxygen. Figure 5.12 portrays the variations of brake specific nitrogen oxide (BSNO) emission with brake power for diesel, JME and the JMETPO blends. The BSNO emission for diesel, JME and all the JMETPO blends increases as the brake power increases. This is expected, because with increasing brake power, the temperature prevailing in the combustion chamber increases. The BSNO emission is higher for JME and the JMETPO blends compared to that of diesel at all loads. This may be due to the availability of the excess oxygen present in JME.

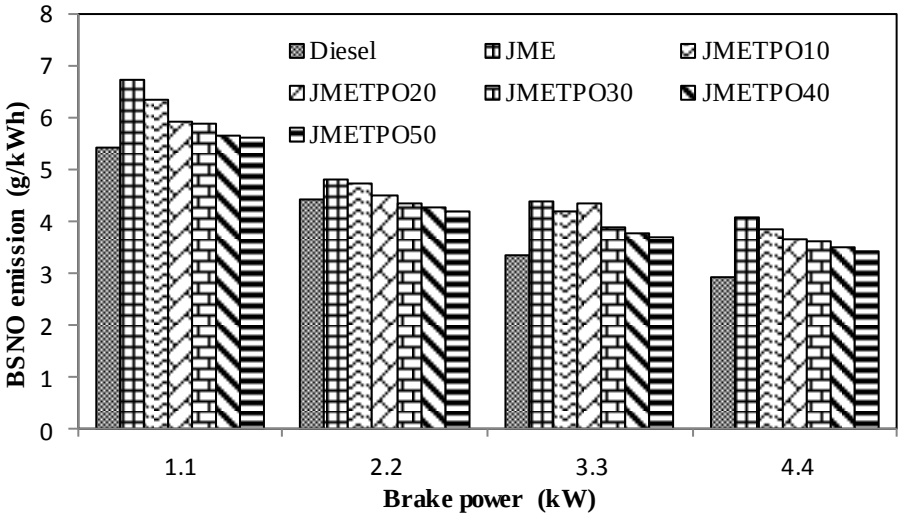

Fig. 5.12 Variation of BSNO emission with brake power

This result indicates that higher oxygen levels in the combustion chamber when using JME and its blend, which helps to promote NO formation reactions. This statement can be justified with the reason stated by Tan et al. [223] in their research paper. While increasing the TPO percentage, the BSNO emission decreases, because of lower heat release rates attained in the premixed combustion phase than that of JME. This can also be evidenced from Fig. 5.3 The values of BSNO emission for diesel, JME, JMETPO10, JMETPO20, JMETPO30, JMETPO40 and JMETPO50 are 2.91, 4.04, 3.81, 3.63, 3.59, 3.49, and 3.4 g/kWh respectively, at full load operation.

5.2.3.4 Smoke opacity

Smoke opacity strongly depends on engine load and is the result of incomplete combustion which is formed in the rich mixture zone in the combustion chamber [224]. Figure 5.13 illustrates the smoke opacity measured in the engine exhaust, for the fuels

tested in this study. With increase in the brake power, the air fuel ratio decreases as the fuel injected increases, and hence results in higher smoke.

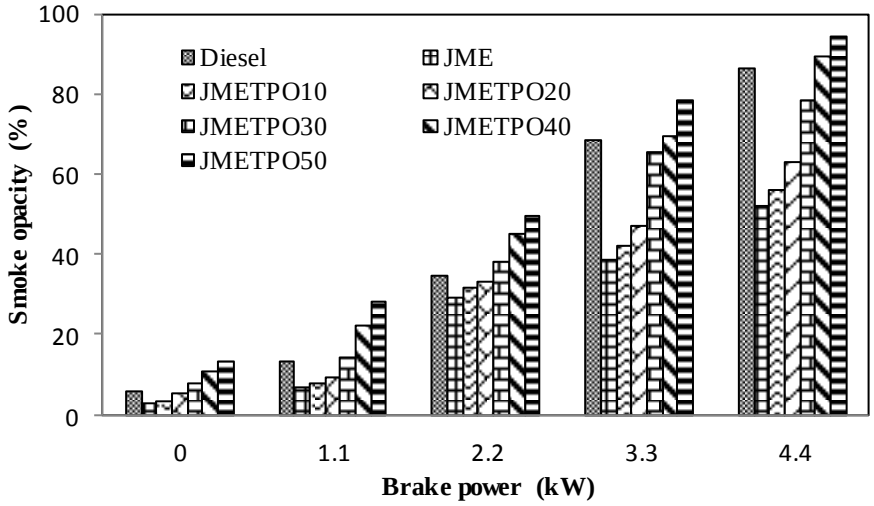

Fig. 5.13 Variation of smoke opacity with brake power

In comparison with diesel, the smoke opacity is less for JME, JMETPO10 and JMETPO20, and more for JMETPO30, JMETPO40 and JMETPO50 at all loads. The presence of oxygen in the JME may be helpful in breaking the aromatic content that is available in less percentage with JMETPO10 and JMETPO20. But, further increase of the TPO percentage, results in an increased aromatic content, which gives higher smoke opacity. The longer ignition delay and longer combustion duration are also the reasons for higher smoke opacity in the case of JMETPO30, JMETPO40 and JMETPO50. The smoke opacity values for diesel, JME, JMETPO10, JMETPO20, JMETPO30, JMETPO40 and JMETPO50 are by about 86.3, 52.2, 56.2, 63.1 78.3, 89.1, and 94.2% respectively, at full load.

5.2.4 Summary

In this study, five different JMETPO blends namely JMETPO10, JMETPO20, JMETPO30, JMETPO40 and JMETPO50 were used as alternative fuels in a single cylinder, four stroke, air cooled, DI diesel engine, and combustion, performance and emission behaviour of the engine fueled with JMETPO blends, were compared with those of diesel and JME operation. There was a marginal reduction in the brake thermal efficiency with 30%, 40% and 50% TPO in the blend at full load compared to other blends. The combustion and emission behaviour of the engine deviated after 20% TPO in

the blend. During the tests, the engine ran satisfactorily through the entire duration, and did not show any difficulty, when fueled with the JMETPO20 blend.

The summary of the values obtained at full load for some of the important parameters related to the combustion, performance and emission parameters of the test engine run on diesel, JME and JMETPO blends are given in Appendix 6.

The next section presents the optimization of JMETPO blends. In that chapter, in the proposed model, principal component analysis (PCA) was integrated with technique for VlseKriterijumska Optimizacija I Kompromisno Resenje (in Serbian) (VIKOR) to determine the optimum blend.

5.3 The best JMETPO blend selection based on MCDM-VIKOR

In the previous section, experiments were carried out in a naturally aspirated single cylinder, four stroke, air cooled, direct injection (DI) diesel engine with a rated power of 4.4 kW at a constant speed of 1500 rpm that was run on different Jatropha methyl ester (JME)-tyre pyrolysis oil (TPO) blends. This section describes an application of hybrid Multi Criteria Decision Making (MCDM) technique for the selection of optimum JMETPO blend for the test engine.

5.3.1 VIKOR computation

The testing of engine under all possible conditions and fuel cases is both time consuming and expensive too. In the aspect of attaining sustainability of engine performance, it is essential to identify the best blend. Several engine parameters have to be considered before selecting the optimum blend. Therefore a new approach has been employed to develop hybrid MCDM techniques namely VlseKriterijumska Optimizacija I Kompromisno Resenje (in Serbian) (VIKOR) for ranking the blend alternatives. The proposed model, principal component analysis was integrated with a technique VIKOR to determine an optimum JMETPO blend. The experimental results of combustion, performance and emission parameters of the diesel engine operated with different JMETPO blends at different load conditions were used for optimization. The optimization method has already been discussed in Chapter 4. The results obtained in this optimization are discussed in this chapter.

The experimental results were normalized using Eq. 4.8 given in Chapter 4. The resulting normalized decision matrix is shown in Table 5.3. The normalized values of the multiple responses lie between 0 and 1.

The PCA is used for deciding the weight for each parameter. The sum of total weights is equal to unity. Minitab 16.0 software was used to calculate the principal components for combustion, performance and emission parameters of the diesel engine operated with different JMETPO blends at different load conditions. The brake thermal efficiency (BTE), maximum cylinder pressure (P_{max}), maximum heat release rate (MHRR) were considered as higher-is-better (HB) type characteristic while brake specific energy consumption (BSEC), brake specific carbon monoxide (BSCO) emission, brake specific hydrocarbon (BSHC)

emission, brake specific nitric oxide (BSNO) emission and smoke opacity lower is better (LB) criteria was preferred for diesel engine point of view. The weightage for BTE, BSEC, exhaust gas temperature (EGT), ignition delay (ID), combustion duration (CD), P_{max}, maximum rate of pressure rise (MRPR), MHRR, BSCO, BSHC, BSNO and smoke opacity are 0.15, 0.08, 0.09,0.1,0.05.0.11,0.08,0.11,0.03,0.03,0.08 and 0.08 respectively. The final weights obtained for the criteria are calculated by using Eq. 4.16 and are shown in Table 5.3. Table 5.4 shows the utility and regret measure values corresponding to each test.

Table 5.1 Experimental values of combustion, performance and emission parameters for diesel, JME and JMETPO blends

Trial no	Input parameters		Output parameters											
	Load (%)	Fuel	BTE	BSEC	EGT	ID	CD	P_{max}	MRPR	MHRR	BSCO	BSHC	BSNO	Smoke
1	0	Diesel	0	0.00	120	13.67	25.6	59.31	2.63	29.45	0.00	0.00	0.00	5.6
2	0	JME	0	0.00	128	12.76	24.59	58.46	2.33	23.8	0.00	0.00	0.00	2.8
3	0	JMETPO10	0	0.00	126	13.89	25.41	59.08	2.45	28.54	0.00	0.00	0.00	3.4
4	0	JMETPO20	0	0.00	122	13.71	25.2	60.33	2.74	30.04	0.00	0.00	0.00	5.4
5	0	JMETPO30	0	0.00	136	13.83	25.24	58.84	2.51	26.32	0.00	0.00	0.00	7.9
6	0	JMETPO40	0	0.00	131	14.81	23.53	58.18	2.37	29.46	0.00	0.00	0.00	10.6
7	0	JMETPO50	0	0.00	130	13.84	24.69	58.7	2.52	27.92	0.00	0.00	0.00	13.2
8	25	Diesel	17.2	20.45	152	12.47	28.3	65.6	3.76	41.3	8.93	0.18	5.43	13.2
9	25	JME	16.5	21.65	163	11.69	27.66	66.51	3.83	34.51	7.22	0.12	6.71	6.9
10	25	JMETPO10	16.51	21.78	157	12.29	28.7	64.83	3.41	35.35	7.47	0.15	6.34	7.9
11	25	JMETPO20	16.89	21.12	152	12.31	27.9	65.79	3.75	36.34	7.71	0.17	5.91	9.4
12	25	JMETPO30	17.29	22.39	166	12.54	29.66	63.29	3.15	31.34	9.22	0.21	5.85	14.2
13	25	JMETPO40	19.4	22.48	159	13.47	29.07	62.85	3.13	36.08	9.45	0.23	5.64	22.3
14	25	JMETPO50	19.6	23.05	160	12.85	29.63	62.3	3.05	33.27	10.45	0.25	5.61	28
15	50	Diesel	25.2	13.93	196	11.81	31.02	73.17	5.02	49.73	4.68	0.10	4.40	34.5
16	50	JME	27.25	14.44	209	10.82	31.3	71.07	3.79	34.94	3.62	0.08	4.81	29.3
17	50	JMETPO10	25.25	14.60	199	11.79	29.77	71.16	4.42	44.34	3.85	0.08	4.72	31.5
18	50	JMETPO20	25.96	14.11	192	11.71	30.8	71.68	4.38	42.02	4.22	0.11	4.47	33.1
19	50	JMETPO30	25.96	14.96	210	12.01	37.23	65.15	3.37	35.01	4.94	0.12	4.31	38.2
20	50	JMETPO40	28.4	15.10	203	12.81	34.54	66.36	3.45	39.72	5.30	0.13	4.26	45.1
21	50	JMETPO50	26.8	15.25	220	12.8	47.47	64.45	3.19	34.42	6.04	0.16	4.18	49.3
22	75	Diesel	29.12	12.05	247	11.62	35.24	78.18	5.47	56.53	3.19	0.07	3.33	68.2
23	75	JME	28.62	12.55	265	10.26	34.14	76.07	3.55	42.87	2.62	0.06	4.36	38.5
24	75	JMETPO10	28.69	12.75	265	11.69	33.86	75.44	4.33	45.51	2.75	0.06	4.17	42
25	75	JMETPO20	32.46	12.02	255	11.52	34.4	75.71	4.17	44.01	3.13	0.08	4.31	47

26	75	JMETPO30	28.56	13.29	282	11.89	46.96	68.42	3.06	36.14	3.38	0.08	3.85	65.2
27	75	JMETPO40	29.9	13.35	282	12.77	53.7	67.39	3.26	36.01	3.68	0.10	3.74	69.3
28	75	JMETPO50	30.21	13.49	291	12.48	48.59	67.7	3.24	36.69	4.07	0.11	3.67	78.2
29	100	Diesel	29.89	11.87	303	11.51	38.34	80.96	5.25	56.41	2.45	0.06	2.91	86.3
30	100	JME	28.61	12.55	329	10.15	37.89	80.6	3.41	52.43	1.99	0.05	4.05	52.2
31	100	JMETPO10	29.8	12.67	297.3	11.49	37.32	79.15	4.16	49.15	2.07	0.05	3.82	56.2
32	100	JMETPO20	29.88	12.18	288	11.36	37.8	79.95	3.79	50.36	2.23	0.05	3.63	63.1
33	100	JMETPO30	26.6	13.50	376	11.86	56.88	66.81	2.91	40.05	2.61	0.07	3.60	78.3
34	100	JMETPO40	26.9	13.70	371	12.7	65.4	68.61	2.92	41.16	2.95	0.08	3.49	89.1
35	100	JMETPO50	27.86	13.93	369	12.14	58.85	68.5	2.96	40.58	3.29	0.09	3.41	94.2

Table 5.2 Normalized data matrix of output responses

Load (%)	**Fuel**	**BTE**	**BSEC**	**EGT**	**ID**	**CD**	**P_{max}**	**MRPR**	**MHRR**	**CO**	**HC**	**NO**	**Smoke**
0	Diesel	0.00	0.00	0.30	0.43	0.34	0.38	0.35	0.36	0.00	0.00	0.00	0.14
0	JME	0.00	0.00	0.31	0.42	0.34	0.38	0.33	0.32	0.00	0.00	0.00	0.10
0	JMETPO10	0.00	0.00	0.30	0.44	0.34	0.38	0.34	0.35	0.00	0.00	0.00	0.11
0	JMETPO20	0.00	0.00	0.30	0.43	0.34	0.39	0.36	0.36	0.00	0.00	0.00	0.14
0	JMETPO30	0.00	0.00	0.31	0.43	0.34	0.38	0.34	0.34	0.00	0.00	0.00	0.17
0	JMETPO40	0.00	0.00	0.31	0.45	0.33	0.38	0.34	0.36	0.00	0.00	0.00	0.19
0	JMETPO50	0.00	0.00	0.31	0.43	0.34	0.38	0.35	0.35	0.00	0.00	0.00	0.22
25	Diesel	0.35	0.49	0.33	0.41	0.36	0.40	0.42	0.42	0.56	0.53	0.47	0.22
25	JME	0.35	0.51	0.34	0.40	0.36	0.41	0.43	0.38	0.50	0.43	0.53	0.16
25	JMETPO10	0.35	0.51	0.34	0.41	0.36	0.40	0.40	0.39	0.51	0.48	0.51	0.17
25	JMETPO20	0.35	0.50	0.33	0.41	0.36	0.40	0.42	0.39	0.52	0.51	0.49	0.18
25	JMETPO30	0.35	0.51	0.35	0.41	0.37	0.40	0.39	0.37	0.57	0.56	0.49	0.23
25	JMETPO40	0.38	0.52	0.34	0.43	0.37	0.39	0.39	0.39	0.58	0.59	0.48	0.28
25	JMETPO50	0.38	0.52	0.34	0.42	0.37	0.39	0.38	0.38	0.61	0.62	0.48	0.32
50	Diesel	0.43	0.41	0.38	0.40	0.38	0.43	0.49	0.46	0.41	0.39	0.43	0.35

50	JME	0.44	0.41	0.39	0.38	0.38	0.42	0.42	0.39	0.36	0.34	0.45	0.32
50	JMETPO10	0.43	0.42	0.38	0.40	0.37	0.42	0.46	0.44	0.37	0.36	0.44	0.34
50	JMETPO20	0.43	0.41	0.37	0.40	0.38	0.42	0.46	0.42	0.39	0.40	0.43	0.34
50	JMETPO30	0.43	0.42	0.39	0.41	0.41	0.40	0.40	0.39	0.42	0.42	0.42	0.37
50	JMETPO40	0.45	0.42	0.38	0.42	0.40	0.41	0.40	0.41	0.43	0.45	0.42	0.40
50	JMETPO50	0.44	0.42	0.40	0.42	0.47	0.40	0.39	0.38	0.46	0.49	0.42	0.42
75	Diesel	0.46	0.38	0.42	0.40	0.40	0.44	0.51	0.49	0.34	0.33	0.37	0.49
75	JME	0.46	0.39	0.44	0.37	0.40	0.43	0.41	0.43	0.30	0.30	0.42	0.37
75	JMETPO10	0.46	0.39	0.44	0.40	0.39	0.43	0.45	0.44	0.31	0.31	0.42	0.39
75	JMETPO20	0.49	0.38	0.43	0.40	0.40	0.43	0.44	0.43	0.33	0.34	0.42	0.41
75	JMETPO30	0.46	0.40	0.45	0.40	0.46	0.41	0.38	0.39	0.34	0.35	0.40	0.48
75	JMETPO40	0.47	0.40	0.45	0.42	0.50	0.41	0.39	0.39	0.36	0.39	0.39	0.50
75	JMETPO50	0.47	0.40	0.46	0.41	0.47	0.41	0.39	0.40	0.38	0.41	0.39	0.53
100	Diesel	0.47	0.37	0.47	0.40	0.42	0.45	0.50	0.49	0.29	0.30	0.35	0.56
100	JME	0.46	0.39	0.49	0.37	0.42	0.45	0.40	0.47	0.26	0.27	0.41	0.43
100	JMETPO10	0.47	0.39	0.47	0.40	0.41	0.44	0.44	0.46	0.27	0.27	0.40	0.45
100	JMETPO20	0.47	0.38	0.46	0.39	0.42	0.44	0.42	0.46	0.28	0.29	0.39	0.48
100	JMETPO30	0.44	0.40	0.52	0.40	0.51	0.41	0.37	0.41	0.30	0.32	0.39	0.53
100	JMETPO40	0.44	0.40	0.52	0.42	0.55	0.41	0.37	0.42	0.32	0.35	0.38	0.57
100	JMETPO50	0.45	0.41	0.52	0.41	0.52	0.41	0.37	0.42	0.34	0.38	0.38	0.58

Table 5.3 Weighted normalized matrix

Load (%)	Fuel	BTE	BSEC	EGT	ID	CD	P_{max}	MRPR	MHRR	BSCO	BSHC	BSNO	Smoke
0	Diesel	0.15	0.00	0.00	0.08	0.00	0.10	0.07	0.09	0.00	0.00	0.00	0.01
0	JME	0.15	0.00	0.00	0.06	0.00	0.11	0.08	0.11	0.00	0.00	0.00	0.00
0	JMETPO10	0.15	0.00	0.00	0.08	0.00	0.11	0.08	0.09	0.00	0.00	0.00	0.00
0	JMETPO20	0.15	0.00	0.00	0.08	0.00	0.10	0.07	0.08	0.00	0.00	0.00	0.01
0	JMETPO30	0.15	0.00	0.01	0.08	0.00	0.11	0.07	0.10	0.00	0.00	0.00	0.01
0	JMETPO40	0.15	0.00	0.01	0.10	0.00	0.11	0.08	0.09	0.00	0.00	0.00	0.02
0	JMETPO50	0.15	0.00	0.00	0.08	0.00	0.11	0.07	0.09	0.00	0.00	0.00	0.02
25	Diesel	0.04	0.08	0.01	0.05	0.01	0.07	0.04	0.05	0.03	0.03	0.07	0.02
25	JME	0.04	0.08	0.02	0.04	0.01	0.07	0.04	0.07	0.02	0.02	0.08	0.01
25	JMETPO10	0.04	0.08	0.02	0.05	0.01	0.08	0.05	0.07	0.03	0.02	0.08	0.01
25	JMETPO20	0.04	0.08	0.01	0.05	0.01	0.07	0.04	0.06	0.03	0.02	0.08	0.01
25	JMETPO30	0.04	0.08	0.02	0.05	0.01	0.08	0.06	0.08	0.03	0.03	0.07	0.02
25	JMETPO40	0.03	0.08	0.02	0.07	0.01	0.09	0.06	0.06	0.03	0.03	0.07	0.03
25	JMETPO50	0.03	0.08	0.02	0.06	0.01	0.09	0.06	0.07	0.03	0.03	0.07	0.04
50	Diesel	0.02	0.06	0.03	0.04	0.01	0.04	0.01	0.02	0.02	0.02	0.06	0.04
50	JME	0.01	0.06	0.04	0.02	0.01	0.05	0.04	0.07	0.02	0.02	0.07	0.04
50	JMETPO10	0.02	0.06	0.03	0.04	0.01	0.05	0.02	0.04	0.02	0.02	0.07	0.04
50	JMETPO20	0.02	0.06	0.03	0.04	0.01	0.04	0.02	0.04	0.02	0.02	0.07	0.04
50	JMETPO30	0.02	0.06	0.04	0.04	0.02	0.07	0.05	0.07	0.02	0.02	0.06	0.04
50	JMETPO40	0.01	0.06	0.04	0.06	0.02	0.07	0.05	0.05	0.02	0.02	0.06	0.05
50	JMETPO50	0.01	0.07	0.04	0.06	0.03	0.08	0.05	0.07	0.02	0.02	0.06	0.05
75	Diesel	0.01	0.06	0.05	0.03	0.02	0.01	0.00	0.00	0.02	0.02	0.06	0.07
75	JME	0.01	0.06	0.06	0.00	0.02	0.02	0.04	0.04	0.02	0.01	0.06	0.05
75	JMETPO10	0.01	0.06	0.06	0.04	0.01	0.03	0.03	0.03	0.02	0.02	0.06	0.05
75	JMETPO20	0.00	0.06	0.05	0.03	0.02	0.02	0.03	0.04	0.02	0.02	0.06	0.05
75	JMETPO30	0.01	0.06	0.06	0.04	0.03	0.06	0.06	0.06	0.02	0.02	0.06	0.06
75	JMETPO40	0.01	0.06	0.06	0.06	0.04	0.06	0.05	0.06	0.02	0.02	0.06	0.07

75	JMETPO50	0.01	0.06	0.07	0.05	0.03	0.06	0.05	0.06	0.02	0.02	0.06	0.07
100	Diesel	0.01	0.06	0.07	0.03	0.02	0.00	0.00	0.00	0.01	0.01	0.05	0.08
100	JME	0.01	0.06	0.08	0.00	0.02	0.00	0.05	0.01	0.01	0.01	0.06	0.06
100	JMETPO10	0.01	0.06	0.07	0.03	0.02	0.01	0.03	0.02	0.01	0.01	0.06	0.06
100	JMETPO20	0.01	0.06	0.06	0.03	0.02	0.00	0.04	0.02	0.01	0.01	0.06	0.06
100	JMETPO30	0.01	0.06	0.09	0.04	0.04	0.07	0.06	0.05	0.01	0.02	0.06	0.07
100	JMETPO40	0.01	0.06	0.09	0.06	0.05	0.06	0.06	0.05	0.02	0.02	0.06	0.08
100	JMETPO50	0.01	0.06	0.09	0.05	0.04	0.06	0.06	0.05	0.02	0.02	0.06	0.08

Table 5.4 Utility and regret measure values corresponding to each test

Load (%)	**Fuel**	**Utility measure (Ui)**	**Regret measure (Ri)**
0	Diesel	0.50	0.15
0	JME	0.51	0.15
0	JMETPO10	0.51	0.15
0	JMETPO20	0.49	0.15
0	JMETPO30	0.53	0.15
0	JMETPO40	0.55	0.15
0	JMETPO50	0.53	0.15
25	Diesel	0.49	0.08
25	JME	0.49	0.08
25	JMETPO10	0.52	0.08
25	JMETPO20	0.50	0.08
25	JMETPO30	0.57	0.08
25	JMETPO40	0.58	0.09
25	JMETPO50	0.59	0.09
50	Diesel	0.37	0.06
50	JME	0.43	0.07

50	JMETPO10	0.41	0.07
50	JMETPO20	0.41	0.07
50	JMETPO30	0.52	0.07
50	JMETPO40	0.51	0.07
50	JMETPO50	0.57	0.08
75	Diesel	0.33	0.07
75	JME	0.39	0.06
75	JMETPO10	0.40	0.06
75	JMETPO20	0.40	0.06
75	JMETPO30	0.54	0.06
75	JMETPO40	0.57	0.07
75	JMETPO50	0.56	0.07
100	Diesel	0.35	0.08
100	JME	0.37	0.08
100	JMETPO10	0.39	0.07
100	JMETPO20	0.39	0.06
100	JMETPO30	0.58	0.09
100	JMETPO40	0.60	0.09
100	JMETPO50	0.59	0.09

Table 5.5 VIKOR index and preference order

Trial No.	Load (%)	Fuel	VIKOR Index (Qi)	Rank
1.	0	Diesel	0.81	30
2.	0	JME	0.83	32
3.	0	JMETPO10	0.83	31
4.	0	JMETPO20	0.79	29
5.	0	JMETPO30	0.87	34
6.	0	JMETPO40	0.89	35
7.	0	JMETPO50	0.87	33
8.	25	Diesel	0.36	14
9.	25	JME	0.39	17
10.	25	JMETPO10	0.43	19
11.	25	JMETPO20	0.39	16
12.	25	JMETPO30	0.56	23
13.	25	JMETPO40	0.58	24
14.	25	JMETPO50	0.62	27
15.	50	Diesel	0.08	2
16.	50	JME	0.21	12
17.	50	JMETPO10	0.16	11
18.	50	JMETPO20	0.15	10
19.	50	JMETPO30	0.41	18
20.	50	JMETPO40	0.35	13
21.	50	JMETPO50	0.53	22
22.	75	Diesel	0.01	1
23.	75	JME	0.11	5
24.	75	JMETPO10	0.12	7
25.	75	JMETPO20	0.12	8
26.	75	JMETPO30	0.39	15

27.	75	JMETPO40	0.45	20
28.	75	JMETPO50	0.47	21
29.	100	Diesel	0.10	3
30.	100	JME	0.15	9
31.	100	JMETPO10	0.12	6
32.	**100**	**JMETPO20**	**0.10**	**4**
33.	100	JMETPO30	0.62	26
34.	100	JMETPO40	0.65	28
35.	100	JMETPO50	0.61	25

At the end, the VIKOR index (Qi) value was calculated by utilizing Eqn 4.13. The best alternative is selected based on preference ranking as shown in Table 5.6. The alternative with smallest Qi value is identified as close to the optimal solution.

Form Table 5.6, it can be seen that experimental trial number 32 has the smallest VIKOR index (Qi) value for JMETPO20 blend compared to other JMETPO blends. Thus, it is concluded that the minimum VIKOR index can be obtained when engine is operated with the JMETPO20 blend at full load. Thus, the final ranking for the JMETPO blends based on VIKOR analysis is JMETPO20> JMETPO10> JMETPO30> JMETPO40> JMETPO50.

5.3.2 Summary

The selection of best blend plays an imperative role for its usage in diesel engine. There are a number of combustion, performance, and emission parameters that are to be considered before choosing the best blend which involves a multidimensional perspective. Therefore effective decision-making approach is essential to resolve the problem. PCA integrated VIKOR decision making methods have been used to evaluate the best JMETPO blend in this study.

5.4 Effect of injection timings on combustion, performance and emission characteristics of a diesel engine fueled with the JMETPO20 blend

The experimental results obtained in the previous section revealed that, a blend of 80% Jatropha methyl ester (JME) and 20% Tyre pyrolysis oil (TPO) referred to as JMETPO20 blend exhibited a better performance and lower emissions compared to that of other JMETPO blends and considered as an optimum blend. Being a fuel derived from a non-petroleum source, the original injection timing, nozzle opening pressure and compression ratio of diesel engine may not be suitable for the JMETPO20 blend. In this context, the influence of the injection timing on the combustion, performance and emission characteristics of the test engine used in this study were experimentally investigated, when the engine was run with the JMETPO20 blend, at five different injection timings (26, 24.5, 23, 21.5 and 20 ˚CA bTDC). The results related to the combustion, performance and emission characteristics of the test engine fueled with the JMETPO20 blend at different injection timings were compared with those of the JME and diesel operation and are presented in this section. The designations used in this study for diesel, JME and the JMETPO20 blend at different injection timings are given below. In this section, the JMETPO20 blend is designated as the blend "X".

Test fuels	Designation
Diesel at injection timing of 23 ˚CA bTDC	diesel
JME at injection timing of 23 ˚CA bTDC	JME
Blend X at injection timing of 26 ˚CA bTDC	X@ 26 ˚CA bTDC
Blend X at injection timing of 24.5 ˚CA bTDC	X@ 24.5 ˚CA bTDC
Blend X at injection timing of 23 ˚CA bTDC	X@ 23 ˚CA bTDC
Blend X at injection timing of 21.5 ˚CA bTDC	X@ 21.5 ˚CA bTDC
Blend X at injection timing of 20 ˚CA bTDC	X@ 20 ˚CA bTDC

5.4.1 Combustion parameters

5.4.1.1 Cylinder pressure history

The cylinder pressure variation with respect to the crank angle data can be used to obtain quantitative information on the progress of combustion [225]. Figure 5.14 illustrates the variation of the cylinder pressure with crank angle, for diesel, JME, and the test blend X with different injection timings at full load. It can be observed from the figure that, the variation of injection timing affects the cylinder pressure of the test blend remarkably.

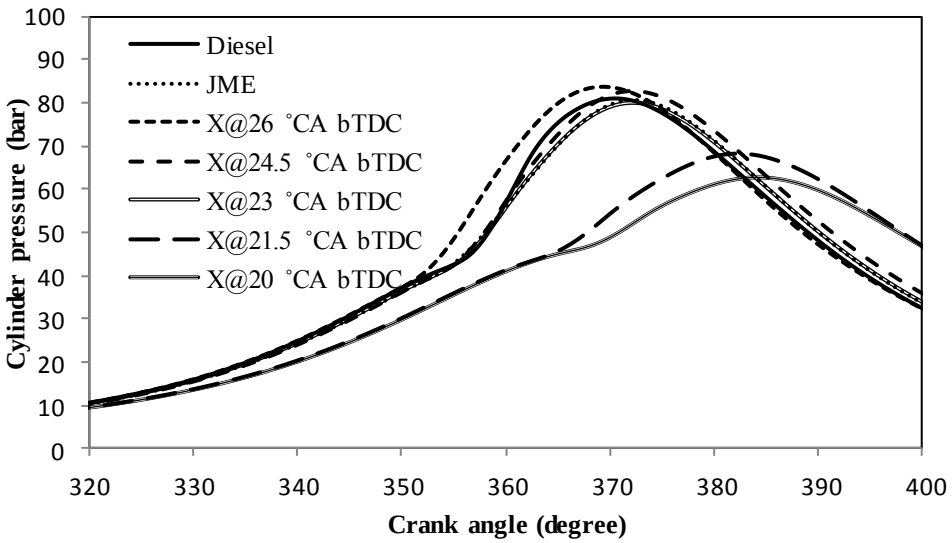

Fig. 5.14 Variation of the cylinder pressure with crank angle at different injection timings and full load

It is found that at full load and the original injection timing, the start of combustion occurs at about 348.5, 347.2 and 348.4 ˚CA in the case of diesel, JME and the test blend X respectively. It can also be observed that, at the original injection timing and full load, the combustion starts a little earlier for JME, compared to that of diesel and the test blend X. This is due to the higher cetane number and the oxygen bound combustion of JME [226]. For the test blend X, at an advanced injection timings of 26 and 24.5 ˚CA bTDC, the start of combustion occurs at about 348.7 and 348.3 ˚CA respectively, while for a retarded injection timings of 21.5 and 20 ˚CA bTDC, it occurs at 349.3 and 348.1 ˚CA respectively at full load. It is evident from the figure, that the start of combustion occurs earlier for advanced injection timings, compared to that of the original and retarded injection timings at full load. This is due to a faster burning rate in the premixed combustion phase [227]. At retarded injection timings, reduced cylinder pressures are observed, which may be due to the delayed burning of fuel, which continues after top dead centre in the expansion stroke. Similar results are reported by Bari et al. [228] in their investigation of a diesel engine, fueled with biodiesel obtained from waste cooking oil.

5.4.1.2 Ignition delay

Figure 5.15 presents the variation of the ignition delay for diesel, JME, and the test blend X at different injection timings and full load. It is apparent from the figure that, with the increase in the engine load, the ignition delay decreases for all the test fuels in this study.

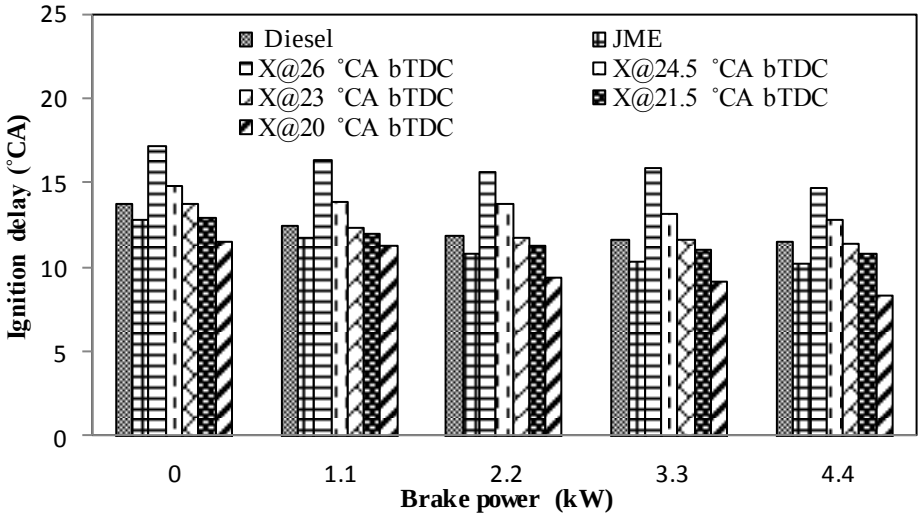

Fig. 5.15 Variation of the ignition delay with brake power at different injection timings

This is because, as the engine load increases, the heat loss during compression decreases, resulting in higher temperature and pressure of the compressed air and a shorter ignition delay is obtained [229]. The values of ignition delay for diesel, JME and the test blend X at full load and original injection timing are by about 11.51, 10.2, and 11.4 ˚CA respectively. The ignition delay of diesel is found to be longer compared to those of JME, and the test blend X at full load and the original injection timing. The higher cetane number of JME and the test blend X makes auto ignition easy which gives a better ignition quality and results in a shorter ignition delay. With the advanced injection timings of 26 and 24.5 ˚CA bTDC, the values are found to be about 14.6 and 12.8 ˚CA respectively, while at the retarded injection timings of 21.5 and 20 ˚CA bTDC the values are about 10.7 and 8.3 ˚CA respectively, at full load. It is observed that, the test blend X exhibits a marginally longer ignition delay at full load and advanced injection timings. This is because at the early start of fuel injection, the cylinder air temperature and pressure are get reduced; resulting in an increase in ignition delay. The reasons are in a good agreement with those of Gumus et al [230], when the diesel engine was fueled with canola oil methyl ester-diesel blends. Compared to the original injection timing, when injection starts close to top dead centre (retardation), the shorter values of ignition delay are found for the test blend X. This is because, the spray experiences comparatively high temperature and pressure of air and this result in a decrease in ignition delay.

5.4.1.3 Heat release rate

Figure 5.16 illustrates the heat release rate pattern with respect to the crank angle for diesel, JME, and the test blend X at full load and different injection timings.

The maximum heat release rate is found for diesel, among all the three test fuels at original injection timing and at full load. This may be due to the higher calorific value of diesel, and accumulation of more fuel owing to the longer ignition delay of diesel. At the original injection timing and at full load, the maximum heat release rate for diesel, JME and, the test blend X are found to be about 56.4, 52.4 and 50.4 J/˚CA respectively. Similarly, at full load and advanced injection timings of 26 and 24.5 ˚CA bTDC, the values of the maximum heat release rate for the test blend X are found to be about 52.2 and 51.4 J/˚CA respectively. The maximum heat release rate is higher at advanced injection timing for the test blend X, and this is attributed to the accumulation of more fuel due to a longer ignition delay. This increases the amount of fuel burnt during the premixed combustion phase which also results in a higher heat release rate.

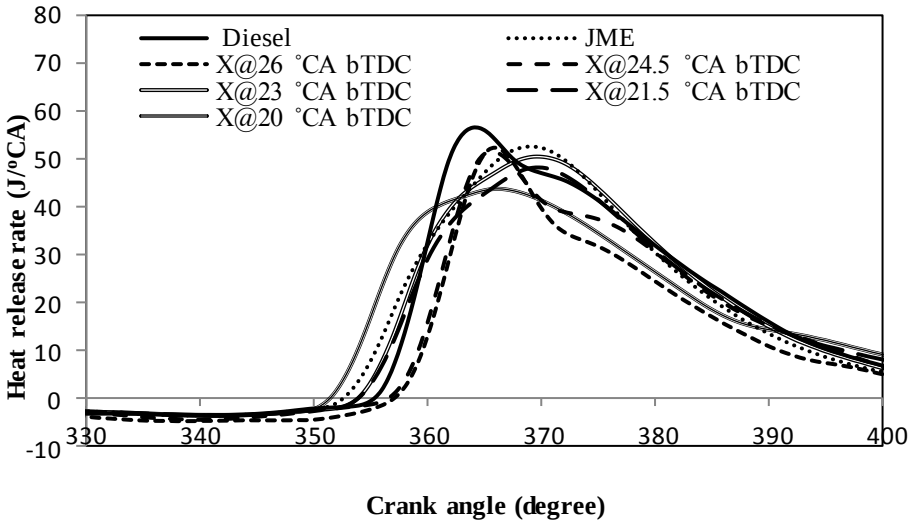

Fig. 5.16 Variation of the heat release rate with crank angle at different injection timings and full load

The values of maximum heat release rate for the test blend X at full load and retarded injection timings of 21.5 and 20 ˚CA bTDC are found 48.1 and 43.6 J/˚CA respectively. At retarded injection timings, the maximum heat release rate for the test blend X is found to be lower, because as the fuel is injected near the top dead centre (TDC), more amount of heat goes to the exhaust.

5.4.1.4 Combustion duration

Figure 5.17 depicts the variation of the combustion duration for all the test fuels at different injection timings. The combustion duration increases with the increase in the engine load for all the test fuels in this study due to an increase in the quantity of fuel injected. It is also evident from the figure, that at the original injection timing and full load the combustion duration is found to be shorter for the JME and the test blend X, compared to that of diesel. This is due to the high cetane number and the oxygen content of JME which helped the complete combustion. The values of the combustion duration for diesel, JME, and the test blend X are found to be about 38.3, 37.9 and 37.8 ˚CA respectively, at full load and the original injection timing. With the advanced injection timings, the combustion duration is found to be reduced, while at retarded injection timings, it is found to be increased for the test blend X. This is due to the longer ignition delay at advanced injection timing which results in faster burning rate of the fuel and rapid rise of the pressure and temperature inside the cylinder.

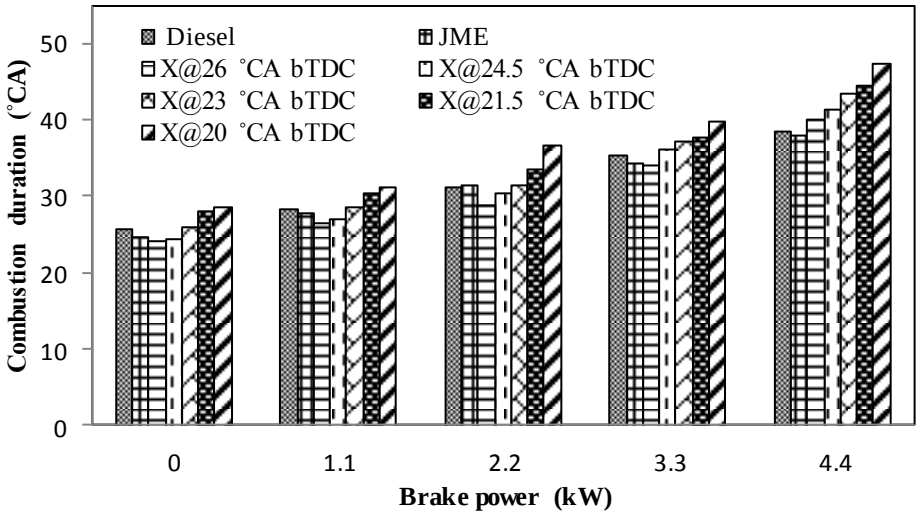

Fig. 5.17 Variation of the combustion duration with brake power at different injection timings

Therefore, most of the air-fuel mixture burns in the premixed phase and causes maximum heat release rate and shorter combustion duration. At retarded injection timings, comparatively less air-fuel mixture is accumulated resulting in shorter ignition delays. It leads to slower burning rate and gradual rise in pressure and temperature inside the cylinder. Therefore, relatively more air-fuel mixture burns in the diffusion phase than in the premixed phase leading to lower maximum heat release rate and longer combustion duration. The similar reason was reported by Jayashankara et al. [231] in their review

article on the effect of fuel injection timing and intake pressure on the performance of a DI diesel engine. The values of the combustion duration are found to be about 40.1, 41.3, 44.4 and 47.4 ˚CA, with an injection timing of 26, 24.5, 21.5 and 20 ˚CA bTDC respectively, at full load.

5.4.1.5 Maximum cylinder pressure

The effects of injection timings on maximum cylinder pressure are compared between diesel, JME, and the JMETPO20 blend, and shown in Figure 5.18. The maximum cylinder pressure values for diesel, JME, and the test blend X at the standard injection timing and full load are found to be about 81, 80.6 and 80 bar respectively. It is apparent from the figure that, advancing the injection timing raises the maximum cylinder pressure for the blend.

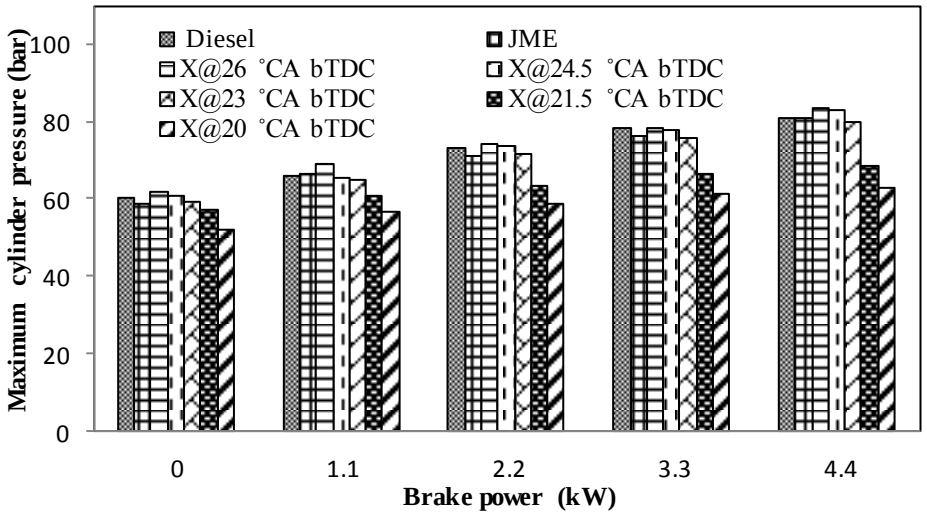

Fig. 5.18 Variation of the maximum cylinder pressure with brake power at different injection timings

At full load and advanced injection timings of 26 and 24.5 ˚CA bTDC, the maximum cylinder pressure values for test blend X are found to be about 83.7 and 82.7 bar respectively. It is due to early starting of fuel injection that results in a more amount of mixture accumulated that undertakes combustion process, which results in an increase in a maximum cylinder pressure. The reason is in a good agreement with the reason documented by Agrawal et al. [232] for the results they obtained from a single cylinder, four stroke, air cooled, diesel engine run on karanja biodiesel-diesel blends at different injection timings. While retarding the injection timing, a lower maximum cylinder pressure is attained as a result of less fuel being accumulated in the delay period for blend.

At full load and the retarded injection timings of 21.5 and 20 ˚CA bTDC, the values of the maximum cylinder pressure are recorded as 68.2 and 62.7 bar respectively for the test blend X.

5.4.1.6 Maximum rate of pressure rise

The rate of pressure rise of an engine refers to the smoothness of the engine operation. Ideally, the rate of pressure rise should not exceed 5 bar/˚CA in a single cylinder, four stroke, DI diesel engine [233]. The variations of the maximum rate of pressure rise with brake power for diesel, JME, and the test blend X at different injection timings, are shown in Figure 5.19. The maximum rate of pressure rise at the original injection timing for diesel varies from 2.6 to 5.3 bar/˚CA and for test blend X it varies from 2.7 to 5 bar/˚CA with respect to load**.** The rate of pressure rise is found to be higher with advanced injection timings because of faster combustion. The values of maximum rate of pressure rise at full load and injection timings of 26, 24.5, 21.5, 20 ˚CA bTDC are found to be about 5.6, 5.3, 4.8 and 4.1 bar/˚CA respectively for test blend X. It can be observed from the figure that, at advanced injection timings, maximum rate of pressure rise increases for test blend X.

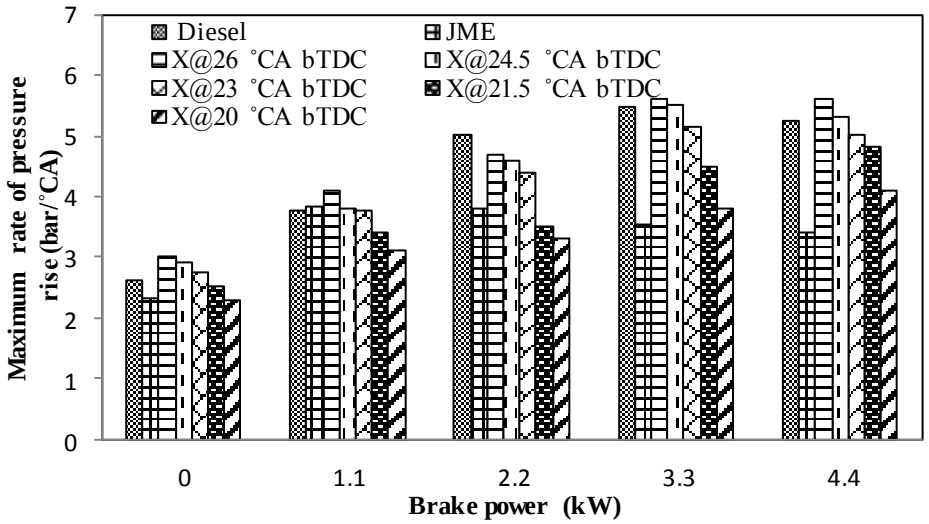

Fig. 5.19 Variation of the maximum rate of pressure rise with brake power at different injection timings

The reason is that, the cylinder air pressure and temperature at the point of injection fall, resulting in more fuel being burnt during uncontrolled combustion phase, because of longer ignition delay and, finally this leads to, an increased maximum rate of pressure rise [234].

5.4.2 Performance parameters

5.4.2.1 Brake thermal efficiency

The brake thermal efficiency reflects quality of combustion and provides comparable of assessing how efficient the energy in the fuel was converted to mechanical power output [235]. Figure 5.20 depicts the comparison of the brake thermal efficiency with brake power for diesel, JME, and the test blend X at different injection timings. The brake thermal efficiency of JME is found to be lower than that of diesel at original injection timing, due to high density and lower calorific value of the JME. At original injection timing, the brake thermal efficiency for diesel, JME, and the test blend X are found to be 29.89%, 28.6% and 29.87% respectively at full load. It can be observed from the figure, that the test blend X at the advanced injection timing of 26 ˚CA bTDC and 24.5 ˚CA bTDC, the engine delivered the brake thermal efficiency of 29.1% and 30.5% respectively at full load. At retarded injection timings of 21.5 and 20 ˚CA bTDC, the brake thermal efficiency is found to be 29% and 28.1% respectively at full load. It can also be observed, that advancing the injection timing by 1.5 ˚CA increased the brake thermal efficiency, however additional advancement is not thus helpful at full load. With the advanced injection timing of 24.5 ˚CA bTDC, the brake thermal efficiency is increased by about 2.1% and 6.3% than that of diesel and the JME respectively at full load.

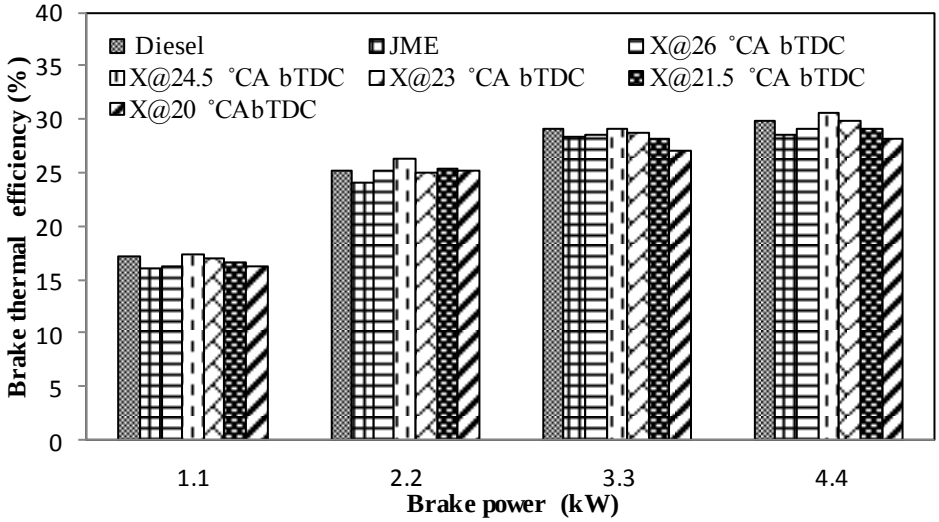

Fig. 5.20 Variation of the brake thermal efficiency with brake power at different injection timings

Advanced injection timing leads to better air-fuel mixing which results in improved combustion and in turn results in the maximum brake thermal efficiency. But, with the

retarded injection timings, the brake thermal efficiency is decreased owing to incomplete combustion, resulting in a lowered power output.

5.4.2.2 Brake specific energy consumption

Figure 5.21 illustrates the variation of the BSEC for diesel, JME, and the test blend X with load at different injection timings. As shown in the figure, the BSEC for the JME is found to be higher compared to that of diesel, because of the lower energy content of JME. At the original injection timing and full load, the values of BSEC for diesel, JME, and the test blend X are recorded as 11.86, 12.79 and 12.55 MJ/kWh respectively. In the case of the test blend X, when the injection timing is advanced by 1.5 and 3 ˚CA bTDC, the BSEC decreased by about 7.1% and 4.5% compared to that of the original injection timing at full load. But, with the retarded injection timing of 1.5 and 3 ˚CA bTDC, the BSEC increased by about 4.6% and 10.3% respectively compared to that of the original injection timing at full load. Retarding the injection timing means delayed combustion, which causes a loss of power and, hence, a higher BSEC is noticed [236].

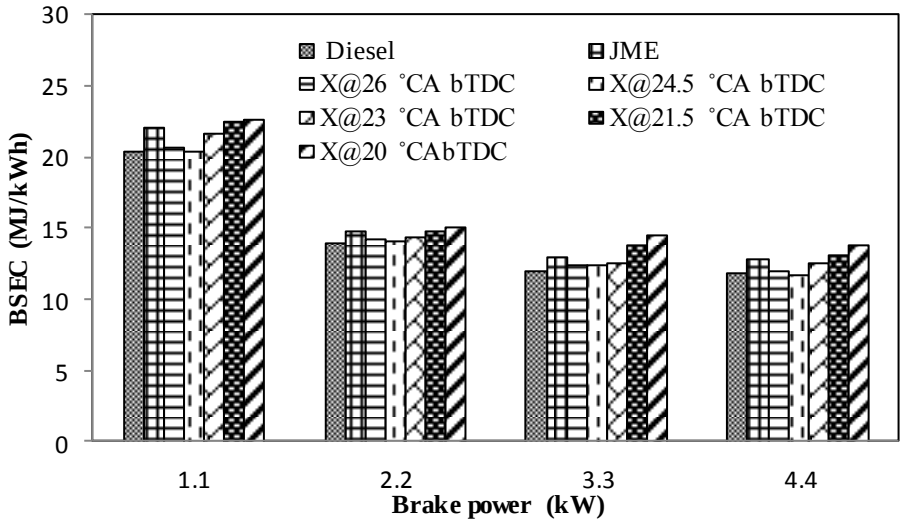

Fig. 5.21 Variation of the BSEC with brake power at different injection timings

The lowest value of BSEC for the test blend X is found to be about 11.7 MJ/kWh, at full load and an advanced injection timing of 24.5 ˚CA bTDC.

5.4.2.3 Exhaust gas temperature

The exhaust gas temperature provides qualitative information about the progress of combustion in the engine [237]. The variation of the exhaust gas temperature with diesel, JME, and the test blend X at different injection timings is graphically depicted in Figure

5.22. The exhaust gas temperature increases with an increase in the engine load, as a result of increased cylinder gas temperature. It is evident from the figure that, the exhaust gas temperature increases, when the injection timing is retarded in comparison with the original injection timing and full and for the test blend X. This is because, with the delayed combustion, more amount of heat goes to the exhaust. At the original injection timing and full load, the values of exhaust gas temperature are recorded to be about 303, 333 and 335 ˚C for diesel, JME, and the test blend X respectively.

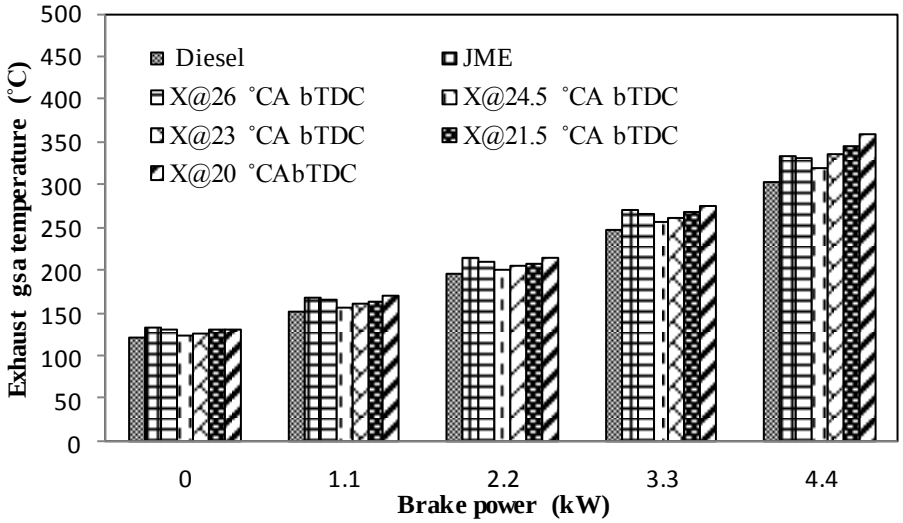

Fig. 5.22 Variation of the exhaust gas temperature with brake power at different injection timings

For the test blend X, at the advanced injection timing of 26 and 24.5 ˚CA bTDC, the values of exhaust gas temperature are found to be 330 and 320 ˚C respectively, and at the retarded injection timing of 21.5 and 20 ˚CA bTDC, the values of exhaust gas temperature are recorded as 344 and 358 ˚C respectively, at full load. It can be observed from figure for the test blend X that, the exhaust gas temperature decreased as injection timing was advanced from 23 to 24.5 ˚CA bTDC at full load. The exhaust gas temperature reduced by about 4.5% when injection timing is advanced by 1.5 ˚CA bTDC at full load. This may be attributed to the fact that, at advanced injection timing, wall heat transfer is more owing to earlier start of combustion. This leads to the lowering of the exhaust gas temperature [238].

5.4.3 Emission parameters

5.4.3.1 Brake specific carbon monoxide emission

During a compression ignition (CI) engine operation, the parameters that affect the carbon monoxide (CO) formation are the equivalence ratio, fuel type, combustion chamber

geometry, atomization rate, injection timing, injection pressure, engine load and speed [239]. Normally, the CO emission from a CI engine is negligible, because the engine operates with the excess air. Figure 5.23 depicts the variation of the brake specific carbon monoxide (BSCO) emission for various test fuels with brake power at different injection timings. The test results reveal that, for the test blend with the advanced injection timings of 26 and 24.5 ˚CA bTDC, the BSCO emission is found to be lower compared to that with the original injection timing by about 4.8% and 13.3% respectively, at full load. This is due to the fact that, more time is being available for the complete combustion in case of advanced injection timings. Contradictory to this, the BSCO emission is found to be increased by about 7.1% and 16.8% with the retarded injection timing of 21.5 and 20 ˚CA bTDC respectively, compared to that at the original injection timing and full load. This is because of late burning of the fuel injected, and incomplete combustion.

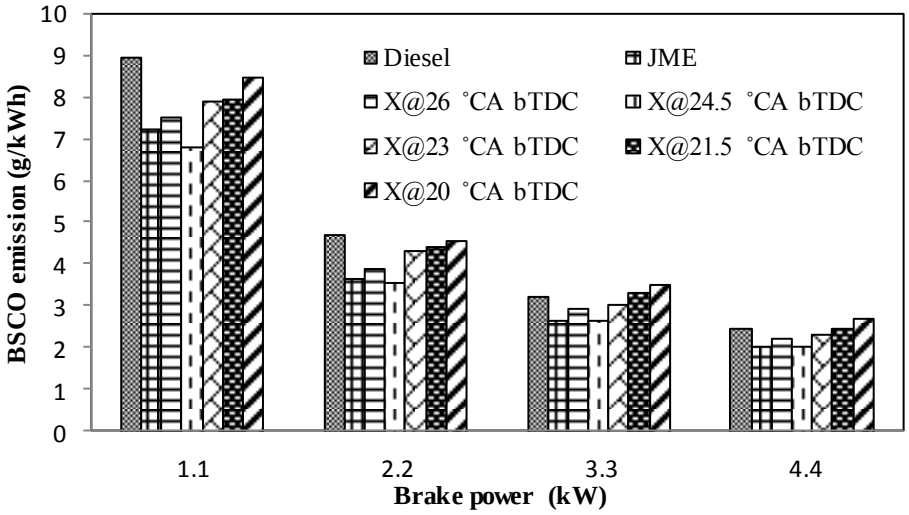

Fig. 5.23 Variation of the BSCO emission with brake power at different injection timings

Further, a relatively lower value of the BSCO emission is recorded for the test blend X at full load and advanced injection timing of 24.5 ˚CA bTDC, which is lower by about 19.3% and 1% than that of diesel and JME at full load.

5.4.3.2 Brake specific hydrocarbon emission

Figure 5.24 presents the change in the brake specific hydrocarbon (BSHC) emission from the engine, using diesel, JME, and the test blend X at different injection timings. The BSHC emissions for the JME and test blend X at all injection timings are found to be lower compared to that of diesel at full load. It can also be noted that, with the advanced injection timing, the BSHC emission decreases. This is because of the earlier start of combustion comparative to top dead centre (TDC), which helps in the complete

combustion as the fuel-air mixture gets compressed with the piston moving to the TDC, resulting in a relatively higher temperature [240]. Similar reason was reported by Belagur et al. [241] in their research work on utilization of Honne oil methyl ester (HOME) at different injection timings with variable compression ratios. It can also be observed that, when the injection timing is retarded, the BSHC emissions are found to be more as compared to those with original and advanced injection timings.

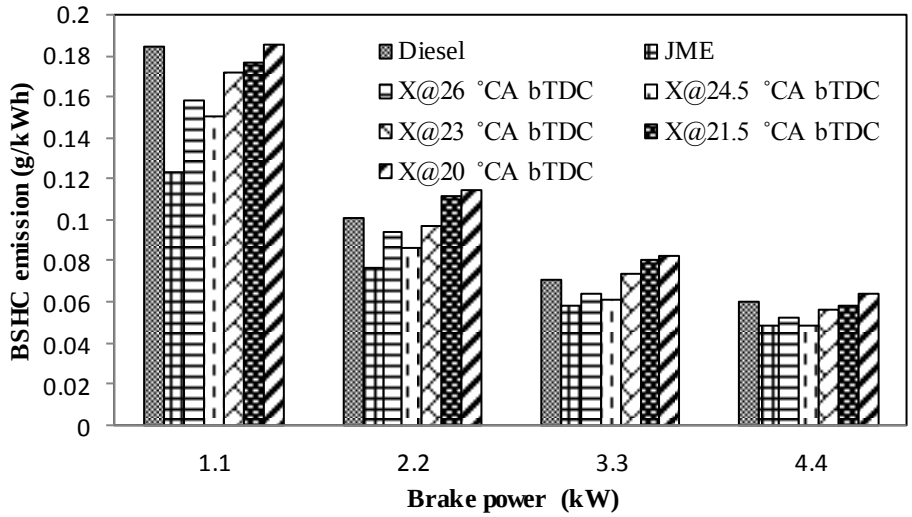

Fig. 5.24 Variation of the BSHC emission with brake power at different injection timings

It is evident from the figure, the advanced injection timings of 26 and 24.5 ˚CA bTDC cause a reduction in the BSHC emission by about 7.53% and 14.2%, respectively and the retarded injection timing of 21.5 and 20 ˚CA bTDC raise the BSHC emission by about 4.1% and 14.6%, respectively compared to that of the original injection timing of 23 ˚CA bTDC for the test blend X, at full load.

5.4.3.3 Brake specific nitric oxide emission

The nitric oxide (NO) formation in a CI engine is predominantly influenced by the maximum combustion temperature, residence time and the oxygen concentration [242]. The effects of the injection timings on the brake specific nitric oxide (BSNO) emission for diesel, JME, and the test blend X are compared in Figure 5.25. The BSNO emission increases with the increase in the engine load, due to the rise in combustion temperature. With the increase in the engine load, more fuel needs to be burned, which results in a rise in combustion temperature and subsequently a greater amount of BSNO emission [243]. The results show that, when the injection timing is advanced, the BSNO emission for the

test blend increases significantly under all engine loads, due to a higher combustion temperature caused by better fuel-air mixture burning. The BSNO emission for the test blend X at an advanced injection timing 26 and 24.5 ˚CA bTDC is higher by about 4.9% and 2.1% than that of the original injection timing at full load. With the retarded injection timing of 21.5 and 20 ˚CA bTDC, the test blend X produces a lower BSNO emission by about 12% and 14.9%, compared to that of the original injection timing at full load.

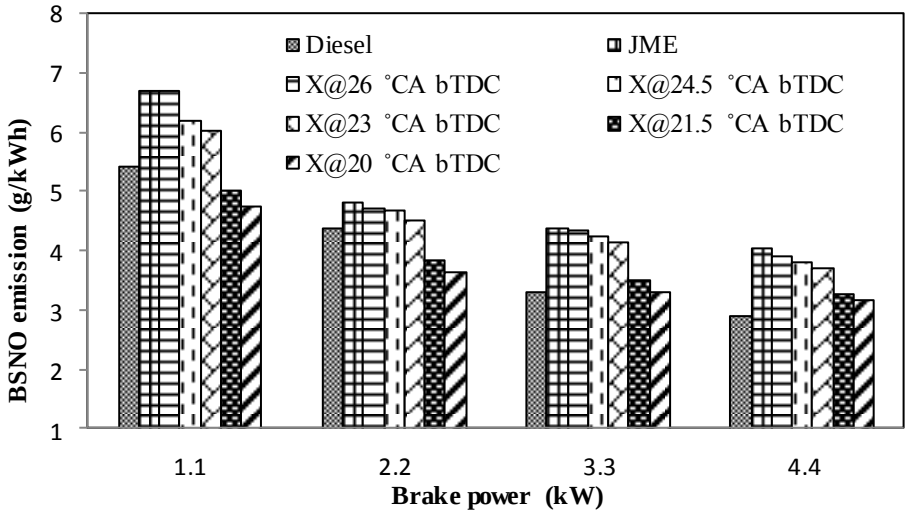

Fig. 5.25 Variation of the BSNO emission with brake power at different injection timings

The BSNO emission decreases at retarded injection timings compared to original and advanced injection timings. This is due to the fact that, at retarded injection timing, fuel is injected near the TDC and most of the fuel burns after TDC. It causes higher amount of heat going as waste in the exhaust which results in lowering of maximum cylinder pressure and temperature.

5.4.3.4 Smoke opacity

The variation of the smoke opacity with brake power for diesel, JME, and the test blend X at different injection timings are depicted in Figure 5.26. At the original injection timing and full load, the smoke opacity is found to be about 86.3%, 52.2% and 63.1% for diesel, JME, and the test blend X respectively. The smoke opacity for the test blend X is lower by 9.3% at an advanced injection timing of 24.5 ˚CA bTDC, compared to that of original injection timing. This is due to the availability of more time for the oxidation process between carbon and oxygen molecules which results better combustion process by the early start of fuel injection [244].

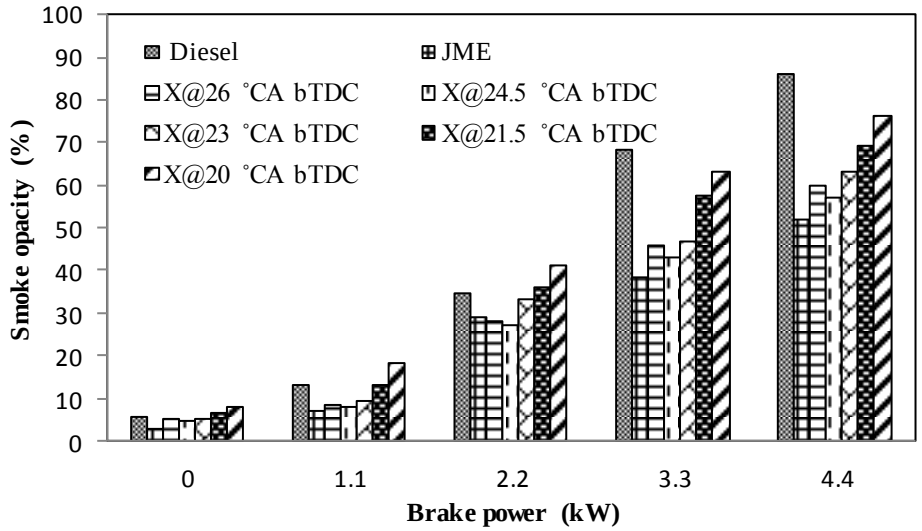

Fig. 5.26 Variation of the smoke opacity with brake power at different injection timings

Similar reasons are given by Purushotham et al. [245], in their work on the performance and emissions characteristics of a diesel engine fueled with Pongamia pinnata methyl ester and its diesel blends. It is also found that, at retarded injection timing results in a higher particulate emission, which is attributed to the increased fraction of diffusion combustion. At full load, the values of smoke opacity for the test blend X are about 60.2%, 57.2%, 69.3% and 76.5% at the injection timings of 26, 24.5, 21.5 and 20 ˚CA bTDC, respectively.

5.4.4 Summary

Fuel injection timing is undoubtedly an important parameter that influences the combustion, performance and emission characteristics of any diesel engine. In this study, the influence of the injection timing on these characteristics of a single cylinder, four stroke, air cooled, naturally aspirated, DI diesel engine were experimentally investigated, when the engine was run with the JMETPO20 blend, at five different injection timings (26, 24.5, 23, 21.5 and 20 ˚CA bTDC). It is summarized that, the advanced injection timing of 24.5 ˚CA bTDC was the optimum injection timing, which gives better results in terms of the combustion, performance and lower emission characteristics of the engine fueled with the test blend.

Appendix 7 provides summary of values on combustion, performance and emission parameters for diesel, JME and the JMETPO20 blend at full load and different injection timings.

The next section presents the effect of nozzle opening pressure on the combustion, performance and emission characteristics of a DI diesel engine fueled with the JMETPO20 blend which would enable us to find the optimum nozzle opening pressure for the blend.

5.5. Effect of nozzle opening pressure on combustion, performance and emission characteristics of a diesel engine fueled with the JMETPO20 blend

The experimental results from the previous study indicated that the JMETPO20 blend gave a better performance and lower emissions when operated with an advanced injection timing of 24.5 ˚CA bTDC compared to the other injection timings of the test engine. With the optimum injection timing of 24.5 ˚CA bTDC, further investigations were carriedout to study the effects of different nozzle opening pressure on the combustion, performance and emission characteristics of a compression ignition (CI) engine run on the JMETPO20 blend. Experiments were conducted at the optimized injection timing with the five nozzle opening pressures viz. 210, 220, 230, 240 and 250 bar in addition to the original nozzle opening pressure of 200 bar, and the findings were compared with those of diesel operation and are presented in this section.

In this section, the JMETPO20 blend is designated as the blend "X". The designations used in this study for diesel, JME and the test blend X at different nozzle opening pressures are given below.

Test fuels	Designation
Diesel at injection timing of 23 ˚CA bTDC and nozzle opening pressure of 200 bar	Diesel
JME at injection timing of 23 ˚CA bTDC and nozzle opening pressure of 200 bar	JME
X at injection timing of 23 ˚CA bTDC and nozzle opening pressure of 200 bar	X@200 bar
X at injection timing of 24.5 ˚CA bTDC and nozzle opening pressure of 210 bar	X@210 bar
X at injection timing of 24.5 ˚CA bTDC and nozzle opening pressure of 220 bar	X@220 bar
X at injection timing of 24.5 ˚CA bTDC and nozzle opening pressure of 230 bar	X@230 bar
X at injection timing of 24.5 ˚CA bTDC and nozzle opening pressure of 240 bar	X@240 bar
X at injection timing of 24.5 ˚CA bTDC and nozzle opening pressure of 250 bar	X@250 bar

5.5.1 Combustion parameters

5.5.1.1 Cylinder pressure history

Figure 5.27 compares the cylinder pressure variations with respect to the crank angle, with diesel and the blend, at full load and different nozzle opening pressures. The highest cylinder pressures for diesel and the test blend X are obtained as 81 bar at 370.3 ˚CA and 80 bar at 371 ˚CA respectively, at the original nozzle opening pressure. It is evident from Figure 5.27 that the commencement of combustion for the test blend X occurs marginally later compared to that of diesel at the original nozzle opening pressure. This may be due to higher viscosity of the test blend X, which results in marginally poorer atomization and fuel-air mixture preparation.

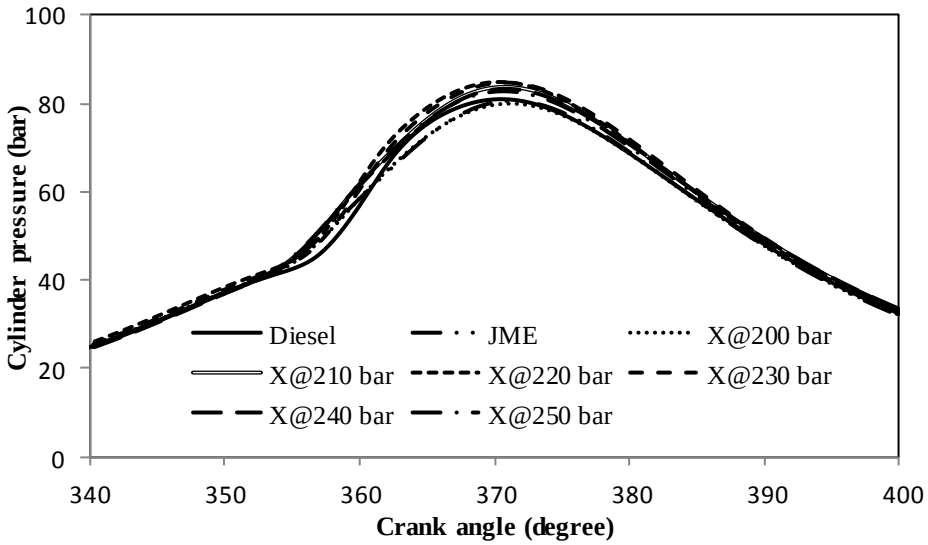

Fig. 5.27 Variation of cylinder pressure with crank angle at different nozzle opening pressures and full load

Among all the tested nozzle opening pressures with the test blend X operation, 220 bar nozzle opening pressure shows the highest cylinder pressure of 84.9 bar at 370.38 ˚CA and it occurs 0.63 ˚CA earlier compared to that of the original nozzle opening pressure. This may be owing to the improved air entrainment and hence, results in better air-fuel mixing. Increasing the nozzle opening pressure beyond 220 bar, results in a reduction in the cylinder peak pressure, because a higher nozzle opening pressure does not show any considerable improvement. This is due to the consequent increase in the ignition delay, as some of the fuel particles will impact on the cylinder wall, and may not participate in the combustion process, which leads to poor combustion [246]. At full load and nozzle opening pressures of 210, 220, 230, 240 and 250 bar, the values of the maximum cylinder pressures for the test blend X are 83.8, 84.9, 84.7, 83.3 and 82.8 bar respectively.

5.5.1.2 Ignition delay

The significant factors which affect ignition delay of a CI engine are intake-air temperature, type of fuel used, air-fuel ratio, compression ratio, engine speed, and fuel injection pressure [247]. Figure 5.28 depicts the ignition delay for diesel and the test blend X at different nozzle opening pressures. At full load and original nozzle opening pressure of 200 bar, the values of the ignition delay for diesel and the test blend X are by about 11.5 and 11.4 ˚CA respectively. At full load and nozzle opening pressures of 210, 220, 230, 240 and 250 bar the values of ignition delay for the test blend X are 10.1, 9.6, 10.3, 10.9 and 11.4 ˚CA respectively.

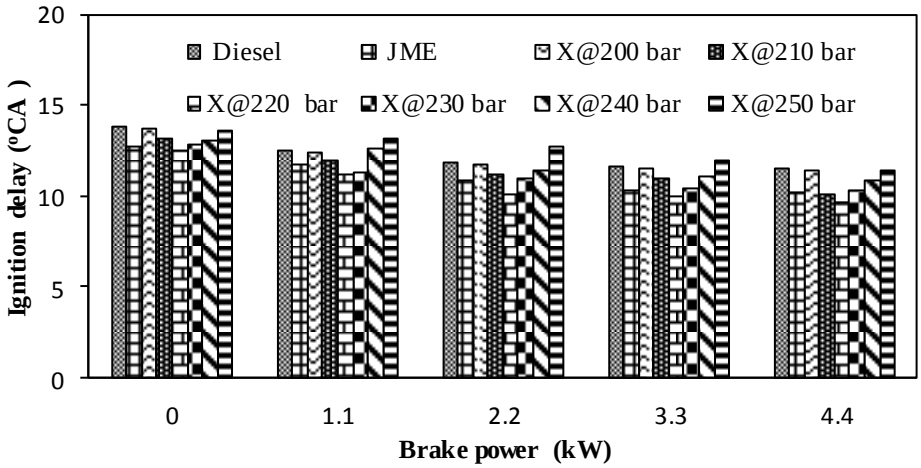

Fig. 5.28 Variation of ignition delay with brake power at different nozzle opening pressures

Among all the tested nozzle opening pressures, the lowest ignition delay of 9.6 ˚CA is recorded at 220 bar with the test blend X at full load. The ignition delay at full load and nozzle opening pressure of 220 bar is found to be shorter by about 1.9 and 1.75 ˚CA, compared to those at 200 bar for diesel and the test blend X respectively. Increasing the nozzle opening pressure from 200 to 220 bar results in better atomization of fuel and well mixing of the fuel with air leading to decrease in the ignition delay is obtained.

5.5.1.3 Heat release rate

The comparison of the heat release rate at full load and different nozzle opening pressures for diesel and the test blend X is depicted in Figure 5.29. The maximum heat release rate is found with diesel compared to that of the test blend X at all nozzle opening pressures. This is owing to fact of the higher calorific value of diesel and more fuel accumulation as a result of longer ignition delay.

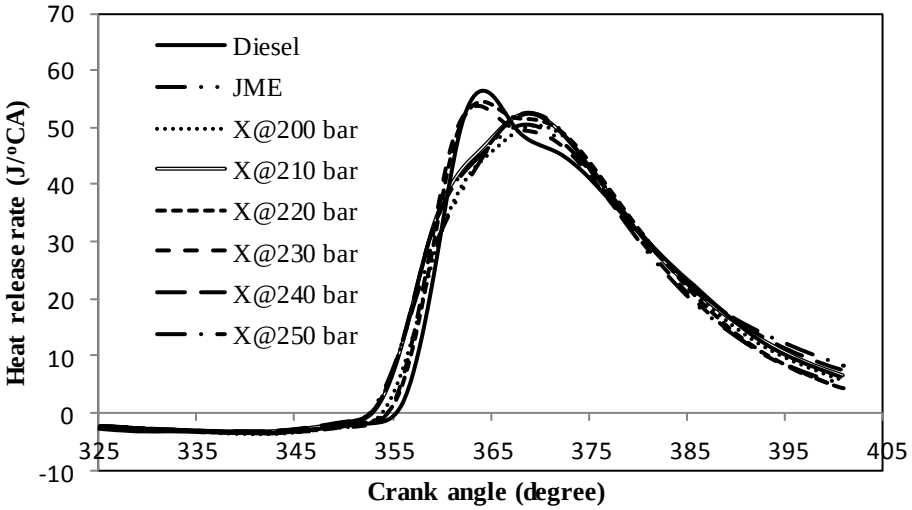

Fig. 5.29 Variation of heat release rate at different nozzle opening pressures and full load

At the original nozzle opening pressure and full load, the maximum heat release rates for diesel and the test blend X are found to be about 56.4 and 50.4 J/˚CA respectively. The maximum heat release rate of 54.5 J/˚CA is obtained for the test blend X at nozzle opening pressure of 220 bar, which is approximately 8.26% higher than that of the original nozzle opening pressure. When the nozzle opening pressure is increased for the test blend X, the quantity of fuel injected during the ignition delay period enhances, because of the high injection rate [248]. Nanthagopal [249] reported similar reasons in their work on the effects of fuel injection pressures on Calophyllum inophyllum methyl ester fueled direct injection (DI) diesel engine. The mixing process of fuel with air is also improved with the higher nozzle opening pressures which results in a strong combustible mixture and higher premixed combustion takes place. Further increase in the nozzle opening pressure, results in a lower heat release rate due to lesser air entrainment, subsequently the fuel droplets are finer and they do not find sufficient air to form a homogeneous mixture. The values of the maximum heat release rate for the test blend X are 52.5, 54.5, 53.8, 52.6 and 50.5 J/˚CA at nozzle opening pressures of 210, 220, 230, 240 and 250 bar respectively.

5.5.1.4 Combustion duration

Figure 5.30 depicts the variations of the combustion duration with brake power for diesel and the test blend X at different nozzle opening pressures. The combustion duration increases with the increase in the engine load for both the test fuels, due to the increase in the quantity of fuel injected. At the original nozzle opening pressure and full load, the values of the combustion duration for diesel and the test blend X are found to be about

38.3 and 43.3 ˚CA respectively. The longer combustion duration obtained with the test blend X, at the original nozzle opening pressure is the result of its higher viscosity than that of diesel. The values of the combustion duration at full load are found to be about 42.9, 35.4, 35.8, 42.6 and 44.2 ˚CA, at the nozzle opening pressures of 210, 220, 230, 240 and 250 bar respectively. The lowest value of combustion duration of 35.4 ˚CA is observed with the nozzle opening pressure of 220 bar for the test blend X, at full load.

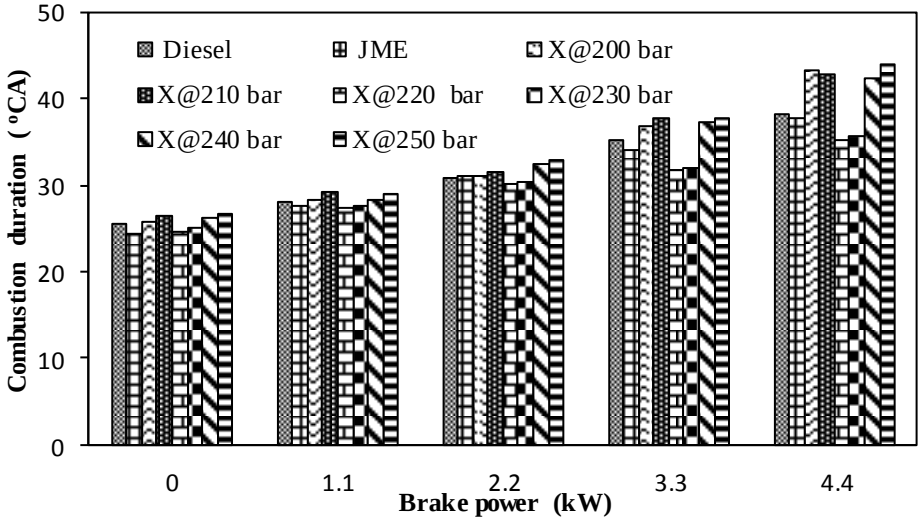

Fig. 5.30 Variation of combustion duration with brake power at different nozzle opening pressures

The combustion duration increases as the nozzle opening pressure is increased from 230 bar to 250 bar, as a result of a longer diffusion combustion phase**.** Similar reasons are reported by Sayin et al. [250] in their work on the effects of fuel injection pressure on the combustion and emissions of a diesel engine run on the canola oil methyl esters-diesel fuel blends.

5.5.1.5 Maximum cylinder pressure

The effects of different nozzle opening pressures on the maximum cylinder pressure are compared between diesel, and the test blend X and shown in Figure 5.31. The maximum cylinder pressure mainly depends on the combustion rate in the initial stages, which is affected by the fuel taking part in uncontrolled combustion phase [251]. The maximum cylinder pressure for diesel and the test blend X at the original nozzle opening pressure are found to be about 81 and 80 bar respectively at full load. The value of maximum cylinder pressures for the test blend X is 83.8, 84.9, 84.7, 83.3 and 82.8 bar at full load and nozzle opening pressure of 210, 220, 230, 240 and 250 bar respectively. It can be observed that the cylinder pressure for the test blend X is higher at 220 bar nozzle opening pressure. The

maximum cylinder pressure decreases after 220 bar nozzle opening pressure for the test blend X due to a lesser heat release rate during uncontrolled combustion phase, owing to lesser spray penetration inside the combustion chamber.

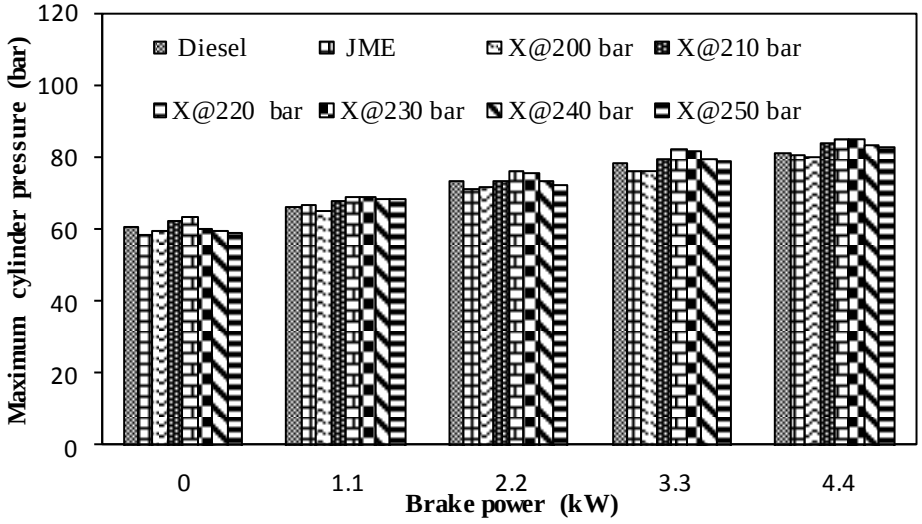

Fig. 5.31 Variation of maximum cylinder pressure with brake power at different nozzle opening pressures

5.5.1.6 Maximum rate of pressure rise

The variation of the maximum rate of pressure rise with brake power for diesel and the test blend X at different nozzle opening pressures is shown in Fig. 5.32. The maximum rate of pressure rise for diesel varies from 2.63 bar/°CA at no load to 5.25 bar/°CA at full load.

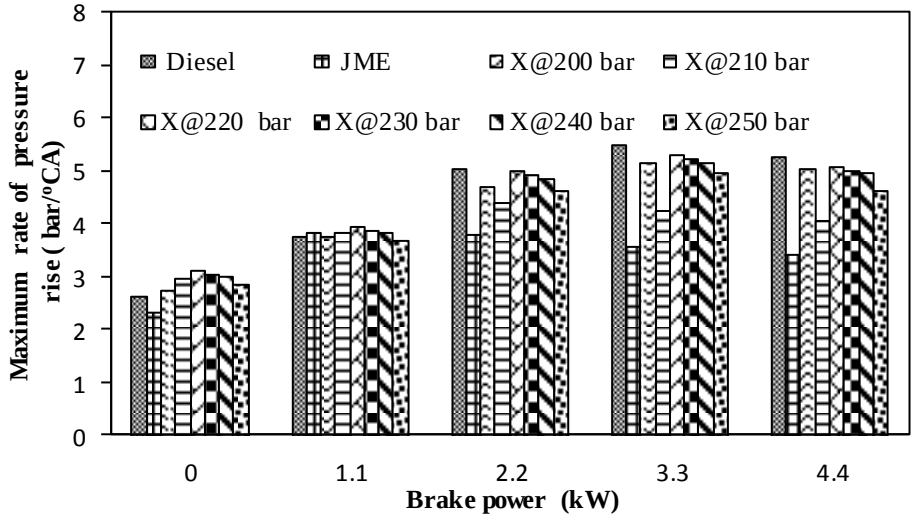

Fig. 5.32 Variation of maximum rate of pressure rise with brake power at different nozzle opening pressures

The maximum rate of pressure rise is found to be higher with the nozzle opening pressure of 220 bar, because of finer spray formation resulting in better combustion. The increase in the nozzle opening pressure above 220 bar reduces the maximum rate of pressure rise compared to the other nozzle opening pressures for the test blend X. This may be due to the lesser spray penetration of the test blend X, which gives in a lower rate of pressure rise [252]. The values of the maximum rate of pressure rise at full load and nozzle opening pressures of 210, 220, 230, 240 and 250 bar are found to be about 4.1, 5.1, 5, 4.96 and 4.6 bar/˚CA respectively, for the JMETPO20 blend.

5.5.2 Performance parameters

5.5.2.1 Brake thermal efficiency

The brake thermal efficiency provides information regarding how efficient the energy in the fuel is transformed to power output [253]. The brake thermal efficiency of the engine for diesel and the test blend X, at different nozzle opening pressures is shown in Fig. 5.33.

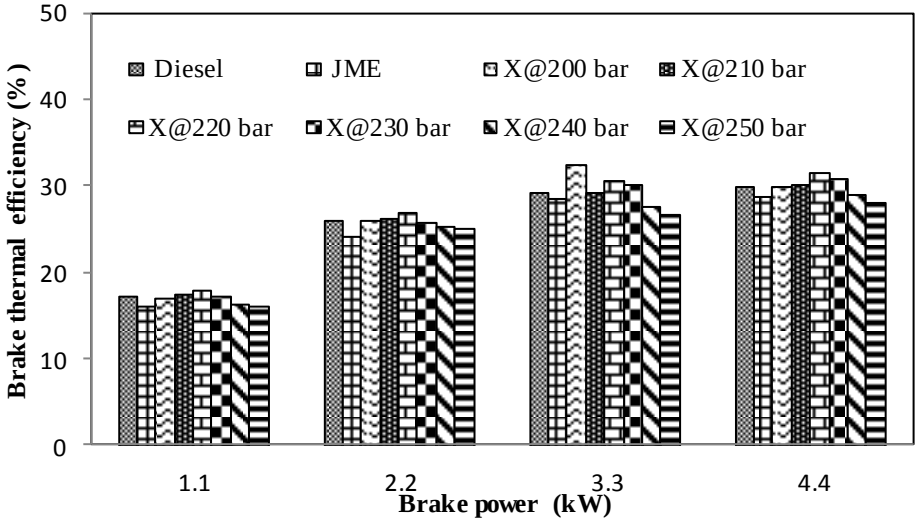

Fig. 5.33 Variation of brake thermal efficiency with brake power at different nozzle opening pressures

The brake thermal efficiency increases with the increase in brake power for all the test fuels, as expected. The values of brake thermal efficiency for diesel and the test blend X are attained almost equal at the original nozzle opening pressure and full load. At full load and the nozzle opening pressure of 220 bar the test blend X gave 5.8% and 5.12% increase in the brake thermal efficiency for diesel and the test blend X compared to that of the standard settings of the test engine, due to better air-fuel mixing which gives complete combustion. When the nozzle opening pressure is increased, the fuel particle diameter

would become smaller and the mixing of the fuel with the air becomes better during ignition delay period [254]. Similar kind of results was reported by Senthil et al. [255] when biodiesel from Nerium oil was blended with diesel. It is also observed that, increasing the nozzle opening pressure above 220 bar reduced the brake thermal efficiency. This may be due to more decrease in the fuel droplet size, as much smaller fuel droplets would have a lesser momentum and that affects the fuel distribution in air [256]. Also, the decrease in the relative velocity of fuel droplets corresponding to the air gives poor air entrainment leading to incomplete combustion. The brake thermal efficiency for the test blend X is obtained as 29.9%, 31.4%, 31.1%, 29% and 28.1%, at full load and nozzle opening pressures of 210, 220, 230, 240 and 250 bar respectively.

5.5.2.2 Brake specific energy consumption

Figure 5.35 illustrates the variation of brake specific energy consumption (BSEC) at different nozzle opening pressure of diesel, and test blend X. For the nozzle opening pressure of 220 bar with test blend X, the BSEC of test engine for the entire load range was lower compared to other nozzle opening pressures. This may be due to the increased penetration length and spray cone angle and due to more area coverage of spray formed in the combustion chamber and utilizing the air effectively resulting optimum peak pressure, better fuel air mixing and higher spray atomization [257]. However, beyond the nozzle opening pressure 220 bar, the performance has suffered significantly because of low penetration of fuel droplets due to low momentum of fuel droplets.

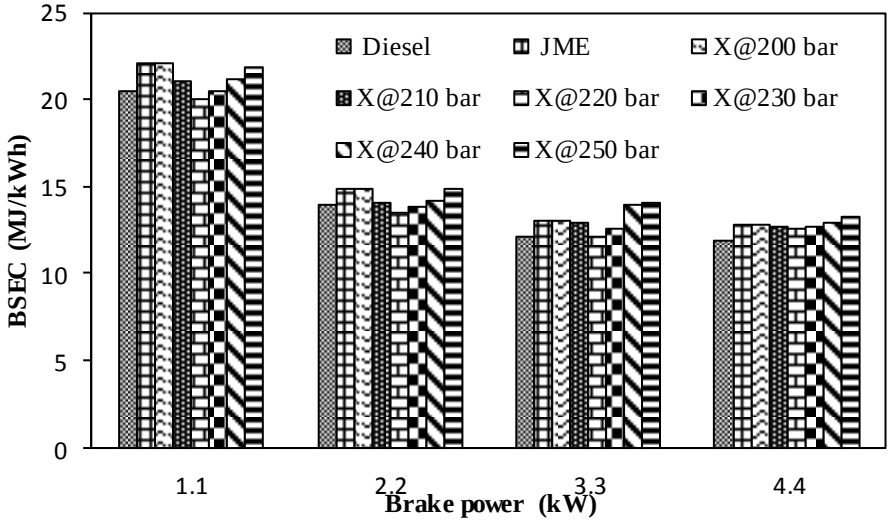

Fig. 5.34 Variation of BSEC with brake power at different nozzle opening pressures

5.5.2.3 Exhaust gas temperature

Figure 5.35 portrays the comparison of the exhaust gas temperature of diesel and the test blend X at different nozzle opening pressures. It is apparent from the figure that, the exhaust gas temperature always increased with increase in engine load, because of the increase in fuel quantity injected. At full load, the original nozzle opening pressure, the values of exhaust gas temperature are found to be about 303 and 325 ˚C for diesel and the test blend X respectively.

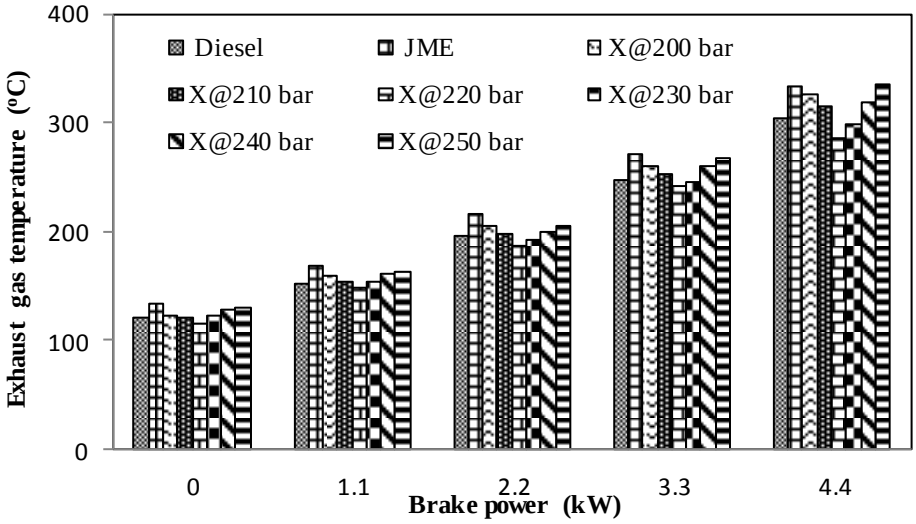

Fig. 5.35 Variation of exhaust gas temperature with brake power at different nozzle opening pressures

At full load and the nozzle opening pressures of 210, 220, 230, 240 and 250 bar, the values of exhaust gas temperature are recorded as 315, 285, 298, 318 and 334 ˚C respectively. The exhaust gas temperature is found to increase with the increase in the nozzle opening pressure after 220 bar. This is because at very high injection pressure of beyond 220 bar, a poor entrainment of air with surrounding fuel results in lesser fuel-air mixing leading to the occurrence of premixed heat release further away from the top dead center, which increased the exhaust gas temperature [258].

5.5.3 Emission parameters

5.5.3.1 Brake specific carbon monoxide emission

The rate of brake specific carbon monoxide (BSCO) emission results during combustion process due to deficiency of oxygen molecule. In the presence of sufficient oxygen, the carbon monoxide is converted into carbon dioxide (CO_2). The BSCO emission results are illustrated in Figure 5.36, for different nozzle opening pressures of the test blend X, in

comparison with diesel at different brake power. The BSCO emission for the JMETPO20 blend is marginally lower on increasing the nozzle opening pressure up to 220 bar, compared to that of the original nozzle opening pressure. This could be due to the fact that, with an increase in the nozzle opening pressure, better atomization of the fuel resulted in the smaller droplet size, faster vaporisation of fuel sprays and improved reaction between the fuel and the air.

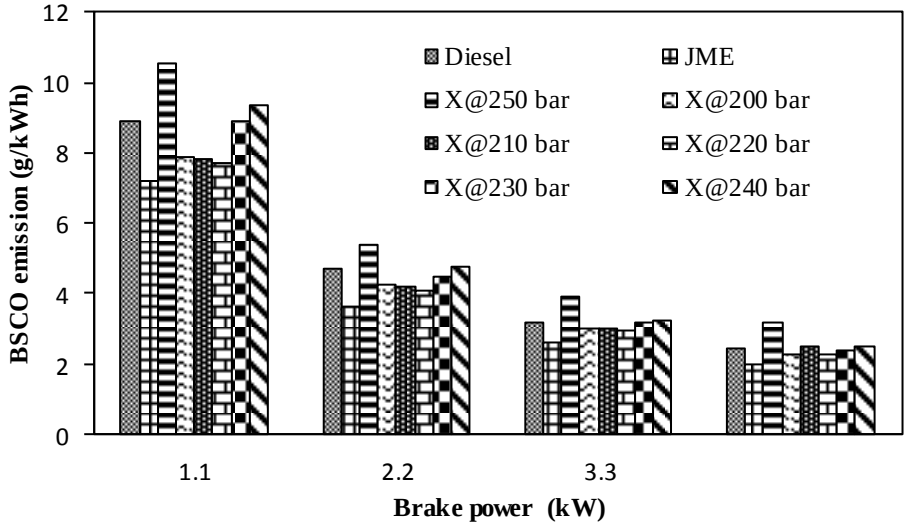

Fig. 5.36 Variation of the BSCO emission with brake power at different nozzle opening pressures

The lesser BSCO emission can be correlated with the higher heat release rate and peak in-cylinder pressure of the test blend X at 220 bar injection pressure. The lower value of BSCO emission for the test blend X is found to be 2.24 g/kWh, at full load and the nozzle opening pressure of 220 bar. When the nozzle opening pressure increases from 220 bar, the fuel droplet travels with a high velocity, and may hit the wall of combustion chamber, which results in incomplete combustion and may lead to higher BSCO [259]**.** This reason can be supported by Pei Lin Zhou [260], in his research work.

5.5.3.2 Brake specific hydrocarbon emission

The brake specific hydrocarbon (BSHC) emission consists of fuel that is completely unburned or only partially burned. The hydrocarbon emission is influenced by the fuel and air mixing and is largely affected by the overall air-fuel equivalence ratio [261]. The BSHC emission results at different nozzle opening pressures for diesel and the test blend X is illustrated in Figure 5.37. The BSHC emissions for diesel and the test blend X at full load and the original are about 0.59 and 0.55 g/kWh respectively.

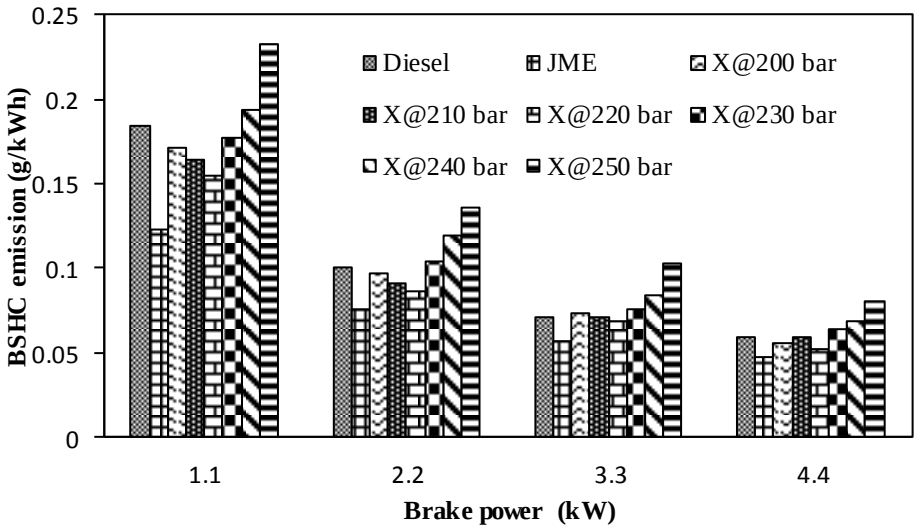

Fig. 5.37 Variation of BSHC emission with brake power at different nozzle opening pressures

As seen from the figure, for the test blend X, when the nozzle opening pressure increases up to 220 bar, the BSHC emission decreases. At full load and nozzle opening pressure of 220 bar, the minimum BSHC emission of about 0.52 g/kWh is obtained with the test blend X, which is lower by about 6.12%, compared to that of the original nozzle opening pressure. This is because at higher injection pressure the fuel has better atomization characteristics, and the fuel droplets gain better momentum and deeper penetration leading to complete combustion. However, increasing the nozzle opening pressure beyond 220 bar accelerates the formation of BSHC emission. This is because at very high injection pressure, a poor entrainment of air with the surrounding fuel results in incomplete combustion favoring higher concentration of BSHC. The BSHC emission for the test blend X is approximately 0.58, 0.52, 0.64, 0.69 and 0.80 g/kWh for the nozzle opening pressures of 210, 220, 230, 240, and 250 bar, respectively, and at full load.

5.5.3.3 Brake specific nitric oxide emission

The formation of nitric oxide (NO) emission is highly dependent on the maximum temperature of burning gas, oxygen concentration, and time available for the reactions to take place. Figure 5.38 presents the brake specific nitric oxide (BSNO) emission values for diesel and the test blend X at different nozzle opening pressures. It is quite obvious that, due to improved combustion, the temperature in the combustion chamber is expected to be higher and also presence of oxygen in the test blend X results in the higher amount of BSNO emission. As observed in this figure, for the test blend X, when the nozzle opening pressure is increases up to 220 bar, the BSNO emission is increases. This can also

be evidenced from the heat release rate curve. The BSNO emissions for the test blend X at full load and nozzle opening pressures of 200, 210, 220, 230, 240, and 250 bar are noticed to be about 3.72, 4.17, 4.29, 3.92, 3.62 and 3.94 g/kWh respectively. Increasing nozzle opening pressure initially generates faster combustion rates in the premixed phase combustion, resulting in higher heat release rate.

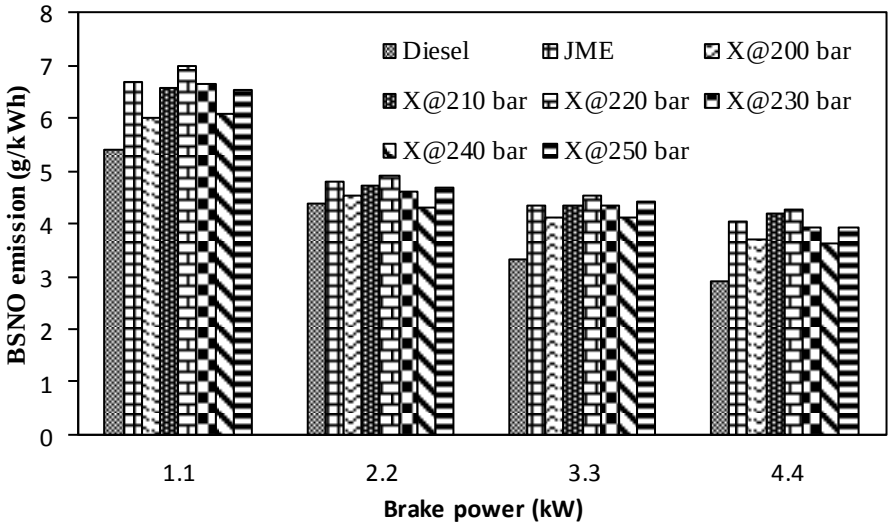

Fig. 5.38 Variation of the BSNO emission with brake power at different nozzle opening pressures

The BSNO emission decreases for the test blend X, while increasing the nozzle opening pressure beyond 220 bar compared to that of the original nozzle opening pressure, because of the lower premixed heat release rates, resulting in lower cylinder temperatures.

5.5.3.4 Smoke opacity

The smoke formation depends on fuel composition and is formed during premixed and diffusion combustion phase of the fuel rich mixtures [262]. The variations of smoke opacity with brake power for diesel and test blend X are illustrated in Figure 5.39. It can be observed from the figure that, the smoke opacity increases with the increase in the engine load, because, when the load increases more fuel is injected and this raises the smoke opacity [263]. At full load and the original nozzle opening pressure, the value of the smoke opacity for diesel and the test blend X is found to be about 86.3% and 63.1% respectively at full load. Smoke opacity is lower for the test blend X compared to that of diesel at full load. This is due to the presence of oxygen molecule in the test blend X which may help to break the aromatic content of the TPO. Increasing the nozzle opening pressure up to 220 bar, decreases the smoke opacity, as shown in the figure.

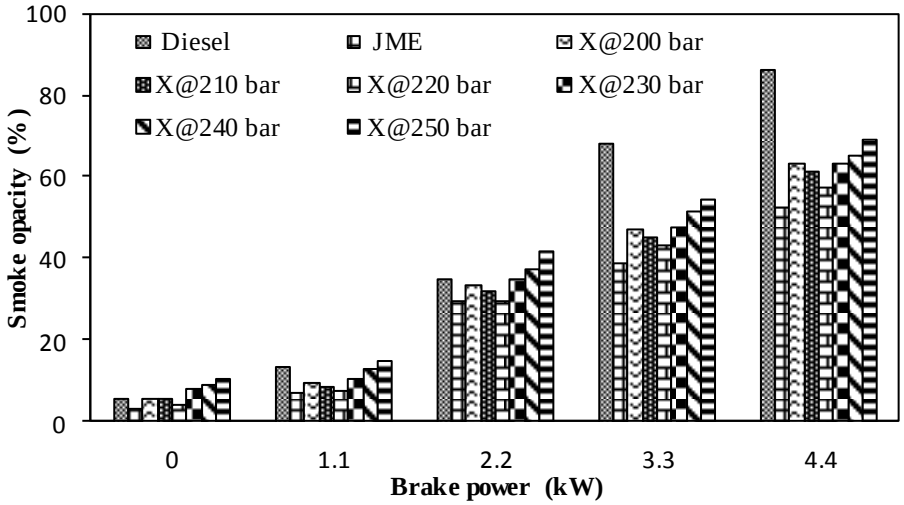

Fig. 5.39 Variation of smoke opacity with brake power at different nozzle opening pressures

This may be due to the small diameter of the particles which enable better mixing of fuel with air, resulting in better combustion. For the test blend X at full load and the nozzle opening pressure of 220 bar, the smoke opacity is lower by about 9.5%, compared to that of the original nozzle opening pressure. By increasing the nozzle opening pressure beyond 220 bar, an inverse trend is noticed. This can also be evidenced from the combustion duration Figure 5.30 The values of smoke opacity for the test blend X are about 61.2%, 57.1%, 63%, 65.3% and 69.1%, at nozzle opening pressures of 210, 220, 230, 240, and 250 bar respectively and full load.

5.4.4 Summary

In this chapter, the experimental results obtained for the combustion, performance and emission parameters of a single cylinder, four stroke, air cooled DI diesel engine running at optimized injection timing of 24.5 ˚CA bTDC with the different nozzle opening pressures (from 200 to 250 bar in a step of 10 bar) are presented. Based on the test results, it was observed that the higher nozzle opening pressure of 220 bar, gave significantly better results of the engine behavior run on the JMETPO20 blend compared to other nozzle opening pressures. On the whole, it can be summarized that, the advanced injection timing of 24.5 ˚CA bTDC and the higher nozzle opening pressure of 220 bar was the optimum combination for the JMETPO blend operated engine at which the engine gave better results.

The summary of the values obtained at full load for some of the important parameters related to the combustion, performance and emission parameters of the test engine run on diesel, JME and the JMETPO20 blend at different nozzle opening pressures are presented in Appendix 8.

The next section presents the effect of operating the engine fueled with the JMETPO20 blend at different compression ratios, keeping the injection timing and nozzle opening pressure of the engine at optimum conditions which would enable us to find the optimum compression ratio for the blend.

5.6 Effect of compression ratios on combustion, performance and emission characteristics of a diesel engine fueled with the JMETPO20 blend

After performing the experimental investigation on the test engine by varying the fuel injection timing and nozzle opening pressure, and analysing the results, the optimum injection timing and nozzle opening pressure were chosen as 24.5 ˚CA bTDC and 220 bar respectively. Furthermore, the effect of varying the compression ratio of the JMETPO20 blend fueled engine on the combustion, performance and emission characteristics were studied. Experiments were conducted for the JMETPO20 blend at the optimum injection timing of 24.5 ˚CA and nozzle opening pressure of 220 bar, for the compression ratios of 16.5, 17.5 and 18.5. The experimental results of the JMETPO20 blend were compared with those of the diesel operation under standard test conditions and are presented in the subsequent sections.

In this section, the JMETPO20 blend is designated as the blend "X". The designations used in this study for diesel, JME and the test blend X at different compression ratios are given below.

Test fuels	Designation
Diesel at injection timing of 23 ˚CA bTDC, nozzle opening pressure of 200 bar and compression ratio of 17.5	Diesel
JME at injection timing of 23 ˚CA bTDC, nozzle opening pressure of 200 bar and compression ratio of 17.5	JME
X at injection timing of 23 ˚CA bTDC, nozzle opening pressure of 200 bar and compression ratio of 17.5	X@standard
X at injection timing of 23 ˚CA bTDC, nozzle opening pressure of 200 bar and compression ratio of 16.5	X@16.5
X at injection timing of 23 ˚CA bTDC, nozzle opening pressure of 200 bar and compression ratio of 17.5	X@17.5
X at injection timing of 23 ˚CA bTDC, nozzle opening pressure of 200 bar and compression ratio of 18.5	X@17.5

5.6.1 Combustion parameters

5.6.1.1 Cylinder pressure history

The peak pressure in a compression ignition (CI) engine depends primarily on the combustion rate in the initial stages, and is influenced by the fuel taking part in the premixed combustion phase [264]. The variations of the cylinder pressure with respect to the crank angle at different compression ratios, for diesel and the blend at full load are shown in Figure 5.40. The cylinder pressures for diesel and the test blend X are obtained

as 81 bar at 370.30 ˚CA and 80 bar at 371 ˚CA respectively, at the original compression ratio and full load.

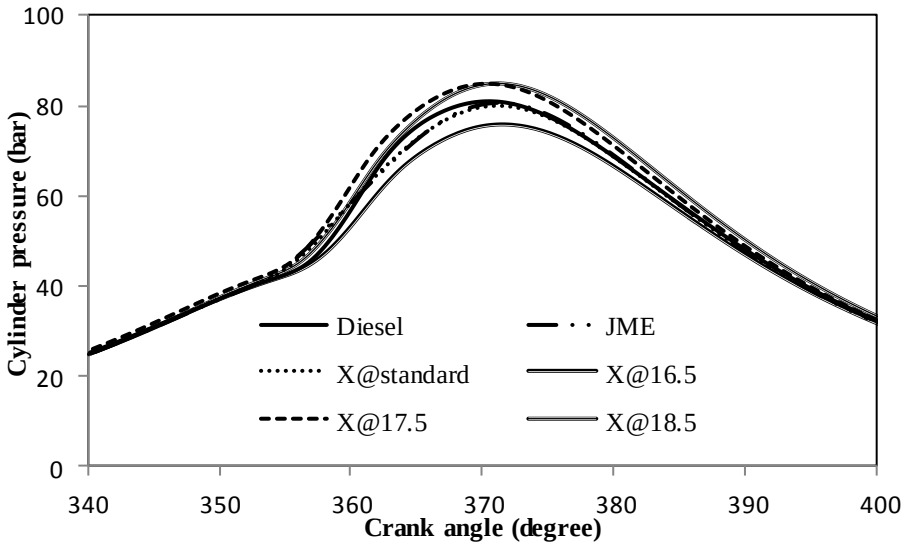

Fig. 5.40 Variation of cylinder pressure with crank angle at different compression ratios and full load

It can be observed from the figure that, the combustion starts marginally earlier for the blend than for diesel at the original compression ratio. This is because of the higher cetane number and presence of oxygen in the blend, which results in improved combustion. The values of the maximum cylinder pressure for the blend at full load have been recorded as 75.8 bar at 371.7 ˚CA, 84.8 bar at 370.4 ˚CA and 84.9 bar at 371.4 ˚CA at compression ratios of 16.5, 17.5 and 18.5, respectively. It can also be observed from the figure, that from a lower to a higher compression ratio, the maximum cylinder pressure is increased for the blend. The reason is that with the increase in the compression ratio, the intake air temperature increases, which provides better fuel atomization and mixture preparation with the air, and accelerates the complete combustion process. Similar reasons are documented by Nagaraja et al. [265], in their work on variable compression ration DI diesel engine fueled with diesel, Corn oil methyl ester, and Palm oil methyl ester. The maximum cylinder pressure for the blend is found to be enhanced by about 6.2% at full load by increasing the compression ratio to 18.5 compared to that of the original compression ratio. For the test blend X at the lower compression ratio of 16.5, the maximum cylinder pressure is found to be lower compared to those of the original and the higher compression ratio, because of the relatively slower premixed combustion phase that ends up in a lower maximum cylinder pressure.

5.6.1.2 Ignition delay

Figure 5.41 compares the ignition delay curve of diesel and the test blend X for different brake powers at three different compression ratios.

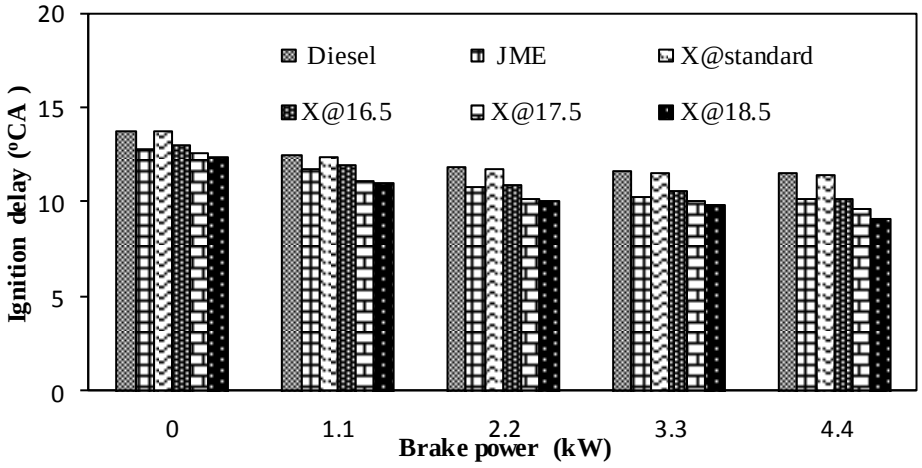

Fig. 5.41 Variation of ignition delay with brake power at different compression ratios

As shown in the figure, as the load increases, the ignition delay decreases for both the fuels at all compression ratios. This is because, as the engine load increases, the heat loss during compression decreases, resulting in higher temperature and pressure of the compressed air, and a shorter ignition delay is obtained. A similar reason was reported by Gumus [266], for the results they obtained from the experimental investigation carriedout on a diesel engine run on Hazelnut kernel oil methyl ester at different compression ratios. At the original compression ratio and full load, the values of the ignition delay for diesel and the test blend X are about 11.5 and 11.4 ˚CA respectively. For the test blend X at full load, the values of ignition delay are 10.1, 9.6 and 9.1 ˚CA at the compression ratios of 16.5, 17.5 and 18.5 respectively. The lowest value of ignition delay is recorded as 9.1 ˚CA, at the compression ratio of 18.5 and full load for the test blend X and, it is found to be shorter by about 2.3 ˚CA, compared to the values at the original compression ratio. The increase in the compression ratio increases the compressed air temperature, which reduces the viscosity of the blend, by breaking down the intermolecular bonds, and decreasing the self ignition temperature of the fuel; and hence, the ignition delay is found shorter [267].

5.6.1.3 Heat release rate

The comparison of the heat release rate curve at full load for diesel and the blend at different compression ratios is depicted in Figure 5.42.

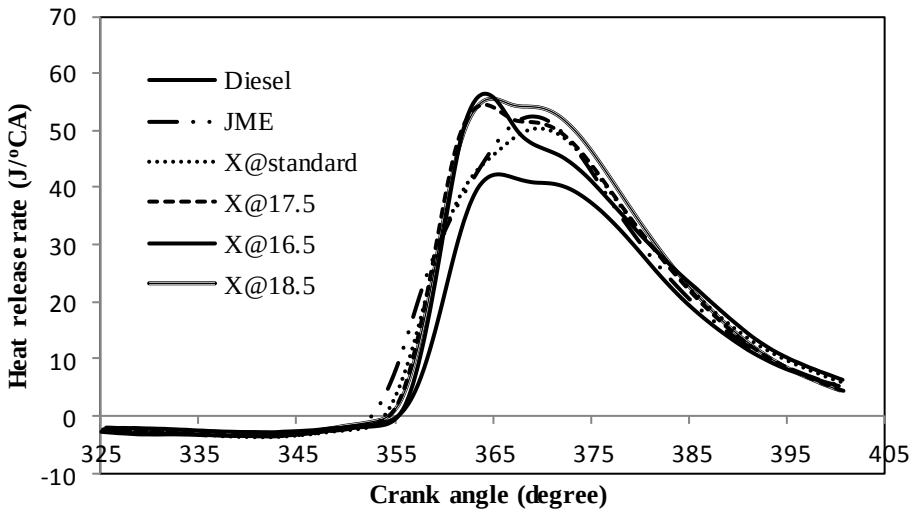

Fig. 5.42 Variation of heat release rate at different compression ratios and full load

Figure 5.47 indicates that, the value of the peak heat release rate is the higher for diesel, compared to that of the blend at all compression ratios. This may be attributed to the higher calorific value of diesel; and more fuel accumulating owing to longer ignition delay would increase the amount of fuel burnt during the premixed combustion phase, causing a higher heat release rate. At full load, the values of the heat release rate for diesel and the blend are found to be about 56.4 and 50.4 J/˚CA respectively, at the original compression ratio. At full load, the values of the maximum heat release rate in case of the blend are by about 42.3, 54.5 and 55.6 J/˚CA, for the compression ratios of 16.5, 17.5 and 18.5 respectively. The heat release rate of 55.6 J/˚CA is obtained for the blend at the compression ratio of 18.5, which is 10.3% higher than that of the original compression ratio at full load. The higher compression ratio enhanced the heat release rate for the blend due to the reduction in viscosity, and this might promote a better spray formation as the intake air temperature increases with a higher compression ratio. The reasons are in good agreement with those of Muralidharan and Vasudevan [268], when the tests were conducted on variable compression ratio diesel engine was fueled with methyl esters of waste cooking oil and diesel blends. The lower heat release rate is observed for the test blend X at a lower compression ratio of 16.5, due to the slower air-fuel mixture formation, weak air entrainment and poorer combustion of the fuel.

5.6.1.4 Combustion duration

Figure 5.43 depicts the variations of the combustion duration for diesel and the test blend X at different compression ratios. The combustion duration becomes longer with the

increase in the engine load for both the fuels, owing to the increase in the quantity of fuel injected.

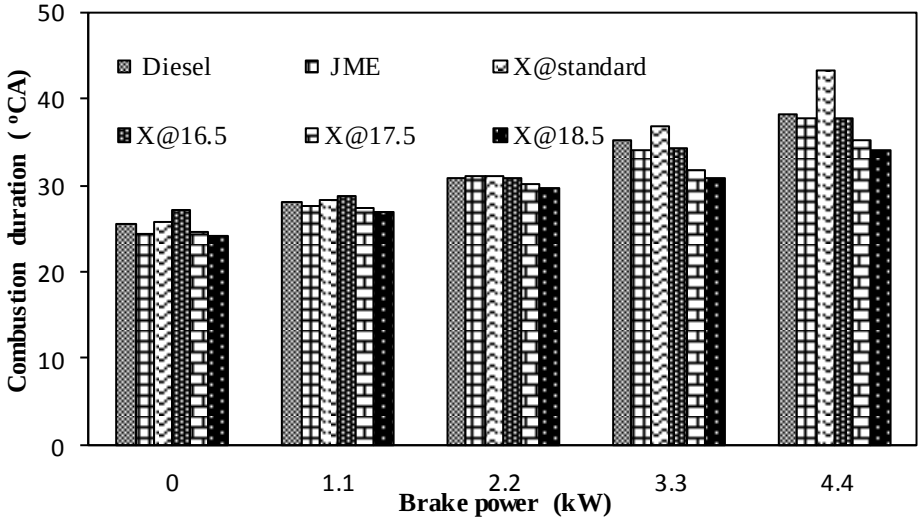

Fig. 5.43 Variation of combustion duration with brake power at different compression ratios

At the original compression ratio and full load, the values of the combustion duration for diesel and the blend are found to be about 38.3 and 43.3 ˚CA respectively. The longer combustion duration obtained with the test blend X, at the original compression ratio is the result of an increase in the quantity of fuel consumed, to maintain the engine speed stable at different loads, as the calorific value of the blend is lower than that of diesel. The values of the combustion duration are found to be about 38, 35.4 and 34.2 ˚CA, at the compression ratios of 16.5, 17.5 and 18.5 respectively, at full load. The lowest value of combustion duration of 34.2 ˚CA is observed with the compression ratio of 18.5 for the blend, at full load. The increase in combustion duration causes a rise in the in-cylinder air temperature and pressure that provides faster fuel vaporization, and accelerates the complete combustion process and a decrease in the combustion duration. Similar reasons are given by Ibrahim et al. [269], in their work on the impact of changing the compression ratio of a diesel engine fueled with waste-cooking-oil biodiesel and its diesel blends.

5.6.1.5 Maximum cylinder pressure

The variation of maximum cylinder pressure with brake power at different compression ratios for test fuels are shown in Figure 5.44. It is observed that maximum cylinder pressure for diesel and the test blend X is 81 and 80 bar respectively at original compression ratio. The maximum cylinder pressure increased with increasing the

compression ratio [270]. The maximum cylinder pressure is higher for the test blend at higher compression ratio of 18.5 compared to lower compression ratio of 16.5. This is due to the faster and complete combustion of fuel inside the combustion chamber.

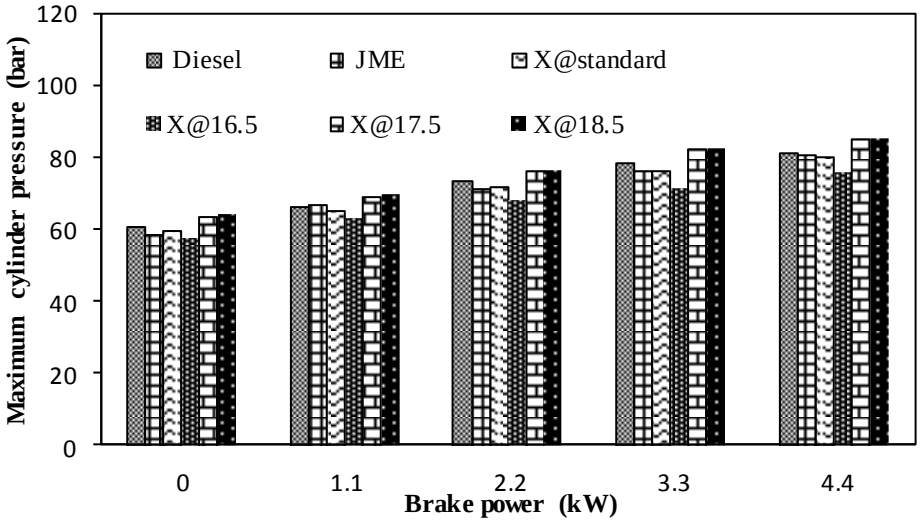

Fig. 5.44 Variation of maximum cylinder pressure with brake power at different compression ratios

5.6.1.6 Maximum rate of pressure rise

The variation of the maximum rate of pressure rise with brake power for diesel and the test blend X at different compression ratios, is shown in Figure 5.45.

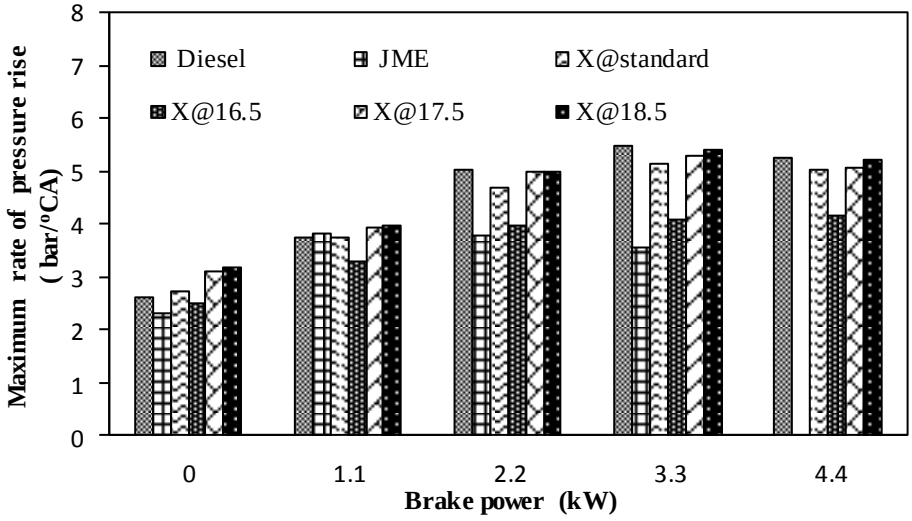

Fig. 5.45 Variation of maximum rate of pressure rise with brake power at different compression ratios

The maximum rate of pressure rise at the original compression ratio for diesel varies from 2.6 bar/˚CA at no load to 5.3 bar/˚CA at full load, and for the blend it varies from 2.7 bar/˚CA at no load to 5 bar/˚CA at full load**.** The maximum rate of pressure rise is found to

be rising with increase in compression ratio for the blend from no load to full load. The maximum rate of pressure rise at full load is found to be the highest as 5.2 bar/°CA for the blend at the compression ratio of 18.5. The oxygen enrichment in the blend due to the addition of JME accelerates the reactions, and this result in more complete combustion of fuels. This is the reason for the increase in the maximum rate of pressure rise at a higher compression ratio. This reason can also be supported from the research work documented by Mozhi et al. [271]. The values of the maximum rate of pressure rise at compression ratios of 16.5, 17.5 and 18.5, are found to be about 4.2, 5.1 and 5.2 bar/°CA respectively, for the test blend X at full load.

5.6.2 Performance parameters

5.6.2.1 Brake thermal efficiency

Figure 5.46 shows the effect of the compression ratios on the brake thermal efficiency for diesel and the test blend X.

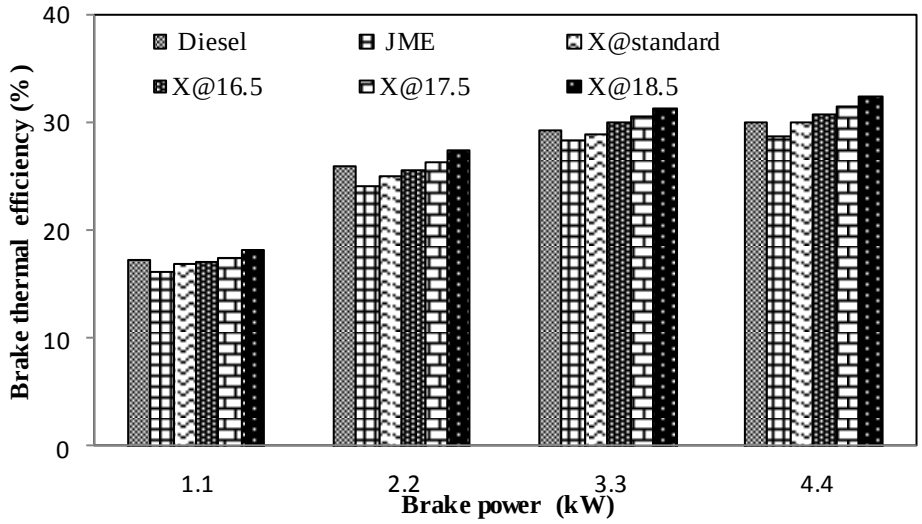

Fig. 5.46 Variation of brake thermal efficiency with brake power at different compression ratios

It is evident from the figure, that the thermal efficiency is found to increase considerably with the increase in the load as a reduction in the heat loss and increase in power are encountered at higher loads. The values of thermal efficiency for diesel and the blend are very close to each other. The results indicate that the thermal efficiency of diesel and the test blend X at full load are about as 29.89% and 29.88% respectively at the original compression ratio. Generally, increasing the compression ratio improves the thermal efficiency of the engine. This is because, at a higher compression ratio, the compressed air

temperature is higher, which ends up in better combustion of the fuel [272]. At full load, the values of brake thermal efficiency for the test blend X at compression ratios of 16.5, 17.5 and 18.5 was obtained as 30.7%, 31.4% and 32.3% respectively. The test blend X exhibits the highest thermal efficiency with 32.3% at the compression ratio of 18.5, and it is about 8% higher than that of diesel. The possible reason for this may be the proper mixing of the fuel-air, and improved fuel spray characteristics that occur with the higher compression ratio of 18.5. At full load, the thermal efficiency for the blend at the compression ratio of 16.5 was decreased by about 2.2% and 4.8% compared to that of the compression ratios of 17.5 and 18.5, respectively.

5.6.2.2 Brake specific energy consumption

Figure 5.47 illustrates the variations of the BSEC for diesel and the blend with the brake power at different compression ratios. At the original compression ratio and full load, the values of BSEC for diesel and the blend were recorded as 11.9 and 12.6 MJ/kWh respectively.

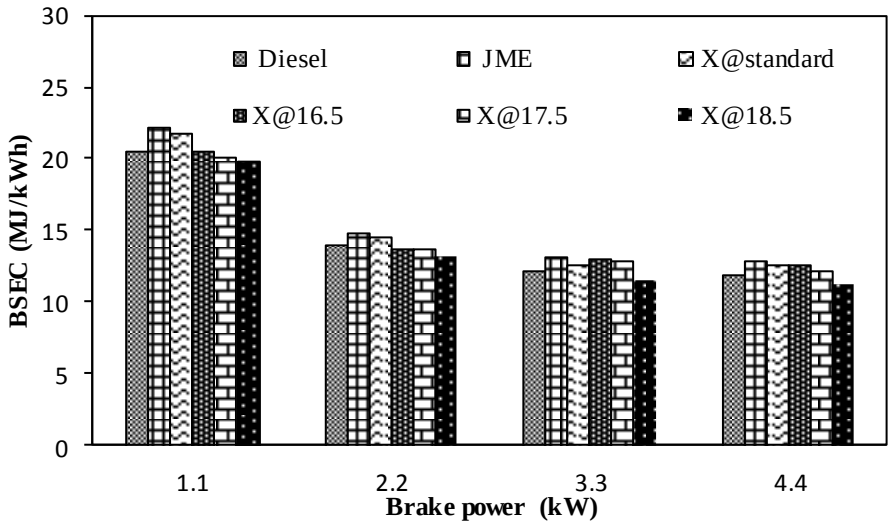

Fig. 5.47 Variation of BSEC with brake power at different compression ratios

The BSEC for the test blend X at full load is obtained as 12.52, 12.1 and 11.15 MJ/kWh at compression ratios of 16.5, 17.5 and 18.5, respectively. It can be observed from the figure that, while increasing the compression ratio of the engine the BSEC will be reduced for the blend. The lowest value of BSEC for the test blend X is found to be about 11.2 MJ/kWh, at full load and original compression ratio. The possible reason may be that higher compression ratio enhances the extent of evaporation and subsequently the combustion process [273]. But, with the lower compression ratio, the BSEC increases

owing to incomplete combustion, resulting in a lowered power output and decreased brake thermal efficiency.

5.6.2.3 Exhaust gas temperature

The variations of the exhaust gas temperature for different compression ratios are depicted in Figure 5.48. With the increase in engine load, the exhaust gas temperature is found to increase due to higher combustion temperature inside the cylinder as more fuel is burnt with increasing load. At the original compression ratio, the values of exhaust gas temperature are found to be about 303 and 335 ˚C for diesel, and the blend respectively, at full load. For the blend as the compression ratio increases, the exhaust gas temperature decreases. At full load the values of exhaust gas temperature for the blend are recorded as 310, 290 and 285 ˚C for the compression ratios of 16.5, 17.5 and 18.5 respectively. The blend has the lowest value of exhaust gas temperature at compression ratio of 18.5 and it is lower by about 18 ˚C as compared to that for diesel at full load. This may be due to the fact that air entered during the suction stroke at higher compression ratio is compressed, which increases the air temperature.

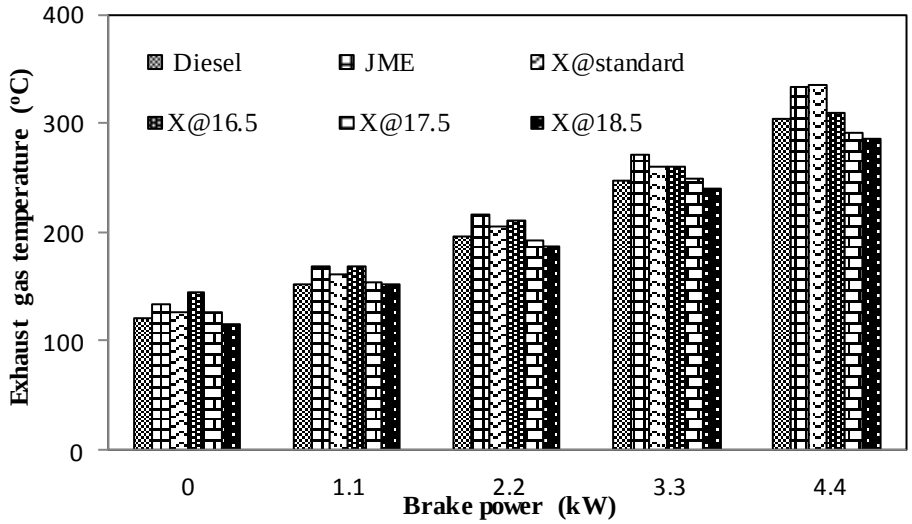

Fig. 5.48 Variation of exhaust gas temperature with brake power at different compression ratios

The increased air temperature helps for better atomization of fuel which contributing more complete combustion and resulting reduction in the exhaust gas temperature [274]. At lower compression ratio of 16.5 the exhaust gas temperature for the blend is higher as to more amount of heat is released during diffusion phase resulting in more amount of heat going along with exhaust gas.

5.6.3 Emission parameters

5.5.3.1 Brake specific carbon monoxide emission

It is known that the rate of carbon oxide (CO) emission is a function of the unburned fuel availability and mixture temperature, which controls the rate of fuel decomposition and oxidation [275].

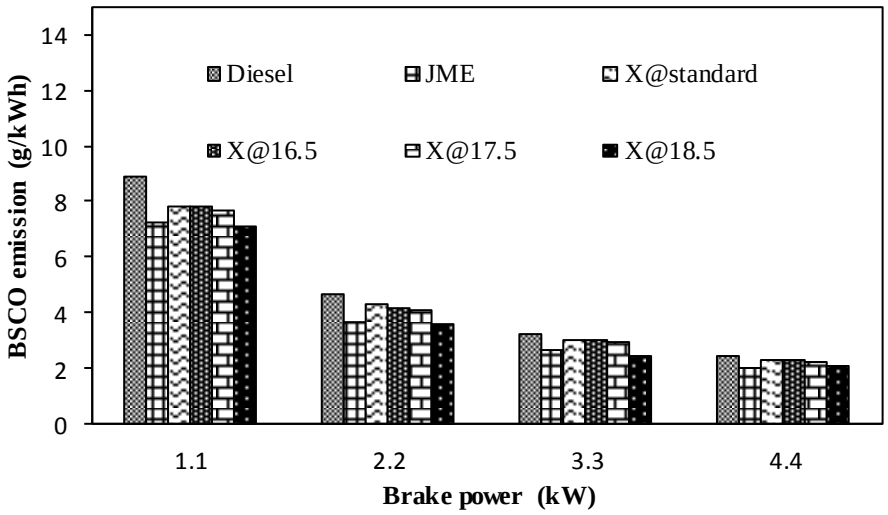

Fig. 5.49 Variation of BSCO emission with brake power at different compression ratios

The brake specific carbon monoxide (BSCO) emission results are illustrated in Figure 5.49 at different compression ratios of the blend, in comparison with those for diesel. The BSCO emissions for diesel and for the blend at the original compression ratio and full load are about 2.45 and 2.28 g/kWh respectively. The BSCO for the blend at full load was obtained as 2.3, 2.24 and 2.04 g/kWh at compression ratios of 16.5, 17.5 and 18.5, respectively. The BSCO emission for the blend is marginally lower on increasing the compression ratio to 18.5, compared to the original compression ratio. This could be due to the fact that, the increased compression ratio increases the air temperature inside the cylinder subsequently reducing the delay period leading to better and more complete burning of the fuel and so lower BSCO emission. This reason can also be supported from the research article published by Kassaby and Nemitallah [276] for a similar work carriedout. The lower value of BSCO emission at full load for the blend was found to be 2.04 g/kWh, at the compression ratio of 18.5.

5.6.3.2 Brake specific hydrocarbon emission

The hydrocarbon (HC) emission consists of fuel that is completely unburned or alone partially burned. The HC emission is influenced by the fuel-air mixing, and is abundantly

affected by the overall air-fuel equivalence ratio, as the equivalence ratio varies broadly from very rich at the core of the spray to very lean at the spray boundaries [277]. The brake specific hydrocarbon (BSHC) emission results at different compression ratios for diesel and the blend are illustrated in Figure 5.50. The BSHC emissions for diesel and the blend at the original compression ratio are about 0.059 and 0.055 g/kWh respectively at full load.

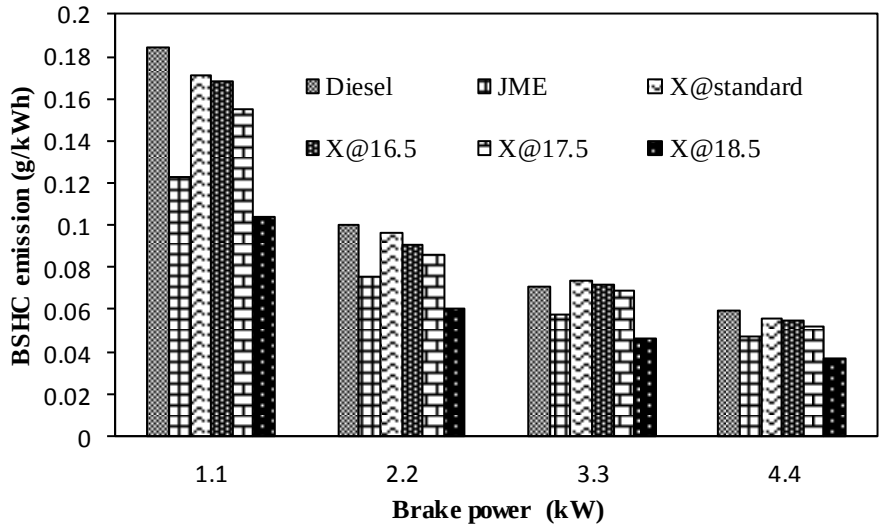

Fig. 5.50 Variation of BSHC emission with brake power at different compression ratios

The figure indicates that, the BSHC emission of the test blend X, is lower at the higher compression ratio of 18.5. At the compression ratio of 18.5, the minimum BSHC emission of about 0.037 g/kWh is obtained with the blend, which is lower by about 32%, compared to the original compression ratio at full load. The increase in compression ratio enhances the air density and temperature in the cylinder, resulting in better fuel-air mixing in the combustion chamber, which contributes to the more complete combustion of the fuel. The BSHC emission for the test blend X is found measured to be 0.055, 0.052, and 0.037 g/kWh, at the compression ratios of 16.5, 17.5 and 18.5, respectively and full load.

5.6.3.3 Brake specific nitric oxide emission

The formation of nitric oxide (NO) emission is highly dependent on the maximum temperature of burned gases during the premixed combustion phase, oxygen concentration, and the time available for the reactions to take place [278]. Figure 5.51 depicts the BSNO emission values for diesel and the blend at different compression ratios.

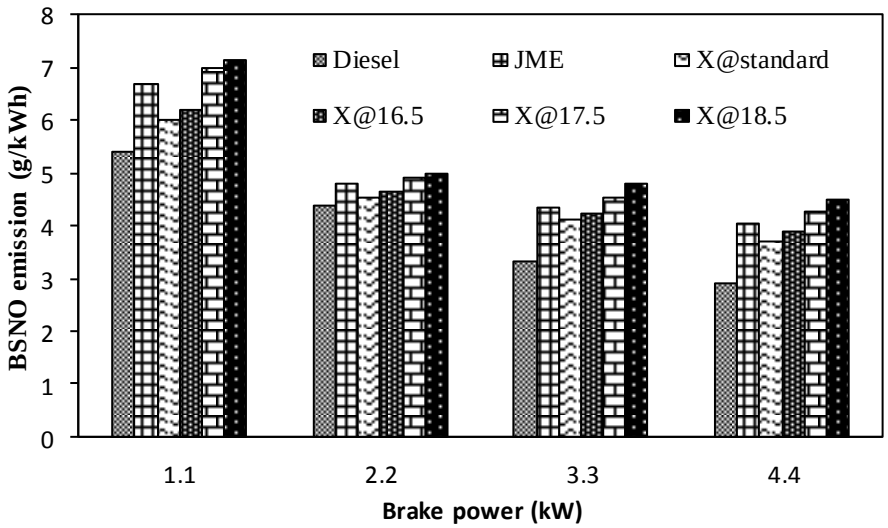

Fig. 5.51 Variation of BSNO emission with brake power at different compression ratios

The BSNO emissions for the blend at full load are found to be about 3.9, 4.3, and 4.5 g/kWh, at the compression ratios of 16.5, 17.5 and 18.5, respectively. As observed in this figure, for the blend, at the higher compression ratio of 18.5, the BSNO emission is found to be higher compared to the original and lower compression ratio. It is quite obvious that, at the higher compression ratio, the temperature in the combustion chamber is higher due to improved combustion, and also the amount of oxygen present in the blend, results in higher amount of NO formation. The increase in the air intake temperature due to the rise in the compression ratio generates faster combustion rates, resulting in higher burned gas temperatures. The BSNO emission is decreased for the blend, while decreasing the compression ratio to 16.5, compared to that of the original compression ratio, because of lower premixed heat release rates, which cause a lower combustion temperature.

5.6.3.4 Smoke opacity

The smoke formation depends mainly on the incomplete burning of the hydrocarbon fuel, and partially reacted carbon content in the liquid fuel [279]. The results of smoke opacity are depicted in Figure 5.52 at different compression ratios. It is apparent from the figure that, the smoke opacity increases with rise in the engine load due to the overall richer combustion, longer duration of the diffusion phase and reduced oxygen concentration [280]. At the original compression ratio, the smoke opacity for diesel and the blend is about 86.3% and 63.1% respectively, at full load. At the original compression ratio, the smoke opacity for the test blend X is relatively less in comparison with diesel, due to the presence of oxygen in the blend that contributes to a complete fuel oxidation. This actually

leads to a significant drop in smoke opacity. For the blend at the compression ratio of 18.5, the smoke opacity is lower by about 17.4%, compared to that of the original compression ratio at full load.

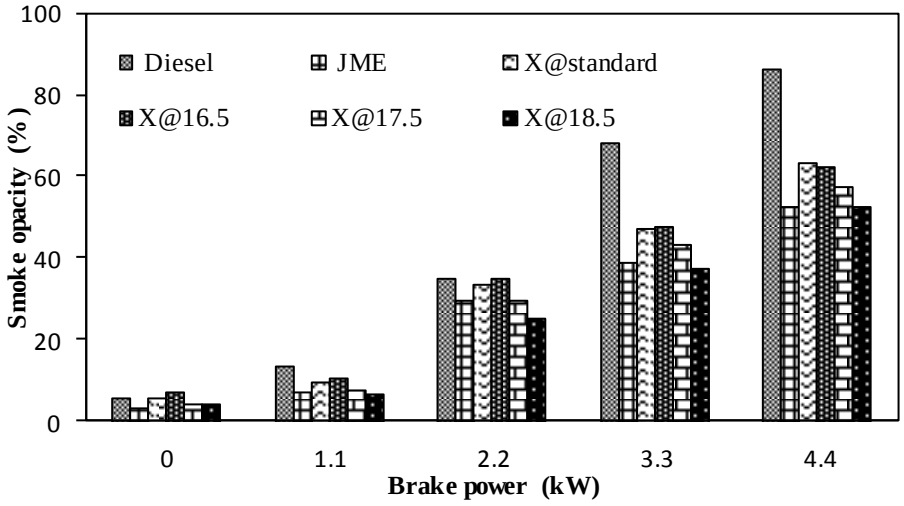

Fig. 5.52 Variation of smoke opacity with brake power at different compression ratios

At full load, the values of smoke opacity for the blend are about 62.3%, 57.1%, and 52.1%, at the compression ratios of 16.5, 17.5 and 18.5, respectively. The smoke opacity reduced at the higher compression ratio of 18.5 compared to the original and lower compression ratios, because as the compression ratio increases, the combustion temperature increases due to improved fuel atomization, and this leads to the reduction in smoke opacity.

5.6.4 Summary

This experimental investigation was aimed to study the effects of compression ratio (one higher (18.5) and one lower (16.5) in addition to the original compression ratio of 17.5) of the engine fueled with the blend X, keeping the injection timing (24.5 ˚CA bTDC) and nozzle opening pressure (220 bar) of the engine at optimum conditions. The above experimental findings suggest that the combustion, performance and emission characteristics for the test blend X are relatively better at the higher compression ratio of 18.5 as compared to those at standard operating conditions. Overall it can be summarized that the advanced injection timing of 24.5 ˚CA bTDC, nozzle opening pressure of 220 bar and compression ratio of 18, improved the overall performance of the engine compared to that of standard settings, and established this combination as the optimum engine operating parameters for the engine run on the JMETPO20 blend.

The summary of the values obtained at full load for some of the important parameters related to the combustion, performance and emission parameters of the test engine run on diesel, JME and the JMETPO20 blend at different compression ratios are given in Appendix 9.

The next section presents, the effect of blending different amounts of tyre pyrolysis oil (TPO) with Jatropha methyl ester (JME) on the oxidation stability of the different JMETPO blends. In addition to this, an experimental investigation was also carriedout by using the JMETPO20 blend, to evaluate the behaviour of the diesel engine run on the biodiesel blend, with and without synthetic antioxidants

5.7 Effect of blending tyre pyrolysis oil with Jatropha methyl ester on oxidation stability

Tyre pyrolysis oil (TPO) derived from waste automobile tyres through pyrolysis contains a few phenolic compounds. The phenolic compounds present in the TPO may act as natural antioxidants to Jatropha methyl ester (JME). In this investigation, an attempt was made to study the effect of blending different amounts of TPO with JME on the oxidation stability. For this purpose, 20%, 40% and 60% (on volume basis) of TPO were blended with the JME and the blends were designated as JMETPO20, JMETPO40 and JMETPO60 respectively. The oxidation stabilities of the blends were determined and as they did not reach the required values as per the standard specifications, three commercially available antioxidants namely tert-butyl hydroquinone (TBHQ), pyrogallol (PY) and propyl gallate (PG) were added in small quantity (200 ppm) to the JMETPO20 blend. In addition to this, an experimental investigation was also carriedout by using the JMETPO20 blend, to evaluate the behaviour of the diesel engine run on the JMETPO20 blend, with and without synthetic antioxidants. The compositions of different JME-TPO in comparison with the diesel-JME blends have already been given in chapter 4 Experimental methodology section. The designations of the test fuels are given below;

Blends	JME	Diesel	TPO
B80	80%	20%	
B60	60%	40%	
B40	40%	60%	
JMETPO20	80%		20%
JMETPO40	60%		40%
JMETPO60	40%		60%

5.7.1 Oxidation stability of test fuels

Figure 5.53 shows the oxidation stability of JME, B80, B60, B40, JMETPO20, JMETPO40 and JMETPO60 blends. It can be observed from the figure that, the JME meets the oxidation stability limit of 3 h as per ASTM D-6751 limit, but failed according to the IS-15607 limits for biodiesel and its blends. Because according to the ASTM D-6751 and IS-15607 limit for the diesel-biodiesel blend (up to B20), the induction period is 6 h and 20 h respectively. It can be observed from the figure, that as the percentage of diesel increases in the diesel-JME blend; the induction period also increases, resulting in

the increase in the oxidation stability owing to the decrease of unsaturated fatty acid in the blend.

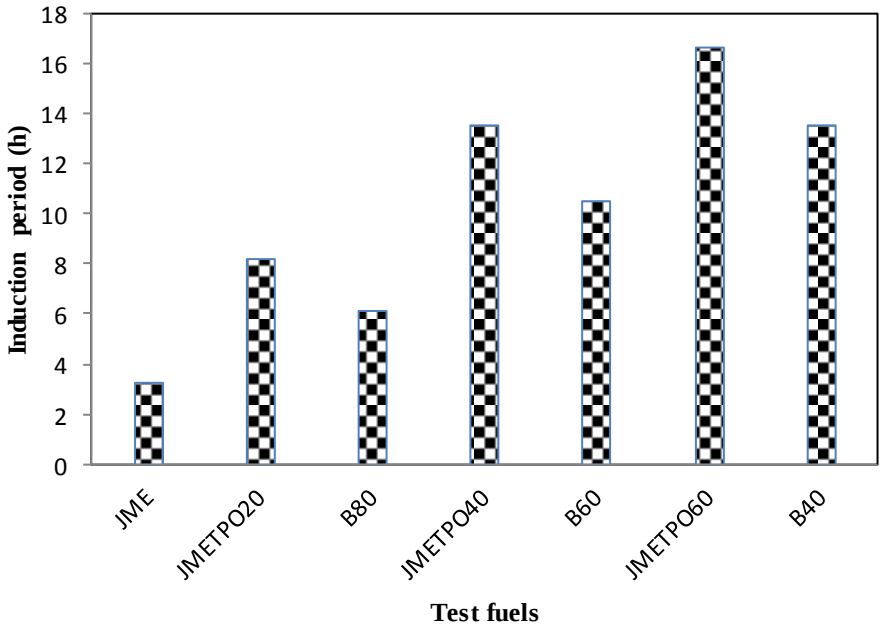

Fig. 5.53 Oxidation stability of test fuels

It is evident from figure that, as the percentage of TPO increases in the blend, the induction period also increases, showing improvement in the oxidation stability. This can be attributed to the presence of some of phenolic compounds present in TPO which act as antioxidant [281]. The induction period of the JMETPO20, JMETPO40 and JMETPO60 blends increases in comparison with the JME, but then also fails as per IS-15607 limits. However, by adding a very small amount of synthetic antioxidants, the required limit could be achieved for the JMETPO blends. Also, it can be understood from the figure that, the JMETPO blends have more oxidation stability than those of the B80, B60 and B40 blends, even than the same amount of JME is available in the respective blends.

5.7.2 Effect of antioxidants on the oxidation stability

The induction period for different fuels tested with the synthetic antioxidants in this investigation is depicted in Figure 5.54. Although, it is possible to obtain the required oxidation stability of the blends using antioxidants, it will increase the cost of the resultant fuel as the antioxidants are expensive chemicals. It is reported in the literature that, the minimum amount of 600 ppm of α-tocopherol (α-T) antioxidant would be required to meet the oxidation stability of JME as per EN 14112 specification [282]. On the other hand, as the percentage of JME increases in the diesel-JME blend, the dosage of antioxidants

required to maintain induction period up to 20 h would also increase. It can be observed that, by doping antioxidant with 200 ppm, the oxidation stability of the JMETPO20 blend increases. It can also be observed from the figure that addition of 200 ppm of PY antioxidant increases the oxidation stability of the JMETPO20 blend, which meets the IS-15607 specification limits of oxidation stability for the biodiesel blend. For the same concentration of JME in the diesel-JME blend, the dosage of antioxidants required is 400 ppm. Thus, it is possible to reduce the dosage of antioxidant for the JMETPO20 blend by blending the TPO.

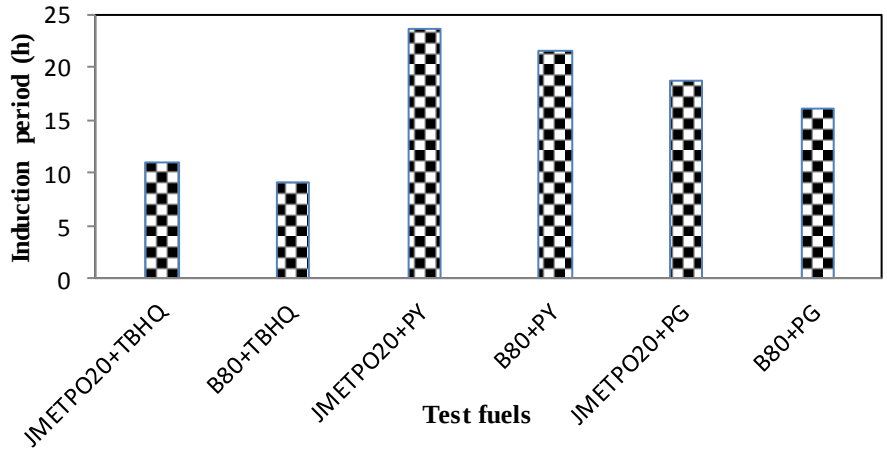

Fig. 5.54 Effect of antioxidants on the oxidation stability

5.7.3 Performance parameters

Brake specific energy consumption (BSEC) is a popular term used now a days related to performance of a diesel engine when two different fuels are blended and used in an engine [283]. Figure 5.55 shows the variation of the BSEC for diesel, JME and its blends with respect to brake power. The BSEC for diesel, JME and JMETPO20 blend is approximately 11.9, 12.5 and 12.8 MJ/kWh at full load respectively. The BSEC decreases with the rise in the brake power for all the test fuels. The engine requires more fuel with the blend than with diesel, to develop the same power output, owing to the lower calorific value, higher density of the blend and combustion attributes. The addition of antioxidants TBHQ, PY and PG to the JMETPO20 blend resulted mean reduction in BSEC by about 2.3%, 7% and 5.4% respectively at full load compared to that of JMETPO20 blend without antioxidant.

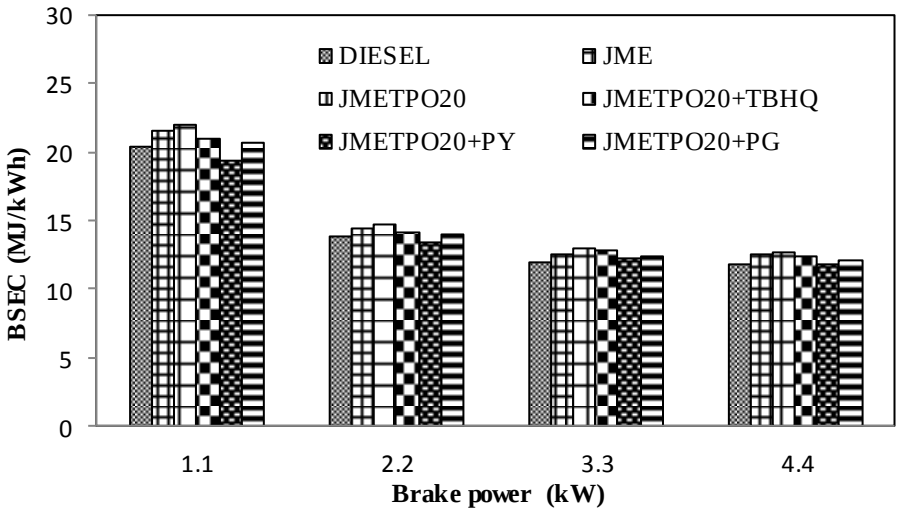

Fig. 5.55 Variation of BSEC with brake power

The antioxidants PY is found to be the most effective antioxidant for reducing BSEC. Similar findings have also been reported by Varatharajan et al. [284] in the past for jatropha biodiesel when they used BHT antioxidant with concentration of 0.025%-m.

5.7.4 Emission parameters

5.7.4.1 Brake specific nitric oxide emission

The prime factors which affect the nitric oxide (NO_x) formation of in a diesel engine are the higher combustion temperature and the accessibility of excess oxygen. The elevated combustion temperature (above 1700 K) breaks the strong triple bond of nitrogen molecules and generates highly reactive nitrogen which reacts with oxygen and produces NO_x [284]. Figure 5.56 illustrates the variation of brake specific nitric oxide (BSNO) emission with brake power for different test fuels. The BSNO emission is higher for JME and the JMETPO20 blend in comparison with diesel at all loads. This may be owing to the rich oxygen content of the JME which leads to complete combustion and resulted in higher combustion temperature [285-286]. At full load operation, the values of BSNO emission for diesel, JME and the JMETPO20 blend are about 2.9, 4.1, and 3.6 g/kWh respectively. The antioxidants are effective in reducing the formation of BSNO emission from the combustion of the JMETPO20 blend. The optimum reduction is found with the PY antioxidant when tested with the JMETPO20 blend due to decrease in the prompt BSNO formation by reducing free radicals during combustion process.

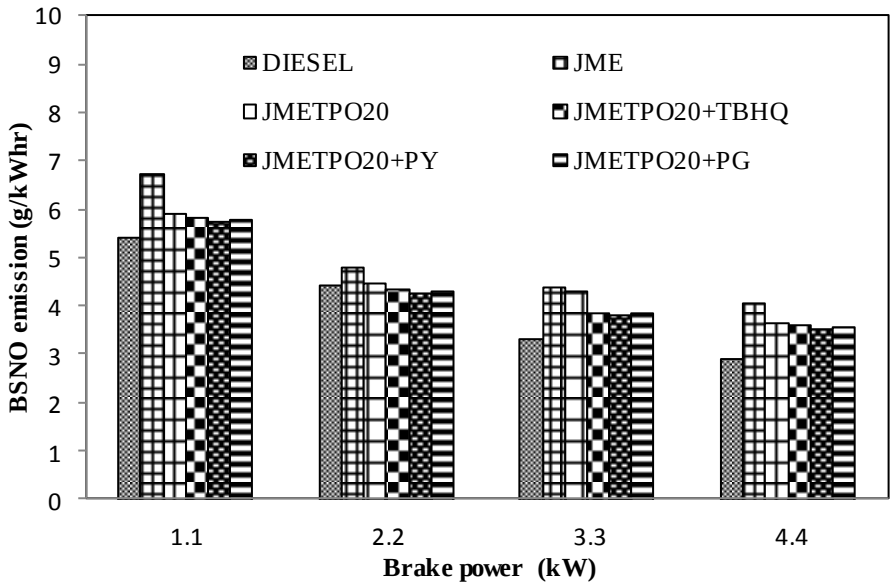

Fig. 5.56 Variation of BSNO emission with brake power

The concentration of 200 ppm of PY mixed with the JMETPO20 blend yields better results and a mean decrease of 3.6% is obtained with this additive in comparison without antioxidant. Also it can be assumed that the phenolic hydroxyl group present in the TPO interface with the prompt NO_x mechanism.

5.7.4.2 Brake specific hydrocarbon emission

The hydrocarbon (HC) emission mainly due to incomplete combustion comes in different forms such as vapour, drop of unburned fuel droplets etc. [287]. The brake specific hydrocarbon (BSHC) emissions for diesel, JME and its blends with brake power are shown in Figure 5.57. It can be noted from figure that, at full load the JME and JMETPO20 blend resulted reduction in BSHC emission by about 19% and 8.6% respectively, compared to that of diesel. This is due to the presence of oxygen molecule in the blend. But, by adding the TPO with the JME results in increase in BSHC emission, due to the increase in the aromatic content in the blend as the TPO has higher aromatic content. It can be noticed from the figure that by adding the antioxidant to the JMETPO20 blend leads to a marginal increase in the BSHC emission at all loads. This rise in the BSHC emission may be due to decrease in oxidative free radical formed by the antioxidants. The lowest BSHC emission for the JMETPO20 blend is found with the PY antioxidant at full load.

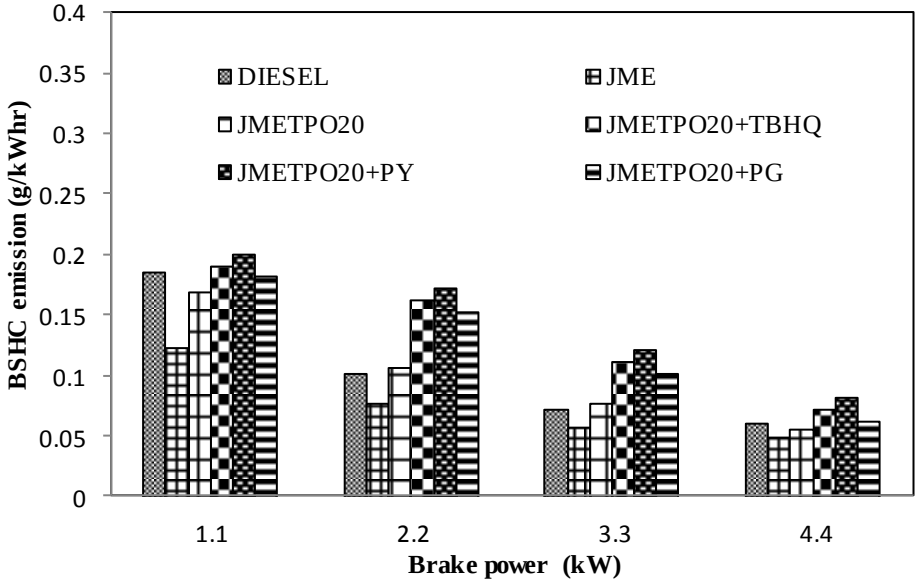

Fig. 5.57 Variation of BSHC emission with brake power

5.7.4.3 Smoke opacity

Smoke opacity is the result of incomplete combustion of hydrocarbon fuel and is formed in the rich mixture zone in the combustion chamber [288]. The smoke opacity measured in the engine exhaust for the test is shown in Figure 5.58. The smoke opacity increased with the rise in the engine load, because more fuel is injected when the load increases and this causes increase in the smoke opacity. The smoke opacity for diesel, JME and the JMETPO20 blend are found to by about 86.3%, 52.2%, and 63.1% respectively, at full load.

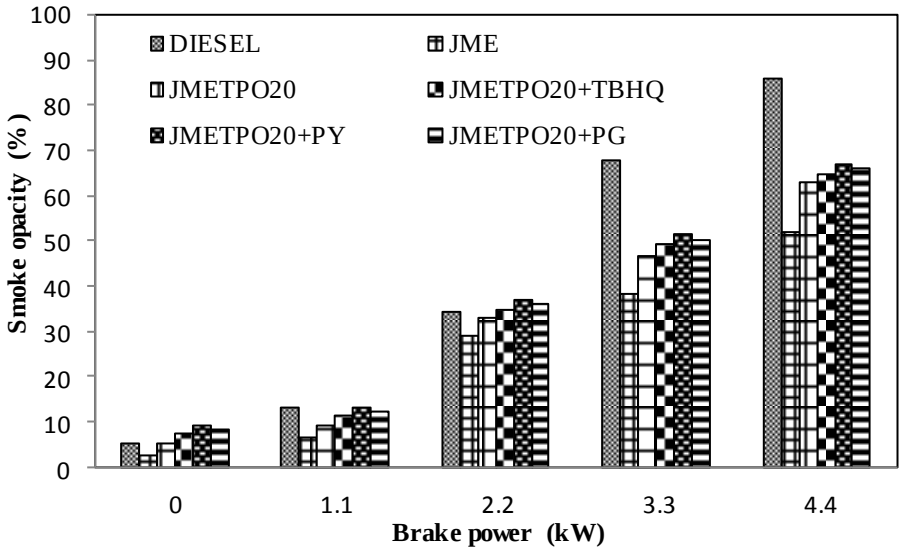

Fig. 5.58 Variation of smoke opacity with brake power

Smoke opacity is lower for the JME and the JMETPO20 blend compared to that of diesel at full load. This is due to the presence of oxygen in the JME which may help to break the aromatic content of the TPO. Addition of antioxidant to the JMETPO20 blend marginally increases the smoke opacity at all load operations. For the TBHQ, PY and PG added to the JMETPO20 blend, the values of smoke opacity are 65.1%, 68% and 66.8% respectively, at full load. Similar result has been reported by Balaji and Cheralathan [289] and the reason mentioned was improper combustion resulting from antioxidant addition.

5.7.5 Summary

The oxidation stability of biodiesel plays an important role for its long term storage. The oxidation stability of biodiesel is very poor and it needs antioxidant to get the storage requirements and also to ensure the fuel quality at performance level. Although it is possible to obtain the required oxidation stability of any biodiesel by using synthetic antioxidants, it will at the same time increase the cost of the resultant fuel as antioxidants are expensive chemicals. The investigation results on the effects of adding TPO as an natural antioxidant in terms of oxidation stability and the engine performance and emission when the test engine was run on the JMETPO20 blend + different antioxidants addition as fuels are presented in this chapter. The JME has poor oxidation stability; on the other hand the TPO contains some phenolic compounds which give a positive effect on improvement of oxidation stability while blended with the JME. This study recommends that by blending 20% TPO with 80% JME can reduce dosage of antioxidant by about 50%.

The next section presents a comparative study on the durability issues of a the test engine run on the JMETPO20 blend and diesel, when the engine operated with the JMETPO20 blend and diesel for 100 h, which consist of 14 test cycles of 7 h each as per the IS 10000 standards.

5.8 Durability analysis of single cylinder DI diesel engine operating with the JMETPO20 blend

A comparative study reported in this section is aimed to examine the durability issues of the test engine run on the JMETPO20 blend and diesel. The engine was run for 100 h, adopting 14 test cycles of 7 h each as per the IS 10000 standards. A visual examination of the vital parts of the engine components such as cylinder head, piston crown, and nozzle injector tip etc. was carried out to find the carbon deposit after the durability test. After the durability test, several tribological characteristics of the used lubricating oil were evaluated after every 25 h of engine operation in order to analyze the consequence of fuel chemistry on the life of the lubricating oil. Measurement of different metal debris concentrations present in the lubricating oil samples drawn from the JMETPO20 blend and diesel operated engine was also carriedout by the atomic absorption spectroscopy (AAS). The analysis of experimental results was categorized into two sections: visual inspection of engine components and lubricating oil analysis, and the results are presented in the subsequent sections.

5.8.1 Visual inspection of engine components

5.8.1.1 Cylinder head and piston crown

Carbon deposits on the vital components of the engine such as cylinder head, piston crown, and injector tip happen due to the thermal and oxidative degradation of lubricants, and incomplete combustion. These deposits reduce the engine performance, and create operational issues leading to an increase in the maintenance cost. Sometimes heavy deposits may also lead to engine failure. After completing 100 h run of the engine fueled with the JMETPO20 blend, the engine was dismantled and a qualitative analysis of carbon deposits on several engine components was carriedout with the help of photograph taken before and after the durability test. The photographs of various in-cylinder engine components, such as, cylinder head, piston crown, and nozzle injector tip, were captured for both the cases i.e. before and after the durability test. The black carbon deposits were clearly detected on these engine parts as shown in Figure 5.59. The photograph of the cylinder head before and after the durability test, carried out with the JMETPO20 blend is also shown in Fig. 5.63. It is apparent from the figure that, more carbon deposits were observed with the JMETPO20 blend after the endurance test. The JME consists of saturated and unsaturated fatty acids [290], and these fatty acids undergo chemical reactions in the high temperature combustion chamber. The thermal cracking of

compounds, especially the double bonds, supports combustion by the formation of low volatile compounds at the fringes of the spray. However, polymerization of the fuel in the liquid core accounts for the contraction at the core of the spray [291]. These compounds can no longer evaporate fully and deposits on different available surfaces in the combustion chamber which on further heating change into black carbon deposits.

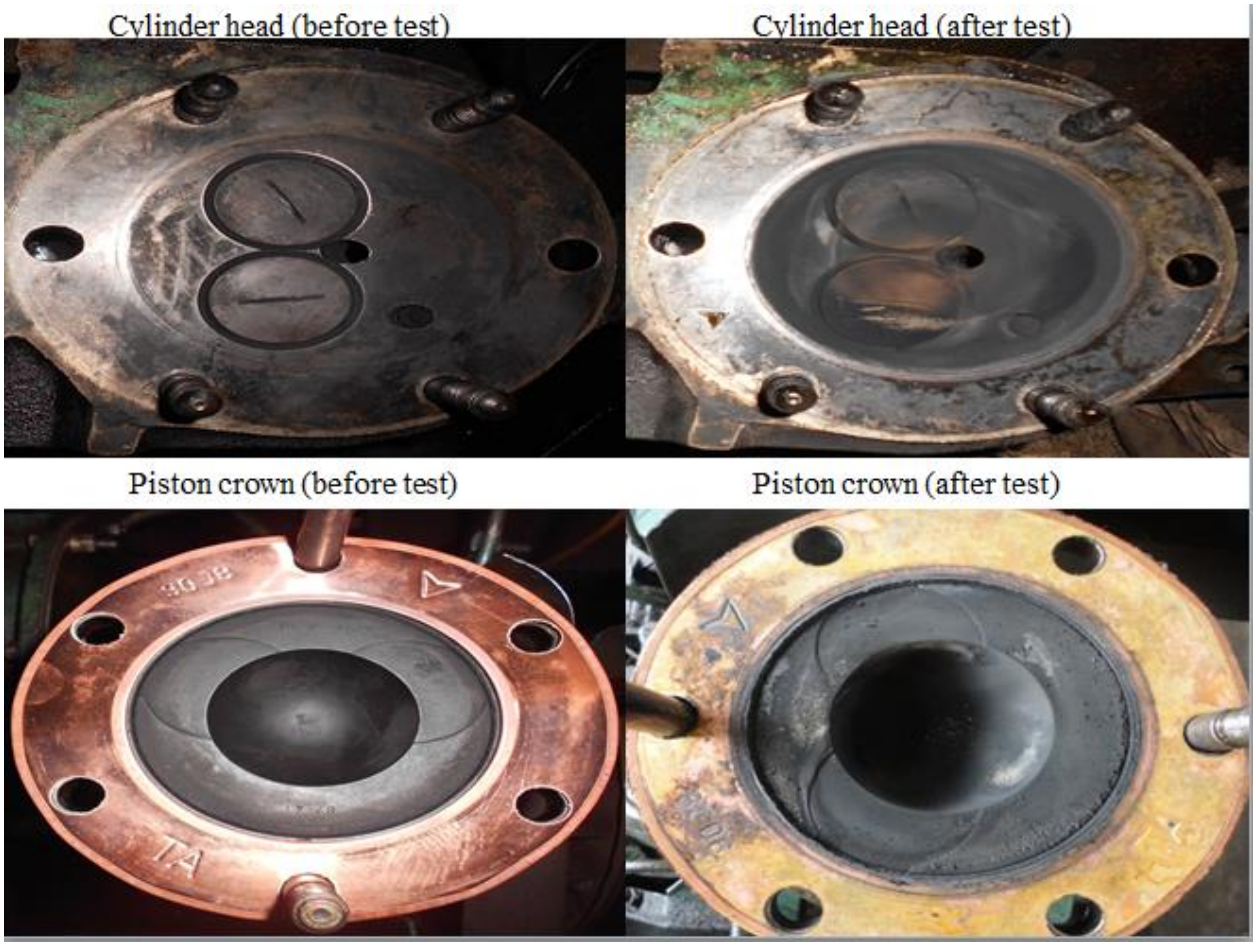

Fig. 5.59 Photographs of cylinder head and piston crown before and after the durability test

5.8.1.2 Fuel injector and fuel filter

The fuel injector components were dismantled after running the engine by 100 h with the test blend. Important parts such as the needle and injector tip were visually inspected and analyzed. Figure 5.60 shows the photographic views of the fuel injector tip and fuel filter, before and after the endurance test. The carbon deposits on the nozzle injector tip of the JMETPO20 fueled engine after 100 h of run is illustrated in Fig. 5.60. It is noticed that, the quantity of carbon deposits on the nozzle injector tip is more after the durability test compared to that of the injector before subjected to the examination before the test. The carbon deposits are found in the injector nozzle and in between the holes.

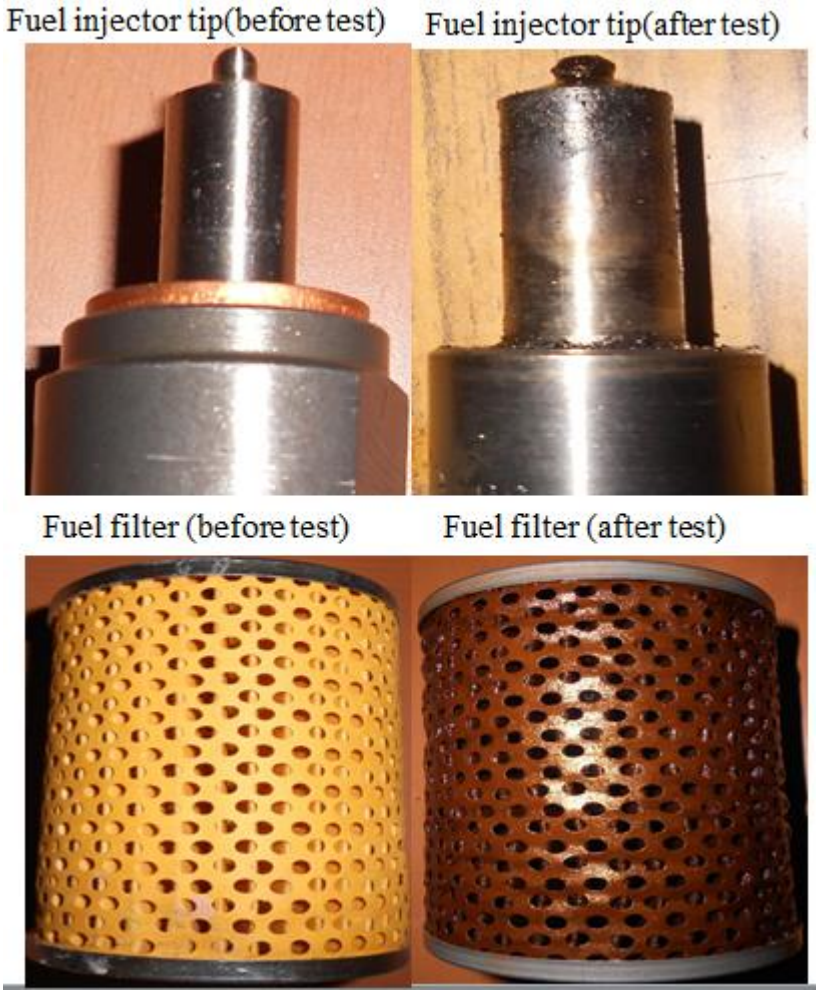

Fig. 5.60 Photographs of injector tip and fuel filter before and after the durability test

The carbon content (wt.%) was measured with the help of the weight balance, which is presented in Table 5.6.

Table 5.6 Carbon deposits (wt. %) on different parts of the engine fueled with the JMETPO20 blend

Different Engine Parts	**JMETPO20 blend**
Carbon deposits on cylinder head (mg)	5.2
Carbon deposits on injector tip (mg)	3.6
Carbon deposit on piston crowns (mg)	4.5

5.8.1.3 Fuel injection pump components

The photographs of the different components of dismantled fuel injection pump before and after the durability test are shown in Figure 5.61. The traces of wear on the plunger of the disassembled fuel injection pump were observed by visual inspection. This wear is important because, under severe conditions, it might have an effect on the sealing between

the plunger and the barrel, thereby may cause a reduction of pressure in the injection system, which subsequently influences the fuel injection phenomenon [292].

Fig. 5.61 Photographs of Fuel pump before and after the endurance test

5.8.2 Lubricating oil properties

Lubricating oil tribology was studied by operating 100 h short term durability test in a DI diesel engine operated with diesel and the JMETPO20 blend. The evolution in engine lubricating oil after every 25 h of engine operation was done in order to analyze the health of the lubricating oil by determining various properties.

5.8.2.1 Kinematic viscosity

The viscosity of a fluid is known as the measure of its resistance to flow at specified temperature. The kinematic viscosity is considered as one of the most essential factors to evaluate the life of engine lubricating oil. If the viscosity of lubricating oil increases by about 20% or more, or decreases by 10% or more, then it must be replaced by fresh lubricating oil [293]. The kinematic viscosity evolution of lubricating oil during 100 h operation of diesel and the JMETPO20 fueled engines are presented in Figure 5.62. Kalam et al. [294] reported that during engine operation, fuel in a very small amount gets diluted in lubricating oil which tends to deteriorate its kinematic viscosity. The test consequences revealed that the drop in kinematic viscosity of the lubricating oil in the JMETPO20 blend operated engine is higher than that in case of diesel operated engine. In fact, though the kinematic viscosity of the blend is more compared to diesel, it may be assumed that the viscosity of lubricating oil should rise concerning fuel dilution. But, the opposite trend was found, which may be due to moisture content in the blend which causes a decrease in the lubricating oil viscosity. [295].

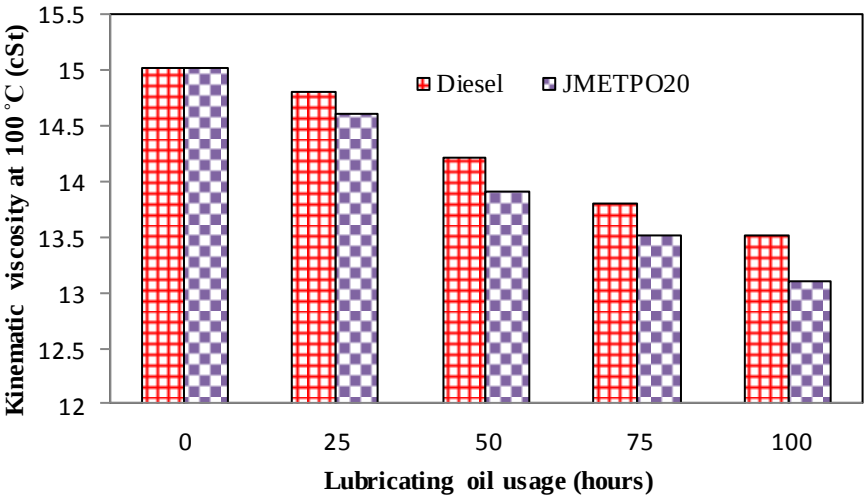

Fig. 5.62 Changes in kinematic viscosity versus hours of lubricating oil usage

5.8.2.2 Flash point

The flash point is largely affected by the Van der Waal's forces. The more amount of energy will be needed for vaporizing the oil if the van der Waal's forces are greater and this is desirable for higher flash point of engine lubricating oil [296]. The variation of flash point of the lubricating oil with engine running time is presented in Figure 5.63.

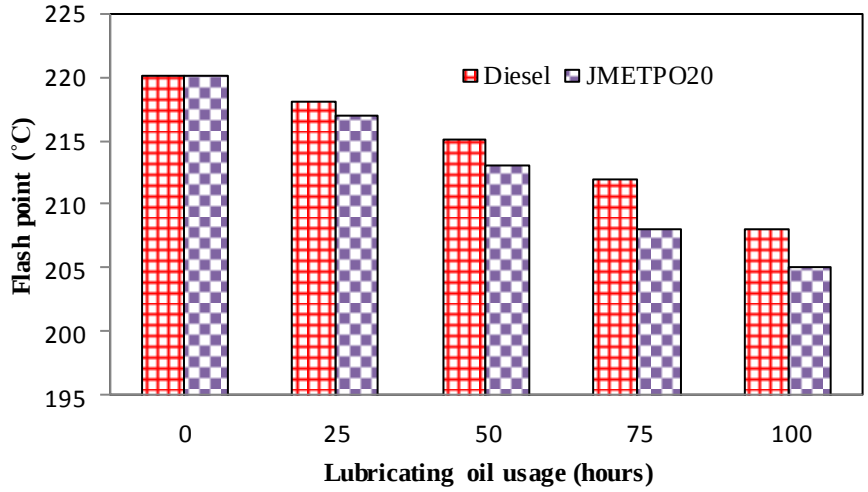

Fig. 5.63 Changes in flash point versus hours of lubricating oil usage

It can be observed from the figure that, the flash point of both the lubricating oil samples decreased with usage. The flash point is reduced to 205 ˚C from 220 ˚C for the JMETPO20 blend and to 208 ˚C for the diesel operated engine after 100 h of engine run. The decrease in the flash point of the lubricating oil for the JMETPO20 blend operated engine is higher than that of diesel. The possible cause for this decrease may be due to

availability of more moisture and free fatty acid contained in the blend. A similar reason was reported by Gopal et al. [295] when they carriedout lubricating oil tribology study of a diesel engine run on a pongamia oil methyl ester-diesel blend.

5.8.2.3 Moisture Content

The presence of moisture content in the engine lubricating oil has adverse impact as it oxidizes Fe^{2+} ion to Fe^{3+} ion and this can cause corrosion inside an engine. The variation in the moisture content of the lubricating oil versus engine running time is shown in Figure 5.64.

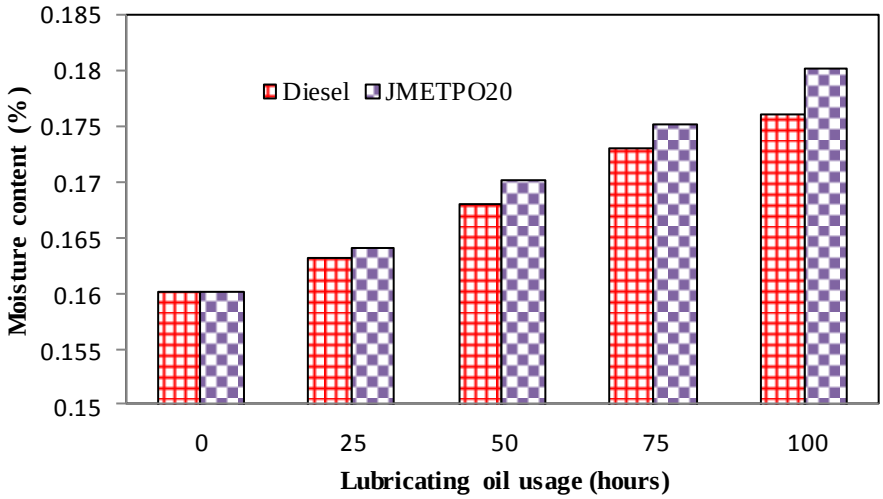

Fig. 5.64 Changes in moisture content versus hours of lubricating oil usage

The presence of moisture content in the lubricating oil increases with its usage for engine operated with diesel and the JMETPO20 blend. This increase is the sign of more fuel dilution and additive drop out (precipitation of additive from lubricating oil) [297]. The change in the moisture content of the lubricating oil is greater for the JMETPO20 blend operated engine than that of the engine run on diesel. This increase is due to the presence of more moisture content in the JMETPO20 blend.

5.8.2.4 Ash content

The ash content in the lubricating oil reveals percentage of mass of non-carbonaceous material. Ash content primarily specifies metallic wear debris and abrasive foreign particles such as sand entering the system. The excess ash content in the lubricating oil can block engine oil filter, increases the fuel consumption and decreases life of the engine. The gradual change in ash content in the lubricating oil samples drawn after a regular interval is shown in Figure 5.65. It can be observed from the figure that, the ash content

for the JMETPO20 fueled engine oil is found to be higher in comparison with the diesel fueled one.

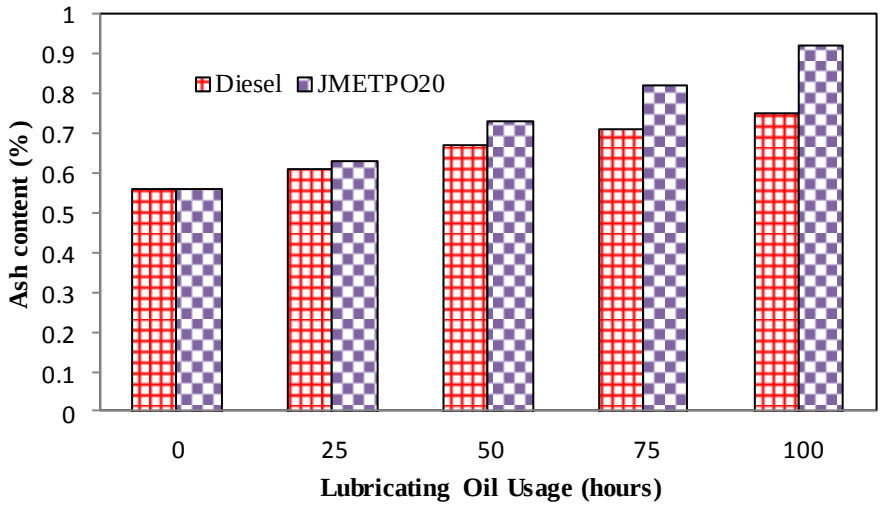

Fig. 5.65 Changes in ash content versus hours of lubricating oil usage

This is because biodiesel has a higher ash content compared to diesel, and is also owing to greater wear debris formation in the JMETPO20 blend fueled engine. Similar reason is reported by Dhar and Agrawal [298] for the results they obtained for durability study from running a DI diesel engine fueled with Karanja biodiesel-diesel blend.

5.8.3 Wear trace metals present in the lubricating oil

5.8.3.1 Iron

The concentration of iron in the lubricating oil versus engine running time is presented in Fig. 5.66.

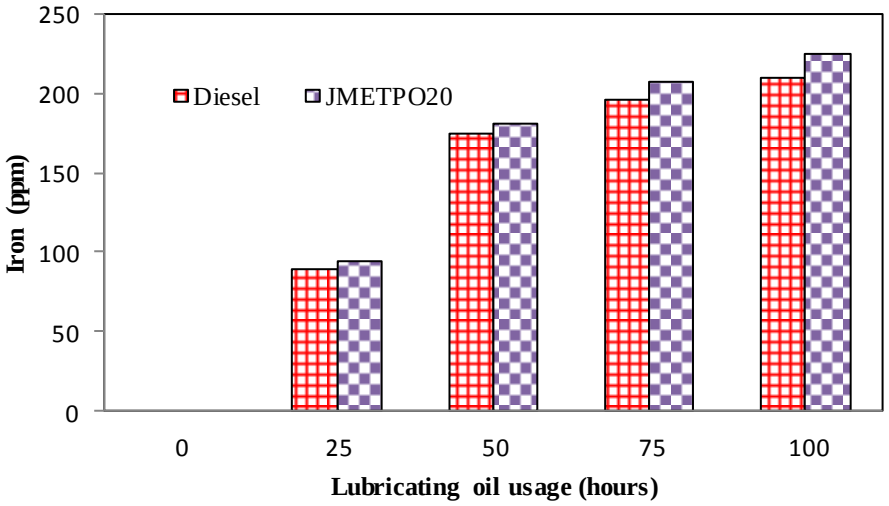

Fig. 5.66 Variation of iron concentration

The possible ways of iron in wear debris are cylinder head, cylinder liner, piston, rings, valves, crankshaft, camshaft, bearings, valve guide and wrist pin etc. [299]. It can also be observed that, for both the fuels, iron increased as a usage time of lubricating oil increased. The concentration of iron is observed to be more for the JMETPO20 fueled engine in comparison with the diesel engine under all ranges of the operations. One of the possible reasons is its more dilution with the lubricating oil resulting in partially dissolved lubricant, a mechanism which is presumably more serious on the cylinder wall lubricating film. This causes an increase of friction constant of the engine's moving components, leading to higher concentration of iron. Similar reason can be seen in research document published by Fontaras et al. [300], when they conducted a test on diesel engine fueled with soybean oil methyl ester-diesel blend.

5.8.3.2 Copper

The variations of copper concentration in the lubricating oil samples drawn after a regular interval are presented in Figure 5.67.

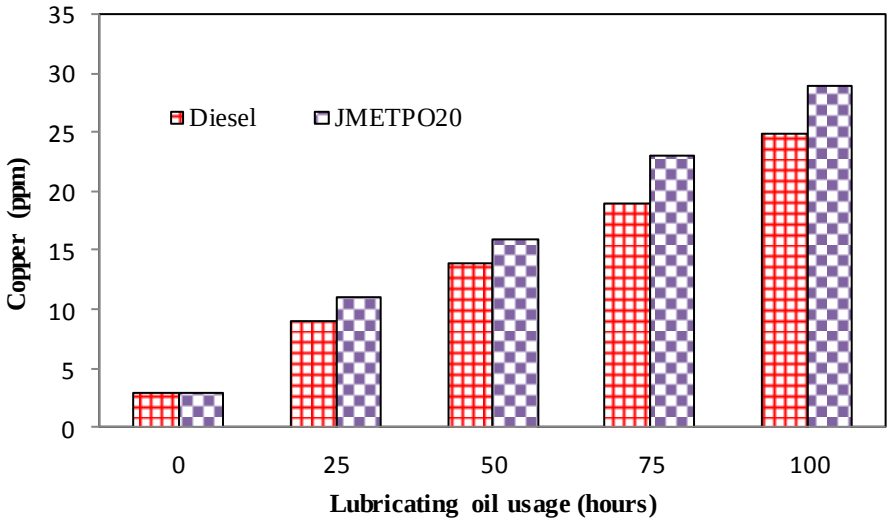

Fig. 5.67 Variation of copper concentration

It is evident from the figure that, for both fuels, copper increases at a constant rate. The copper in the wear debris originates from bearings, bushings, valve guides etc. It is apparent that, copper concentration in the lubricating oil is somewhat more in JMETPO20 fueled engine than that of diesel. This is due to the possibility of inferior lubricity of the blend after the oxidation of the lubricating oil [298].

5.8.3.3 Zinc

The zinc containing additive compound di-alkyl-di-thio-phosphates (ZDDP) is used as multi-functional additives for engine lubricating oil which acts as an anti-oxidant, corrosion inhibitor and anti-wear agent in the lubricating oil [301].

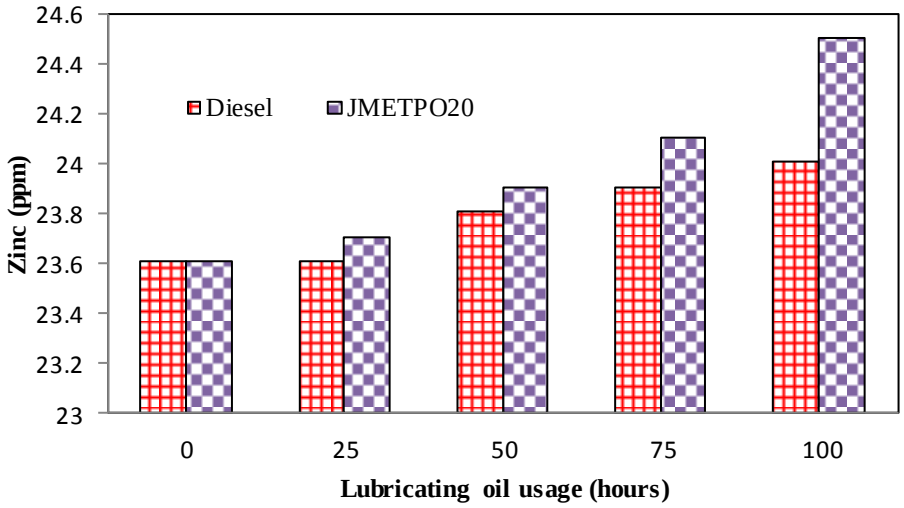

Fig. 5.68 Variation of zinc concentration

The variation of zinc concentration in the lubricating oil versus engine running time is shown in Figure 5.68. After 100 h of engine operation, the concentration of zinc in the lubricating oil is noticed to have increased due to the wear of several moving components of the engine. The zinc concentration is considerably more in the JMETPO20 blend fueled engine due to more additive depletion of lubricating oil with blend.

5.8.3.4 Chromium

The concentration of chromium in the lubricating oil as a function of oil usage is presented in Figure 5.69. The possible sources of chromium in the lubricating oil results from the wear of the cylinder liner, crank shaft, gear and compression rings etc [302]. It is apparent from the figure that, the engine run on the JMETPO20 blend exhibits more chromium concentration than that of diesel operation, which might result from greater wear of engine components during long term operation.

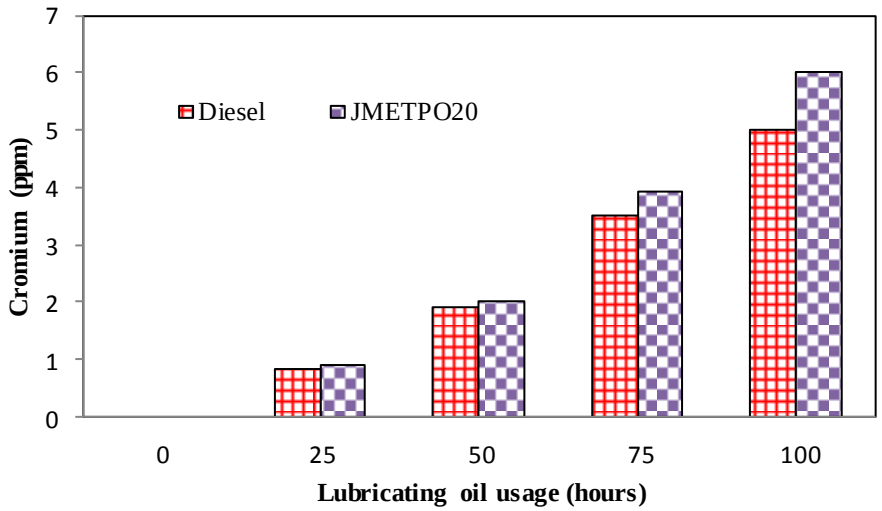

Fig. 5.69 Variation of chromium concentration

5.8.3.5 Magnesium

The values of magnesium concentration in the lubricating oil samples in a regular interval of engine operation are shown in Figure 5.70.

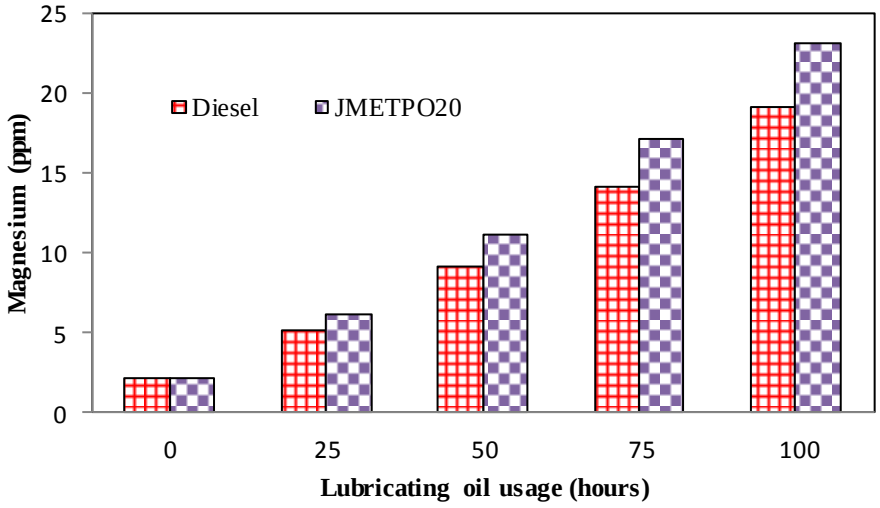

Fig. 5.70 Variation of magnesium concentration

Magnesium is used as an additive to the lubricating oil. The magnesium concentration in the engine lubricating oil may originate from wear of bearing and gearbox housing etc. [303]. After 100 h of engine run, it is noticed that the presence of magnesium in the lubricating oil is marginally higher for the JMETPO20 blend fueled engine than that of diesel operation.

5.8.3.6 Lead

It is used as an additive to the lubricating oil. In addition to this, the lead concentration in engine lubricating oil originates from wear of bearings, paint and greases etc. [304]

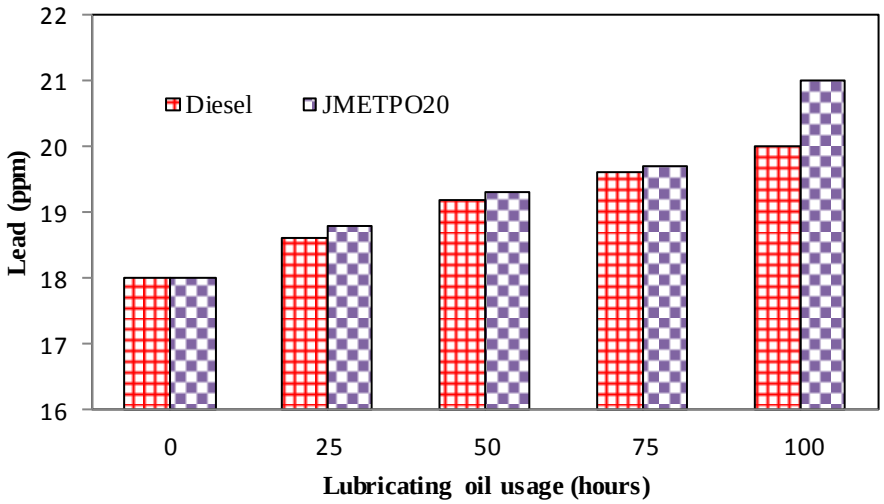

Fig. 5.71 Variation of lead concentration

The lead concentration in the lubricating oil samples of both the test fuels is presented in Figure 5.71. The result indicates that the lead concentration in the lubricating oil samples drawn from the JMETPO20 blend operated engine is marginally higher than that of the diesel operated engine.

5.8.4 Summary

A 100 h durability test was carriedout with the JMETPO20 blend as the fuel in a modified engine and with diesel in the unmodified engine under similar test conditions. After the 100 h of engine operation with the JMETPO20 blend, visual inspection of several engine components was carriedout and carbon deposits were found in the combustion chamber and nozzle injector tip. Afer 100 h of operation, decrease in kinematic viscosity and flash point of the lubricating oil were noticed in the JMETPO20 blend operated engine compared to that of diesel operation. This may be due to more moisture content in the blend which causes a decrease in lubricating oil viscosity. The ash content in the lubricating oil for the JMETPO20 fueled engine is found to be higher in comparison with the diesel fueled engine. This may be due to more ash content in biodiesel compared to diesel, hence indicates higher degree of wear debris formation in the JMETPO20 blend fueled engine. Lubricating oil samples were tested using AAS for measurement of different metal debris present in the lubricating oil samples collected from the JMETPO20

blend and diesel fueled engines. The results revealed that, the concentration of metal elements in the lubricating oil was marginally higher when the engine operated with the JMETPO20 blend compared to that of the engine operated with diesel. On the other hand, there was no operational or durability problems, while the engine was operated with the JMETPO20 blend.

The next chapter presents a summary of the research findings and the specific conclusions drawn from these investigations. It also outlines various scopes for future research in the related field.

Chapter 6

Conclusion and Scope for Future Research

6.1 General

The combustion, performance and emission characteristics of a single cylinder, four stroke, air cooled, direct injection diesel engine capable of producing 4.4 kW at a constant speed of 1500 rpm, fueled with JME-TPO blend with fuel and engine modifications, were analysed, compared with diesel and JME operations of the engine. Further, a new approach has been employed to develop hybrid multi criteria decision making technique namely VlseKriterijumska Optimizacija I Kompromisno Resenje (in Serbian) (VIKOR) for ranking the blend alternatives to find the optimum blend. Also the experimental investigations were carriedout at varied injection timing, nozzle opening pressure and compression ratio with the optimum blend. Also, an attempt was made to analyse the influence of blending different amounts of TPO with JME on the oxidation stability of the blend. Further, a short term endurance test was also carried out to ensure the technical feasibility of the engine fueled with the optimum blend. The conclusions of each technique are given in this section.

6.1.1 Combustion, performance and emission characteristics of the engine fueled with JMETPO blends

- On the whole it is concluded, that the JMETPO blend can be used as fuel in a diesel engine directly, without any engine modification. JMETPO20 gives the optimum result, compared to the other blends.
- The cylinder peak pressure lowers by about 1 bar for JMETPO20 in comparison with diesel at full load.
- It is found that the ignition delay for JMETPO20 is almost equal to that of diesel at full load operation.
- The combustion duration for diesel is 38.34oCA at full load. It decreased by about 0.54oCA for JMETPO20.

- At full load, the brake thermal efficiency is almost the same, i.e., 29.88 and 29.89% for JMETPO20 and diesel respectively, at full load.
- The EGT is higher for JMETPO20 compared to that of diesel at full load.
- The BSEC for diesel is 11.86MJ/kWh at full load. The BSEC increased by about 7.8% for JMETPO20, than that of diesel operation at full load.
- The CO, HC and smoke emissions were lower by about 9.09, 8.6 and 26% respectively for JMETPO20, compared to diesel at full load.
- Nitric oxide emission was higher by about 24% for JMETPO20, in comparison with diesel at full load.
- Overall, by considering the combustion, performance and emission parameters, it can be concluded that the JMETPO20 blend showed a better performance and lower emissions compared to those of other JMETPO blends.

6.1.2 A hybrid multi-criteria decision modelling approach for the best JMETPO blend selection based on PCA-VIKOR

The selection of best blend plays an imperative role for usage in test engine. There are a number of performance, emission and combustion parameters that are to be considered before choosing the best blend. It was seen that experimental trial number 32 has the smallest VIKOR index (Qi) value for JMETPO20 blend compared to other JMETPO blends. Thus, it is concluded that the minimum VIKOR index can be obtained when engine is operated with the JMETPO20 blend at full load. Thus, the final ranking for the JMETPO blends based on VIKOR analysis is JMETPO20> JMETPO10> JMETPO30> JMETPO40> JMETPO50.

6.1.3 Effect of injection timings on combustion, performance and emission characteristics of a diesel engine fueled with the JMETPO20 blend

- Advanced injection timing results in increase in maximum cylinder pressure and heat release rate, while the reverse trend is noticed in case of retarded injection timing. At an advanced injection timing of 24.5 ˚CA bTDC the maximum cylinder pressure was found to increase by about 2.73 bar, compared to that with the original injection timing at BMEP of 5.6 bar. Similarly, the ignition delay was found to be longer with shorter combustion duration at an advanced injection timing of 24.5 ˚CA bTDC, compared to that with the original and retarded

injection timings. The maximum heat release rate at the advanced injection timing of 24.5 ˚CA bTDC was found to be 51.42 J/˚CA, which is 1.1 J/˚CA higher in comparison with that the original injection timing.

- At the advanced injection timing, BSEC decreased as early start of fuel injection ensures more complete combustion owing to improved reaction between fuel and oxygen. The BSEC at an advanced injection timing of 24.5 ˚CA bTDC is lower by about 7.1% than that with the original injection timing at BMEP of 5.6 bar.
- The experimental investigation revealed that, advancing the injection timing results in reduced the CO, HC and particulate emission. On the other hand the NO emission increased. The CO and HC emission were lower by about 14.2% and 13.26% at the advanced injection timing of 24.5 ˚CA bTDC and BMEP of 5.6 bar, compared to that with the original injection timing. Similarly, the NO emission was higher by about 2.1% at the advanced injection timing of 24.5 ˚CA bTDC, in comparison to that with the original injection timing. The particulate emission was found to be lesser by about 9.3% at the advanced injection timing of 24.5 ˚CA bTDC compared to that with the original injection timing.

On the whole, it is concluded that the advanced injection timing of 24.5 ˚CA bTDC was the optimum injection timing, which gives significant superior results in terms of the combustion, performance and emission characteristics of the engine fueled with the JMETPO20 blend.

6.1.4 Effect of nozzle opening pressure on combustion, performance and emission characteristics of a diesel engine fueled with the JMETPO20 blend

- The peak cylinder pressure and maximum HRR at the NOP of 220 bar is found to higher by about 6.12% and 8.26% respectively, than those for the original operating condition.
- The ID at the NOP of 220 bar is 9.61 ˚CA, which is 1.75 ˚CA lower in value than that for the original operating condition.
- At the NOP of 220 bar, the BTE is increased by about 5.12% compared to that of the original operating condition.
- The reduction in the smoke opacity, BSCO and BSHC emissions by about 9.5%, 1.57% and 6.26% respectively are obtained at the NOP of 220 bar, compared to those in case of the original operating condition.

- The BSNO emission was higher by about 15% at the NOP of 220 bar compared to that of the original operating condition.
- Overall it can be concluded that at the optimum injection timing of 24.5 ˚CA and the higher nozzle opening pressure of 220 bar, significant superior results of the engine behavior run on the JMETPO20 blend were obtained.

6.1.5 Effect of compression ratios on combustion, performance and emission characteristics of a diesel engine fueled with the JMETPO20 blend

- The maximum cylinder pressure and heat release rate at the compression ratio of 18.5 were higher by about 6.2% and 10.3% respectively, than those of the original compression ratio.
- The ignition delay period decreased by about 2.25 ˚CA at the compression ratio of 18.5 than that of the original compression ratio.
- It was found that increasing the compression ratio of the engine, the brake thermal efficiency is enhanced irrespective of the engine load. The maximum brake thermal efficiency obtained at the compression ratio of 18.5 is higher by about 8% than that of the original compression ratio. Also it was found that at the compression ratio of 18.5 the BSEC of the engine running with the blend was reduced by about 11% compared to original compression ratio.
- The reduction in the BSCO, BSHC emissions and smoke opacity by about 10.5%, 32%, and 17.4% respectively, was obtained at the higher compression ratio of 18.5, compared to that in case of the original compression ratio.
- The brake specific nitric oxide emission was found to behigher by about 20% at the compression ratio of 18.5 compared to that of the original operating condition.
- The above experimental findings suggest that the combustion, performance and emission characteristics for the JMEPTO20 blend are relatively better at the higher compression ratio of 18.5 as compared to those at standard operating conditions. Although there is a small increase in the BSNO emission, it still lies within the acceptable range and is quite comparable with that of diesel.

6.1.6 Effect of blending tyre pyrolysis oil with Jatropha methyl ester on oxidation stability

- It is possible to improve the oxidation stability as per the EN 14112 and IS-15607 specification of the JMETPO20 blend by blending 20% TPO in 80% JME and by adding only 200 ppm of PY antioxidant. It was also noticed that the antioxidant dosage could be reduced by about 50% in the above case in comparison when 20% diesel is blended in 80% JME.
- Effectiveness of antioxidants with a concentration of 200 ppm in the JMETPO20 blend, on the oxidation stability was ordered as PY>PG>TBHQ
- A marginal decrease in the BSEC was observed with the JMETPO20+PY antioxidant compared to that of the JMETPO20 blend without antioxidant.
- Antioxidants are vital additives for enhancing the oxidation stability of biodiesel and for reduction of NO emission. It was observed that the PY antioxidant is a promising candidate for reducing the NO emission at marginal expense of increase in HC emission and smoke opacity. The highest NO emission reduction for the JMETPO20 blend was found by about 3.6% with the PY antioxidant compared to that of the JMETPO20 blend without antioxidant.

6.1.7 Durability analysis of single cylinder DI diesel engine operating with the JMETPO20 blend

- The 100 h durability test was carriedout with the JMETPO20 blend as the fuel in modified engine and with diesel in unmodified engine under similar test conditions. After the 100 h of engine operation with the JMETPO20 blend, on visual inspection of several engine parts, carbon deposits were found in the combustion chamber and nozzle injector tip.
- Decrease in kinematic viscosity and flash point of lubricating oil after 100 of engine operations were noticed in the JMETPO20 blend operated engine compared to that of diesel due to more moisture content in the blend which caused a decrease in lubricating oil viscosity. The ash content in lubricating oil for the JMETPO20 fueled engine was higher in comparison with the diesel fueled. This is because of the fact that biodiesel has more ash content compared to diesel and also higher ash content indicates higher degree of wear debris formation in the JMETPO20 blend fueled engine.

- Atomic absorption spectroscopy tests were conducted for measurement of different metal debris concentrations presents in the lubricating oil samples drawn from the JMETPO20 blend and diesel fueled engines. The results revealed that the concentration of metal elements in the lubricating oil was marginally higher when the engine operated with the JMETPO20 blend as compared to the engine operated with diesel. On the other hand, there was no operational or durability problems while engine was operated with the JMETPO20 blend. Thus the JMETPO20 blend has proven to be a suitable alternative fuel to diesel engine and environment friendly substitute fuel for the mineral diesel. A marginal wear was observed in the plunger of the fuel injection pump.

6.2 Scope for Future Work

The present research work leaves a wide scope for future investigators to explore many other aspects of this fuel. Some recommendations for future research include:

- The JMETPO blends can be tested in multi cylinder automotive engines and in gensets.
- By adopting some emission control techniques to bring the emission results closer to that of diesel operation.
- To study the impact of fuel additives on engine characteristics by attempting different additives in different proportions
- Computation Fluid Dynamics (CFD) analysis can be carriedout for the entire process. Detailed combustion modelling may also be carriedout.
- The moisture content in the TPO to be removed to avoid corrosion of engine components.
- The analysis of possible routes for the pyrolysis reaction mechanism of tyre wastes and optimization of parameters involved in the production of TPO.
- Optimisation of particle size in waste tyre pyrolysis.

References

[1] British Petroleum. BP statistical review of world energy. <http:// www.bp.com/statistical review of world energy> (2016).

[2] International Energy Agency (IEA). <http://www.iea.org> (2014).

[3] CIA World Fact book. <https://www.cia.gov/library/publications/the-worldfactbook/ geos/af.html> (2014).

[4] Buragohain B, Mahanta P, Moholkar VS. Biomass gasification for decentralized power generation: The Indian perspective. Renewable and Sustainable Energy Reviews. 2010 Jan 31; 14(1):73-92.

[5] Rao GA, Mohan PR. Effect of supercharging on the performance of a DI Diesel engine with cotton seed oil. Energy Conversion and Management. 2003 Apr 30; 44(6):937-44.

[6] Karaosmanoğlu F, Kurt G, Özaktaş T. Long term CI engine test of sunflower oil. Renewable energy. 2000 Feb 29; 19(1):219-21.

[7] Pryor RW, Hanna MA, Schinstock JL, Bashford LL. Soybean oil fuel in a small diesel engine. Transactions of the ASAE. 1983; 26(2):333-0337.

[8] De Almeida SC, Belchior CR, Nascimento MV, dos SR Vieira L, Fleury G. Performance of a diesel generator fuelled with palm oil. Fuel. 2002 Nov 1; 81(16):2097-102.

[9] Li Q, Backes F, Wachtmeister G. Application of canola oil operation in a diesel engine with common rail system. Fuel. 2015 Nov 1; 159:141-9.

[10] Pramanik K. Properties and use of Jatropha curcas oil and diesel fuel blends in compression ignition engine. Renewable energy. 2003 Feb 28; 28(2):239-48.

[11] Prasad CV, Krishna MM, Reddy CP, Mohan KR. Performance evaluation of non edible vegetable oils as substitute fuels in low heat rejection diesel engines. Proceedings of the Institution of Mechanical Engineers, Part D: Journal of Automobile Engineering. 2000 Feb 1; 214(2):181-7.

[12] Agarwal D, Kumar L, Agarwal AK. Performance evaluation of a vegetable oil fuelled compression ignition engine. Renewable energy. 2008 Jun 30; 33(6):1147-56.

[13] Rao G, Saravanan S. Role of Biofuels in a Sustainable Environment–A Technical Study. CLEAN–Soil, Air, Water. 2008 Nov 1; 36(10-11):830-4.

[14] Rao GA, Mohan PR. Effect of supercharging on the performance of a DI Diesel engine with cotton seed oil. Energy Conversion and Management. 2003 Apr 30; 44(6):937-44.

[15] Narayan CM. Vegetable oil as engine fuels—prospect and retrospect. Proceedings on recent trends in automotive fuels, Nagpur, India. 2002.

[16] Agarwal D, Agarwal AK. Performance and emissions characteristics of Jatropha oil (preheated and blends) in a direct injection compression ignition engine. Applied Thermal Engineering. 2007 Sep 30; 27(13):2314-23.

[17] Haldar SK, Ghosh BB, Nag A. Studies on the comparison of performance and emission characteristics of a diesel engine using three degummed non-edible vegetable oils. Biomass and Bioenergy. 2009 Aug 31; 33(8):1013-8.

[18] Ruan DF, Cheng WL, Lee CF. Comparison of performance and combustion characteristics of diesel fuel and vegetable oils in DI diesel engine. SAE International Journal of Fuels and Lubricants. 2008 Jun 23; 1(2008-01-1639):1049-55.

[19] No SY. Inedible vegetable oils and their derivatives for alternative diesel fuels in CI engines: a review. Renewable and Sustainable Energy Reviews. 2011 Jan 31; 15(1):131-49.

[20] Nwafor OM. The effect of elevated fuel inlet temperature on performance of diesel engine running on neat vegetable oil at constant speed conditions. Renewable Energy. 2003 Feb 28; 28(2):171-81.

[21] Kalam MA, Masjuki HH. Emissions and deposit characteristics of a small diesel engine when operated on preheated crude palm oil. Biomass and Bioenergy. 2004 Sep 30; 27(3):289-97.

[22] Bari S, Lim TH, Yu CW. Effects of preheating of crude palm oil (CPO) on injection system, performance and emission of a diesel engine. Renewable Energy. 2002 Nov 30; 27(3):339-51.

[23] Labeckas G, Slavinskas S. Study of exhaust emissions of direct injection diesel engine operating on ethanol, petrol and rapeseed oil blends. Energy Conversion and Management. 2009 Mar 31; 50(3):802-12.

[24] Forson FK, Oduro EK, Hammond-Donkoh E. Performance of jatropha oil blends in a diesel engine. Renewable Energy. 2004 Jun 30; 29(7):1135-45.

[25] Yilmaz N, Morton B. Effects of preheating vegetable oils on performance and emission characteristics of two diesel engines. Biomass and Bioenergy. 2011 May 31; 35(5):2028-33.

[26] Ramkumar S, Kirubakaran V. Review on Admission of Preheated Vegetable Oil in CI Engine. Indian Journal of Science and Technology. 2016 Jan 31; 9(2).

[27] Nwafor OM. Emission characteristics of diesel engine running on vegetable oil with elevated fuel inlet temperature. Biomass and Bioenergy. 2004 Nov 30; 27(5):507-11.

[28] Pryde EH. Vegetable oils as fuel alternatives-symposium overview. Journal of the American Oil Chemists Society. 1984 Oct 1; 61(10):1609-10.

[29] Atmanlı A, Yüksel B, İleri E. Experimental investigation of the effect of diesel–cotton oil–n-butanol ternary blends on phase stability, engine performance and exhaust emission parameters in a diesel engine. Fuel. 2013 Jul 31; 109:503-11.

[30] Qi DH, Bae C, Feng YM, Jia CC, Bian YZ. Combustion and emission characteristics of a direct injection compression ignition engine using rapeseed oil based micro-emulsions. Fuel. 2013 May 31; 107:570-7.

[31] Narkpakdee J, Permsuwan A, Deethayat T, Kiatsiriroat T. Performance and Emission of Small Diesel Engine Using Diesel-Crude Palm Oil-Water Emulsion as Fuel. Energy Science and Technology. 2012 May 31; 3(2):38-45.

[32] Crookes RJ, Kiannejad F, Nazha MA. Systematic assessment of combustion characteristics of biofuels and emulsions with water for use as diesel engine fuels. Energy Conversion and Management. 1997 Nov 30; 38(15):1785-95.

[33] Kumar MS, Jaikumar M. A comprehensive study on performance, emission and combustion behavior of a compression ignition engine fuelled with WCO (waste cooking oil) emulsion as fuel. Journal of the Energy Institute. 2014 Aug 31; 87(3):263-71.

[34] Melo-Espinosa EA, Piloto-Rodríguez R, Goyos-Pérez L, Sierens R, Verhelst S. Emulsification of animal fats and vegetable oils for their use as a diesel engine fuel: An overview. Renewable and Sustainable Energy Reviews. 2015 Jul 31; 47:623-33.

[35] Niehaus RA, Goering CE, Savage LD, Sorenson SC. Cracked soybean oil as a fuel for a diesel engine. Transactions of the ASAE. 1986 May 1; 29(3):683-0689.

[36] Alencar JW, Alves PB, Craveiro AA. Pyrolysis of tropical vegetable oils. Journal of Agricultural and Food Chemistry. 1983 Nov; 31(6):1268-70.

[37] Idem RO, Katikaneni SP, Bakhshi NN. Thermal cracking of canola oil: reaction products in the presence and absence of steam. Energy & Fuels. 1996 Nov 20; 10(6):1150-62.

[38] Ramadhas AS, Jayaraj S, Muraleedharan C. Use of vegetable oils as IC engine fuels-a review. Renewable Energy. 2004 Apr 30; 29(5):727-42.

[39] Maher KD, Bressler DC. Pyrolysis of triglyceride materials for the production of renewable fuels and chemicals. Bioresource Technology. 2007 Sep 30; 98(12):2351-68.

[40] Zhang Q, Chang J, Wang T, Xu Y. Review of biomass pyrolysis oil properties and upgrading research. Energy Conversion and Management. 2007 Jan 31; 48(1):87-92.

[41] Marchetti JM, Miguel VU, Errazu AF. Possible methods for biodiesel production. Renewable and Sustainable Energy Reviews. 2007 Aug 31; 11(6):1300-11.

[42] Demirbas A. Biodiesel production from vegetable oils via catalytic and non-catalytic supercritical methanol transesterification methods. Progress in Energy and Combustion Science. 2005 Dec 31; 31(5):466-87.

[43] Lapuerta M, Armas O, Rodriguez-Fernandez J. Effect of biodiesel fuels on diesel engine emissions. Progress in Energy and Combustion Science. 2008 Apr 30; 34(2):198-223.

[44] The world's biggest biodiesel producers in 2015, by country (in billion liters) http://www.energy-101.org/renewable-energy/biofuelsbiomass-facts/biofuel biodiesel-facts/biofuel-biodiesel-production (accessed Oct 29, 2016)

[45] Lohan SK, Ram T, Mukesh S, Ali M, Arya S. Sustainability of biodiesel production as vehicular fuel in Indian perspective. Renewable and Sustainable Energy Reviews. 2013 Sep 30; 25:251-9.

[46] Biswas PK, Pohit S, Kumar R. Biodiesel from jatropha: can India meet the 20% blending target? Energy Policy. 2010 Mar 31; 38(3):1477-84.

[47] Ghadge SV, Raheman H. Biodiesel production from mahua (Madhuca indica) oil having high free fatty acids. Biomass and Bioenergy. 2005 Jun 30; 28(6):601-5.

[48] Srivastava PK, Verma M. Methyl ester of karanja oil as an alternative renewable source energy. Fuel. 2008 Jul 31; 87(8):1673-7.

[49] Dixit S, Rehman A. Linseed oil as a potential resource for bio-diesel: A review. Renewable and Sustainable Energy Reviews. 2012 Sep 30; 16(7):4415-21.

[50] National Policy on Biofuels, Government of India. Report by Ministry of New & Renewable Energy (MNRE) New Delhi; Dec 2009. Available from: www.mnre.gov.in/policy/biofuel-policy.pdf

[51] Kureel RS, Singh CB, Gupta AK, Pandey A. Jatropha: an alternate source for biodiesel. National Oilseeds and Vegetable oils Development Board. 2007

[52] Dhyani SK, Kumar RV, Ahlawat SP. Jatropha curcas: a potential biodiesel crop and its current R&D status. Indian Journal of Agricultural Sciences. 2011; 81(4):295-308.

[53] Atadashi IM, Aroua MK, Aziz AA. High quality biodiesel and its diesel engine application: a review. Renewable and Sustainable Energy Reviews. 2010 Sep 30; 14(7):1999-2008.

[54] Kumar A, Sharma S. Potential non-edible oil resources as biodiesel feedstock: an Indian perspective. Renewable and Sustainable Energy Reviews. 2011 May 31; 15(4):1791-800.

[55] Ashraful AM, Masjuki HH, Kalam MA, Fattah IR, Imtenan S, Shahir SA, Mobarak HM. Production and comparison of fuel properties, engine performance, and emission characteristics of biodiesel from various non-edible vegetable oils: A review. Energy Conversion and Management. 2014 Apr 30; 80:202-28.

[56] Aydin H, Bayindir H. Performance and emission analysis of cottonseed oil methyl ester in a diesel engine. Renewable Energy. 2010 Mar 31; 35(3):588-92.

[57] Puhan S, Vedaraman N, Ram BV, Sankarnarayanan G, Jeychandran K. Mahua oil (Madhuca Indica seed oil) methyl ester as biodiesel-preparation and emission characterstics. Biomass and Bioenergy. 2005 Jan 31; 28(1):87-93.

[58] Ozsezen AN, Canakci M, Turkcan A, Sayin C. Performance and combustion characteristics of a DI diesel engine fueled with waste palm oil and canola oil methyl esters. Fuel. 2009 Apr 30; 88(4):629-36.

[59] Agarwal AK. Biofuels (alcohols and biodiesel) applications as fuels for internal combustion engines. Progress in energy and combustion science. 2007 Jun 30; 33(3):233-71.

[60] Rashedul HK, Masjuki HH, Kalam MA, Ashraful AM, Rahman SA, Shahir SA. The effect of additives on properties, performance and emission of biodiesel fuelled compression ignition engine. Energy Conversion and Management. 2014 Dec 31; 88:348-64.

[61] Canakci M, Monyem A, Van Gerpen J. Accelerated oxidation processes in biodiesel. Transactions of the ASAE. 1999; 42(6):1565.

[62] Dunn RO. Effect of temperature on the oil stability index (OSI) of biodiesel. Energy & Fuels. 2007 Dec 21; 22(1):657-62.

[63] Miyashita K, Takagi T. Study on the oxidative rate and prooxidant activity of free fatty acids. Journal of the American Oil Chemists' Society. 1986 Oct 1; 63(10):1380-4.

[64] Jain S, Sharma MP. Stability of biodiesel and its blends: a review. Renewable and Sustainable Energy Reviews. 2010 Feb 28; 14(2):667-78.

[65] Knothe G. Dependence of biodiesel fuel properties on the structure of fatty acid alkyl esters. Fuel Processing Technology. 2005 Jun 25; 86(10):1059-70.

[66] Knothe G, Dunn RO. Dependence of oil stability index of fatty compounds on their structure and concentration and presence of metals. Journal of the American Oil Chemists' Society. 2003 Oct 1; 80(10):1021-6.

[67] Fattah IR, Masjuki HH, Kalam MA, Hazrat MA, Masum BM, Imtenan S, Ashraful AM. Effect of antioxidants on oxidation stability of biodiesel derived from vegetable and animal based feedstocks. Renewable and Sustainable Energy Reviews. 2014 Feb 28; 30:356-70.

[68] Hui YH. Bailey's industrial oil and fat products. 5th ed., vol. 4, 1996. p. 411–415.

[69] Knothe G. Some aspects of biodiesel oxidative stability. Fuel Processing Technology. 2007 Jul 31; 88(7):669-77.

[70] Arisoy K. Oxidative and thermal instability of biodiesel. Energy Sources, Part A. 2008 Jun 17; 30(16):1516-22.

[71] Yaakob Z, Narayanan BN, Padikkaparambil S. A review on the oxidation stability of biodiesel. Renewable and Sustainable Energy Reviews. 2014 Jul 31; 35:136-53.

[72] Planning commission report on biofuels, planning commission, Government of India, 2013.

[73] Torres-Jimenez E, Dorado MP, Kegl B. Experimental investigation on injection characteristics of bioethanol–diesel fuel and bioethanol–biodiesel blends. Fuel. 2011 May 31; 90(5):1968-79.

[74] Noguchi N, Terao H, Sakata C. Performance improvement by control of flow rates and diesel injection timing on dual-fuel engine with ethanol. Bioresource Technology. 1996 Apr 30; 56(1):35-9.

[75] Li DG, Zhen H, Xingcai L, Wu-gao Z, Jian-Guang Y. Physico-chemical properties of ethanol–diesel blend fuel and its effect on performance and emissions of diesel engines. Renewable energy. 2005 May 31; 30(6):967-76.

[76] Kumar BR, Saravanan S. Use of higher alcohol biofuels in diesel engines: A review. Renewable and Sustainable Energy Reviews. 2016 Jul 31; 60:84-115.

[77] Rakopoulos DC, Rakopoulos CD, Giakoumis EG, Dimaratos AM. Characteristics of performance and emissions in high-speed direct injection diesel engine fueled with diethyl ether/diesel fuel blends. Energy. 2012 Jul 31; 43(1):214-24.

[78] Mohanan P, Kapilan N, Reddy RP. Effect of diethyl ether on the performance and emission of a 4-S Di diesel engine. SAE Technical Paper; 2003 Mar 3.

[79] Rubber manufacturers association (RMA). Scrap Tyre Markets in the United States 9th Biennial Report. May, 2009.

[80] Reisman JI. Air Emission from Scrap Tyre Combustion. October, 1997, EPA-600/R-97.

[81] Maschio G, Koufopanos C, Lucchesi A. Pyrolysis, a promising route for biomass utilization. Bioresource Technology. 1992 Jan 1; 42(3):219-31.

[82] Demirbas A, Arin G. An overview of biomass pyrolysis. Energy Sources. 2002 May 1; 24(5):471-82.

[83] Panda AK, Murugan S, Singh RK. Performance and emission characteristics of diesel fuel produced from waste plastic oil obtained by catalytic pyrolysis of waste polypropylene. Energy Sources, Part A: Recovery, Utilization, and Environmental Effects. 2016 Feb 16; 38(4):568-76.

[84] Fukushima M, Wu B, Ibe H, Wakai K, Sugiyama E, Abe H, Kitagawa K, Tsuruga S, Shimura K, Ono E. Study on dechlorination technology for municipal waste plastics containing polyvinyl chloride and polyethylene terephthalate. Journal of Material Cycles and Waste Management. 2010 Jun 1; 12(2):108-22.

[85] López A, De Marco I, Caballero BM, Laresgoiti MF, Adrados A. Dechlorination of fuels in pyrolysis of PVC containing plastic wastes. Fuel Processing Technology. 2011 Feb 28; 92(2):253-60.

[86] López A, De Marco I, Caballero BM, Laresgoiti MF, Adrados A. Dechlorination of fuels in pyrolysis of PVC containing plastic wastes. Fuel Processing Technology. 2011 Feb 28; 92(2):253-60.

[87] Prakash R, Singh RK, Murugan S. Experimental studies on combustion, performance and emission characteristics of diesel engine using different biodiesel bio oil emulsions. Journal of the Energy Institute. 2015 Feb 28; 88(1):64-75.

[88] Solantausta Y, Nylund NO, Westerholm M, Koljonen T, Oasmaa A. Wood-pyrolysis oil as fuel in a diesel-power plant. Bioresource Technology. 1993 Dec 31; 46(1):177-88.

[89] Ikura M, Stanciulescu M, Hogan E. Emulsification of pyrolysis derived bio-oil in diesel fuel. Biomass and Bioenergy. 2003 Mar 31; 24(3):221-32.

[90] Arpa O, Yumrutaş R, Argunhan Z. Experimental investigation of the effects of diesel-like fuel obtained from waste lubrication oil on engine performance and exhaust emission. Fuel Processing Technology. 2010 Oct 31; 91(10):1241-9.

[91] Tajima H, Takasaki K, Nakashima M, Yanagi J, Takaishi T, Ishida H, Osafune SN, Iwamoto K. Combustion of used lubricating oil in a diesel engine. SAE Technical Paper; 2001 May 7.

[92] Behera P, Murugan S. Combustion, performance and emission parameters of used transformer oil and its diesel blends in a DI diesel engine. Fuel. 2013 Feb 28; 104:147-54.

[93] Behera P, Murugan S, Nagarajan G. Dual fuel operation of used transformer oil with acetylene in a DI diesel engine. Energy Conversion and Management. 2014 Nov 30; 87:840-7.

[94] Senthil Kumar M, Ramesh A, Nagalingam B. Investigations on the use of Jatropha oil and its methyl ester as a fuel in a compression ignition engine. Journal of the Institute of Energy. 2001; 74(498):24-8.

[95] Kumar MS, Ramesh A, Nagalingam B. An experimental comparison of methods to use methanol and Jatropha oil in a compression ignition engine. Biomass and Bioenergy. 2003 Sep 30; 25(3):309-18.

[96] Sahoo PK, Naik SN, Das LM. Studies on biodiesel production technology from jatropha curcas and its performance in a CI engine. Journal of Agricultural Engineering. 2005; 42(2):14-20.

[97] Mandpe S, Kadlaskar S, Degen W, Keppeler S. On road testing of advanced common rail diesel vehicles with biodiesel from the Jatropha curcas plant. SAE Technical Paper; 2005 Oct 23.

[98] Mahanta P, Mishra S, Kushwah Y. A comparative study of pongamia pinnata and jatropha curcus oil as diesel substitute. International Energy Journal. 2006 Mar; 7(1):1-2.

[99] Sivaprakasam S, Saravanan CG. Optimization of the transesterification process for biodiesel production and use of biodiesel in a compression ignition engine. Energy & Fuels. 2007 Sep 19; 21(5):2998-3003.

[100] Lakshmi Narayana Rao G, Durga Prasad B, Sampath S, Rajagopal K. Combustion analysis of diesel engine fueled with jatropha oil methyl ester-diesel blends. International Journal of Green Energy. 2007 Nov 15;4(6):645-58.

[101] Reksowardojo IK, Lubis IH, Manggala W, Brodjonegoro TP, Soerawidjaja TH, Arismunandar W, Dung NN, Ogawa H. Performance and exhaust gas emissions of using biodiesel fuel from physic nut (Jatropha Curcas L.) oil on a direct injection diesel engine (DI). SAE Technical Paper; 2007 Jul 23.

[102] Rao YV, Voleti RS, Hariharan VS, Raju AV. Jatropha oil methyl ester and its blends used as an alternative fuel in diesel engine. International Journal of Agricultural and Biological Engineering. 2008 Dec 12; 1(2):32-8.

[103] Anand K, Sharma RP, Mehta PS. Experimental investigations on combustion of jatropha methyl ester in a turbocharged direct-injection diesel engine. Proceedings of the Institution of Mechanical Engineers, Part D: Journal of Automobile Engineering. 2008 Oct 1; 222(10):1865-77.

[104] Sahoo PK, Das LM, Babu MK, Arora P, Singh VP, Kumar NR, Varyani TS. Comparative evaluation of performance and emission characteristics of jatropha, karanja and polanga based biodiesel as fuel in a tractor engine. Fuel. 2009 Sep 30; 88(9):1698-707.

[105] Kywe TT, Oo MM. Production of biodiesel from Jatropha oil (Jatropha curcas) in pilot plant. In Proceedings of World Academy of Science, Engineering and Technology 2009 Feb (Vol. 38, pp. 481-487).

[106] Sahoo PK, Das LM. Combustion analysis of Jatropha, Karanja and Polanga based biodiesel as fuel in a diesel engine. Fuel. 2009 Jun 30; 88(6):994-9.

[107] Puhan S, Saravanan N, Nagarajan G, Vedaraman N. Effect of biodiesel unsaturated fatty acid on combustion characteristics of a DI compression ignition engine. Biomass and Bioenergy. 2010 Aug 31; 34(8):1079-88.

[108] Jindal S, Nandwana BP, Rathore NS. Comparative evaluation of combustion, performance, and emissions of jatropha methyl ester and karanj methyl ester in a direct injection diesel engine. Energy & Fuels. 2010 Jan 7; 24(3):1565-72.

[109] Ejilah IR, Asere AA, Adisa AB, Ejila A. The Effect of Diesel Fuel-'Jatropha curcas' Oil Methyl Ester Blend on the Performance of a Variable Speed Compression Ignition Engine. Australian Journal of Agricultural Engineering. 2010 Jul; 1(3):80.

[110] Prasad L, Pradhan S, Madankar CS, Das LM, Naik SN. Comparative study of performance and emissions characteristics of a diesel engine fueled with jatropha and karanja biodiesel. Journal of Scientific and Industrial Research. 2011 Aug 1; 70:694-8.

[111] Reddy VS, Ranjan KR, Sharma VK, Tyagi SK. Experimental investigation of a diesel engine fuelled with Jatropha curcas L. seed oil. International Journal of Sustainable Energy. 2011 Dec 1;30(sup1):S4-10.

[112] Rao PV. Experimental investigations on the influence of properties of jatropha biodiesel on performance, combustion, and emission characteristics of a DI-CI engine. World Academy of Science, Engineering and Technology. 2011 Mar 23; 75:855-68.

[113] Prasad L, Pradhan S, Das LM, Naik SN. Experimental assessment of toxic phorbol ester in oil, biodiesel and seed cake of Jatropha curcas and use of biodiesel in diesel engine. Applied Energy. 2012 May 31; 93:245-50.

[114] Salamanca M, Agudelo JR, Mondragón F, Santamaría A. Chemical characteristics of the soot produced in a high-speed direct injection engine operated with diesel/biodiesel blends. Combustion Science and Technology. 2012 Jul 1; 184(7-8):1179-90.

[115] Chauhan BS, Kumar N, Cho HM. A study on the performance and emission of a diesel engine fueled with Jatropha biodiesel oil and its blends. Energy. 2012 Jan 31; 37(1):616-22.

[116] Mohammed EK, Nemit-allah MA. Experimental investigations of ignition delay period and performance of a diesel engine operated with Jatropha oil biodiesel. Alexandria Engineering Journal. 2013 Jun 30; 52(2):141-9.

[117] Mofijur M, Masjuki HH, Kalam MA, Atabani AE. Evaluation of biodiesel blending, engine performance and emissions characteristics of Jatropha curcas methyl ester: Malaysian perspective. Energy. 2013 Jun 15; 55:879-87.

[118] Mamilla VR, Mallikarjun MV, Rao GL. Performance analysis of IC engines with bio-diesel jatropha methyl ester (JME) blends. Journal of Petroleum Technology and Alternative Fuels. 2013 May 31;4(5):90-3.

[119] Abedin MJ, Masjuki HH, Kalam MA, Sanjid A, Rahman SA, Fattah IR. Performance, emissions, and heat losses of palm and jatropha biodiesel blends in a diesel engine. Industrial Crops and Products. 2014 Aug 31; 59:96-104.

[120] Ong HC, Masjuki HH, Mahlia TM, Silitonga AS, Chong WT, Yusaf T. Engine performance and emissions using Jatropha curcas, Ceiba pentandra and Calophyllum inophyllum biodiesel in a CI diesel engine. Energy. 2014 May 1; 69:427-45.

[121] Rashed MM, Kalam MA, Masjuki HH, Mofijur M, Rasul MG, Zulkifli NW. Performance and emission characteristics of a diesel engine fueled with palm, jatropha, and moringa oil methyl ester. Industrial Crops and Products. 2016 Jan 31; 79:70-6.

[122] Mehta RN, Chakraborty M, Mahanta P, Parikh PA. Evaluation of fuel properties of butanol− biodiesel− diesel blends and their impact on engine performance and emissions. Industrial & Engineering Chemistry Research. 2010 Jul 15; 49(16):7660-5.

[123] Hulwan DB, Joshi SV. Performance, emission and combustion characteristic of a multicylinder DI diesel engine running on diesel–ethanol–biodiesel blends of high ethanol content. Applied Energy. 2011 Dec 31; 88(12):5042-55.

[124] Kannan D, Pachamuthu S, Nabi MN, Hustad JE, Løvås T. Theoretical and experimental investigation of diesel engine performance, combustion and emissions analysis fuelled with the blends of ethanol, diesel and jatropha methyl ester. Energy Conversion and Management. 2012 Jan 31; 53(1):322-31.

[125] Prakash R, Singh RK, Murugan S. Experimental investigation on a diesel engine fueled with bio-oil derived from waste wood–biodiesel emulsions. Energy. 2013 Jun 15; 55:610-8.

[126] Imtenan S, Masjuki HH, Varman M, Kalam MA, Arbab MI, Sajjad H, Rahman SA. Impact of oxygenated additives to palm and jatropha biodiesel blends in the context of performance and emissions characteristics of a light-duty diesel engine. Energy Conversion and Management. 2014 Jul 31; 83:149-58.

[127] Sanjid A, Masjuki HH, Kalam MA, Rahman SA, Abedin MJ, Reza MI, Sajjad H. Experimental investigation of palm-jatropha combined blend properties, performance, exhaust emission and noise in an unmodified diesel engine. Procedia Engineering. 2014 Dec 31; 90:397-402.

[128] Sanjid A, Masjuki HH, Kalam MA, Rahman SA, Abedin MJ, Palash SM. Production of palm and jatropha based biodiesel and investigation of palm-jatropha combined blend properties, performance, exhaust emission and noise in

an unmodified diesel engine. Journal of Cleaner Production. 2014 Feb 15; 65:295-303.

[129] Imtenan S, Masjuki HH, Varman M, Fattah IR, Sajjad H, Arbab MI. Effect of n-butanol and diethyl ether as oxygenated additives on combustion–emission-performance characteristics of a multiple cylinder diesel engine fuelled with diesel–jatropha biodiesel blend. Energy Conversion and Management. 2015 Apr 30; 94:84-94.

[130] Senthilkumar P, Sankaranarayanan G. Effect of Jatropha methyl ester on waste plastic oil fueled DI diesel engine. Journal of the Energy Institute. 2015 Sep 3.

[131] Nalgundwar A, Paul B, Sharma SK. Comparison of performance and emissions characteristics of DI CI engine fueled with dual biodiesel blends of palm and jatropha. Fuel. 2016 Jun 1; 173:172-9.

[132] Banapurmath NR, Tewari PG, Hosmath RS. Performance and emission characteristics of a DI compression ignition engine operated on Honge, Jatropha and sesame oil methyl esters. Renewable Energy. 2008 Sep 30; 33(9):1982-8.

[133] Dhananjaya DA, Mohanan P, Sudhir CV. Effect of Injection Pressure and Injection Timing on a Semi-Adiabatic CI Engine Fueled With Blends of Jatropha Oil Methyl Esters. SAE Technical Paper; 2008 Jan 9.

[134] Ganapathy T, Gakkhar RP, Murugesan K. An analytical and experimental study of performance on jatropha biodiesel engine. Thermal Science. 2009 Jan 1; 13(3):69-82.

[135] Dhananjaya DA, Sudhir CV, Mohanan P. Combustion and emission characteristics of DI compression ignition engine operated on jatropha oil methyl ester with different injection parameters. International Journal of Mechanical and Materials Engineering. 2009; 4(3):220-31.

[136] Jindal S, Nandwana BP, Rathore NS, Vashistha V. Experimental investigation of the effect of compression ratio and injection pressure in a direct injection diesel engine running on Jatropha methyl ester. Applied Thermal Engineering. 2010 Apr 30; 30(5):442-8.

[137] Dhananjaya DA, Sudhir CV, Mohanan P. Combustion characteristics of diesel engine operating on jatropha oil methyl ester. Thermal Science. 2010 Jan 1; 14(4):965.

[138] Jindal S. Effect of engine parameters on NOx emissions with Jatropha biodiesel as fuel. International journal of Energy and Environment. 2010; 1(2):343-50.

[139] Ganapathy T, Gakkhar RP, Murugesan K. Influence of injection timing on performance, combustion and emission characteristics of Jatropha biodiesel engine. Applied energy. 2011 Dec 31; 88(12):4376-86.

[140] Jindal S. Effect of injection timing on combustion and performance of a direct injection diesel engine running on Jatropha methyl ester. International Journal of Energy and Environment. 2011; 2(1):113-22.

[141] Gomaa M, Alimin AJ, Kamarudin KA. The effect of EGR rates on NOx and smoke emissions of an IDI diesel engine fuelled with Jatropha biodiesel blends. International Journal of Energy and Enviroment. 2011; 2(3):477-90.

[142] Shrivastava N, Varma SN, Pandey M. A study on reduction of oxides of nitrogen with jatropha oil based bio diesel. International Journal of Renewable Energy Research (IJRER). 2012 Sep 18; 2(3):504-9.

[143] Rambabua V, Prasada VJ, Babua PR. Performance Analysis of Di-Diesel Engine at Different Injection Pressures using Jatropha Methyl Ester. International Journal of Thermal Technologies. 2012 June; 2:165-70

[144] Barboza AB, Madhwesh N, Sudhir CV, Sharma YN. Influence of Injection Timing and Injector Opening Pressure on Combustion Performance and P-θ Characteristics of a CI Engine Operating on Jatropha B20 Fuel Operating on Jatropha B20 Fuel. World Academy of Science, Engineering and Technology. 2012; 70:628-33.

[145] Rajashekhar CR, Chandrashekar TK, Umashankar C, Kumar RH. Studies on effects of combustion chamber geometry and injection pressure on biodiesel combustion. Transactions of the Canadian Society for Mechanical Engineering. 2012 Jan 1; 36(4):429-38.

[146] Pandhare A, Padalkar A. Investigations on performance and emission characteristics of diesel engine with biodiesel (Jatropha Oil) and its blends. Journal of Renewable Energy. 2013 Mar 14; 2013.

[147] Deore ER, Jahagirdar RS. Effect of compression ratio on energy and emission performance of single cylinder diesel engine fueled with jatropha and karanja biodiesel. International Journal of Thermodynamics. 2013; 16(3):132-44.

[148] Kumar R, Dixit AK. Combustion and emission characteristics of variable compression ignition engine fueled with Jatropha curcas ethyl ester blends at different compression ratio. Journal of Renewable Energy. 2014 Apr 16; 2014.

[149] Premnath S, Devaradjane G. Improving the performance and emission characteristics of a single cylinder diesel engine having reentrant combustion chamber using diesel and Jatropha methyl esters. Ecotoxicology and Environmental Safety. 2015 Nov 30; 121:10-5.

[150] Tang H, Wang A, Salley SO, Ng KS. The effect of natural and synthetic antioxidants on the oxidative stability of biodiesel. Journal of the American Oil Chemists' Society. 2008 Apr 1; 85(4):373-82.

[151] Botella L, Bimbela F, Martín L, Arauzo J, Sánchez JL. Oxidation stability of biodiesel fuels and blends using the Rancimat and PetroOXY methods. Effect of 4-

allyl-2, 6-dimethoxyphenol and catechol as biodiesel additives on oxidation stability. Frontiers in Chemistry. 2014; 2.

[152] Rashedul HK, Masjuki HH, Kalam MA, Teoh YH, How HG, Fattah IR. Effect of antioxidant on the oxidation stability and combustion–performance–emission characteristics of a diesel engine fueled with diesel–biodiesel blend. Energy Conversion and Management. 2015 Dec 31; 106:849-58.

[153] Jain S, Sharma MP. Oxidation stability of blends of Jatropha biodiesel with diesel. Fuel. 2011 Oct 31; 90(10):3014-20.

[154] Sarin R, Sharma M, Sinharay S, Malhotra RK. Jatropha–palm biodiesel blends: an optimum mix for Asia. Fuel. 2007 Aug 31; 86(10):1365-71.

[155] Sarin A, Arora R, Singh NP, Sharma M, Malhotra RK. Influence of metal contaminants on oxidation stability of Jatropha biodiesel. Energy. 2009 Sep 30; 34(9):1271-5.

[156] Sarin A, Arora R, Singh NP, Sarin R, Malhotra RK, Sharma M, Khan AA. Synergistic effect of metal deactivator and antioxidant on oxidation stability of metal contaminated Jatropha biodiesel. Energy. 2010 May 31; 35(5):2333-7.

[157] Varatharajan K, Cheralathan M, Velraj R. Mitigation of NOx emissions from a jatropha biodiesel fuelled DI diesel engine using antioxidant additives. Fuel. 2011 Aug 31; 90(8):2721-5.

[158] Sarin A, Arora R, Singh NP, Sarin R, Malhotra RK. Blends of biodiesels synthesized from non-edible and edible oils: influence on the OS (oxidation stability). Energy. 2010 Aug 31; 35(8):3449-53.

[159] Chen YH, Chen JH, Luo YM, Shang NC, Chang CH, Chang CY, Chiang PC, Shie JL. Property modification of jatropha oil biodiesel by blending with other biodiesels or adding antioxidants. Energy. 2011 Jul 31; 36(7):4415-21.

[160] Murugan S, Ramaswamy MC, Nagarajan G. Production of tyre pyrolysis oil from waste automobile tyres. Inthe Proceedings of National conference on Advances in Mechanical Engineering 2006 (pp. 899-906).

[161] Murugan S, Ramaswamy MC, Nagarajan G. The use of tyre pyrolysis oil in diesel engines. Waste Management. 2008 Dec 31; 28(12):2743-9.

[162] Murugan S, Ramaswamy MC, Nagarajan G. Assessment of pyrolysis oil as an energy source for diesel engines. Fuel Processing Technology. 2009 Jan 31; 90(1):67-74.

[163] Murugan S, Ramaswamy MC, Nagarajan G. Influence of Distillation on Performance, Emission, and Combustion of a DI Diesel Engine, Using Tyre Pyrolysis Oil Diesel Blends. Thermal Science. 2008 Jan 1; 12(1):157-67.

[164] Murugan S, Ramaswamy MC, Nagarajan G. A comparative study on the performance, emission and combustion studies of a DI diesel engine using distilled tyre pyrolysis oil–diesel blends. Fuel. 2008 Aug 31; 87(10):2111-21.

[165] Murugan S, Ramaswamy MC, Nagarajan G. Performance, emission and combustion studies of a DI diesel engine using Distilled Tyre pyrolysis oil-diesel blends. Fuel Processing Technology. 2008 Feb 29; 89(2):152-9.

[166] Hariharan S, Murugan S, Nagarajan G. Effect of diethyl ether on Tyre pyrolysis oil fueled diesel engine. Fuel. 2013 Feb 28; 104:109-15.

[167] Doğan O, Çelik MB, Özdalyan B. The effect of tire derived fuel/diesel fuel blends utilization on diesel engine performance and emissions. Fuel. 2012 May 31; 95:340-6.

[168] Frigo S, Seggiani M, Puccini M, Vitolo S. Liquid fuel production from waste tyre pyrolysis and its utilisation in a Diesel engine. Fuel. 2014 Jan 15; 116:399-408.

[169] Martínez JD, Rodríguez-Fernández J, Sánchez-Valdepeñas J, Murillo R, García T. Performance and emissions of an automotive diesel engine using a tire pyrolysis liquid blend. Fuel. 2014 Jan 31; 115:490-9.

[170] Yadav VS, Khatri KK, Tanwar D, Sharma D, Soni SL. Performance analysis and exhaust emissions of neem methyl ester operated compression ignition engine. Journal of Renewable and Sustainable Energy. 2013 Mar 1;5(2):023101.

[171] Meher LC, Sagar DV, Naik SN. Technical aspects of biodiesel production by transesterification-a review. Renewable and sustainable energy reviews. 2006 Jun 30; 10(3):248-68.

[172] Miranda M, Pinto F, Gulyurtlu I, Cabrita I. Pyrolysis of rubber tyre wastes: a kinetic study. Fuel. 2013 Jan 31; 103:542-52.

[173] Williams PT. Pyrolysis of waste tyres: a review. Waste management. 2013 Aug 31; 33(8):1714-28.

[174] Bridgwater AV. Review of fast pyrolysis of biomass and product upgrading. Biomass and bioenergy. 2012 Mar 31; 38:68-94.

[175] Hossain AK, Davies PA. Pyrolysis liquids and gases as alternative fuels in internal combustion engines–A review. Renewable and Sustainable Energy Reviews. 2013 May 31; 21:165-89.

[176] Martínez JD, Puy N, Murillo R, García T, Navarro MV, Mastral AM. Waste tyre pyrolysis–a review. Renewable and Sustainable Energy Reviews. 2013 Jul 31; 23:179-213.

[177] Pakdel H, Roy C. Simultaneous gas chromatographic-Fourier transform infrared spectroscopic-mass spectrometric analysis of synthetic fuel derived from used tire

vacuum pyrolysis oil, naphtha fraction. Journal of Chromatography A. 1994 Oct 14; 683(1):203-14.

[178] Seidelt S, Müller-Hagedorn M, Bockhorn H. Description of tire pyrolysis by thermal degradation behaviour of main components. Journal of Analytical and Applied Pyrolysis. 2006 Jan 31; 75(1):11-8.

[179] Krieger RB, Borman GL. Computation of apparent heat release for internal combustion engines. In Mechanical Engineering 1967 Jan 1 (Vol. 89, No. 1, p. 59). 345 E 47TH ST, NEW YORK, NY 10017: ASME-AMER SOC MECHANICAL ENG.

[180] J.B. Heywood. Internal combustion engines fundamentals. McGraw Hill, London, 1989.

[181] Martyr AJ, Plint MA. Engine testing theory and practice. 3rd ed. Oxford: Elsevier; 2007. p. 306–7.

[182] Pundir BP. IC engines combustion and emissions. Oxford: Alpha Science International Ltd; 2010. p. 135.

[183] Bora BJ, Saha UK. Experimental evaluation of a rice bran biodiesel–biogas run dual fuel diesel engine at varying compression ratios. Renewable Energy. 2016 Mar 31; 87:782-90.

[184] Prakash R, Singh RK, Murugan S. An experimental investigation on a diesel engine fueled by biodiesel and its emulsions with wood pyrolysis oil. International Journal of Green Energy. 2012 Nov 1;9(8):749-65.

[185] Exhaust gas analysis. ftp://ftp.energia.bme.hu/pub/Measurements_in_Thermal_ Engineering_BMEGEENMWM1/GasAnalysis.pdf [accessed on dt. 29.09. 2016]

[186] Combustion. http://www.cambustion.com/products/hfr500/fast-fid-principles [accessed on dt. 29.09. 2016]

[187] Electrochemical sensor. http://www.intlsensor.com/pdf/electrochemical.pdf [accessed on dt. 29.09. 2016]

[188] Holman JP. Experimental techniques. Tata McGraw Hill publications, 2003.

[189] Khan A, Maity K. A Novel MCDM Approach for Simultaneous Optimization of some Correlated Machining Parameters in Turning of CP-Titanium Grade 2. InInternational Journal of Engineering Research in Africa 2016 (Vol. 22, pp. 94-111). Trans Tech Publications.

[190] Caresana F. Impact of biodiesel bulk modulus on injection pressure and injection timing. The effect of residual pressure. Fuel. 2011 Feb 28; 90(2):477-85.

[191] Zhu R, Miao H, Wang X, Huang Z. Effects of fuel constituents and injection timing on combustion and emission characteristics of a compression-ignition

engine fueled with diesel-DMM blends. Proceedings of the Combustion Institute. 2013 Dec 31; 34(2):3013-20.

[192] Banapurmath NR, Tewari PG, Gaitonde VN. Experimental investigations on performance and emission characteristics of Honge oil biodiesel (HOME) operated compression ignition engine. Renewable energy. 2012 Dec 31; 48: 193-201.

[193] Agarwal AK, Dhar A, Srivastava DK, Maurya RK, Singh AP. Effect of fuel injection pressure on diesel particulate size and number distribution in a CRDI single cylinder research engine. Fuel. 2013 May 31; 107:84-9.

[194] Liu J, Yao A, Yao C. Effects of diesel injection pressure on the performance and emissions of a HD common-rail diesel engine fueled with diesel/methanol dual fuel. Fuel. 2015 Jan 15; 140:192-200.

[195] Kegl B. Experimental investigation of optimal timing of the diesel engine injection pump using biodiesel fuel. Energy & Fuels. 2006 Jul 19; 20(4):1460-70.

[196] Bhusnoor SS, Babu MG, Subrahmanyam JP. Studies on performance and exhaust emissions of a CI engine operating on diesel and diesel biodiesel blends at different injection pressures and injection timings. SAE Technical Paper; 2007 Apr 16.

[197] Jindal S. Experimental investigation of the effect of compression ratio and injection pressure in a direct injection diesel engine running on Karanj methyl ester. International Journal of Sustainable Energy. 2011 Dec 1; 30(sup1):S91-105.

[198] Debnath BK, Sahoo N, Saha UK. Thermodynamic analysis of a variable compression ratio diesel engine running with palm oil methyl ester. Energy Conversion and Management. 2013 Jan 31; 65:147-54.

[199] European Committee for Standardization (CEN). EN 15751 Automotive fuels-fatty acid methyl ester (FAME) fuel and blends with diesel fuel -determination of oxidation stability by accelerated oxidation method; 2009.

[200] Agarwal AK, Bijwe J, Das LM. Wear assessment in a biodiesel fueled compression ignition engine. Journal of Engineering for Gas Turbines and Power. 2003 Jul 1; 125(3):820-6.

[201] Agarwal AK. Experimental investigations of the effect of biodiesel utilization on lubricating oil tribology in diesel engines. Proceedings of the Institution of Mechanical Engineers, Part D: Journal of Automobile Engineering. 2005 May 1; 219(5):703-13.

[202] Sinha S, Agarwal AK. Experimental investigation of the effect of biodiesel utilization on lubricating oil degradation and wear of a transportation CIDI engine. Journal of Engineering for Gas Turbines and Power. 2010 Apr 1; 132(4):042801.

[203] Liaquat AM, Masjuki HH, Kalam MA, Fattah IR. Impact of biodiesel blend on injector deposit formation. Energy. 2014 Aug 1; 72:813-23.

[204] Wander PR, Altafini CR, Colombo AL, Perera SC. Durability studies of mono-cylinder compression ignition engines operating with diesel, soy and castor oil methyl esters. Energy. 2011 Jun 30; 36(6):3917-23.

[205] Indian Standard Code IS: 10000, Part VIII, 1980, ''Methods of Tests for Internal Combustion Engines: Part VIII Performance Tests.''

[206] Qi DH, Chen H, Geng LM, Bian YZ. Experimental studies on the combustion characteristics and performance of a direct injection engine fueled with biodiesel/diesel blends. Energy Conversion and Management. 2010 Dec 31; 51(12):2985-92.

[207] Liu Z, Karim GA. An examination of the ignition delay period in gas-fueled diesel engines. Journal of Engineering for Gas Turbines and Power. 1998 Jan 1; 120(1):225-31.

[208] Canakci M. Combustion characteristics of a DI-HCCI gasoline engine running at different boost pressures. Fuel. 2012 Jun 30; 96:546-55.

[209] Hansdah D, Murugan S. Bioethanol fumigation in a DI diesel engine. Fuel. 2014 Aug 15; 130:324-33.

[210] Tse H, Leung CW, Cheung CS. Investigation on the combustion characteristics and particulate emissions from a diesel engine fueled with diesel-biodiesel-ethanol blends. Energy. 2015 Apr 1; 83:343-50.

[211] Laresgoiti MF, Caballero BM, de Marco I, Torres A, Cabrero MA, Chomón MJ. Characterization of the liquid products obtained in tyre pyrolysis. Journal of Analytical and Applied Pyrolysis. 2004 Jun 30; 71(2):917-34.

[212] Kumar MS, Ramesh A, Nagalingam B. Complete vegetable oil fueled dual fuel compression ignition engine. SAE Technical Paper; 2001 Nov 1.

[213] Rajendiran G, Subramanian R, Venkatachalam R, Nedunchezhian N, Mayilsamy K. Experimental investigation on combustion analysis of multicylinder direct injected diesel engine using diesel–biodiesel–DEE as alternative fuel. International Journal of Ambient Energy. 2013 Jun 1; 34(2):63-72.

[214] Suryanarayanan S, Janakiraman VM, Rao GL, Sampath S. Comparative study of the performance and emission characteristics of biodiesels from different vegetable oils with diesel. SAE Technical Paper; 2008 Jun 23.

[215] Gopal R, Kavandappa Goundar M, Ramasamy S, Natarajan N, Ramasamy V. Experimental and regression analysis for multi cylinder diesel engine operated with hybrid fuel blends. Thermal Science. 2014 Jan 1; 18(1):193-203.

[216] Kumar S, Prakash R, Murugan S, Singh RK. Performance and emission analysis of blends of waste plastic oil obtained by catalytic pyrolysis of waste HDPE with

diesel in a CI engine. Energy Conversion and Management. 2013 Oct 31; 74:323-31.

[217] Labeckas G, Slavinskas S. The effect of rapeseed oil methyl ester on direct injection diesel engine performance and exhaust emissions. Energy Conversion and Management. 2006 Aug 31; 47(13):1954-67.

[218] Takeda Y. Development study on Jatropha curcas (sabu dum) oil as a substitute for diesel engine oil in Thailand. Journal of the Agricultural Association of China. 1982(120):1-8.

[219] Lin CY, Lin HA. Engine performance and emission characteristics of a three-phase emulsion of biodiesel produced by peroxidation. Fuel Processing Technology. 2007 Jan 31; 88(1):35-41.

[220] Nabi MN, Rahman MM, Akhter MS. Biodiesel from cotton seed oil and its effect on engine performance and exhaust emissions. Applied Thermal Engineering. 2009 Aug 31; 29(11):2265-70.

[221] Cheng CH, Cheung CS, Chan TL, Lee SC, Yao CD, Tsang KS. Comparison of emissions of a direct injection diesel engine operating on biodiesel with emulsified and fumigated methanol. Fuel. 2008 Aug 31; 87(10):1870-9.

[222] Canakci M. Combustion characteristics of a turbocharged DI compression ignition engine fueled with petroleum diesel fuels and biodiesel. Bioresource technology. 2007 Apr 30; 98(6):1167-75.

[223] Tan PQ, Hu ZY, Lou DM, Li ZJ. Exhaust emissions from a light-duty diesel engine with Jatropha biodiesel fuel. Energy. 2012 Mar 31; 39(1):356-62.

[224] Can Ö, Celikten I, Usta N. Effects of ethanol addition on performance and emissions of a turbocharged indirect injection diesel engine running at different injection pressures. Energy conversion and Management. 2004 Sep 30; 45(15):2429-40.

[225] Canakci M, Ozsezen AN, Turkcan A. Combustion analysis of preheated crude sunflower oil in an IDI diesel engine. Biomass and bioenergy. 2009 May 31; 33(5):760-7.

[226] Kalbande SR, Vikhe SD. Jatropha and Karanj bio-fuel: an alternate fuel for diesel engine. ARPN J Eng Appl Sci. 2008 Feb; 3(1):7-13.

[227] Giakoumis EG, Rakopoulos CD, Dimaratos AM, Rakopoulos DC. Exhaust emissions with ethanol or n-butanol diesel fuel blends during transient operation: a review. Renewable and Sustainable Energy Reviews. 2013 Jan 31; 17:170-90.

[228] Bari S, Yu CW, Lim TH. Effect of fuel injection timing with waste cooking oil as a fuel in a direct injection diesel engine. Proceedings of the Institution of Mechanical Engineers, Part D: Journal of Automobile Engineering. 2004; 218(1):93-104.

[229] Shehata MS. Emissions, performance and cylinder pressure of diesel engine fuelled by biodiesel fuel. Fuel. 2013 Oct 31; 112:513-22.

[230] Gumus M, Sayin C, Canakci M. Effect of fuel injection timing on the injection, combustion, and performance characteristics of a direct-injection (DI) diesel engine fueled with canola oil methyl ester− diesel fuel blends. Energy & Fuels. 2010 Apr 9; 24(5):3199-213.

[231] Jayashankara B, Ganesan V. Effect of fuel injection timing and intake pressure on the performance of a DI diesel engine–A parametric study using CFD. Energy Conversion and Management. 2010 Oct 31; 51(10):1835-48.

[232] Agarwal AK, Dhar A, Gupta JG, Kim WI, Choi K, Lee CS, Park S. Effect of fuel injection pressure and injection timing of Karanja biodiesel blends on fuel spray, engine performance, emissions and combustion characteristics. Energy Conversion and Management. 2015 Feb 28; 91:302-14.

[233] Ragland KW, Bryden KM. Combustion engineering. 2nd ed. Boca Raton: CRC Press, Taylor & Francis group; 2011.

[234] Qi DH, Lee CF, Jia CC, Wang PP, Wu ST. Experimental investigations of combustion and emission characteristics of rapeseed oil–diesel blends in a two cylinder agricultural diesel engine. Energy Conversion and Management. 2014 Jan 31; 77:227-32.

[235] Paul A, Bose PK, Panua R, Debroy D. Study of performance and emission characteristics of a single cylinder CI engine using diethyl ether and ethanol blends. Journal of the Energy Institute. 2015 Feb 28; 88(1):1-0.

[236] Mani M, Subash C, Nagarajan G. Performance, emission and combustion characteristics of a DI diesel engine using waste plastic oil. Applied Thermal Engineering. 2009 Sep 30; 29(13):2738-44.

[237] Devan PK, Mahalakshmi NV. Performance, emission and combustion characteristics of poon oil and its diesel blends in a DI diesel engine. Fuel. 2009 May 31; 88(5):861-7.

[238] Nwafor OM. Effect of advanced injection timing on the performance of natural gas in diesel engines. Sadhana. 2000 Feb 1; 25(1):11-20.

[239] Challen B, Baranescu R. Diesel Engine Reference Book. 2nd ed. Woburn, MA: SAE and Butterworth Heinemann, 1999.

[240] Sayin C, Uslu K, Canakci M. Influence of injection timing on the exhaust emissions of a dual-fuel CI engine. Renewable Energy. 2008 Jun 30; 33(6):1314-23.

[241] Belagur VK, Chitimini VR. Influence of static injection timing on combustion, emission and performance characteristics of DI diesel engine fuelled with honne

oil methyl ester. International Journal of Ambient Energy. 2012 Jun 1; 33(2):65-74.

[242] Devan PK, Mahalakshmi NV. A study of the performance, emission and combustion characteristics of a compression ignition engine using methyl ester of paradise oil–eucalyptus oil blends. Applied Energy. 2009 May 31; 86(5):675-80.

[243] Zhu Z, Li DK, Liu J, Wei YJ, Liu SH. Investigation on the regulated and unregulated emissions of a DME engine under different injection timing. Applied Thermal Engineering. 2012 Mar 31; 35:9-14.

[244] Uslu K. Influence on performance and emission on using diesel fuel and ethanol at the different injection timing in the diesel engine (Doctoral dissertation, MSc thesis, Marmara University).

[245] Banapurmath NR, Tewari PG, Hosmath RS. Performance and emission characteristics of a DI compression ignition engine operated on Honge, Jatropha and sesame oil methyl esters. Renewable energy. 2008 Sep 30; 33(9):1982-8.

[246] Kannan GR, Anand R. Effect of injection pressure and injection timing on DI diesel engine fuelled with biodiesel from waste cooking oil. Biomass and bioenergy. 2012 Nov 30; 46:343-52.

[247] Ganesan V, Internal combustion engines. 3rd ed., Tata McGraw-Hill, New Delhi, 2010.

[248] Purushothaman K, Nagarajan G. Effect of injection pressure on heat release rate and emissions in CI engine using orange skin powder diesel solution. Energy Conversion and Management. 2009 Apr 30; 50(4):962-9.

[249] Nanthagopal K, Ashok B, Raj RT. Influence of fuel injection pressures on Calophyllum inophyllum methyl ester fuelled direct injection diesel engine. Energy Conversion and Management. 2016 May 15; 116:165-73.

[250] Sayin C, Gumus M, Canakci M. Effect of fuel injection pressure on the injection, combustion and performance characteristics of a DI diesel engine fueled with canola oil methyl esters-diesel fuel blends. Biomass and bioenergy. 2012 Nov 30; 46:435-46.

[251] Turkcan A, Canakci M. Combustion characteristics of an indirect injection (IDI) diesel engine fueled with ethanol/diesel and methanol/diesel blends at different injection timings. InWorld Renewable Energy Congress-Sweden; 8-13 May; 2011; Linköping; Sweden 2011 Nov 3 (No. 057, pp. 3565-3572). Linköping University Electronic Press.

[252] İçıngür Y, Altiparmak D. Effect of fuel cetane number and injection pressure on a DI Diesel engine performance and emissions. Energy Conversion and Management. 2003 Feb 28; 44(3):389-97.

[253] Das B, Lingfa P. Energy analysis of karanja oil as a supplementary fuel for compression ignition engine. Journal of Urban and Environmental Engineering (JUEE). 2016 Jan 21; 9(2):97-101.

[254] Jaichandar S, Annamalai K. Combined impact of injection pressure and combustion chamber geometry on the performance of a biodiesel fueled diesel engine. Energy. 2013 Jun 15; 55:330-9.

[255] Senthil R, Paramasivam C, Silambarasan R. Influence of Injection Pressure on Performance and Emission Characteristics of Nerium Methyl Ester Operated DI Diesel Engine. In Applied Mechanics and Materials. 2014 (Vol. 592, pp. 1632-1637). Trans Tech Publications.

[256] Bakar RA, Ismail AR. Fuel injection pressure effect on performance of direct injection diesel engines based on experiment. American Journal of Applied Sciences. 2008; 5(3):197-202.

[257] Celıkten I. An experimental investigation of the effect of the injection pressure on engine performance and exhaust emission in indirect injection diesel engines. Applied Thermal Engineering. 2003 Nov 30; 23(16):2051-60.

[258] Hountalas DT, Kouremenos DA, Binder KB, Schwarz V, Mavropoulos GC. Effect of injection pressure on the performance and exhaust emissions of a heavy duty DI diesel engine. SAE Technical Paper; 2003 Mar 3.

[259] Venkanna BK, Venkataramana Reddy C. Effect of injector opening pressure on performance, emission and combustion characteristics of DI diesel engine fueled with diesel and honne oil methyl ester. Environmental Progress & Sustainable Energy. 2013 Apr 1; 32(1):148-55.

[260] P.L. Zhou. An investigation into the atomisation of emulsified fuels. Ph.D thesis. University of Newcastle upon Tyne, 1992.

[261] Fazal MA, Haseeb AS, Masjuki HH. Biodiesel feasibility study: an evaluation of material compatibility; performance; emission and engine durability. Renewable and Sustainable Energy Reviews. 2011 Feb 28; 15(2):1314-24.

[262] Sayin C, Ozsezen AN, Canakci M. The influence of operating parameters on the performance and emissions of a DI diesel engine using methanol-blended-diesel fuel. Fuel. 2010 Jul 31; 89(7):1407-14.

[263] Gumus M, Sayin C, Canakci M. The impact of fuel injection pressure on the exhaust emissions of a direct injection diesel engine fueled with biodiesel–diesel fuel blends. Fuel. 2012 May 31; 95:486-94.

[264] Devan PK, Mahalakshmi NV. A study of the performance, emission and combustion characteristics of a compression ignition engine using methyl ester of paradise oil–eucalyptus oil blends. Applied Energy. 2009 May 31; 86(5):675-80.

[265] Nagaraja S, Sakthivel M, Sudhakaran R. Comparative study of the combustion, performance, and emission characteristics of a variable compression ratio engine fuelled with diesel, corn oil methyl ester, and palm oil methyl ester. Journal of Renewable and Sustainable Energy. 2012 Nov 1; 4(6):063122.

[266] Gumus M. A comprehensive experimental investigation of combustion and heat release characteristics of a biodiesel (hazelnut kernel oil methyl ester) fueled direct injection compression ignition engine. Fuel. 2010 Oct 31; 89(10):2802-14.

[267] Caton PA, Hamilton LJ, Cowart JS. Understanding ignition delay effects with pure component fuels in a single-cylinder diesel engine. Journal of Engineering for Gas Turbines and Power. 2011 Mar 1; 133(3):032803.

[268] Muralidharan K, Vasudevan D. Performance, emission and combustion characteristics of a variable compression ratio engine using methyl esters of waste cooking oil and diesel blends. Applied energy. 2011 Nov 30;88(11):3959-68.

[269] Ibrahim A, El-Adawy M, El-Kassaby MM. The impact of changing the compression ratio on the performance of an engine fueled by biodiesel blends. Energy Technology. 2013 Jul 1.

[270] Debnath BK, Saha UK, Sahoo N. Effect of compression ratio and injection timing on the performance characteristics of a diesel engine running on palm oil methyl ester. Proceedings of the Institution of Mechanical Engineers, Part A: Journal of Power and Energy. 2013 Mar 22:0957650912470907.

[271] Arul Mozhi Selvan V, Anand RB, Udayakumar M. Combustion characteristics of diesohol using biodiesel as an additive in a direct injection compression ignition engine under various compression ratios. Energy & Fuels. 2009 Oct 5; 23(11):5413-22.

[272] Xue J, Grift TE, Hansen AC. Effect of biodiesel on engine performances and emissions. Renewable and Sustainable Energy Reviews. 2011 Feb 28; 15(2):1098-116.

[273] Murugesan A, Umarani C, Subramanian R, Nedunchezhian N. Bio-diesel as an alternative fuel for diesel engines—a review. Renewable and Sustainable Energy Reviews. 2009 Apr 30; 13(3):653-62.

[274] Enweremadu CC, Rutto HL. Combustion, emission and engine performance characteristics of used cooking oil biodiesel—a review. Renewable and Sustainable Energy Reviews. 2010 Dec 31; 14(9):2863-73.

[275] Debnath BK, Sahoo N, Saha UK. Adjusting the operating characteristics to improve the performance of an emulsified palm oil methyl ester run diesel engine. Energy Conversion and Management. 2013 May 31; 69:191-8.

[276] EL_Kassaby M, Nemit_allah MA. Studying the effect of compression ratio on an engine fueled with waste oil produced biodiesel/diesel fuel. Alexandria Engineering Journal. 2013 Mar 31; 52(1):1-1.

[277] Jaichandar S, Annamalai K. Effects of open combustion chamber geometries on the performance of pongamia biodiesel in a DI diesel engine. Fuel. 2012 Aug 31; 98:272-9.

[278] Laguitton O, Crua C, Cowell T, Heikal MR, Gold MR. The effect of compression ratio on exhaust emissions from a PCCI diesel engine. Energy Conversion and Management. 2007 Nov 30; 48(11):2918-24.

[279] Celik MB. Experimental determination of suitable ethanol–gasoline blend rate at high compression ratio for gasoline engine. Applied Thermal Engineering. 2008 Apr 30; 28(5):396-404.

[280] Hariram V, Shangar RV. Influence of compression ratio on combustion and performance characteristics of direct injection compression ignition engine. Alexandria Engineering Journal. 2015 Dec 31; 54(4):807-14.

[281] Williams PT, Besler S, Taylor DT. The pyrolysis of scrap automotive tyres: The influence of temperature and heating rate on product composition. Fuel. 1990 Dec 31; 69(12):1474-82.

[282] Sarin A, Singh NP, Sarin R, Malhotra RK. Natural and synthetic antioxidants: influence on the oxidative stability of biodiesel synthesized from non-edible oil. Energy. 2010 Dec 31; 35(12):4645-8.

[283] Fattah IR, Masjuki HH, Kalam MA, Wakil MA, Ashraful AM, Shahir SA. Experimental investigation of performance and regulated emissions of a diesel engine with Calophyllum inophyllum biodiesel blends accompanied by oxidation inhibitors. Energy Conversion and Management. 2014 Jul 31; 83:232-40.

[284] Varatharajan K, Cheralathan M, Velraj R. Mitigation of NOx emissions from a jatropha biodiesel fuelled DI diesel engine using antioxidant additives. Fuel. 2011 Aug 31; 90(8):2721-5.

[285] Kalaivani K, Balasubramanian N. Energy Consumption and Greenhouse Gas Emission Studies of Jatropha Biodiesel Pathway by Life Cycle Assessment in India. Indian Chemical Engineer. 2015 Jun 12:1-3.

[286] Ganapathy T, Gakkhar RP, Murugesan K. Optimization of performance parameters of diesel engine with Jatropha biodiesel using response surface methodology. International Journal of Sustainable Energy. 2011 Dec 1; 30(sup1):S76-90.

[287] Bora BJ, Saha UK, Chatterjee S, Veer V. Effect of compression ratio on performance, combustion and emission characteristics of a dual fuel diesel engine run on raw biogas. Energy Conversion and Management 2014; 87:1000-1009.

[288] Pullen J, Saeed K. An overview of biodiesel oxidation stability. Renewable and Sustainable Energy Reviews. 2012 Oct 31; 16(8):5924-50.

[289] Balaji G, Cheralathan M. Study of antioxidant effect on oxidation stability and emissions in a methyl ester of neem oil fuelled DI diesel engine. Journal of the Energy Institute. 2014 Aug 31; 87(3):188-95.

[290] Jain S, Sharma MP. Biodiesel production from Jatropha curcas oil. Renewable and Sustainable Energy Reviews. 2010 Dec 31; 14(9):3140-7.

[291] Ziejewski M, Goettler HJ, Haines H, Huang C. EMA durability test on high oleic sunflower and safflower oils in diesel engines. SAE Technical paper 1996; Paper No. 961846.

[292] Bari S, Yu CW, Lim TH. Performance deterioration and durability issues while running a diesel engine with crude palm oil. Proceedings of the Institution of Mechanical Engineers, Part D: Journal of Automobile Engineering. 2002 Sep 1; 216(9):785-92.

[293] Fitch JC. Oil Analysis and Proactive Maintenance-A Complete Users Guide for Maintenance Professionals Diagnostics 1994.

[294] Kalam MA, Majsuki HH. Use of an additive in biofuel to evaluate emissions, engine component wear and lubrication characteristics. Proceedings of the Institution of Mechanical Engineers, Part D: Journal of Automobile Engineering. 2002 Sep 1; 216(9):751-7.

[295] Gopal KN, Raj RT. Effect of pongamia oil methyl ester–diesel blend on lubricating oil degradation of di compression ignition engine. Fuel. 2016 Feb 1; 165:105-14.

[296] Mofijur M, Masjuki HH, Kalam MA, Atabani AE, Shahabuddin M, Palash SM, Hazrat MA. Effect of biodiesel from various feedstocks on combustion characteristics, engine durability and materials compatibility: A review. Renewable and Sustainable Energy Reviews. 2013 Dec 31; 28:441-55.

[297] Agarwal AK. Lubricating Oil Tribology of a Biodiesel-Fuelled Compression Ignition Engine. InASME 2003 Internal Combustion Engine Division Spring Technical Conference 2003 Jan 1 (pp. 751-765). American Society of Mechanical Engineers.

[298] Dhar A, Agarwal AK. Experimental investigations of effect of Karanja biodiesel on tribological properties of lubricating oil in a compression ignition engine. Fuel. 2014 Aug 15; 130:112-9.

[299] Haseeb AS, Fazal MA, Jahirul MI, Masjuki HH. Compatibility of automotive materials in biodiesel: a review. Fuel. 2011 Mar 31; 90(3):922-31.

[300] Fontaras G, Karavalakis G, Kousoulidou M, Tzamkiozis T, Ntziachristos L, Bakeas E, Stournas S, Samaras Z. Effects of biodiesel on passenger car fuel consumption, regulated and non-regulated pollutant emissions over legislated and real-world driving cycles. Fuel. 2009 Sep 30; 88(9):1608-17.

[301] Singh SK, Agarwal AK, Sharma M. Experimental investigations of heavy metal addition in lubricating oil and soot deposition in an EGR operated engine. Applied Thermal Engineering. 2006 Feb 28; 26(2):259-66.

[302] Kumar N, Chauhan SR. Evaluation of endurance characteristics for a modified diesel engine runs on jatropha biodiesel. Applied Energy. 2015 Oct 1; 155:253-69.

[303] Agarwal AK, Dhar A. Karanja oil utilization in a direct-injection engine by preheating. Part 2: experimental investigations of engine durability and lubricating oil properties. Proceedings of the Institution of Mechanical Engineers, Part D: Journal of Automobile Engineering. 2010; 224(1):85-97.

[304] Hasannuddin AK, Wira JY, Sarah S, Aqma WW, Hadi AA, Hirofumi N, Aizam SA, Aiman MA, Watanabe S, Ahmad MI, Azrin MA. Performance, emissions and lubricant oil analysis of diesel engine running on emulsion fuel. Energy Conversion and Management. 2016 Jun 1; 117:548-57.

Appendices

Appendix 1

Technical specifications of the engine

Type	Kirloskar TAF1 Vertical diesel engine
No. of cylinder	1
Type of injection	Direct
Rated power at 1500 rpm, kW	4.41
Bore, mm	87.5
Stroke, mm	110
Compression ratio	17.5
Method of cooling	Air cooled with radial fan
Displacement volume, litres	0.662
Fuel injection timing bTDC, °CA	23
Number of injector nozzle holes	3
Nozzle-hole diameter, mm	0.25
Inlet valve opening bTDC, °CA	4.5
Inlet valve closing aBDC, °CA	35.5
Exhaust valve opening bBDC, °CA	35.5
Exhaust valve closing aTDC, °CA	4.5
Weight, kg	163
Type of fuel injection	Pump-line-nozzle injection system
Connecting rod length, mm	220

Appendix 2

Specification of the pressure transducer

Description	Data
Model	KISTLER, Switzerland 601 A, air cooled
Range	0-100 bar
Sensitivity	25 mV/bar
Linearity	0.1 <+ % FSO
Acceleration sensitivity	< 0.001 bar / g
Operating temperature range	-196 to 200 ^{o}C
Capacitance	5 PF
Weight	1.7 g
Connector, Teflon insulator	M4 x 0.35

Appendix 3

Specification of the charge amplifier

Description	Data
Make	KISLTER instruments, Switzerland
Measuring ranges	12 stages graded pC 10-50000 1:2:5 and stepless 1 to 10
Accuracy of two most sensitive ranges Accuracy of other range stages	<± 3 % <± 1%
Linearity, of Transducer sensitivity	<±0.5%
Calibration capacitor	1000 ± 0.5 pF
Operating temperature range	-196 to 200 ^{o}C
Calibration input sensitivity	1±0.5 pC/mV
Input voltage, maximum with pulses	+ 12 V
Connector, Teflon insulator	M4 x 0.35

Appendix 4

Technical specification of AVL DiGAS 444 analyzer

Measured quantity	Measuring range	Accuracy
CO	0-10%	< 0.6% vol: ±0.03% vol ≥ 0.6% vol: ± 5% of initial value
CO_2	0-20%	< 10% vol: ±0.05% vol ≥ 10% vol: ± 5% of vol
HC	0-20000 ppm vol	< 200 ppm vol: ± 10 ppm vol ≥ 200 ppm vol: ± 5% of initial value
O_2	0-22% vol	< 2% vol: ±0.01% vol ≥ 2% vol: ± 5% of vol
NO	0-5000 ppm vol	< 500 ppm vol: ± 50 ppm vol ≥ 500 ppm vol: ± 10% of initial value
Voltage	11-22 V DC	
Power consumption	≈25W	
Warm up time	≈ 7 min	
Operating temperature	5-45 ^{o}C	
Dimensions (WxDxH)	270x320x85	
Weight	4.5 kg net weight without accessories.	

Appendix 5

Technical specification of AVL 437C Diesel smoke meter

Description	Data
Measuring chamber	0-100% opacity
Accuracy and repeatability	±1 % of full scale
Alarming signal temperature	Lights up when temperature of measuring chamber is below 70 ^{o}C
Linearity check	48.4% - 53.1% or 1.54 m^{-1} - 1.54 m^{-1} of measurement range
Measuring chamber length	430 ± 5 mm
Light source	Halogen lamp, 12V
Sensor	Selenium Photocell
Weight	24 kg

Appendix 6

Summary of values on combustion, performance and emission parameters for diesel, JME and JMETPO blends at full load

Parameters	**Diesel**	**JME**	**JMETPO10**	**JMETPO20**	**JMETPO30**	**JMETPO40**	**JMETPO50**
Combustion Parameters							
Ignition delay (˚CA)	11.5	10.2	11	11.4	11.9	12.7	12.14
Maximum heat release (J/˚CA)	56.4	52.4	49.2	50.4	40.1	41.2	40.6
Combustion duration (˚CA)	38.3	37.9	37.3	37.8	56.9	65.4	58.9
Maximum cylinder pressure (bar)	81	80.6	79.2	80	66.8	68.6	68.5
Maximum rate of pressure rise (bar/ ˚CA)	5.3	3.4	4.2	3.8	2.9	2.9	3
Performance Parameters							
Brake thermal efficiency (%)	29.89	28.61	29.87	29.88	26.6	26.9	27.86
Brake specific energy consumption (MJ/kWh)	11.86	12.55	12.67	12.79	13.50	13.69	13.92
Exhaust gas temperature (˚C)	303	329	297	325	376	371	369
Emission Parameters							
BSCO emission (g/kWh)	2.45	1.99	2.07	2.22	2.6	2.94	3.28
BSHC emission (g/kWh)	0.059	0.047	0.049	0.054	0.065	0.081	0.092
BSNO emission (g/kWh)	2.91	4.04	3.81	3.63	3.59	3.49	3.4
Smoke opacity (%)	86.3	52.2	56.2	63.1	78.3	89.1	94.2

Appendix 7

Summary of values on combustion, performance and emission parameters for diesel, JME and the JMETPO20 blend at full load and different injection timings

Parameters	**Diesel**	**JME**	**X@ 26 ˚CA bTDC**	**X@ 24.5 ˚CA bTDC**	**X@ 23˚CA bTDC**	**X@ 21.5 ˚CA bTDC**	**X@ 20 ˚CA bTDC**
Combustion Parameters							
Ignition delay (˚CA)	11.5	10.2	14.6	12.8	11.4	10.7	8.3
Maximum heat release (J/˚CA)	56.4	52.4	52.2	51.4	50.4	48.1	43.6
Combustion duration (˚CA)	38.3	37.9	40.1	41.3	37.8	44.4	47.4
Maximum cylinder pressure (bar)	81	80.6	83.7	82.7	80	68.2	62.7
Maximum rate of pressure rise (bar/˚CA)	5.3	3.4	5.6	5.3	3.8	4.8	4.1
Performance Parameters							
Brake thermal efficiency (%)	29.89	28.61	29.1	30.5	29.88	29.1	28.1
BSEC (MJ/kWh)	11.86	12.55	12.03	11.6	12.79	13.13	13.8
Exhaust gas temperature (˚C)	303	329	330	320	325	344	358
Emission Parameters							
BSCO emission (g/kWh)	2.45	1.99	2.17	1.97	2.22	2.44	2.66
BSHC emission (g/kWh)	0.059	0.047	0.051	0.047	0.054	0.057	0.063
BSNO emission (g/kWh)	2.91	4.04	3.9	3.8	3.63	3.26	3.17
Smoke opacity (%)	86.3	52.2	60.2	57.2	63.1	69.1	76.5

Appendix 8

Summary of values on combustion, performance and emission parameters for diesel, JME and the JMETPO20 blend at full load and different nozzle opening pressures

Parameters	**Diesel**	**JME**	**X@ 200 bar**	**X@ 210 bar**	**X@ 220 bar**	**X@ 230 bar**	**X@ 240 bar**	**X@ 240 bar**
Combustion Parameters								
Ignition delay (˚CA)	11.5	10.2	11.4	10.1	9.6	10.3	10.9	11.4
Maximum heat release (J/˚CA)	56.4	52.4	50.4	52.5	54.5	53.8	52.6	50.5
Combustion duration (˚CA)	38.3	37.9	37.8	42.9	35.4	35.8	42.6	44.23
Maximum cylinder pressure (bar)	81	80.6	80	83.8	84.9	84.7	83.3	82.8
Maximum rate of pressure rise (bar/ ˚CA)	5.3	3.4	3.8	4.1	5.1	5.01	4.96	4.63
Performance Parameters								
Brake thermal efficiency (%)	29.89	28.61	29.88	29.95	31.4	31.1	28.97	28.1
Brake specific energy consumption (MJ/kWh)	11.86	12.55	12.79	12.77	12.52	12.7	12.9	13.2
Exhaust gas temperature (˚C)	303	329	325	315	285	298	318	334
Emission Parameters								
BSCO emission (g/kWh)	2.45	1.99	2.22	2.47	2.24	2.4	2.5	3.15
BSHC emission (g/kWh)	0.059	0.047	0.054	0.058	0.052	0.064	0.068	0.080
BSNO emission (g/kWh)	2.91	4.04	3.63	4.17	4.29	3.92	3.62	3.94
Smoke opacity (%)	86.3	52.2	63.1	61.2	57.1	63	65.3	69.1

Appendix 9

Summary of values on combustion, performance and emission parameters for diesel, JME and the JMETPO20 blend at full load and different compression ratios

Parameters	**Diesel**	**JME**	**X@ standard**	**X@ 16.5**	**X@ 17.5**	**X@ 18.5**
Combustion Parameters						
Ignition delay (˚CA)	11.5	10.2	11.4	10.12	9.6	9.1
Maximum heat release (J/˚CA)	56.4	52.4	50.4	42.3	54.5	55.56
Combustion duration (˚CA)	38.3	37.9	37.8	38	35.4	34.12
Maximum cylinder pressure (bar)	81	80.6	80	75.8	84.9	84.91
Maximum rate of pressure rise (bar/ ˚CA)	5.3	3.4	3.8	4.2	5.1	5.21
Performance Parameters						
Brake thermal efficiency (%)	29.89	28.61	29.88	29.95	31.41	32.27
Brake specific energy consumption (MJ/kWh)	11.86	12.55	12.79	12.77	12.52	11.15
Exhaust gas temperature (˚C)	303	329	325	325	285	285
Emission Parameters						
BSCO emission (g/kWh)	2.45	1.99	2.22	2.47	2.24	2.04
BSHC emission (g/kWh)	0.059	0.047	0.054	0.058	0.052	0.037
BSNO emission (g/kWh)	2.91	4.04	3.63	4.17	4.29	4.49
Smoke opacity (%)	86.3	52.2	63.1	61.23	57.14	52.12

Dissemination

Internationally indexed Journals (Web of Science, SCI, Scopus, etc.)

1. **Abhishek Sharma** and S. Murugan. Effect of nozzle opening pressure on the behaviour of a diesel engine running with non-petroleum fuel. **Energy,** 2017, May 27; 127: 236-246. (**SCI**, Impact Factor 4.810, Elsevier Publications)

2. **Abhishek Sharma, S Murugan**. Effect of blending waste tyre derived fuel on oxidation stability of biodiesel and performance and emission studies of a diesel engine. **Applied Thermal Engineering**, 2017 May 25; 118:365-74. (**SCI**, Impact Factor 3.269, Elsevier Publications)

3. **Abhishek Sharma** and S. Murugan. Durability analysis of a single cylinder DI diesel engine operating with a non-petroleum fuel. **Fuel**, 2017 Mar 30; 191:393-402. (**SCI**, Impact Factor 4.141, Elsevier publications)

4. **Abhishek Sharma**, S. Murugan. Potential for using a tyre pyrolysis oil-biodiesel blend in a diesel engine at different compression ratios. **Energy Conversion and Management**, 2015 Mar 15; 93:289-97. (**SCI**, Impact Factor 4.80, Elsevier Publications)

5. **Abhishek Sharma** and S. Murugan. Combustion, performance and emission characteristics of a DI diesel engine fuelled with non-petroleum fuel: A study on the role of fuel injection timing. **Journal of the Energy Institute,** 2015 Nov 30; 88(4):364-75. (**SCI**, Impact Factor 1, Elsevier Publications)

6. **Abhishek Sharma** and S. Murugan. Influence of Fuel Injection Timing on the Performance and Emission Characteristics of a Diesel Engine Fueled with Jatropha Methyl Ester-Tyre Pyrolysis Oil Blend. **Applied Mechanics and Materials** 2014, 592:1627-1631. (**Scopus**, Trans Tech Publications)

7. **Abhishek Sharma** and S. Murugan. Investigation on the behaviour of a DI diesel engine fueled with Jatropha Methyl Ester (JME) and Tyre Pyrolysis Oil (TPO) blends. **Fuel**, 2013 Jun 30; 108:699-708. (**SCI**, Impact Factor 4.141, Elsevier Publications)

Book chapter

1. **Abhishek Sharma** and S. Murugan. Chapter 13 entitled as "Experimental evaluation of combustion parameters of a di diesel engine operating with biodiesel blend at varying injection timings" in Proceedings of the First International Conference on Recent Advances in Bioenergy Research by **Springer publication**, 2016. (ISBN 978-81-322-2773-1)

Conferences

1. **Abhishek Sharma** and S. Murugan. Combustion Analysis of Diesel Engine Fueled with Jatropha Oil Methyl Ester Blend at Varying Nozzle Injection Pressure. International Conference on Environment and Energy, Jawaharlal Nehru Technological University Hyderabad, 15-17 December 2014.

2. **Abhishek Sharma** and S. Murugan. Impact of Fuel Injection Pressure on Performance and Emission Characteristics of a Compression Ignition Engine Fueled With Jatropha Methyl Ester Tyre Pyrolysis Blend. SAE 2014 Powertrains, Fuels & Lubricants Meeting, 20 - 23 October 2014, Birmingham, England. Paper No. - 2014-01-2650. DOI: 10.4271/2014-01-2650 (**Scopus Index**)

3. **Abhishek Sharma** and S. Murugan. Performance and Emission Studies of a Diesel Engine Using Biodiesel Tyre Pyrolysis Oil Blends. SAE World Congress & Exhibition, Detroit, US, 8 April 2013. Paper No.-2013-01-1150.
   DOI: 10.4271/2013-01-1150. (**Scopus Index**)

4. **Abhishek Sharma**, R. Senthooran, Subhash Kumar Gupta and S. Murugan. Combustion Studies of a DI Diesel Engine Using Jatropha Methyl Ester Tyre Pyrolysis Oil Blends. Proceedings of International Conference on Alternative Fuels for I.C. engines, Malaviya National Institute of Technology Jaipur, 6-8 February 2013.

Brief Bio-data of the Author

The author, Abhishek Sharma, born on 02-01-1983 graduated in Mechanical Engineering from Shri Shankaracharya College of Engineering and Technology, Bhilai, India in the year 2005. He completed his Post-graduate study (M.Tech.) in Mechanical Engineering with specialization in Thermal Engineering from the Maulana Azad National Institute of Technology, Bhopal, India in the year 2008. Immediately after completion of M.Tech programme, he joined as Lecturer in the Department of Mechanical Engineering at R.K.D.F. Institute of Science and Technology Bhopal, India and served for about 9 months. Later, in October 2009, he joined Technocrats Institute of Science and Technology Bhopal, India as Assistant Professor. He joined National Institute of Technology, Rourkela in the year 2012 as an Institute Research Scholar in the Department of Mechanical Engineering. The author is engaged in active research in the area of alternative fuel for IC engines, energy from waste etc. since January 2012. He has 6 research papers to his credit which have been published in various international journals with SCI index. He has also presented 8 research papers in the area of alternative fuel for diesel engines at various international conferences held in India and abroad. He has also received best research scholar award from the Department of Mechanical Engineeing at **"Research Scholars' Week 2016"** at NIT Rourkela.